

SAVITRIBAI PHULE PUNE UNIVERSITY
DOCTORAL THESIS

Isotopic studies of rainfall and Its reconstruction using Speleothems from **the Indian Subcontinent**

A thesis submitted in fulfillment of the
requirements
for the degree of Doctor of Philosophy

in the

Faculty of Science
Department of Atmospheric and Space Sciences

Author
Nitesh Sinha

Supervisor
Dr. S. Chakraborty

Indian Institute of Tropical Meteorology
Dr. Homi Bhabha Road, Pashan
Pune - 411008, MH, India

SAVITRIBAI PHULE PUNE UNIVERSITY

DOCTORAL THESIS

**ISOTOPIC STUDIES OF RAINFALL AND
ITS RECONSTRUCTION USING
SPELEOTHEMS FROM THE INDIAN
SUBCONTINENT**

*A thesis submitted in fulfillment of the requirements
for the degree of Doctor of Philosophy*

in the

Faculty of Science

Department of Atmospheric and Space Sciences

Author:

Nitesh SINHA

Supervisor:

Dr. S. CHAKRABORTY

Indian Institute of Tropical Meteorology
Pune - 411008, India

October, 2018

CERTIFICATE

CERTIFIED that the work incorporated in the thesis "Isotopic studies of rainfall and its reconstruction using speleothems from the Indian subcontinent" Submitted by Mr. Nitesh Sinha was carried out by the candidate under my supervision. Such material has been obtained from other sources has been duly acknowledged in the thesis.

I am satisfied with the analysis of data, interpretation of results and conclusions drawn.

I recommend the submission of the thesis.

Dr. S. Chakraborty

Signed: 

Date: 01 - Nov - 2018

Declaration of Authorship

I declare that the thesis entitled "Isotopic studies of rainfall and its reconstruction using speleothems from the Indian subcontinent" submitted by me for the degree of Doctor of Philosophy is the record of work carried out by me during the period from August 2013 to Jun 2018 under the guidance of Dr. S. Chakraborty and has not formed the basis for the award of any degree, diploma, associateship, fellowship, titles in this or any other University or other institution of Higher learning.

I further declare that the material obtained from other sources has been duly acknowledged in the thesis.

Signed: 

Date: 01 - Nov - 2018

**Declaration under Rule 4(E) of the rules for the degree of
Doctor of Philosophy (Ph.D.) of the Savitribai Phule Pune
University**

It is declared that in case of all the joint paper incorporated in the thesis, the major contribution to the paper is by the candidate. Contribution by the co-author other than supervisor have been only in respect of providing support, like sampling, processing of data and assistance in computations.



Dr. S. Chakraborty
(Supervisor)



Nitesh Sinha
(Candidate)

Date: 01 - Nov - 2018

Place: Pune

Abstract

Department of Atmospheric and Space Sciences

Doctor of Philosophy

ISOTOPIC STUDIES OF RAINFALL AND ITS RECONSTRUCTION USING SPELEOTHEMS FROM THE INDIAN SUBCONTINENT

by Nitesh SINHA

Indian Institute of Tropical Meteorology

The Asian Summer Monsoon is a primary source of precipitation across India and Southeast Asian countries and plays a vital role in the global energy balance and hydrological cycle. For a better understanding of the monsoon system, it is essential to examine long-term records of monsoon variability that go far beyond the instrument based observational data. This necessitates monsoon reconstruction from the natural archives. One of the fundamental goals of paleoclimatology is to understand past climate change in order to predict and anticipate future changes. The isotopic studies of precipitation have been proven to be a reliable means in understanding the hydrological processes and study of the paleo-monsoon. The oxygen and hydrogen isotopic signature of rainwater, which often gets preserved in cave deposits are considered an important proxy for hydroclimate variability and act as physical tracers for the atmospheric conditions.

The thesis presents an extensive dataset of modern rainfall isotopic composition from a few sites over the Indian subcontinent (viz., central India, eastern and north-east India, Andaman Islands) on daily timescale between 2012 and 2017 to better understand how changes in rainfall amount and source relate to isotopic changes in the rainfall. The isotopic composition of rainwater seems to be controlled by the dynamical nature of the moisture rather than the individual rain events. Rain isotopes undergo systematic depletions in response to the organized convection occurring over a large area and are modulated by the integrated effect of convective activities. During the early to mid monsoon, the amount effect arises primarily due to rain re-evaporation but in the later phase it could be driven by moisture convergence rather than evaporation. The condensation phase of precipitation is mostly a thermo-dynamical process; the dynamical nature of moisture is lost. But our study, like many other investigations shows that the thermo-dynamical, as well as the dynamical nature of moisture, is inherited by the isotopic composition of precipitation. This characteristic of precipitation isotopes seems to offer a better potential in studying the monsoon system.

The results of the isotopic analysis of rain from the Bay of Bengal and the Indian mainland (dual site) suggested an alternative method for the investigation of the moisture dynamical processes, instead of the traditional method of the single (destination) site analysis. It is observed that the Port Blair rainwater oxygen isotope ratios ($\delta^{18}\text{O}$) maintain a temporally dependent correlation with the average rain variation over the Core Monsoon Zone (CMZ) of India, though the rainfall over these two regions appears to be mutually independent. Consequently, the correlation between rainfall over the CMZ and $\delta^{18}\text{O}$ of Port Blair rain provides conclusive evidence of the transport of the Bay of Bengal moisture to some part of the Indian mainland during the summer monsoon season. We observed analogous variation in $\delta^{18}\text{O}$ of island precipitation and $\delta^{18}\text{O}$ of mainland precipitation at the studied sites. Like precipitation, the $\delta^{18}\text{O}$ at these two regions is modulated by the monsoon intra-seasonal oscillation (MISO). The correlation between the two isotopic records appears to arise from the propagation of the rain/cloud band from the Bay to the Indian landmass and the associated moisture transport linked to the MISO.

The study of the isotopic characteristics of rain and vapor and their association with the meteorological variables helped us better understand the isotopic variability of the speleothem which inherits the properties of percolating rainwater into a cave system. The study addresses the "amount effect" and its spatial and temporal variability and linkage with the Indian monsoon intraseasonal oscillations. The study concludes that despite achieving high sampling resolution, the variable nature of the so-called amount effect may limit our ability to reconstruct the past-monsoon rainfall variability on annual to the sub-annual timescales.

The second part of the work investigates Indian Summer Monsoon (ISM) for the period between 1700 and 3200 yr BP deduced from stable oxygen isotope ($\delta^{18}\text{O}$) and trace element (e.g. Sr, Ba, U) analyses of a stalagmite (Kadapa cave, 14.52°N, 77.99°E) from peninsular India. The achieved time resolution ($\sim 1\text{yr}$) for this time period is one of the highest so far from the Indian region. The record showed an overall increasing trend of $\delta^{18}\text{O}$, ca. 1.8‰ in 1460 years, which corresponds to progressively drier conditions over the Indian region. It is noted that the declining trend of the ISM follows the northern hemispheric summer insolation, which is known to influence the position and strength of the Inter tropical convergence zone (ICTZ). There are several notable wet and dry periods ranging from decades-to-centuries in the stalagmite records under investigation, including prolonged dry conditions (e.g. Roman Warm Period). We identified an abrupt climate change event, characterized by the decline of ISM around 2800 yr BP. The study identified a "2800 yr BP event" that was manifested in the form of enriched ^{18}O record, a sharp change in growth rate, and anomalous trace element ratios of the Kadapa stalagmite. Comparison and synthesis of other records of rainfall variability from the Indian subcontinent as well as from southern China (Dongge Cave, Wang et al., 2005), suggest synchronous variations of the Indian and

the East Asian Monsoon (EAM) systems. Furthermore, the increase in $\Delta^{14}\text{C}$ variation around 2800 yr BP coincides with the period of decreased monsoon (Kadapa & Dongge records) are indicative of the effects of the reduced solar activity.

Speleothem bearing caves are widely distributed in India, but sporadic studies by different investigators require an integrated approach of analysis to realize their full potential. The synthesis of 26 studies from 18 caves around the Indian region presents oxygen isotope measurements from speleothem. Compilation of high resolution records for the last 4000 years reveals that the Indian monsoon had been influenced by various major climatic events, such as LIA, MWP, and RWP. Spectral analysis of oxygen isotopic time series from the Indo-China region indicates the presence of a strong periodicity of ~ 50 yrs in almost all the records. Furthermore, 50-70 yrs of periodicity is also found in other paleo-climatic proxies such as tree ring (southern India) and coral (central Pacific). However, recent (2-4 ka) high-resolution records from India and marine data from the neighboring oceans are needed to strengthen our present understanding of the multi-decadal variability of ISM.

This study provides a valuable perspective on trends and variability of the ISM, their association with large-scale climatic phenomena, and helps advance our understanding of the potential drivers of the rain isotopes & their role in studying the past and present monsoon.

Keywords: Indian Monsoon, Rain Isotopes, Bay of Bengal, Speleothem, Climate Variability

List of Publications

The publications during the tenure of the thesis are given below:

- Chakraborty, S., **Nitesh Sinha**, R. Chattopadhyay, S. Sengupta, PM Mohan, A. Datye (2016). Atmospheric controls on the precipitation isotopes over the Andaman Islands, Bay of Bengal. *Scientific Report*, 6, 19555; doi: 10.1038/srep19555.
- **Nitesh Sinha**, Naveen Gandhi, S. Chakraborty, R. Krishnan, M. G. Yadava, R. Ramesh, (2018). Abrupt climate change at ~2800 Yr BP evidenced by high resolution oxygen isotopic record of a Stalagmite from peninsular India. *The Holocene*. doi.org/10.1177/0959683618788647.
- **Nitesh Sinha** and S. Chakraborty (2018). Rain-vapor interaction and its control on isotopic composition of rainfall over the Bay of Bengal. *JGR Atmosphere* (under review).
- **Nitesh Sinha**, R. Chattopadhyay, S. Chakraborty (2018). Bay of Bengal branch of Indian Summer Monsoon and its association with spatial distribution of rainfall patterns over India, *Theoretical and Applied Climatology* (under review).
- **Nitesh Sinha**, S. Chakraborty, R. Chattopadhyay, B. N. Goswami et al., (2018). Isotopic investigation of the moisture transport processes over the Bay of Bengal. *Journal of Hydrology* (under revision).

Other contributions:

- Chakraborty S., Belekar A. R., Datye A., **Nitesh Sinha** (2018). Isotopic study of intraseasonal variations of plant transpiration: an alternative means to characterize the dry phases of monsoon. *Scientific Report* 8: 8647. doi:10.1038/s41598-018-26965-6.
- Pami Mukherjee, **Nitesh Sinha**, Supriyo Chakraborty (2017). Investigating the dynamical behaviour of the Inter-tropical Convergence Zone since the last glacial maximum based on terrestrial and marine sedimentary records. *Quaternary International*, 433: 49-57.
- Fousiya, A., S. Chakraborty, H. Achyuthan, Naveen Gandhi, **Nitesh Sinha**, Amey Datye (2016). Stable isotopic investigation of Porites coral from the Minicoy Island. *Indian Journal of Geo-Marine Sciences*, 45(11):1465-1470.

Acknowledgements

This thesis would not have been possible without the support of many people. I first very gratefully acknowledge Indian Institute of Tropical Meteorology, an autonomous institute under Ministry of Earth Sciences for funding my research. I would like to express my sincere gratitude to my supervisor, Dr. S. Chakraborty, for his great enthusiasm and attentiveness throughout my Ph.D. tenure. His valuable guidance and encouragement to carry out this work is really appreciable. It is his extensive knowledge, abundant enthusiasm to seek new results, and teaching technique which helped me to grow interests in this completely new field. I am thankful for his constant support and providing all possible facilities to carry out this work. Partial financial support for this work was provided by the IAEA through CRP F31004 to S. Chakraborty.

I am very grateful to Dr. Naveen Gandhi for his suggestions and guidance throughout my research work. His extraordinary experimental skill and field work experience left a big impression on me. Suggestions and critical comments from time to time helped me to improve analysis techniques and sample handling. I would like to express my sincere gratitude and trustful respect to Dr. Rajib Chattopadhyay, his expertise and generous offering of time to discuss my ideas. During the course, his feedbacks improved my work and thinking towards a focused goal.

I express my appreciation and indebtedness to Prof. B. N. Goswami for his believe in me and kindness to give me an opportunity to work in this renowned institute. I am thankful to Dr. R. Krishnan and Dr. H. P. Borgaonkar for constant encouragement and I was truly benefited by their suggestions on various stages. The experimental work in the Stable Isotope Laboratory would not have been possible without assistance and support from Mr. Amey Datye. I express my deep gratitude to him.

I am very grateful to Dr. M. G. Yadava for his constructive comments and involvement in sampling and field work related doubts. I would like to acknowledge late Prof. R. Ramesh for his insightful comments and encouragements during my research work.

I am grateful to Prof. P. M. Mohan for his support and care during my stay at Port Blair, and most importantly providing rainwater samples of the Port Blair site continuously since 2012. I also thank the authorities of the Pondicherry University, Port Blair for carrying out the sampling work in their campus. Dr. N. V. Vinith kumar is acknowledged for extending logistic support for vapor and rain collection at NIOT, Port Blair. Many other staff of NIOT, Port Blair extended their support to make my five months stay at a remote island a great success. Mr. S. Saha, D. K. Parua and Dipankar Sarma are thanked for collecting rainwater samples in Nagpur, Kolkata, and Tezpur respectively.

I am incredibly obliged to Director, IITM, for allowing me to work and utilize all the research facilities at IITM. I also thank P. Mukhopadhyay (ex) Coordinator of Academic cell, IITM and all other members for their unconditional support during

the PhD work. I am grateful to all the staff-members in Library, Establishment, Administration and Accounts sections of IITM for their help and support.

I am also grateful for being invited to participate in the Karst Record VIII conference at University of Texas, USA and Summer School on Speleothem Science (S4), Burgos, Spain and thankful to the financial support by PAGES and DST. Both these conferences helped me a lot in widening my knowledge in the field of past climate studies. Special thanks to Prof. Ian Fairchild for his valuable comments during the S4 conference and also I indebtedness a special appreciation for his generous offering of time to discuss my work through email communications. I will always remember the sincere and timely effort of Satheesh Deekshith (Thermo-Fisher) and V. Mohan (LGR) for their help in maintaining and smooth functioning of stable isotope measurement instruments in our laboratory.

The life at IITM would not have been so enjoyable without friends like Jyoti, Ankur, Maheswar, Snehlata, Shilpa, Mercy, and many more. I thank my friend Jyoti for her support at every stage. Special thanks to Siddhartha, Nishant, Supriya, Rekha, Swati, Amita, Rajendra for their inspiration and continuous encouragement. Thanks to Dr. S. Sengupta and Dr T. Bose for their initial helps in experimental work.

Last but not the least, I would like to express my deep involvement with my family members, especially my father whose constant support helped me to realize my childhood dream.

– Nitesh Sinha

Contents

Declaration of Authorship	v
Abstract	ix
List of Publications	xiii
Acknowledgements	xv
1 Introduction	1
1.1 Background	1
1.1.1 Environmental Stable Isotopes	1
1.1.2 Stable isotopes in rainwater	5
1.1.3 Speleothems as past climate proxy	7
1.2 Motivation, Aim and Structure of this study	9
1.2.1 Motivation	9
1.2.2 Aim	11
1.2.3 Structure of this study	12
2 Materials and Methodology	15
2.1 Rainwater Samples	15
2.1.1 Sampling Methods	15
2.1.2 Isotopic Analysis ($\delta^{18}\text{O}$ & $\delta^2\text{H}$)	17
Isotope Ratio Mass Spectrometer (IRMS)	17
Liquid Water Isotope Analyzer (LWIA)	18
2.2 Speleothem Samples	20
2.2.1 Isotopic Analysis ($\delta^{13}\text{C}$ & $\delta^{18}\text{O}$)	21
2.2.2 An overview of the fieldwork	22
3 Atmospheric controls on the rain isotopes	25
3.1 Introduction	25
3.1.1 Moisture Source Identification	27
Rain Isotope Implementation	28
3.1.2 Rationale for selecting the BoB region	29
3.2 Strategy for the sampling	29
3.3 Data and Methods	30
3.3.1 Rainfall Data	30
3.3.2 Other Meteorological Data, Methods and Analysis Used	31

3.4 Results and Discussion	32
3.4.1 Atmospheric controls on the rain isotopes	33
Deuterium Excess	34
Isotopic variability of the low pressure systems	39
Rain Isotopes Lead-lag Analysis	41
Section Conclusion	43
3.4.2 Isotopic investigation of the moisture transport processes	43
Source Area: - BoB	45
Propagation of the rain band	46
Spatial variability of the isotope-rainfall relationship	49
Lag relations between the Island and mainland $\delta^{18}\text{O}$ time series	50
Reversal of south BoB moisture	53
Seasonality in rain isotopes	57
Section Conclusions	59
3.4.3 Rain - Vapor Interaction	59
$\delta^{18}\text{O}$ and $\delta^2\text{H}$ of rain and vapor	60
Rain and vapor isotopic characteristics	61
Role of source moisture	64
Rain and vapor isotopic interaction	66
Section Conclusion	68
3.4.4 Spatial and temporal variability in amount effect	68
Compilation of GNIP database: Indian Region	69
Observation: Rain Isotopes	69
Isotope Enabled Model: Rain Isotopes	75
3.5 Chapter Conclusions	76
4 Reconstruction of high-resolution monsoonal record using stalagmite	79
4.1 ISM rainfall reconstruction using a stalagmite record from peninsular India	79
4.1.1 Introduction	79
4.1.2 Cave location and regional climate	80
4.1.3 Methods	82
4.1.4 Results	83
U-Th based chronology	83
XRD data	84
Oxygen Isotope	85
Hendy's Test	86
Trace Elements	86
4.1.5 Discussion	87
Indian Monsoon Variability	87
Growth rate and Mineralogy	90
Trace elements as evidence of abrupt climatic change	90

Influence of Solar activity on ISM	91
4.2 Synthesis of proxies derived past ISM variability	92
4.2.1 Introduction	92
4.2.2 Speleothem records from the Indian subcontinent	93
Compilation of rainfall record for the last 4000 years	94
4.2.3 ISM Multi-decadal Variability	98
4.3 Chapter Conclusions	100
5 Summary, Discussion & Outlook	103
5.1 Summary	103
5.2 Discussion	104
5.2.1 Modern Rain Isotope Study	104
5.2.2 Past Monsoon Study	107
5.3 Outlook	109
A Chapter I	113
A.1 Spectral Analysis	114
A.2 Source Moisture over Port Blair	115
A.3 Relative humidity and Wind	115
A.4 Cyclone Tracks	116
A.5 CMZ Rain and Port Blair- $\delta^{18}\text{O}$ anomaly	116
A.6 Timescale of moisture transport	117
A.7 Circulation pattern of the south BoB branch during ISM	117
A.7.1 Spatial rainfall distribution during the summer monsoon	118
A.8 Vapor Sampling Site	120
B Chapter II	123
B.1 Moisture Source Region: Kadapa Cave	124
B.2 Monthly Climatology: Andhra Pradesh Region	124
B.3 $\delta^{18}\text{O}$ and $\delta^{13}\text{C}$ Correlation	125
B.4 Crystallography Results: Kadapa Stalagmite Sample	125
B.5 Amount Effect: Kadapa Region	126
B.6 U-Th Dating: Kadapa Stalagmite Samples	127
Bibliography	129

List of Figures

1.1 Rain Fractionation	3
1.2 Speleothem Formation	5
1.3 Thesis Structure	12
2.1 Rain and Vapor Sampler	16
2.2 Mass Spectrometer	18
2.3 Laser Isotope Analyzer	20
2.4 Speleothem cutter and driller	21
2.5 IRMS Lab Work	22
2.6 Pictures from field work	24
3.1 Wind Climatology	26
3.2 Rain- $\delta^{18}\text{O}$ 2012-13	34
3.3 d-excess anomaly 2012-13	35
3.4 Moisture Convergence (d-excess)	36
3.5 OLR Anomaly	37
3.6 Moisture Convergence	39
3.7 Isotope and Rain/OLR	41
3.8 Spatial Correlation $\delta^{18}\text{O}$ and Rain	42
3.9 PB- $\delta^{18}\text{O}$ & CMZ	44
3.10 PB- $\delta^{18}\text{O}$ 2014-15	45
3.11 Hovmöller diagram	46
3.12 $\delta^{18}\text{O}$ Spectral Analysis	47
3.13 Active-Break Response	48
3.14 Spatial Correlation	50
3.15 $\delta^{18}\text{O}$ comparison: BoB and Mainland	51
3.16 Normal and Reversal Trajectories	53
3.17 Surface pressure & temperature	55
3.18 Two distinct pathways of the Bay of Bengal branch	56
3.19 $\delta^{18}\text{O}$ time series, 2014-17	58
3.20 $\delta^{18}\text{O}$ Climatology	58
3.21 Rain & Vapor Correlation	62
3.22 Rain-vapor isotope time series 2015	64
3.23 GNIP Database	70
3.24 Kumar et al., 2010 Database	71

3.25 Port Blair Amount Effect	72
3.26 Port Blair ^{18}O & Spatial Rain	73
3.27 Amount effect on monthly timescale: Port Blair	74
3.28 Amount Effect: Global	75
3.29 Amount Effect: Indian subcontinent	76
4.1 Kadapa Cave Location	81
4.2 Kadapa Speleothem Sample	82
4.3 COPRA Age Depth Model	84
4.4 Kadapa $\delta^{18}\text{O}$ time series	85
4.5 Hendy's Test	88
4.6 Trace Elements	88
4.7 Kadapa $\delta^{18}\text{O}$ Comparision	92
4.8 Speleothem Sites	94
4.9 Speleothem Record Sythesis	96
4.10 Last 4k years record	97
4.11 Power Spectrum	99
4.12 Wavelet Analysis	99
A.1 Spectral Methods Comparision	114
A.2 Moisture Trajectory	115
A.3 Relative Humidity & Wind Port Blair	115
A.4 Cyclone Tracks	116
A.5 CMZ Rain & Port Blair $\delta^{18}\text{O}$ 2015	116
A.6 Mositure Travel Time	117
A.7 Specific Humidity Vs. Height	119
A.8 Rainfall Composites	120
A.9 Vapor Sampling Site: C-G Model	121
B.1 Kadapa Cave - Moisture Source	124
B.2 Monthly Climatology: Kadapa Cave	124
B.3 Kinetic Fractionation	125
B.4 XRD: Kadapa Sample	125
B.5 Amount Effect: Kadapa Region	126
B.6 U-Th dates: Kadapa Stalagmite	127

List of Tables

2.1 Rain and Vapor sampling sites	16
2.2 Water Standards	19
2.3 Cave Sites	21
3.1 Normalized d-excess	38
3.2 Summer and Winter $\delta^{18}\text{O}$	57
3.3 Vapor Sampling	60
3.4 Rain-vapor correlation coefficient	65
4.1 Speleothem Records	95
A.1 Years Examined: Reversal Event	118

List of Abbreviations

ASM	Asian Summer Monsoon
BP	Before Present
CI	Central India
CMZ	Core Monsoon Zone
DJF	December-January-February
EASM	East Asian Summer Monsoon
ENSO	El Niño-Southern Oscillation
GCM	General Circulation Model
GNIP	Global Network of Isotopes in Precipitation
IAEA	International Atomic Energy Agency
IITM	Indian Institute of Tropical Meteorology
IMD	India Meteorological Department
IO	Indian Ocean
IOD	Indian Ocean Dipole
IRMS	Isotope Ratio Mass Spectrometry
IsoGSM	Isotope incorporated Global Spectral Model
ISM	Indian Summer Monsoon
ISMR	India Summer Monsoon Rainfall
ISOs	Intraseasonal oscillations
ITCZ	Intra Tropical Convergence Zone
JJAS	June-July-August-September
LIA	Little Ice Age
LPS	Low Pressure Systems
MWP	Medieval Warm Period
MISOs	Monsoon Intraseasonal Oscillations
NIOT	National Institute of Ocean Technology
OLR	Outgoing Longwave Radiation
RH	Relative humidity
RWP	Roman Warm Period
SCS	South China Sea
SMOW	Standard Mean Ocean Water
SST	Sea Surface Temperatures
VSMOW	Vienna Standard Mean Ocean Water

To my Father

Chapter 1

Introduction

1.1 Background

1.1.1 Environmental Stable Isotopes

Isotopes of an element are having the same atomic number but the different mass number, and stable isotopes which do not disintegrate with time (or by any known mode of decay). For example, oxygen (O) has 13 isotopes from ^{12}O to ^{24}O , but ^{16}O , ^{17}O , ^{18}O are the stable isotopes of the oxygen, with ^{16}O being the most abundant in our environment. The work in this thesis uses environmental stable isotopes, e.g. isotopes of O, H, and C, as they are the principle elements of the hydrological and geological systems. The study will be using stable isotopic composition in the water (rain, vapor, and ocean) and cave deposits (speleothem, cave dripwater) to understand the hydrological components and reconstruct past monsoonal variability respectively.

Stable water isotopologues, namely the molecules $^1\text{H}^1\text{H}^{16}\text{O}$, $^1\text{H}^2\text{H}^{16}\text{O}$, $^1\text{H}^1\text{H}^{18}\text{O}$ due to the difference in the masses of each of these molecules have different saturation vapor pressures (P_s), which results in variations in the partitioning of each molecule during phase changes. The P_s is the pressure of vapor when it is in equilibrium with the liquid phase. It is solely dependent on the temperature. As temperature raises the saturation vapor pressure rises as well. The lighter isotopologue, $^1\text{H}^1\text{H}^{16}\text{O}$, has the highest P_s and tends to collect in the vapor phase, while the heavier isotopologues ($^1\text{H}^2\text{H}^{16}\text{O}$, $^1\text{H}^1\text{H}^{18}\text{O}$) have lower P_s and thus accumulate in the liquid phases. The partitioning of the different water molecules in a reservoir of liquid or vapor is called fractionation. For example, a reservoir of liquid-water under evaporation will become isotopically heavier as lighter isotopes evaporate; on the other hand, a reservoir of water-vapor will become lighter during condensation as the heavier isotopes condense more readily. As the rate of fractionation is dependent on the bond energies of the molecules, when temperature increases, the rate of fractionation decreases (Gat, 1996). Non-equilibrium (or kinetic) fractionation is the result of each molecule having a different diffusivity, which is also weakly dependent on temperature by a factor of $T^{1/2}$ (Mook, 2001). Such as, water molecules through a viscous boundary layer at the water-air interface result in additional isotopic fractionation governed by the so-called kinetic fractionation process.

Environmental stable isotopes are measured as ratio of heavy to the lighter (e.g., $^{18}\text{O}/^{16}\text{O}$). This ratio is often expressed in per mil (‰) using delta notation (δ), which is calculated from the following equation:

$$\delta = \left(\frac{R_{\text{sample}}}{R_{\text{reference}}} - 1 \right) \times 1000\text{‰} \quad (1.1)$$

Where R_{sample} is the measured ratio in the sample and $R_{\text{reference}}$ is the ratio from the laboratory reference or working standard, the value must then be converted to an international reference, such as Vienna Standard Mean Ocean Water (VSMOW) or Vienna PeeDee Belemnite (VPDB) (Gonfiantini, 1981).

The isotopic studies of precipitation have been proven to be a reliable means in understanding the atmospheric and hydrological processes. The isotopic compositions of atmospheric moisture, either as rainwater or analysis of ground level vapor, have been widely used to understand the hydrological and moisture transport processes (Gat, 1996; Lawrence et al., 2004; Deshpande et al., 2010). The isotopic compositions in most components of the hydrological cycle (e.g., ocean water, vapor, rain, etc) serve as physical tracers for the atmospheric conditions and used to understand the possible sources of observed spatio-temporal climatic variability (Gat, 1996; Clark and Fritz, 1997; Kendall and McDonnell, 1998). Stable isotopes in precipitation are affected by meteorological processes that provide a characteristic fingerprint of their origin and appear to depend on the meteorological conditions at the time of the precipitation (Dansgaard, 1964; Rozanski et al., 1992). Thus, isotopic analysis of water provides a means to determine the contributions of land and ocean derived moisture due to their distinct isotopic ratios. Isotopic ratios in precipitation and atmospheric vapor can be used to simulate the isotopic composition of moisture sources modified by the fractionation associated with the mechanism of precipitation during its transport from ocean to a continental site (Dansgaard, 1964; Rozanski et al., 2013; Gat, 2000; Araguás-Araguás et al., 2000; Gat, 2005; Yoshimura, 2015).

A primary process that controls the rain water isotopic composition is Rayleigh distillation whereby cumulative fractionation during condensation and subsequent removal of the condensate through precipitation makes the remaining vapor depleted in heavier isotopes (Figure 1.1(a)). Post condensation processes, such as evaporation of rain drops in low humidity condition and diffusive exchange of isotopes between the raindrops and the ambient vapors also make the liquid phase enriched and ambient vapors depleted in heavy isotopes (Figure 1.1(b)). These processes manifest in the form of amount effect (Dansgaard, 1964) - whereby the heavier isotopes are progressively removed during rainout process resulting an inverse correlation between the rainfall amount and the isotope ratios of the rainwater. This is known to be a fundamental reason of rainwater isotopic fractionation especially in the tropical region.

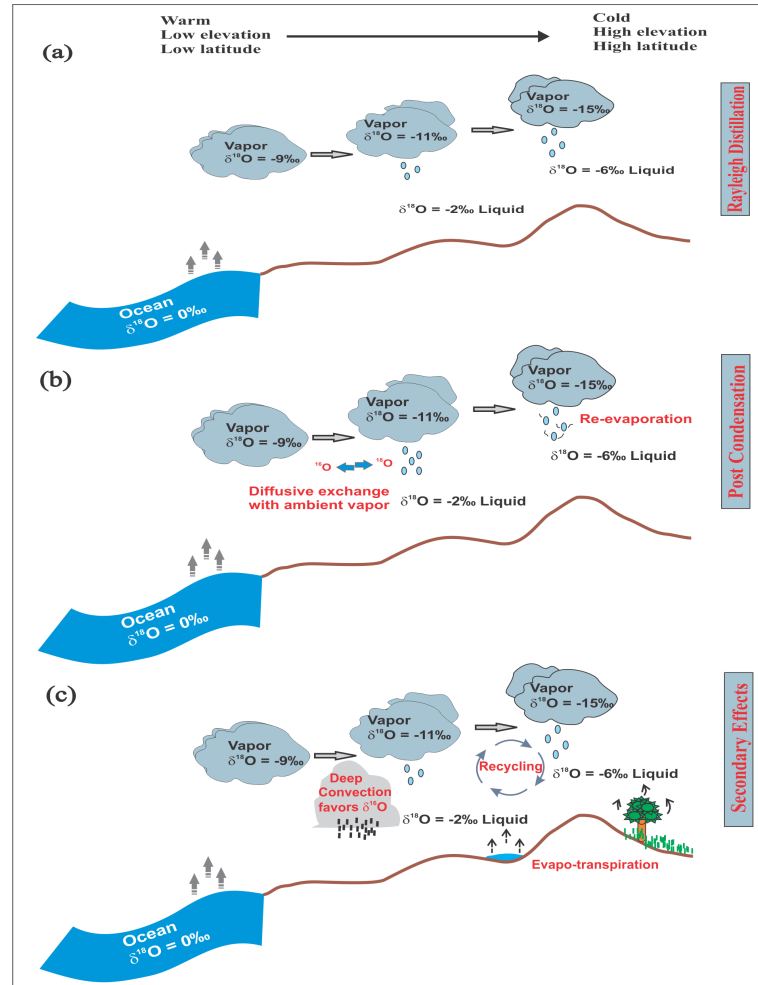


FIGURE 1.1: Schematic illustration of fractionation during evaporation of ocean surface water and (a) removal of the condensate through rain-fall, in turn, depleted residual vapor (b) post condensation processes and their controls on isotopic composition of raindrops and ambient vapor, and (c) secondary effects that favors ^{16}O in the atmospheric vapor, hence, subsequent depleted rainfall.

Condensation temperature, another primary factor controlling the isotopic characteristics often gets overshadowed by the amount effect in the tropics. Secondary effects, such as recycling of water vapor within the convective cells (Figure 1.1(c)) could reduce the rainwater isotopic composition during the heavy convective events (Lawrence et al., 2004; Risi et al., 2008). The amount effect, however, shows spatial variability and needs to be quantified for a specific region in order to study the effects of regional hydrological processes (such as evapotranspiration) on isotopic fractionation (Figure 1.1(c)). It has also been used to reconstruct the past rainfall variability from centennial to millennium time scales using the natural archive. An archive can preserve the isotopic variability (due to the changing environments or climates) which can be measured with sufficient precision using a mass spectrometer or by laser water isotope analyser (discussed in the chapter 2).

The isotope based rainfall reconstruction relies on the premise that $\delta^{18}\text{O}$ of rainfall is inversely correlated with the rainfall amount (The amount effect). This inverse relation is the basis of rainfall reconstruction.

The amount effect, quantified as (in ‰/mm):

$$\frac{d\delta^{18}\text{O}}{dp} \quad (1.2)$$

Where, p is precipitation over the cave region. Customarily this parameter is determined based on analysis of a few years of rainfall data. As mentioned earlier that the amount effect shows considerable variability, the reason however, is not well understood. Hence, it is important to understand the causative mechanism(s) that control the amount effect. On the other hand, to establish the amount effect for specific site where archives based rainfall reconstruction is/are envisaged. If the effect is assumed to have remained constant within the period of interest of rainfall reconstruction the isotopic ratios is calibrated with the rainfall record thus enabling a simple way to estimate the past rainfall amount.

When a tree uptakes water for its physiological process or the rainwater that percolates through subsurface fractures, cracks and conduits and eventually seeps in a cave system to form carbonate deposits, an archive dominantly used in paleo-environmental reconstruction (e.g. speleothems). The percolation of water downward results in leaching of CaCO_3 in the presence of excess CO_2 (high $p\text{CO}_2$), which is typically made available by the respiration of the plants into the soil. Subsequent degassing of CO_2 from CaCO_3 saturated seepage water, when this water is exposed to the cave atmosphere (low $p\text{CO}_2$), leads to deposition of speleothems (Figure 1.2) due to the $p\text{CO}_2$ gradient between the seepage water and the cave atmosphere (Schwarcz, 1986). Speleothem is a family name for secondary cave carbonates (such as stalagmites, stalactites and flowstones) and can be used as paleoclimatic proxies as their formation depends on water and vegetation availability above the surface of a cave site.

The availability and variability of water and vegetation are mainly controlled by climate dynamics over cave areas. The isotopic signature of the rain water through these processes is believed to get transferred and recorded in the oxygen isotopic ratios of tree ring or the carbonate layers of the speleothem. The climatic signals might be recorded in the chemical and isotopic composition (^{13}C and ^{18}O) of speleothems, which reflect those compositions in parent seepage water (Yadava and Ramesh, 2005; Shakun et al., 2007; Lachniet, 2009; Lewis et al., 2011), trace elements (Griffiths et al., 2010), etc. However, deciphering the climate records in speleothems requires proper understanding of the physicochemical processes that controlled the formation, isotopic and chemical composition of speleothems (Hendy, 1971; Fairchild and Treble, 2009; Dreybrodt and Scholz, 2011).

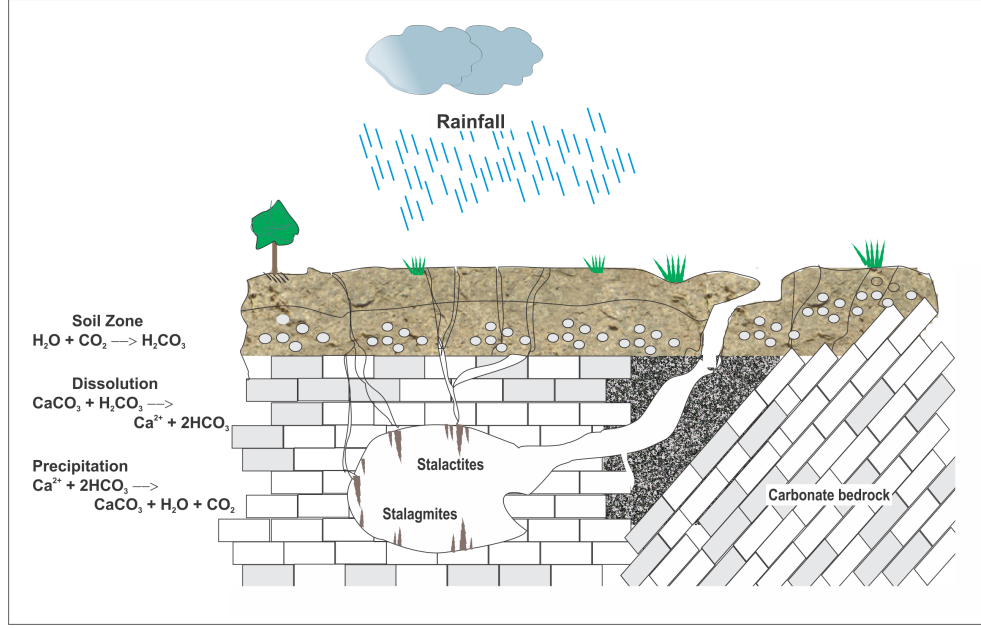


FIGURE 1.2: Conceptual model of the karst system, rainwater percolates through plant, epikarst soil and rock cracks dissolve CO_2 and $CaCO_3$. The upper part of the unsaturated zone (the epikarst), having both higher porosity and permeability. The speleothem deposits in the deep cave environment due to the degassing of CO_2 from the dripwater. The left-hand column shows the step of reactions from soil zone to precipitation of carbonate inside the cave environment.

1.1.2 Stable isotopes in rainwater

The complexity of the hydrological cycle, in turn, made the isotopic fractionations of water in the atmosphere a complex system. Despite the complications ^{18}O and 2H behave in predictable manner. Globally, the stable isotopic compositions of freshwater ($\delta^{18}O$ and δ^2H) show a linear correlation, explained in the form of a global meteoric water line (GMWL) introduced by (Craig, 1961):

$$\delta^{18}O = 8 \times \delta^2H + 10 (\text{‰}, SMOW) \quad (1.3)$$

Craig's line is only global in application, and is actually an average of many local or regional meteoric water lines which differ from the global line due to varying climate and geographic parameters. That is, if the water samples of interest are site/location specific, it will be called as local meteoric water line (LMWL). Local line will differ from the global line in both slope and intercept. So, the meteoric waterline can be represented in its generalized form as $\delta^2H = A \times \delta^{18}O + d$, where A represents the slope and d represents the intercept or d -excess (2H excess). The relationship between ^{18}O and 2H arises from fractionation, starting from evaporation from the oceans to the condensation from the vapor mass, and most importantly the effects of meteorological parameters in between the pathways. This isotopic differentiation is commonly described by the fractionation factor α which is defined as the ratio of the heavy isotope content of the liquid (solid) and of the vapor phase. The fractionation

may happen in physicochemical reactions under equilibrium and non-equilibrium (kinetic) conditions, or fractionation by molecular diffusion. The isotopic difference between two phases (e.g. water(w) - vapor(v)) is simply expressed as enrichment factor (ϵ) and defined by $(\alpha - 1) \times 10^3\text{‰}$ (Clark and Fritz, 1997). For oceans at 25°C, the equilibrium isotopic composition of water vapor should be (Majoube, 1971):

$$\delta^{18}O_{vapor} = \delta^{18}O_{seawater} + \epsilon^{18}O_{v-w} = -9.3\text{‰} \quad (1.4)$$

$$\delta^2H_{vapor} = \delta^2H_{seawater} + \epsilon^2H_{v-w} = -76\text{‰} \quad (1.5)$$

However, under natural conditions, thermodynamic equilibrium between water and vapor phase is not always established, for example, during evaporation of an open ocean into an unsaturated atmosphere. In this case, small differences in transferring of light and heavy water molecules through a viscous boundary layer at the water-air interface result in additional isotopic fractionation governed by the so-called kinetic fractionation process. The model that describes isotope effects accompanying evaporation into an open (unsaturated) atmosphere was formulated by (Harmon and Gordon, 1965), known as C-G Model. According to the C-G model, the isotopic ratio of the evaporating vapor is estimated by the following equation:

$$R_e = \alpha_k \frac{\frac{R_l}{\alpha} - h R_a}{1 - h} \quad (1.6)$$

Where R_e , R_l and R_a are isotopic ratios of evaporated vapor, ocean surface water, and preexisting vapor in the atmosphere. α and α_k are the equilibrium and kinetic fractionation factors, respectively, h is the relative humidity above the sea surface normalized to saturation at the sea surface temperature (SST). The C-G Model estimated that the mean isotopic composition of global precipitation is $\delta^{18}O = -4\text{‰}$ and $\delta^2H = -22\text{‰}$ (Harmon and Gordon, 1965).

The kinetic fractionation suggested that the deviation of the global meteoric water line from seawater makes sense. The kinetic fractionation of ^{18}O exceeds that of 2H , effects are not observed in the large water reservoir (e.g. the ocean) but in the vapor, and the rain from this vapor. The measure of relative proportions of ^{18}O and 2H in water is defined as deuterium excess or d-excess (d) and is calculated for any precipitation sample by:

$$d = \delta^2H - 8 \times \delta^{18}O \quad (\text{Dansgaard, 1964}) \quad (1.7)$$

The d is a second order isotopic parameter acts as an index of deviation from the global meteoric water line ($d_{GMWL} = 10\text{‰}$). The d -excess is correlated with the humidity, air temperature, and sea surface temperature of the oceanic source area of the precipitation (Merlivat and Jean, 1979). It can be used to identify the vapor source region, interaction or mixing of local moisture. High d -excess in precipitation can also

arise from the significant addition of re-evaporated moisture from continental basins or recycling of moisture to the water vapor. Studies on seasonality in the deuterium excess reveal that it will be low (high) during summer (winter) and high (low) during winter (summer) months over the northern (southern) hemisphere (Froehlich et al., 2002). However, the changes in d-excess depend on ^{18}O and ^2H , thus, the uncertainties can be relatively higher than its natural variability. In a $\delta^{18}\text{O}$ - $\delta^2\text{H}$ space, the result is a deviation from the global meteoric water line along a line with variable slopes depends largely on the various factors (as discussed above). The stable isotopes of rain have been widely used to characterize the precipitation and other sources of water in a region or area (Dansgaard, 1964; Gat, 1981; Gedzelman and Lawrence, 1990; Krishnamurthy and Bhattacharya, 1991; Rozanski et al., 1992; Rozanski et al., 2013; Gat, 1996; Araguás-Araguás et al., 1998). The Global Network of Isotopes in Precipitation (GNIP) is the only source that monitors the isotopic composition of precipitation over 50 years (<https://websso.iaea.org>), was initiated by the International Atomic Energy Agency (IAEA) of Vienna, Austria, in collaboration with the World Meteorological Organization (WMO). The data produced from this network serve as an indispensable database to inform a range of scientific disciplines, including, hydrology, meteorology and climatology.

1.1.3 Speleothems as past climate proxy

For paleoclimate, the past two decades have been the age of the ice core. The next two may be the age of the speleothem (Gideon Henderson, 2006). In the recent decades, speleothems have been recognized as a powerful continental paleoclimate archive because of extremely precise dating using uranium-series, U-series dating (Edwards et al., 1987; Li et al., 1989; Cheng et al., 2016), wide geographic distribution (i.e., spans low and high latitudes) and high resolution chemical and isotopic microstratigraphy (Johnson et al., 2006; Ridley et al., 2014). The emphasis of early research on speleothems was on the estimation of paleo-temperature based upon oxygen isotope fractionation between carbonate and water (Harmon et al., 2004; Gascoyne et al., 1980). Due to complexities in the estimation of paleo-temperature in speleothems, recent research on speleothems focuses on qualitative interpretations (e.g., wet/dry) of their well-dated stable isotope records. As precipitation, another primary factor controlling the isotopic characteristics often gets prominent and manifest as amount effect in the tropics (Dansgaard, 1964).

This quantitative approach requires the knowledge of three aspects: (1) understanding of the surface geomorphology and physicochemical processes that control the formation of speleothems (Hendy, 1971; Fairchild and Treble, 2009; Fairchild and Baker, 2012), (2) whether the carbonate formed in isotopic equilibrium or in non-equilibrium with their drip water, and (3) the appropriate equation to estimate the precipitation from the oxygen isotope fractionation determined from speleothems. The latter two aspects are ambiguous and controversial, thus hampering the estimation of paleo-monsoon in speleothem-based records. For instance, the Hendy

test has been utilized as a routine test to check isotopic non-equilibrium in ancient speleothems. However, performing Hendy test on a few growth layers in an individual stalagmite does not guarantee the deposition of the whole stalagmite in isotopic equilibrium. Moreover, the main criteria for Hendy test (i.e., no correlation between $\delta^{18}\text{O}$ and $\delta^{13}\text{C}$ in carbonates along a single growth layer) might falsely indicate isotopic equilibrium in a small radius stalagmite or a short selected transect within the stalagmite apex (few centimetres). Another aspect over the tropical and some semi-arid regions in particular, is that the isotopic composition is inversely related to the amount of rainfall. It has been observed in monsoon regions that the most depleted $\delta^{18}\text{O}$ values correspond to heavier monsoon rain intensity (Dominik et al., 2003; McDermott, 2004). This empirical observation, which can be observed in annual or monthly records, or individual events, is referred to as the amount effect. However, the amount effect is scale dependent, spatially as well as temporally. For example, Treble et al. (2005) showed that there was a strong amount effect in individual rainfall events in Tasmania, whereas monthly means showed only a relationship to temperature. On the other hand, daily rainfall data from certain tropical islands failed to show the effect, even though it was obvious in seasonal data (Kurita et al., 2009). In some locations, the effect is non-stationary: Fuller et al. (2008) found that using monthly data from the GNIP site at Wallingford, southern England, the effect was present in certain years whereas there were co-variations with temperature in others. On the other hand, $\delta^{13}\text{C}$ isotope ratio interpreted as changes in overlying vegetation (C_3 versus C_4 plants) and vegetation density (Dorale et al., 1998; Baldini et al., 2008).

Other speleothem proxy parameters for past environment and climate are growth rate, trace elements concentration (i.e., changes in trace element to Ca), and secondary changes (e.g. change of aragonite to calcite). In practice, these parameters in particular contexts have proved especially valuable. The growth rate variations, determined from the thickness of the speleothem layers, have been shown to reflect climatic variables in several cases and have been applied particularly to modern climate calibrations and understanding the climatology. Likewise, seepage water contains various ions (e.g. Mg, Ba, Sr) at trace levels (in ppm to ppb), known as trace elements, which subsume in speleothem lamina during carbonate precipitation. The trace elements from the bedrock are generally expected to remain constant over long periods of time, unless seepage water pathways have changed in the course of time (Gascoyne, 1983). Evidence of climatic change and paleo-hydrological conditions in the past can be inferred from trace element profiles derived from stalagmites (Treble et al., 2003; Johnson et al., 2006; Fairchild and Treble, 2009). Next is the crystallography of the precipitated carbonate, processes determining speleothem isotopic and elemental composition, however, are complex (Fairchild et al., 2006; Lachniet, 2009). Most stalagmites currently used for paleo-climate reconstruction are calcitic, while aragonitic stalagmites are less abundant (Holmgren et al., 2003). If the precipitated carbonate in speleothem is a mixture of calcite and aragonite, then the $\delta^{18}\text{O}$ of the

speleothem is the weighted mean of the calcite- $\delta^{18}\text{O}$ and aragonite- $\delta^{18}\text{O}$ (Yadava et al., 2014). The presence of aragonite in cave deposits can be interpreted as a consequence of arid climatic conditions or seasonal aridity (McMillan et al., 2005; Wassenburg et al., 2012). The precise dating of speleothem was mainly used for transferring the speleothems chronology to calibrate the timing of paleo-climate fluctuations on the timescales of 10^3 - 10^4 years. Counting of physical or chemical lamina allows the duration of climatically significant intervals to be determined. To study the influences of various global climate phenomena such as, Roman Warm Period (Vollweiler et al., 2006), the Medieval Warm Period (Hughes and Diaz, 1994; Mann, 2002), and the Little Ice Age, e.g., (Mann, 2002) on the regional monsoon system during the mid to the late Holocene. To identify the climate forcing factors by allowing direct comparison with natural and anthropogenic phenomenon (Wang et al., 2008; Cheng et al., 2012) and detecting the teleconnections in the global climate system (Wang et al., 2001; Yuan et al., 2004; Cheng et al., 2016).

1.2 Motivation, Aim and Structure of this study

1.2.1 Motivation

Limited but significant rain isotope work has been done over the Indian region. Most of the early work (starting 1960s) of precipitation isotope analysis in India has been done through the IAEA network (Datta et al., 1991; Bhattacharya et al., 2003; Gupta and D., 2005). However, these studies were limited to only a few sites in India and also done on monthly composite rain sample. Some other sporadic work has been done that gave only short term results and so uninterrupted long-term records are lacking (Bhattacharya et al., 1985; Krishnamurthy and Bhattacharya, 1991; Ramesh and Sarin, 1992). In the last decade more systematic effort has been made such as stable isotope evidence in source, rain-vapor interaction, isotopic characterization of precipitation on a wide scale (Sengupta and Sarkar, 2006; Deshpande et al., 2010; Kumar et al., 2010) as part of a national level program called Isotope Fingerprinting of Waters of India or IWIN (Deshpande et al., 2011). However despite these enhanced activities systematic studies of daily rainfall analysis is still lacking.

Precise knowledge of the site specific amount effect is important in order to understand the regional hydrological processes. Rainwater analysis in most of the places in the Indian subcontinent exhibits amount effect, however places like northeast and some parts of southwest India are notable exceptions (Yadava et al., 2007; Breitenbach et al., 2012; Lekshmy et al., 2014). Amount effect is scale dependent; a better knowledge of its scale dependency may help us improve our understanding about the organization of the convective system, which in turn is likely to improve our understanding on the hydrological processes. The intensity of the amount effect varies

throughout the South-East Asia (Araguás-Araguás et al., 2000). The maximum correlation ($\delta^{18}\text{O}$ vs. rainfall on monthly time scale) is observed for stations from the Indian subcontinent (such as, India, Pakistan, Sri Lanka, and Myanmar) is -0.52 (namely, New Delhi). The IAEA-GNIP data for Mumbai and Kozhikode show no amount effect on annual and seasonal time scales (Bhattacharya et al., 2003; Managave et al., 2011). Conventionally the precipitation isotope ratios are interpreted within the framework of a Rayleigh distillation model and correlated with the amount of precipitation in tropical areas (Dansgaard, 1964). However, amount dependencies of isotopes are influenced by moisture source and transport pathways but our current knowledge is not enough to predict its behavior either in modern precipitation or in paleo-climate records (Lee et al., 2007; Sime et al., 2009). Many attempts have been made to understand its dependency using rain samples on monthly/weekly time scale and also by isotope equipped general circulation models (GSMs), but they fail to explain observed seasonal or inter-annual variations on a regional or local scale (Schmidt et al., 2005; Lee et al., 2007).

In order to reconstruct the past monsoon variability, oxygen isotopic records of speleothems from caves over the Indian subcontinent (Yadava et al., 2004; Sinha et al., 2007; Sinha et al., 2011a; Kotlia et al., 2012; Sanwal et al., 2013) have widely been used. The isotope based rainfall reconstruction relies on the premise that $\delta^{18}\text{O}$ of rainfall is inversely correlated with the rainfall amount (as discussed earlier). A large part of speleothem studies have focused on centennial-millennial scale climate variability, whereas monthly to annually resolved speleothem proxy records (Treble et al., 2003) are still extremely rare. Speleothem growth rates vary by at least two orders of magnitude (0.01-1.0 mm/year), depending on factors such as temperature and calcium ion concentration of the drip waters (Baker et al., 1998; Genty et al., 2001a; Genty et al., 2001b). The conventional sampling techniques resolve stable isotope measurement typically from few years to several decades. Several works have been done on Indian speleothems. For example, (Yadava et al., 2004; Yadava and Ramesh, 2005) reconstructed rainfall for centennial to millennium time scale using speleothem samples from peninsular India (Akalagavi cave, Gupteswar and Dandak cave, respectively). Sinha et al., 2007 analysed oxygen isotope records of a stalagmite from Dandak cave (19°N, 82°E) and observed that monsoon rainfall was significantly weak (ca. 30%) during the Little Ice Age (LIA) around 1360 AD. Kotlia et al., 2012 and Sanwal et al., 2013 reported major climatic variability of past using speleothems from the Himalayan region. Laskar et al., 2013 analyzed a speleothem sample from the Andaman region and observed that the global climatological events such as Medieval Warm Period (MWP) were recorded in the oxygen isotopic composition. Despite these efforts, there are many issues that need to be addressed. For example, isotopic study of stalagmite from Dandak cave (Sinha et al., 2007) observed reduced monsoon intensity during the LIA which does not conform to the observation of Kotlia et al., 2012 who observed a wetter LIA with multi-annual dry spells at 1590-1595 AD, 1725-1730 AD and

1840-1850 AD using speleothem from the Himalayan region. So the anomaly needs to be investigated whether it is due to regional differences in rainfall distribution or the sensitivity of the samples. Secondly though the MWP signal has been found in case of Andaman speleothem (Laskar et al., 2013) but the reason is not well understood how $\delta^{18}\text{O}$ of this speleothem responded to this global event. Thirdly, the BoB experiences heavy cyclonic disturbances and it is known that very heavy rainfall during the cyclonic events cause anomalous isotopic depletion (Lawrence et al., 2004). So such kind of activities in the past may have caused isotopic depletion in speleothem. This kind of studies has not yet been done in Indian context. The speleothem samples in Andaman Island and the coastal areas of eastern India that are subjected to cyclonic activities are expected to carry the cyclonic signatures in their isotopic ratios. Such kind of studies falling under the domain of paleotempestology remained un-attempted in the Indian context.

1.2.2 Aim

The aim of this study is to investigate the atmospheric controls on isotopic composition of the rain/vapor, in turn, understand the moisture transport processes using environmental stable isotopes as a tool. The amount effect needs to be studied to investigate its anomalous behavior on annual to sub-annual timescales, particularly, for a specific site region where speleothem based rainfall reconstruction is envisaged. Further, to reconstruct the high-resolution speleothem records with an aim to study the monsoonal variability for the last several millennia from the Indian subcontinent. Other than this, we will endeavor to correlate the other proxy records vis-à-vis speleothem based rainfall reconstruction within the overlapping time-frame. The main research question:

WHAT ARE THE METEOROLOGICAL CONTROLLING FACTORS OF RAIN AND THEIR ROLE IN CHARACTERIZING ITS ISOTOPIC COMPOSITION OVER A SPECIFIC REGION, WHICH IN TURN ASSOCIATED WITH THE MOISTURE TRANSPORT PROCESSES AND PRESERVED IN AN ARCHIVE AS A PROXY?

is answered by addressing four research objectives:

- **Objective 1:** Investigation of precipitation isotopes and their relationship with the meteorological parameters.
- **Objective 2:** Systematic study of the amount effect from different areas including the speleothem sampling sites.
- **Objective 3:** Reconstruction of monsoon rainfall using the isotopic analysis of speleothem from the Indian subcontinent.
- **Objective 4:** Synthesis of speleothems and other proxy derived rain data in and around the Indian subcontinent.

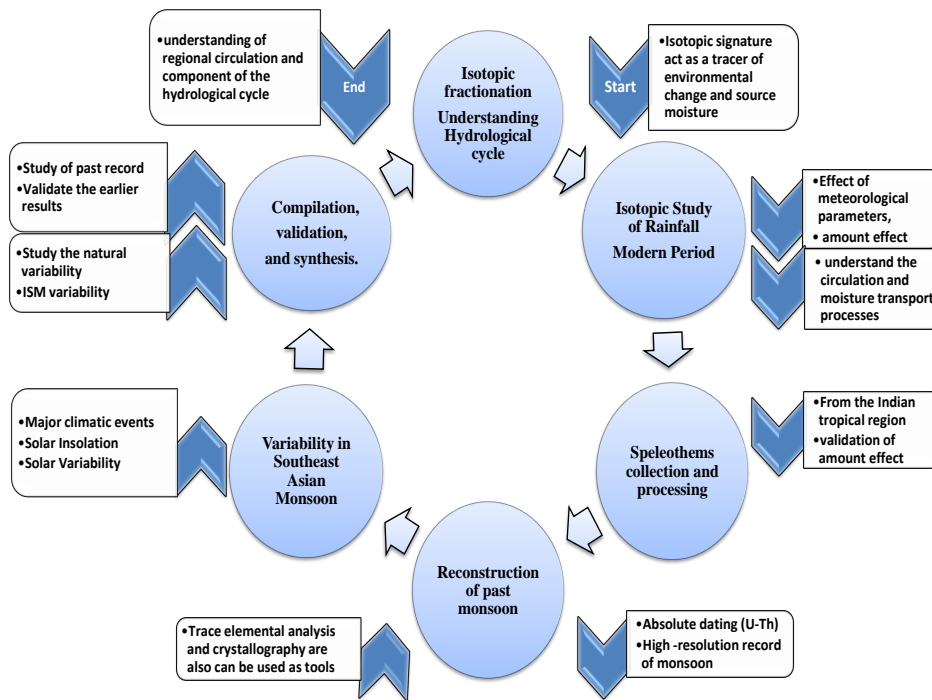


FIGURE 1.3: Flow chart representing the structure of the study.

1.2.3 Structure of this study

To address the aforementioned objectives of the Ph.D. research, the following work has been carried out: **(a)** Introducing the research problems based on detailed literature survey on isotopic fractionation and its association with the hydrological cycle, identification of scientific gap areas and need for further research. One of the most important, yet poorly understood aspects of atmospheric controls on the rainfall isotopes over the Indian region, in particular the moisture transport processes during the summer monsoon season. Therefore, the main focus of this thesis is the isotopic studies of rainfall over the Indian subcontinent during the Indian Summer Monsoon (ISM) to get insight of the amount effect and its spatial variability. The summer monsoon intraseasonal variability is largely governed through the variations over the Bay of Bengal (Gadgil, 2003). Thus, we extensively worked on rain-isotopic connection of the Port Blair, the Andaman Islands to Indian mainland. **(b)** In continuation to that, the moisture transport process from the BoB to Indian landmass has also been investigated. The isotopic study of the hydrological process over the Indian subcontinent enhances our understanding towards the isotopic variability in cave deposits (e.g. speleothem) that form through the meteoric water. **(c)** Further, the field serve and collection of the speleothems from different regions (namely, Peninsular India and Andaman Islands) over the Indian subcontinent have been successfully executed to study the past monsoonal variations. Towards this, a U-Th dated speleothem sample

from Kadapa cave, Andhra Pradesh was processed (cutting and drilling) and sub-samples in the form of carbonate powder have been analysed for $\delta^{13}\text{C}$ and $\delta^{18}\text{O}$. **(d)** Reconstructed high resolution time series of $\delta^{18}\text{O}$ potentially reflects the Indian summer monsoonal variability on sub-annual to multi-decadal timescales. **(e)** A detailed investigation of the natural forcing, such as, solar variability, solar insolation, and major past climatic events on Indian monsoon have been studied. **(f)** Moreover, the synthesis of reconstructed speleothem records and available proxy records (paleomonsoon) from the Indian subcontinent has been performed. The analysis focuses on the mechanisms of multi-decadal variability in ISM using robust statistical methods, to estimate the periodicity and, explain their coherent behavior. **(g)** The research work is expected to provide a valuable perspective on the trends and variability in the ISM, their association with large-scale climatic phenomena, and help advance our understanding of the potential drivers of the rain isotopes & their role in studying the regional hydrological cycle. The structure of the study has been described using a flow chart shown in Figure 1.3.

So, the present Ph. D. work has been divided into two major components, first is the study related to rain isotopes and second is focused on the past monsoon reconstruction using speleothems from Indian subcontinent. The thesis is organized as follows:

Chapter 2 describes the various observed and reanalysis datasets used in thesis work and the details of the instruments used for the rain and carbonate sample processing and analysis. Methods and experimental setups are also discussed in this chapter, including a report on the field works in remote areas of the Andhra Pradesh and the Andaman Islands.

Chapter 3 covers first two objectives that focus on rain isotopes and understanding the amount effect on temporal as well as spatial scales, presents observational rain-isotope daily time series from the various sites over the Indian subcontinent. A systematic effort has been made to get more insight on rain-isotope spatial correlation on wide scale, as well as stable isotope evidences in vapor source, rain-vapor interaction. Applications of isotope hydrology to study the moisture transport processes. The dynamical behavior of moisture namely, its genesis in the Indian Ocean and possible mechanism of observed transport pathways to the Indian continent has been presented. Observational, GNIP as well as Modelled (IsoGSM¹) rain-isotope database for the validation of amount effect over a few sites on the Indian subcontinent, including the speleothem sites have been established.

Chapter 4 presents the reconstructed time series of ISM using speleothem (e.g. stalagmite) from Kadapa, Andhra Pradesh. It help investigates the monsoonal change

¹Isotope incorporated Global Spectral Model

deduced from stable oxygen isotope ($\delta^{18}\text{O}$) and trace element (e.g. Sr, Ba, U) of a stalagmite. There are several notable wet and dry periods ranging from decades to centuries in the stalagmite records under investigation, including prolonged dry conditions (e.g. Roman Warm Period). This chapter also includes synthesis of available paleoclimate data from speleothems as well as other proxy records from the Indian subcontinent. Using rigorous statistical analysis, we investigated the oxygen isotope derived ISM variability on decadal to multi-decadal timescales, thereby studied the natural mode of periodicity in ISM. The observed results are also analysed using other proxy records (including speleothems) from the Indian subcontinent. Statistical analyses have been performed and possible causes of variability on different timescales are discussed.

Chapter 5 summarizes the major findings of the Ph.D. research work and an outlook for future research is presented.

Chapter 2

Materials and Methodology

2.1 Rainwater Samples

The rainwater samples from a few sites in the Indian subcontinent were collected, mainly during the summer monsoon months. Daily rainwater was collected at the Pondicherry University, Port Blair (2012-2014 and 2016-2017). In 2015, rainwater was collected at the National Institute of Ocean Technology (NIOT) campus, which is approximately 4km aerielly north-west of the Pondicherry University. Ground level vapor (GLV) was sampled on a daily timescale for the year 2015 at the NIOT campus between May and October. Rainwater samples were also collected at Indian mainland sites, such as Nagpur, Kolkata and Tezpur for the year 2015. The details of collected rainwater and GLV on a daily timescale are listed in Table [2.1](#)

2.1.1 Sampling Methods

To collect rainwater samples, a two litre plastic bottle fitted with a 20.3 cm diameter funnel was used (Figure [2.1a](#)). A tube was attached to the tip of the funnel that touched the bottom of the plastic bottle that helped reduce the exposed surface area, in turn, evaporation. The collected rainwater was converted to rain rate (mm/day) using a calibration equation (available in IAEA/GNIP Precipitation Sampling Guide, v2.02 September 2014). The rainfall record was also obtained from India Meteorological Department (IMD) site for all the studied years. GLV was collected in Port Blair at the NIOT campus from (from 24th May to 4th October), using a cryogenic trapping method^[1]. Briefly, a metal trap (Figure [2.1b](#)) was cooled to about -80°C temperature using a mixture of ethanol and liquid nitrogen. The air flow rate was controlled at 800 ml/min to ensure an adequate amount (~2 ml) of vapor collected in 3 hours (0800-1100 hour). The sampling of the GLV was carried out using the method similar to Deshpande et al. ([2010](#)). The average amount of collected GLV was 2.9 ml, ranging from 1.4 ml to 4.5 ml in 3 hours. Additionally, a separate arrangement was made to collect rainwater samples synchronized with the vapor sampling time in order to study their isotopic interaction.

¹http://www-naweb.iaea.org/napc/ih/documents/miba/water_vapor_protocol.pdf

TABLE 2.1: Details of rain and vapor collection sites, location, and number of samples collected from the Indian sub-continent.

Rain water collection site	Coordinates	Year (No. of samples)
Pondicherry University, Port Blair	11.66°N, 92.73°E	2012 (82)
		2013 (94)
		2014 (112)
		2016 (139)
		2017 (105)
National Institute of Ocean Technology, Port Blair	11.63°N, 92.70°E	2015 (112)
Nagpur	21.15°N, 79.09°E	2015 (18)
Kolkata	22.56°N, 88.36°E	2015 (47)
Tezpur	26.63°N, 92.80°E	2015 (52)
Ground level vapor collection site	Coordinates	Year (No. of samples)
National Institute of Ocean Technology, Port Blair	11.63°N, 92.70°E	2015 (107)

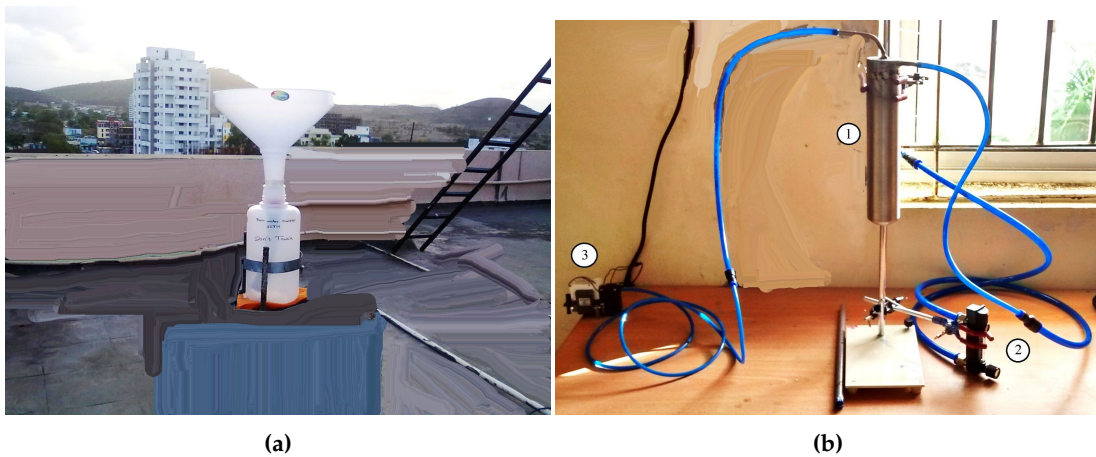


FIGURE 2.1: (a) Rainwater sampler, (b) Ground level vapor sampler and setup (1: Metallic vapor sampler, 2: Flow meter, 3: Diaphragm Pump).

2.1.2 Isotopic Analysis ($\delta^{18}\text{O}$ & $\delta^2\text{H}$)

The rain and GLV samples were transferred to leak proof plastic bottle and then shipped to Indian Institute of Tropical Meteorology (IITM), Pune for isotopic analysis. Initially, the rainwater samples were analyzed using an isotope ratio mass spectrometer. Later, when a LGR liquid water isotope analyzer was installed at IITM in early 2014, all other samples including the previously measured samples by the IRMS were re-analyzed for $\delta^{18}\text{O}$ and $\delta^2\text{H}$. The isotopic ratios measured using both the instruments matched well; most of them were well within the $\pm 1\sigma$ variability. A few samples that did not match within the $\pm 1\sigma$ variability were discarded. The overall analytical precision obtained for $\delta^{18}\text{O}$ ($\delta^2\text{H}$) was about 0.1‰ (<1‰). The working principle of the instruments and analysis methods are discussed below.

Isotope Ratio Mass Spectrometer (IRMS)

Mass Spectrometry is a powerful technique for identifying small abundances of isotopes and their small variations in different phases and probing the fundamentals of isotope geochemistry. The major components of a mass spectrometer are shown by block diagram (Figure 2.2a). The inlet transfers the samples through the gas chamber to the analyzer. The analyzer has three major parts; the source region that ionizes the sample molecules, the mass analyzer separates the ions in space or time depending upon their masses and counted by the detector. The signal transferred to a data system for the analysis and ratio calculation. It is important to have a vacuum system to maintain the low pressure inside the analyzer, which is required to minimize ion and molecule interactions, ions scattering, and neutralization of the ions.

The principle of the mass spectrometry is based upon the motion of a charged particle in an electric or magnetic field. The mass to charge ratio of the ion affects the motion of ions under the influence of established constant force field. For the same ionization, ions of different masses follow different radial paths inside the magnetic field and are collected in Faraday cups, located at appropriate positions for different masses. Delta V Plus from Thermo Fisher Scientific IRMS (Figure 2.2b) is used in the present study. It has triple collectors and is a gas source type stable isotope ratio mass spectrometer. The instrument was standardized and checked for reproducibility/accuracy with a large number of primary and secondary laboratory standards of water and carbonate samples.

For isotopic ratio measurement of water, basically $\text{CO}_2 + \text{H}_2\text{O}$ and $\text{H}_2 + \text{H}_2\text{O}$ equilibration method for $\delta^{18}\text{O}$ and $\delta^2\text{H}$ respectively was followed (Epstein and Mayeda, 1953; Gonfiantini, 1981). Water sample (0.5ml) was filled in a standard glass bottle and sealed with air tight neoprene septum. A batch of 40-50 such bottles filled with samples and secondary laboratory standards (calibrated with respect to VSMOW) were loaded in sequence. Firstly, vials were flushed with air and filled with a $\sim 0.3\%$

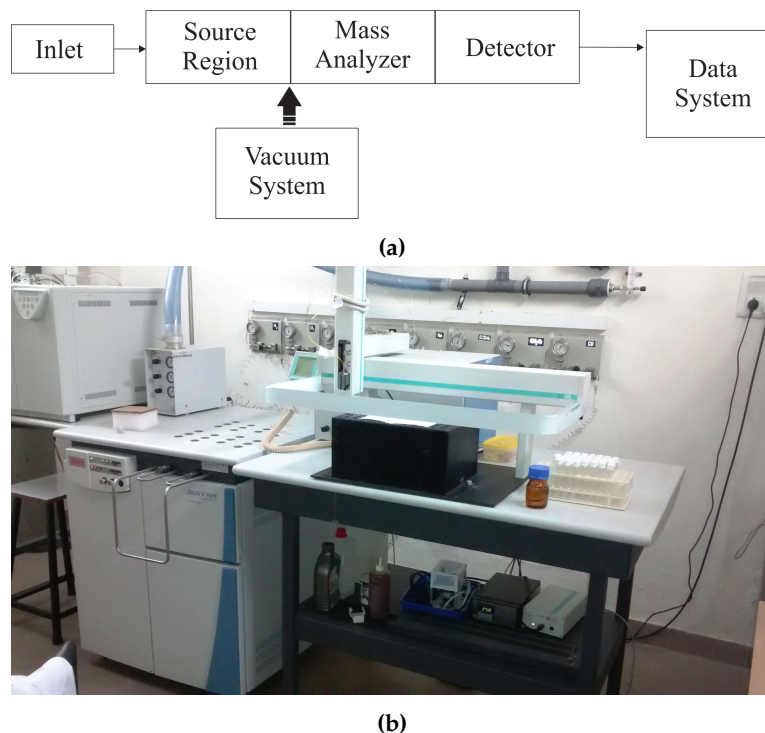


FIGURE 2.2: (a) Illustrates a simplified block diagram of a mass spectrometer and (b) shows a picture of Delta V Plus IRMS installed at IITM, Pune.

CO_2 (H_2) and 99.7% He mixture, then CO_2 (H_2) from a reference reservoir is allowed to exchange oxygen (hydrogen) isotopes with the water at constant temperature for 24 hours (3 hours). In $\text{H}_2 + \text{H}_2\text{O}$ equilibration, additional platinum catalyst pellets are kept inside the bottles to enhance the rate of the isotopic exchange between the gaseous hydrogen and water. The equilibrated CO_2 (H_2) gas is introduced into the mass spectrometer for the isotopic measurement, i.e. $\delta^{18}\text{O}$ ($\delta^2\text{H}$). The flushing and measurements were carried out in automatic mode. In the present study, a few (at least three) secondary laboratory standards with the range of isotopic values (depleted to enriched) have been used. A few secondary standards with their $\delta^{18}\text{O}$ and $\delta^2\text{H}$ with respect to VSMOW are listed in Table 2.2. A batch (3 or 4) of secondary standards was placed after every 8 to 10 samples and analyzed under identical conditions. The final $\delta^{18}\text{O}$ and $\delta^2\text{H}$ values of sample with respect to VSMOW were calculated and displayed on the interface of Isodat 3.0 software. The three point calibration method has been used to calculate the isotopic ratios of the water samples.

Liquid Water Isotope Analyzer (LWIA)

Recent advancement of optical techniques for measurement of water isotope ratio overcame some of the shortcomings of IRMS. Such as, $\delta^{18}\text{O}$ and $\delta^2\text{H}$ can be measured simultaneously, reduced time of measurement, no consumption of pure reference or carrier gases, and relatively inexpensive operation. Optical technique of isotope ratio measurements utilizes laser absorption property; the system comprises an optical

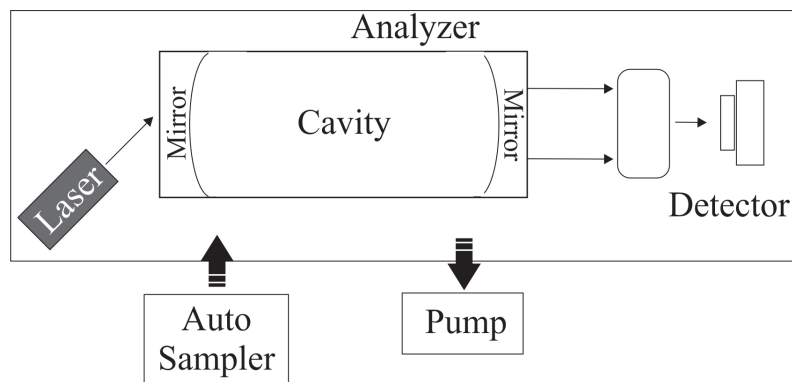
TABLE 2.2: Secondary laboratory standards used in this work. The names are coded in order to identify the source and properties of the standards, such as QD₂O - double distilled water prepared in a quartz distillation plant; En- stands for isotopically enriched water.

S.No.	Secondary Standard	$\delta^{18}\text{O}$ (‰)	δD (‰)
1.	QD ₂ O-B	-4.39	-29.30
2.	IITM-A	-2.04	-10.08
3.	IITM-En	3.71	11.03
4.	IITM-En2	7.97	26.37

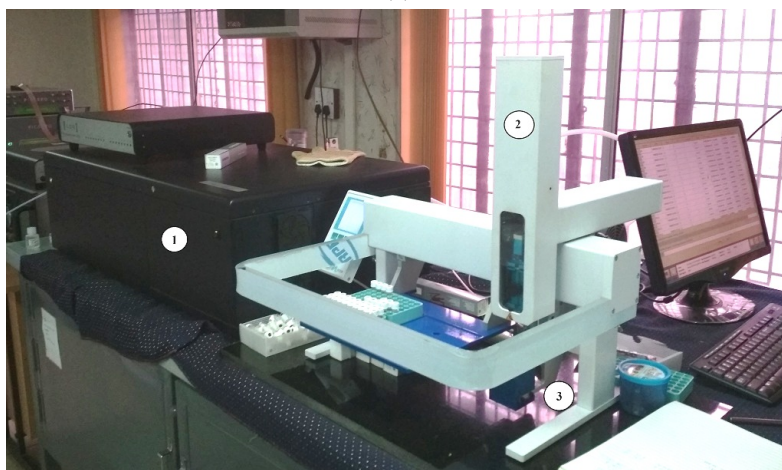
cavity with high-reflectivity mirrors (reflectance >99.9%) at both ends of the cavity. The major parts of a laser based water isotope analyzer are shown as a block diagram (Figure 2.3a). The reflectivity of the mirrors allows photons propagate for the prolonged time, in turn, making an effective absorption path length of several kilometers. The time behavior of the light intensity inside the cavity is monitored by the small fraction of light that is transmitted through the other mirror and detected by a fast photo-detector. The intensity of the light pulse inside the cavity decreases by a fixed percentage during each round trip due to absorption and scattering by the medium within the cell and reflectivity losses. The setup known as cavity ring-down spectroscopy (CRDS) used to measure time that takes for the light to decay to $1/e$ of its initial intensity called the "ring down time". It can be used to calculate the concentration of the absorbing substance in the gas mixture in the cavity.

In the present study, the LGR's patented liquid water isotope analyzer (LWIA) coupled with a liquid auto-sampler was used for simultaneous measurements of $\delta^{18}\text{O}$ and $\delta^2\text{H}$ ratios in water samples (Figure 2.3b). Measurement protocol employs an off-axis integrated cavity output spectroscopy (OA-ICOS), basically a fourth-generation CRDS technique. A major difference between CRDS and OA-ICOS is that OA-ICOS uses off-axis, non-resonant alignment of the laser beam to the cavity. It can directly measure the stable isotope ratios because of the molecular mass dependency of the individual absorption lines with a particular wavelength. That is, a single laser scan can include absorption lines assigned to several isotopologues, for example, H_2^{18}O , H_2^{17}O , and $^1\text{H}^2\text{H}^{16}\text{O}$. The working of LWIA can be described as follows: the auto-sampler is used to inject water sample from the sample tray using a $1.2\mu\text{L}$ syringe to an injector block (vaporization chamber) heated at 70°C which is connected to the analyzer. A Teflon tube is connected to transfer vaporized water sample via an installed filter at the outlet of the tube to the pre-evacuated (using pump) optical cavity.

All water samples and calibrated laboratory standards are generally kept into a 2 mL vials capped with pre sealed silicone septa. The LWIA software interface allows the user to enter sample information for analyses. The analyzer measures concentrations of the individual isotopologues of H_2O and calculates absolute ratios. Therefore,



(a)



(b)

FIGURE 2.3: (a) A block diagram representing major components of an isotopic ratio measuring optical device. (b) Shows a picture of LGR's liquid water isotope analyzer installed at IITM, Pune, 1: Analyzer; 2: Auto sampler; 3: Injector block.

to convert isotopic ratios relative to the VSMOW standard, the absolute ratios are recalculated using calibrated laboratory working standards (Table 2.2) and their ratios relative to VSMOW.

2.2 Speleothem Samples

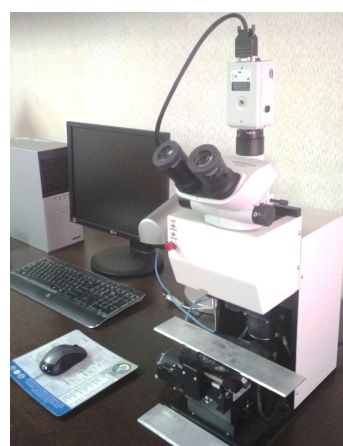
In view of the aim of the study to reconstruct the Indian monsoon, regions those come under high rainfall variability and directly influenced by the Indian monsoon were selected. Accordingly, the speleothem samples were explored from the Indian subcontinent, namely from peninsular India and Andaman Islands. With the focus on particular speleothem forms (stalactites and stalagmites, growth over the ceiling and the floor of the cave from cave drips, respectively), in the present study, stalagmites were collected to generate archives because their internal structure is simpler than stalactites (Fairchild and Baker, 2012). Details of collected stalagmite samples from the Indian subcontinent sites during the study period are reported in Table 2.3.

TABLE 2.3: Speleothem collection sites, their location and periods covered. *Analysis and results are discussed in the present thesis; other samples will be discussed elsewhere. **Age reversal and hiatus found.

S.No.	Region	Site	Location	Year	Analysis	Age (kyr BP)
1.	Andhra Pradesh	Kadapa	14.52°N 77.99°E	2013	completed*	1.72 - 3.18
2.	Andaman Islands	Baratang	12.05°N 92.70°E	2015	cutting & dating	~0.03 - 0.60
3.	Andhra Pradesh	Kadapa	14.52°N 77.99°E	2016	cutting & dating	0.05 1.70
4.	Andhra Pradesh	Kurnool	15.15°N 77.81°E	2016	cutting & dating	15.3 - 16.7** 24.7 - 50.3**



(a)



(b)

FIGURE 2.4: (a) Diamond band saw cutter (PRL, Ahmedabad) and (b) Micro-Mill (IITM, Pune)

The collected samples used to be cut from one of its cross-section using DRAMET-BS270 diamond band saws cutter (Figure 2.4a) installed at Physical Research Laboratory (PRL) in Ahmadabad, India. Further, New Wave Research Micro-Mill was used to drill at every 100-150 μ m of the speleothem sample along the growth axis, and the powered sub-samples were used for the isotopic analysis (Figure 2.4b).

2.2.1 Isotopic Analysis ($\delta^{13}\text{C}$ & $\delta^{18}\text{O}$)

For carbon and oxygen isotope compositions of carbonate (speleothem) samples, the drilled subsamples ($\sim 150 \mu\text{g}$) were loaded, capped with a new septum and then flushed with 99.999% He gas. The flushed vial was then injected with 0.2 mL of the 100% orthophosphoric acid (H_3PO_4) solution using a 1.0 mL syringe. Pure H_3PO_4 acid was prepared in the laboratory, commercially available ($\sim 98\%$) acid mixed with phosphorus pentoxide (P_2O_5) and heated at 180°C for 3 hrs and then left for overnight at 120°C . Afterwards, the prepared acid was stored immediately in the amber bottles

to reduce the chance of getting moisture and the acid density was calculated to check the purity (1.88 g/cm^3). Figure 2.5a & 2.5b shows sampling and acid addition by the author at Stable Isotope Laboratory, IITM. The H_3PO_4 reacted with CaCO_3 in the speleothem samples to produce CO_2 for a minimum of 2 hr at 72°C , followed by the isotopic analysis by the Delta V Plus IRMS. The samples were measured against three isotopic reference materials (i.e., Makrana Marble (PRL standard), NBS-18, and NBS-19), where PRL standard has $\delta^{13}\text{C} = 3.8 \pm 0.1\text{‰}$ and $\delta^{18}\text{O} = -10.6 \pm 0.2\text{‰}$ (Yadava and Ramesh, 1999). The sequence of standards and samples was similar to water analysis discussed above.



(a)



(b)

FIGURE 2.5: (a) Measurement (micro-mill) and loading of carbonate samples in the vials; (b) Acid was added manually into the loaded vials using a 1mL syringe.

2.2.2 An overview of the fieldwork

Exploring caves in a forest region, that too in India is a complicated task. Not only because of the complexity in searching and reaching out over the cave regions, but the major concern in India is the religious sentiment attached with the cave deposit by the local people, who do not easily allow entering the cave and collecting the samples. On the other hand, many of the forest regions known to harbour limestone caves are declared as Reserved Forest by the government agencies. Some other aspects one has to consider if planning for a cave expedition in India are: 1) to get permission from the competent authority to explore the region, 2) to accompany local persons who know

the area well and preferably speak the local language. Speleothems take hundreds or even thousands of years to grow in a natural environment, preserves regional as well as global climatic events. So, each cave may have its unique characteristic and provide valuable records of the past environmental changes. Reconnaissance survey reveals that several good quality speleothems are available in remote caves in peninsular India as well as in the Andaman Islands.

The state of Andhra Pradesh belonging to the Peninsular India receives 80% of its rainfall during the ISM. Regional climate is semi-arid and the major moisture comes from the Arabian Sea during the ISM. Andhra Pradesh has varied geology and is a treasure house for a wide variety of minerals (such as, gold, diamond, limestone, coal, etc). Specifically, limestone as a major mineral occurs in a few districts of Andhra Pradesh, such as Kurnool, Kadapa, Guntur, Krishna, and Anathapur. We have explored several caves in and around the Kadapa and Kurnool district during the study period. An ideal cave was found in the Kadapa region (Nakarallu cave, 14.52°N, 77.99°E) with well preserved archives potentially useful to reconstruct the past ISM variability. The cave is ideal in the perspective of its location, its neighborhood, and most importantly the cave's outside and inside environment. The cave is poorly ventilated with humidity close to 100%, a single entrance and rugged pathway as well as vertically down sections requires strenuous efforts to reach the speleothem location. After successful collection and preliminary analysis of a few stalagmite samples from Nakarallu cave in 2013, the region has been proven to be a potential site for such kind of studies. Considering the precision and high-resolution record obtained in the earlier sample, the same cave was revisited in 2016 to collect a few more samples with the aim to reconstruct the last 2000 years of record of the monsoon rainfall. To our knowledge, this cave was not explored previously for any paleoclimate studies. In the same expedition, the Valmiki cave (15.15°N, 77.81°E), Kurnool district was also explored. A few stalagmite samples were collected from the innermost section of the Valmiki cave. It is one of the deepest known caves in India with a length of 318m and depth of 77m below the surface; however, few earlier studies have reported the past records from the same cave (e.g. Lone et al., 2014). The glimpses of the fieldwork in the Andhra Pradesh region are shown in the form of pictures in Figure 2.6(a).

Andaman and Nicobar Islands of India are located between 6°N and 14°N latitudes in the northeast Indian Ocean. The region is directly influenced by the ISM rainfall as well as cyclonic activities that occur in Bay of Bengal. The major parts of the islands are untouched and less explored in perspective of natural archives. An expedition was planned and successfully executed for limestone caves exploration in the Andaman Islands in 2015. We conducted a 3-day field trip covering a major portion of the Andaman Island from north to south and found several caves. However, not many were of limestone cave and so had no speleothem. The limestone caves on

the south west side of Baratang Island are known for its carbonate deposits and stalagmites from one of these caves (known as "Baratang Cave", now open to tourist) had already been used to study the variations in the ISM (Laskar et al., 2013). However, there are many other caves in the Baratang Island (dozens, as per local information) which were never explored and hence maintained their pristine characteristics. We have collected a few samples from one such cave (12.05°N, 92.70°E), which is around 300-400 m away from the Baratang cave location. The cave has ~10 m thick bedrock and a narrow opening and extends deep inside. Unlike the Baratang cave, the inside of this cave is completely dark. A few pictures of the cave expedition are shown in Figure 2.6(b). The collected stalagmite samples from the cave were sent to IITM, Pune for processing and isotopic analysis.

(a) Kadapa, Andhra Pradesh



(b) Andaman Islands



FIGURE 2.6: Pictures showing the caves from where speleothem samples were collected for this study. (a) the Andhra Pradesh region (2013 & 2016), (b) the Andaman Islands (2015).

Chapter 3

Atmospheric controls on the rain isotopes

The chapter focuses on atmospheric factors that govern the monsoon circulation and moisture transport processes using the modern isotope geochemical observations including modern rainwater. The rainwater isotopes are regulated by rainfall events or by the moisture fluxes that is believed to influence the intraseasonal characteristics of monsoon. The Bay of Bengal (BoB) region is a major moisture contributor to the Indian mainland, and Indian summer monsoon rainfall distribution is linked to the variation of the convection over the BoB. Here, for the first time, the BoB rainwater isotopes linkage with the monsoon intraseasonal oscillations (MISOs) is shown, successively, correlation of rainwater isotopes with rainfall amount during monsoon active and break phases is investigated. Further, it discusses the nature of the amount effect over BoB and if it is association with MISOs. The chapter also presents a systematic study of temporal and spatial variations in the amount effect using observation, GNIP, and model data. This chapter aims to answer objectives 1 and 2.

3.1 Introduction

Moisture generation and transportation is an important aspect of the hydrological cycle; this is especially important in the context of Indian monsoon as the agricultural and economic activities of the country significantly depend on summer monsoon rainfall. A large part of the Indian Ocean including the northern Indian Ocean produces and exports major amount of moistures to the Indian subcontinent that contributes most of the rainfall during the summer seasons. Knowledge of moisture transport processes is essential in order to understand the monsoon variability. Therefore, the dynamical behaviour of moisture namely, its genesis in the Indian Ocean and transport pathways to the Indian continent has been studied by several investigators (e.g., Findlater, 1969a; Krishnamurti and Bhalme, 1976).

Figure 3.1 shows the climatological moisture convergence (specific humidity \times wind) at 850 mbar for the (a) summer monsoon (May to September) and (b) the non-monsoon or winter monsoon (November to March) seasons over the South Asian region. It is

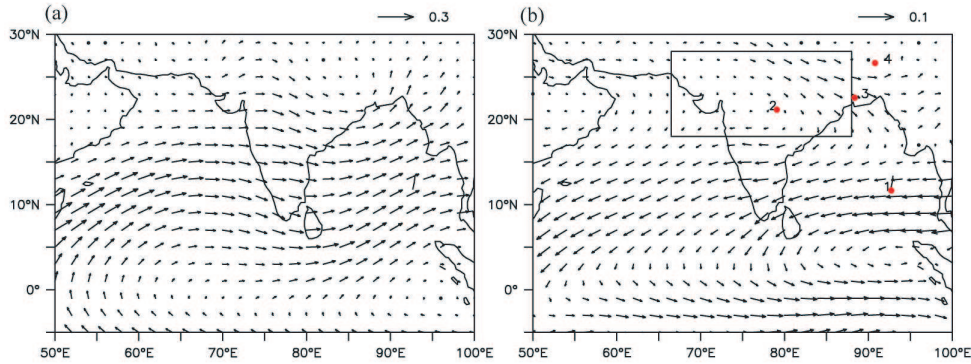


FIGURE 3.1: (a) Climatological mean (2006-2015) of the moisture transport at 850mb level for the months of May to September and (b) similarly, November to March. The box region in the right panel depicts the Core Monsoon Zone of India; the sampling sites are shown as circles, 1. Port Blair, 2. Nagpur, 3. Kolkata, 4. Tezpur.

evident from this figure that major moisture flow during the summer months to the Indian landmass is sustained by a strong south-westerly circulation. However, the moisture content of the Arabian Sea branch is progressively reduced due to rainout process as it reaches the middle of the Peninsular India (Bavadekar and Mooley, 1981). As the moist air from the Arabian Sea enters the Indian coast, it is orographically up-lifted by the Western Ghats mountain range and produces heavy rain. Thus, the relatively dry air is recharged with moisture derived from BoB and moves to eastern India and northern Indo-Gangetic plain following the wind pattern shown in Figure 3.1(a). On the other hand, Figure 3.1(b) shows no such strong circulation from the BoB to the Indian landmass, particularly over the core monsoon zone (rectangular box) during the winter season. The BoB, an integral component of the Indian Ocean contributes a significant amount of moistures amounting to precipitation over the central Indian region, in the eastern parts of India and the neighboring countries. Despite being a significant moisture source the knowledge of the BoB branch of moisture transport to the Indian continent remained poorly documented relative to Arabian Sea moisture transport processes. Therefore, a pertinent and important assignment regarding seasonal mean rainfall over central India is the partitioning of moisture source from the Arabian Sea and BoB. The BoB strongly responds to monsoon intraseasonal variability (see Box 3.1) and it is believed that the bay plays a crucial role in driving/modulating this process. Its subsurface salinity and temperature structure often display distinct variability signatures within the season (Sengupta and Ravichandran, 2001). It is hypothesized that the air-sea fluxes of moisture and momentum influence the intraseasonal variability/oscillation (ISO) of the monsoon atmosphere (Krishnamurti and Bhalme, 1976). During the ISO propagation growth of rainfall takes place in the northwest, while it decays in the southeast direction across the Bay of Bengal (Sengupta and Ravichandran, 2001).

Box 3.1**Monsoon Intra Seasonal Oscillation**

The Indian summer monsoon (ISM) rainfall is characterised with the active and break spells within the monsoon season (Ramamurthi, 1969) governed by northward propagating summer monsoon intraseasonal oscillation (MISO, Yasunari, 1979; Yasunari, 1980; Goswami and Ajaya, 2001). The MISOs represent a broadband spectrum with periods between 10 and 90 days but have two preferred bands of periods (Krishnamurti and Bhalme, 1976; Yasunari, 1980), one between 10 and 20 days and the other between 30 and 60 days. The MISO modulates the frequency of occurrence of the low pressure system (LPS) with 4-5 times more number of LPS occurring during the active phases compared to the break phases (Goswami and Xavier, 2005). Thus, the contribution of BoB moisture to the monsoon precipitation is likely to be modulated strongly on intraseasonal time scales. Monsoon precipitation over the Core Monsoon Zone (CMZ) (Rajeevan et al., 2008) arises from the convergence of moisture partly coming directly from the Arabian Sea and partly coming from the BoB. However, the northward propagating monsoon intraseasonal oscillations (MISO) contributes significantly to the seasonal mean rainfall (Goswami, 2006). The anomalous winds associated with the active (break) spells strengthen (weaken) the climatological moisture transports (see Figure 3.1) and thereby increase or decrease the contribution of BoB moisture to the rainfall over CMZ. Therefore, characterization of sources and transport of BoB moisture to the core monsoon zone on intraseasonal time scale is critical in understanding the seasonal mean monsoon as well as monsoon intraseasonal variability.

3.1.1 Moisture Source Identification

Identifying source or sinks of atmospheric moistures are done mainly by numerical means, such as model calculation, and numerical water tracer analysis (Velde et al., 2010; Gimeno et al., 2012). Some early studies estimated the moisture flux from the Indian Ocean to India. For example, vapor flux was calculated by Pisharoty (1965), Findlater (1969b), and Saha (1970) and other climate researchers. Dewan and authors (1984) measured the flux of air and moisture over the BoB during the summer season. Cadet and Greco (1987) determined the cross equatorial vapor flux to India and observed that the flux was maximum for a longitudinal range of 50°E - 65°E (the western Arabian Sea), but its characteristics were very different for 65°E - 95°E (the eastern Arabian Sea and the BoB). These studies, however, are based on limited data and hence lack statistical significance. Ordóñez et al. (2012) made a detailed investigation of the origin of the atmospheric water arriving in the western and southern parts

of India (during 2000-2004) using a Lagrangian diagnostic technique. While these authors focused their attention mainly to the Indian Ocean and the Arabian Sea, they also identified a BoB vapor source to the above mentioned study region. The method is based on tracking atmospheric moisture along trajectories calculated using the Lagrangian particle dispersion model FLEXPART (Stohl et al., 1998) driven by meteorological analysis data from the European Centre for Medium-Range Weather Forecasts (ECMWF, White, 2002). The limitations of the method arise from errors in particle tracking and can be found in the studies of Stohl and James (2004), Stohl and James (2005). On the daily time scale significant errors in moisture source can arise from particle tracking errors resulting from drying and moistening due to the convective parameterization scheme used in the ECMWF model.

Rain Isotope Implementation

A third approach is the physical tracer analysis, that is, the study of stable isotopes in precipitation which is considered a reliable means in obtaining source related information (Pfahl and Wernli, 2009). Recently isotope based studies provided evidence of BoB vapor reaching the eastern and north-eastern regions of India. For example, it is shown that the BoB vapor enters India through Kolkata and the vapor source to Kolkata remains invariant throughout the year (Sengupta and Sarkar, 2006). Breitenbach et al. (2010) demonstrated that north east India receives moisture from the Arabian Sea as well as from the BoB during the monsoon season but post monsoon moisture mainly comes from the BoB. Gupta and authors (2005) investigated the isotopic composition of shallow ground water and river water from the Central Indian Peninsular region and concluded that the eastern part of the region received significant vapor flux from the BoB. Modification of the isotopic signature of the vapor mass originated in the Arabian Sea during its transit due to the addition of evaporated moisture from the BoB prior to their arrival at Kolkata; in eastern India has been reported (Dar and Ghosh, 2017).

However, despite it being a powerful tool there are some issues, such as, the relationship between water isotope signature and precipitation sources need to be addressed as the isotope fractionation during air-mass transport may alter source signature (Sodemann et al., 2008). As the basic premise of identifying the BoB derived rainfall is its depleted isotopic values relative to that of the rainfall originated through the Arabian Sea moisture. But the isotopic depletion in rainfall may also be caused by other processes, such as organized convection. Lekshmy et al. (2014) demonstrated that rainwater at the Kerala coast underwent systematic depletions due to large scale convection. Hence the isotopic analysis of rainfall at a given place may not provide sufficient information in identifying the moisture source. The identification of moisture sources consists of an important aspect of the hydrological study which can address issues like understanding the monsoon variability, water security, managing and mitigating the extreme rainfall events caused by tropical cyclone etc. In this regard, it is crucial to improve our understanding of how moisture sources affect rain

isotopes, which will also be helpful in interpreting the paleoclimatic archives, such as tree rings, ice cores, cave deposits etc. (Gimeno et al., 2012).

To study the nature of the rainwater isotopes in the BoB region and how they are controlled by the ocean-atmosphere variability, measurements of isotopes of rainwater on a network of stations on a daily timescale are investigated. With an aim to understand the spatial pattern of rainfall in relation to isotopic variability, large scale convection controls on rain isotopes, etc. Further, the chapter discusses the atmospheric factors that control the moisture transport processes from the BoB to the Indian mainland and BoB precipitation isotopes linkage with the monsoon active and break phases, in turn, with the MISOs. The last section focuses on the nature of the amount effect and if it is controlled by the intra seasonal variability of monsoon.

3.1.2 Rationale for selecting the BoB region

The BoB possesses certain unique characteristics which are believed to play an important role in moisture generation and transport process. Firstly, it maintains a relatively high sea surface temperature (SST) especially during the monsoon season than the rest of the Indian Ocean (Shenoi et al., 2002) which often exceeds 28°C, being the threshold for deep convection. The northern BoB is also characterized by genesis of low pressure systems (LPS) which often move westward over India that cause heavy rainfall over central and northern India (Sikka, 1977; Goswami, 1987; Mooley and Shukla, 1989). For the continuous observation and study over the BoB region, the Andaman Islands (namely, Port Blair) have been chosen. The Andaman Islands is a group of island strategically located in BoB as far as monsoon circulation is concerned. Being an island and with a large forest cover (~92%) the secondary source of moisture (i.e. soil moisture) is expected to be low and hence the isotopic study of its rainwater is likely to provide valuable input in understanding the moisture dynamical processes. To our knowledge no systematic study of isotopic analysis of rainwater in this region was available prior to the work, except a short time series (25 May - 31 July, 2010) of $\delta^{18}\text{O}$ of Port Blair rain by Laskar et al. (2011). Therefore, the characteristics behavior of rainwater isotopes largely remains unknown, especially on short time scales.

3.2 Strategy for the sampling

The study argues that the collection and isotopic analysis of rainwater simultaneously in the moisture source area (BoB) and at the target area (Indian mainland) would provide better information of moisture transport. Therefore, the daily rainfall sampling in Port Blair, the Andaman Islands is considered as representative of the BoB (the source area). The core monsoon zone (CMZ) in Indian mainland is considered as the target area (e.g., Nagpur) of the BoB moisture. Using a comparative study of isotopic variations supported by wind trajectory visualization, it is proposed that BoB moisture indeed reaches the central Indian region. To test this hypothesis, we consider two

more sites, namely Kolkata in east India and Tezpur in northeast India. Kolkata is located at the edge of CMZ and Tezpur is outside this zone, but is known to receive a significant amount of moisture from BoB. Figure 3.1(b) shows the rain collection sites and boxed region in this map represents CMZ as defined in Rajeevan et al. (2010). The rainwater isotopic records of the Port Blair site (11.67°N, 92.73°E) for the years 2012 to 2015 are presented. For the target sites, namely Nagpur (21.15°N, 79.09°E), Kolkata (22.56°N, 88.36°E) and Tezpur (26.63°N, 92.80°E), daily rainwater samples have been collected only for the year 2015. Isotopic analysis has been performed on collected daily rainwater samples from all the sites.

An auxiliary effort to study the rain-vapor interaction

The isotopic variations on daily to seasonal timescales in vapor and rain phases can be used to diagnose different moisture sources, especially the influences of the large monsoon systems and convection (Yu et al., 2015). Theoretical studies predicted that isotopic exchange between raindrops and water vapor could be significant, which necessitates quantification of this process causing isotopic fractionation in rainwater, preferably in a field based observational framework. This information is also important to estimate the extent of isotopic fractionation in rainwater subjected to intense cyclonic activities (Lawrence and Gedzelman, 1996) and for a better understanding of the elusive nature of the amount effect (Dansgaard, 1964). A field based observational strategy would require synchronous analysis of ground level vapor and rainwater preferably in a site that experiences high humidity throughout the monsoon season. High humidity will help achieve near equilibration of rainwater and ambient vapor and impart a negligible effect of raindrop evaporation. Secondly, if the moisture is sourced primarily from an open ocean but negligible amount from evapotranspiration, then it will provide an additional constraint to this exercise. With these considerations, a specific field campaign to collect ground level vapor was arranged in Port Blair during the summer of 2015. The isotope study of vapor and rainwater in this site is likely to provide valuable insight in understanding their interaction vis-à-vis source and ambient vapor control on the variations in isotopic composition of regional rainfall.

3.3 Data and Methods

3.3.1 Rainfall Data

The rain gauge data of Indian Meteorological Department (IMD) station was provided by the National Data Center (www.imdpune.gov.in/ndc_new/ndc_index.html), IMD, Pune. The data consists of rainfall averaged over 24 hours at 0830hr. Daily gridded rainfall data of the Tropical Rain Measuring Mission (TRMM 3b42 v2; 0.25×0.25 ; Huffman et al. 2007) was used to investigate the response of rainwater $\delta^{18}\text{O}$ to rainfall

over a wider spatial scale. The rainfall data ($1^\circ \times 1^\circ$) from Global Precipitation Climatology Project (GPCP, (Adler et al., 2003)) was also used in the study.

3.3.2 Other Meteorological Data, Methods and Analysis Used

The other data includes temperature, pressure, wind, sea surface temperature, relative humidity, and specific humidity from National Center for Environmental Prediction (NCEP) reanalysis data (Kalnay et al., 1996) and Era-Interim (Dee et al., 2011). The description of data periods, pressure levels, and regions considered for the particular analyses are mentioned in respective sections.

OLR analysis

Kalpana-1 VHRR (Mahakur et al., 2013) outgoing longwave radiation (OLR) data were used to quantify the convective activities and to visualize its propagation. The time latitude (longitude) Hovmöller diagram was plotted for daily OLR anomaly averaged over specified areas to reveal the northward (westward) propagation of the convection band. Other meteorological data, information on low pressure systems etc were provided by the National Data Center and Weather Section of the Indian Meteorological Department, Pune, India. To monitor the convective activities, OLR (Outgoing Longwave Radiation) anomaly was calculated on pentad scale using a web-tool (<http://iridl.ldeo.columbia.edu/>).

Trajectory analysis

Forward/backward trajectories analyses were performed using the NOAA Hybrid Single-particle Lagrangian Integrated Trajectory (HYSPLIT) model (Stein et al., 2015) in order to predict the moisture pathways and transport travel time from a source region. The data, run time, pressure levels, etc are reported in the respective sections.

Spectral analysis

Since rainfall and hence its $\delta^{18}\text{O}$ data is not available on a daily basis, the method which account the presence of missing values were used for the spectral analysis, such as Lomb-Scargle periodogram (Lomb, 1976; Scargle, 1982). This method is a well-known algorithm for detecting and characterizing periodic signals in unevenly-sampled data. A MATLAB code² has been applied on uneven rainwater isotope data. The function "plomb" computes the spectral power as a function of frequency of a time series which are not necessarily evenly spaced. The routine will calculate the spectral power for an increasing sequence of frequencies up to highest frequency times the average Nyquist frequency, with an oversampling factor of typically $>=$

²<https://in.mathworks.com/matlabcentral/fileexchange/20004-lomb-lomb-scargle-periodogram>

4 (Appendix A.1). Further, to examine the spectral characteristics of the rain isotopic data, FFT was performed on the interpolated rainwater $\delta^{18}\text{O}$ time series using the open software NCAR Command Language (NCL) (<http://dx.doi.org/10.5065/D6WD3XH5>). So, the gaps in $\delta^{18}\text{O}$ of rainwater were estimated by interpolating the original $\delta^{18}\text{O}$ time series using the cubic spline interpolation scheme. The interpolated values were constrained by maintaining the slope and intercept of the post-interpolated local meteoric line (LML) the same as those of the pre-interpolated LML within the limits of uncertainty level. Additionally, the correlation coefficient of the $\delta^{18}\text{O}$ vs. $\delta^2\text{H}$ regression line after interpolation was maintained similar to that of the $\delta^{18}\text{O}$ - $\delta^2\text{H}$ regression line of the original data (i.e., before interpolation). In this context, it is to be noted that the interpolated isotopic values (for non-rainy days), which are nothing but ratios of two numbers, may not be physically viable. However, it has been found that the interpolated values could be reliably used if the number of interpolations is small. Towards this, here we present an indirect proof by estimating the spectral properties of the isotopic values of ground level vapors. Interpolation of vapor isotope data does not suffer from the same problem as the rain isotope, since vapor is always present in the atmosphere. Hence missing values of vapor isotope data, which was not available due to logistic reason, could reliably be interpolated and a continuous record generated. On the other hand, since the isotopic record of rainfall in the Andaman region, primarily reflects the isotopic composition of moisture rather than the individual rain events, the spectral behaviour of $\delta^{18}\text{O}$ of moisture is expected to be manifested in rain isotopes as well. With this consideration, we collected vapor samples and produced a near continuous vapor isotopic record.

3.4 Results and Discussion

This section is divided in four subsections, first discusses the atmospheric controls on the rainwater isotopes, considering moisture dynamics, convective activities, monsoon intraseasonal variability (Section 3.4.1). Under the background of the results from first, the second section focuses on moisture transport processes between BoB and Indian mainland by means of isotopic analysis of rainwater at the moisture source and receiver sites (Section 3.4.2). The third section is describing an attempt to quantify the effect of rain-vapor interaction on isotopic composition of atmospheric vapor and rainfall (Section 3.4.3). The last section is about the observed variability in amount effect over the Indian subcontinent using observation (namely Port Blair, Nagpur, Kolkata, and Tezpur), GNIP (New Delhi, Hyderabad, Bombay, etc.) and IsoGSM2.0 model spatial data (Section 3.4.4).

3.4.1 Atmospheric controls on the rain isotopes

Large parts of this section are published in

Chakraborty, S., Nitesh Sinha, R. Chattopadhyay, S. Sengupta, PM Mohan, A. Datye (2016). Atmospheric controls on the precipitation isotopes over the Andaman Islands, Bay of Bengal. Sci. Rep., 6, 19555; <https://doi.org/10.1038/srep19555>.

The isotopic analysis of Port Blair rainwater samples carried out for the year 2012 and 2013 in order to study the atmospheric controls on isotopic variations. Figure 3.2 displays the oxygen isotope time series for the year 2012 (upper panel) and 2013 (lower panel). The typical values of minima and maxima of $\delta^{18}\text{O}$ ($\delta^2\text{H}$) are approximately -7 and 0‰; (-50 and +6‰, relative to VSMOW) for the year 2012. The winter season is represented only by a few samples hence its isotopic characteristics may not be generalized. The monsoon onset in the Andaman area usually takes place on 20th May (Joseph et al., 1994), though pre-monsoon showers start in early May. The oxygen isotopic values during the early season had a narrow range (-1 to -4‰) with occasional depletions until late August. Henceforth, high depletion was observed which continued till the first week of September. The $\delta^{18}\text{O}$ became less than -6‰ and $\delta^2\text{H}$ recorded below -40‰. The low values persisted for several days and in the middle of September the $\delta^{18}\text{O}$ again increased but remained somewhat lower than the mean value registered in the months of May to July.

The year 2013 showed somewhat different behavior. Unlike 2012 the May-June isotopic record in 2013 does not show any depletion, rather pulses of positive values were observed in the month of June. Depleted isotopic values began to occur in July and like 2012 the September 2013 rainfall also showed significant negative excursion. In this year the $\delta^{18}\text{O}$ had a little higher amplitude (0 to -8‰) compared to 2012. In both the year the early monsoon (May) showed a mean $\delta^{18}\text{O}$ ca. -2 to -3‰. These are the typical values observed in tropical islands (Araguás-Araguás et al., 2000). But the isotopic values could be modulated by large scale processes, such as organized convection associated with the monsoonal intra-seasonal oscillation (Kurita et al., 2011). Additionally low pressure systems can significantly reduce the rain water isotopic compositions (Lawrence et al., 2004).

The local meteoric water lines for the years 2012 and 2013 are given below.

$$\delta^2\text{H} = (6.92 \pm 0.19) \times \delta^{18}\text{O} + (9.14 \pm 0.84); R^2 = 0.93, n = 90 - > 2012 \quad (3.1)$$

$$\delta^2\text{H} = (7.01 \pm 0.12) \times \delta^{18}\text{O} + (5.82 \pm 0.55); R^2 = 0.97, n = 94 - > 2013 \quad (3.2)$$

Both the slope and the intercept are lower than that of the global meteoric water line (8 and 10 respectively). The calculated slope for a temperature range of 24°C to 30°C (typical temperature range for Port Blair) is 8.2 - 8.6 considering equilibrium fractionation factor between vapor and the condensate. Observed slope being close to

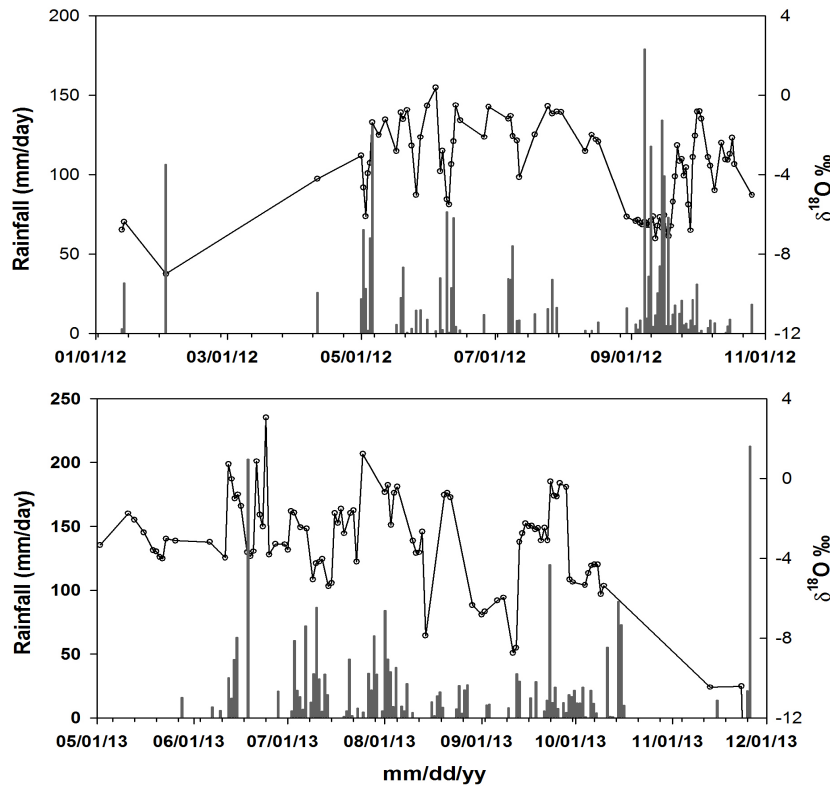


FIGURE 3.2: The daily precipitation record of the IMD weather station, Port Blair (gray bar). Black line represents $\delta^{18}\text{O}$ time series of Port Blair rainwater. The upper panel represents the year 2012 and lower panel for 2013. An inverse correlation between rainfall and $\delta^{18}\text{O}$ record is apparent for 2012.

7 indicates kinetically controlled fractionation, to some extent, is involved during the vapor formation. The slope remains the same within the limits of uncertainty level for both the year 2012 and 2013 asserting that overall (time averaged) kinetic effect, more or less, remained the same. But the intercept differed considerably in 2012 and 2013, representing a variable vapor source and/or a varying degree of recycled moisture contributing significant amount of rainfall in this region.

Deuterium Excess

The deuterium excess (*d-excess*) ranges from 4‰ to 25‰ and -12‰ to 18‰ in years 2012 and 2013 respectively. Figure 3.3(a) and (b) show the *d-excess* anomaly for the respective years. The winter/spring and pre-monsoon times are characterized by positive anomaly while the monsoon season typically shows negative anomaly. However, the September month in both the year is characterized by positive anomaly when the precipitation isotopes suffered from high depletion. On the other hand positive anomaly was observed during the month of November 2013, when severe cyclonic activities were reported. One important aspect is that positive *d-excess* anomalies are usually

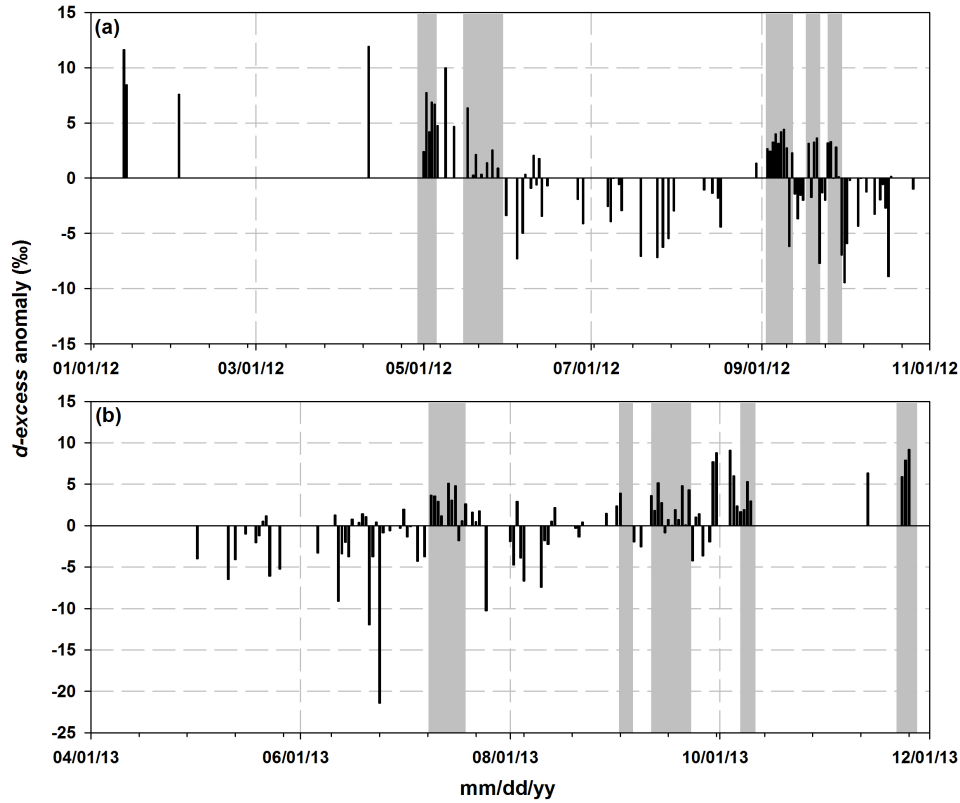


FIGURE 3.3: d-excess anomaly plots: (a) Upper panel for the year 2012 shows distinct seasonality; positive anomaly occurs mainly during the winter/spring and negative anomaly during the summer season. (b) Lower panel is for the year 2013, which also shows mainly negative anomaly during the summer season. But both the years show positive anomaly during the month of September when the delta values show anomalous depletion. Positive anomaly during November 2013 coincided with the heavy cyclonic activities. Orange lines represent $\pm 1\sigma$ variability.

associated with large scale organized convection during the summer monsoon season. The shaded regions in the above mentioned diagrams represent the convective activities (based on pentad OLR anomaly) wherein d-excess displayed higher values.

The seasonal variations of d-excess could be explained by means of moisture source. Firstly we categorized d-excess data in two sets. For this purpose d-excess has been normalized by subtracting the mean value from the individual values and then dividing by its standard deviation. The first (second) data set consists of normalized d-excess < 1 ($> +1$). These two data sets yield two sets of dates in which normalized d-excess is either < 1 or $> +1$. These two sets of dates have been shown in Table 3.1. Moisture flux vector was calculated over an area ($10^{\circ}\text{S} - 45^{\circ}\text{N}$, $40^{\circ}\text{E} - 140^{\circ}\text{E}$) for the corresponding sets of dates yielding (normalized) d-excess < 1 and $> +1$ respectively.

Figure 3.4, clearly shows strong (weak) moisture flux in the case of normalized d-excess < 1 ($> +1$). To demonstrate further we have taken three subsets of arbitrary

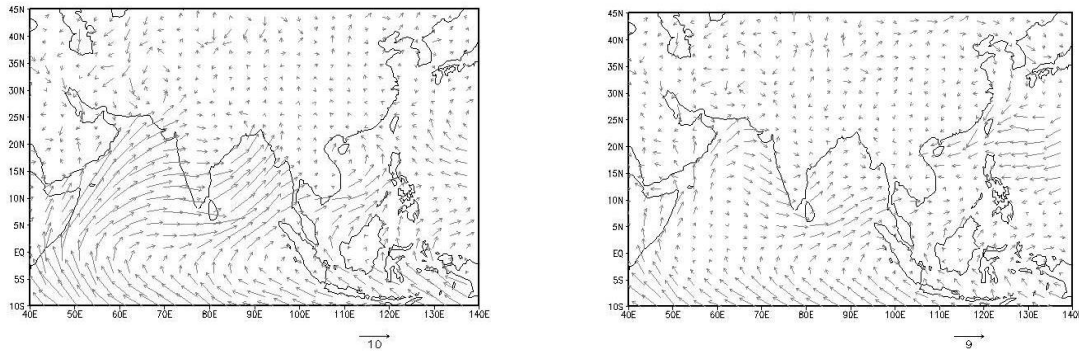


FIGURE 3.4: Calculation of moisture convergence over an area (10°S - 45°N ; 40°E - 140°E). The dates for the two cases have been estimated based on the (normalized) d-excess anomaly < 1 (left panel) and > 1 (right panel).

dates (04/06/2012, 25/07/2013, 10/08/2013) belonging to monsoon (i.e. d-excess < 1) and three non-monsoon dates (viz. 13/01/2012, 11/04/2012, 23/11/2013) (i.e., d-excess $> +1$). 98hr back trajectories using the HYSPLIT model have been calculated on these dates to trace the moisture source (Appendix A.2). Figure A.2 clearly shows that in case of the first (second) set, which is characterized by d-excess < 1 ($> +1$) moisture was mainly sourced from the equatorial Indian Ocean (continental/non-Indian Ocean) region. This demonstrates that low d-excess values typically seen during the monsoon season arise due to moistures coming from the equatorial area across the Indian Ocean. But the moistures during non-monsoon time are characterized by higher d-excess and usually originate in continental and/or non-Indian Ocean region.

On monthly time scale d-excess also shows some variability. The positive d-excess anomaly in early May is due to a deep convection originating over a wide area in south Bay of Bengal including the Andaman Islands as shown in pentad OLR anomaly for May 1-5, 2012 (Figure 3.5a); 24hr back trajectory analysis reveals that moisture was sourced from the neighboring oceanic region, ca. 9°N , 89°E (Figure A.2 (a)) which produced high d-excess rain in Port Blair. Similarly the positive anomalies observed during the later part of May-2012, and July-2013 are also due to varying degree of convective activities as revealed in pentad OLR anomalies (Figure 3.5b). Recycling of water vapor within the convective cell makes the rainfall low in isotopic values but high in d-excess results in inverse correlation between these two parameters (Lawrence et al., 2004). Such kind of correlation between OLR and d-excess has also been reported for the tropical regions (Risi et al., 2008). On the other hand non-convective processes cause lower d-excess in precipitation. The negative d-excess anomaly of summer precipitation suggests that the humidity of the ocean surface is relatively higher than the average relative humidity (RH) of 81% observed in tropical region (Feng et al., 2009) and secondly the major moisture source is the remote oceans (Xie et al., 2011). This is corroborated by 98 hrs back trajectory to the sampling site derived from Hysplit model which shows (Figure A.2 (b)) that the moisture source

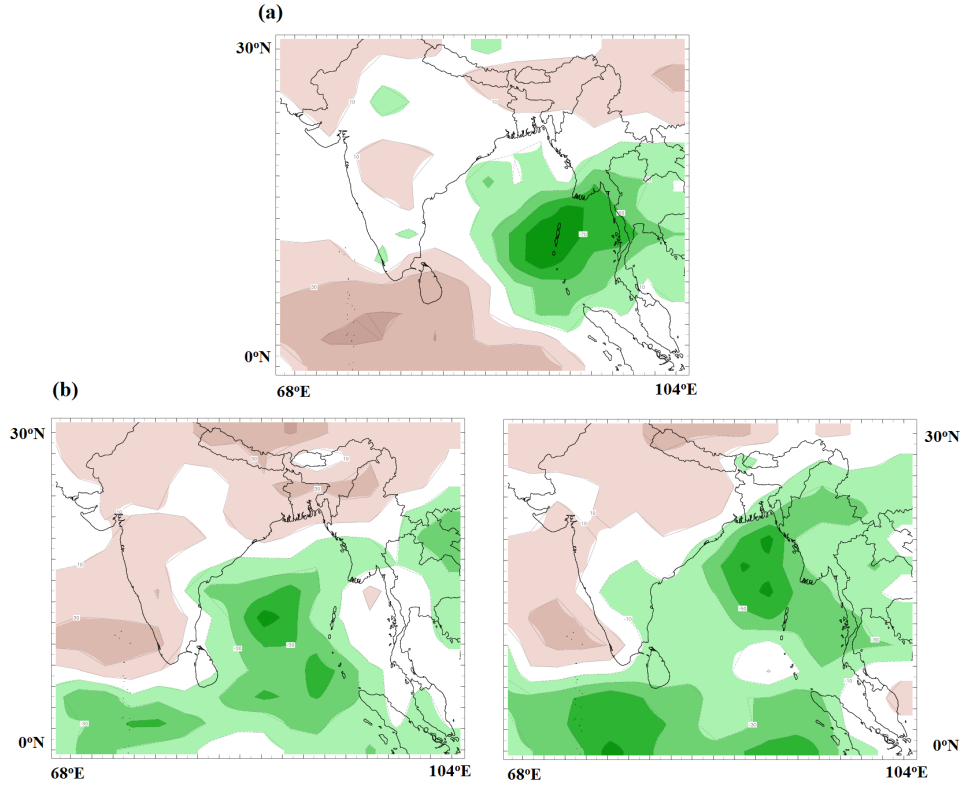


FIGURE 3.5: (a) Pentad OLR anomaly for 1-5 May 2012 showing deep convection in the north Indian Ocean region. (b) Pentad OLR anomaly for 21-25 May (left) and 26-30 May 2012 (right). Map was created using a web-tool (<http://iridl.ldeo.columbia.edu/>). Green represents negative anomaly.

was mainly confined to the equatorial Indian Ocean during the JJAS season.

The relation between RH and d-excess has also been used to assess the effect of RH on rainwater evaporation as raindrop evaporation results an inverse correlation between $\delta^{18}\text{O}$ and d-excess (Gat, 1996). We have observed strong correlation between $\delta^{18}\text{O}$ (i.e., non-interpolated) and d-excess in early monsoon, $r^2 = 0.35$, $n = 10$; $p = 0.1$ and $r^2 = 0.78$; $n = 17$; $p = 0.001$ in June 2012 and 2013 respectively, for the Port Blair. Though the RH during the early monsoon (May-June) remains relatively lower than the later part of monsoon (in 2012; Figure A.3, upper panel).

However, the lack of similar behavior for the year 2013 (Figure A.3, lower panel) indicates that consideration of humidity alone may not fully explain the observed relation between $\delta^{18}\text{O}$ and d-excess. The early phase of monsoon is characterized by strong change in circulation pattern. For example, in 2012 wind speed shows sharp rise from about 6 ms^{-1} in mid May to more than 19 ms^{-1} in mid June. In the year 2013 the wind speed ranges from $< 6 \text{ ms}^{-1}$ to about 17 ms^{-1} (mid May to 3rd week of June). Since strong wind favors raindrop evaporation, $\delta^{18}\text{O}$ – d-excess show strong inverse correlation in early monsoon. After the middle of June wind speed shows a gentle decreasing trend in both the years. It may also be noted that in the early phase of monsoon, wind speed and RH nearly co-vary but after June their variations

TABLE 3.1: the table shows two sets of dates in which normalized d-excess < -1 (left column) and normalized d-excess $> +1$ (right column), based on which moisture convergence has been calculated and plotted in Figure 3.4

Normalized d-excess (< -1)	Normalized d-excess ($> +1$)
1, May 2012	13, 14, Jan 2012
4, 6, Jun 2012	2, Feb 2012
19, 25, 27, 29, Jul 2012	11, Apr 2012
11, 22, 30, Sept 2012	2, 4, 5, 9, 17, May 2012
1, 2, 17, Oct 2012	14, 16, July 2013
11, 23, 26, May 2013	13, 20, 29, 30, Sept 2013
12, 21, 24, Jun 2013	4, 5, 9, Oct 2013
25, Jul 2013	13, 23, 25, Nov 2013
2, 5, 10, Aug 2013	–

are somewhat out of phase (Figure A.3). This means, relatively higher humidity and lower wind strength after June result in weak $\delta^{18}\text{O}$ - d-excess correlation, as is evidenced from the r^2 value which reduces to about 0.18 in September (in both years).

Apart from $\delta^{18}\text{O}$ – d-excess, we have also observed a modest correlation between d-excess and RH. A strong positive correlation between these two parameters emerges when raindrops evaporate significantly (Landais et al., 2010). For the months of May to July, r^2 for RH vs. d-excess linear fit is 0.2. With the progress of monsoon the environmental conditions change (relatively higher RH and lower wind speed) the relation between d-excess and RH weakens. The above observations imply re-evaporation of raindrops, to some extent is present especially during the early to mid monsoon season, which also contributes to amount effect (Dansgaard, 1964). This is also consistent with our earlier observation that the evaporated vapor (hence low in $\delta^{18}\text{O}$) is fed into the convective system and gets influenced by earlier convective events (Risi et al., 2008), which essentially causes amount effect operating efficiently within a time frame of 18 - 27 days.

As mentioned earlier due to the changes in environmental conditions (determined mainly by RH and wind speed) during the later phase of monsoon the correlation between d-excess and RH weakens. For the month of September the correlation nearly vanishes ($r^2 = 0.0002$, $n = 25$). Such kind of situation may be responsible in producing high and persistent depletion of isotopic records, observed more or less in both the years during September (Figure 3.2) resulting an amount effect that could be explained by the hypothesis proposed by Moore et al. (2013). According to these authors when precipitation exceeds evaporation in a given region that is convectively active, amount effect is largely a result of isotopically depleted vapor converging in the lower and middle troposphere with smaller contributions from surface evaporation. Bay of

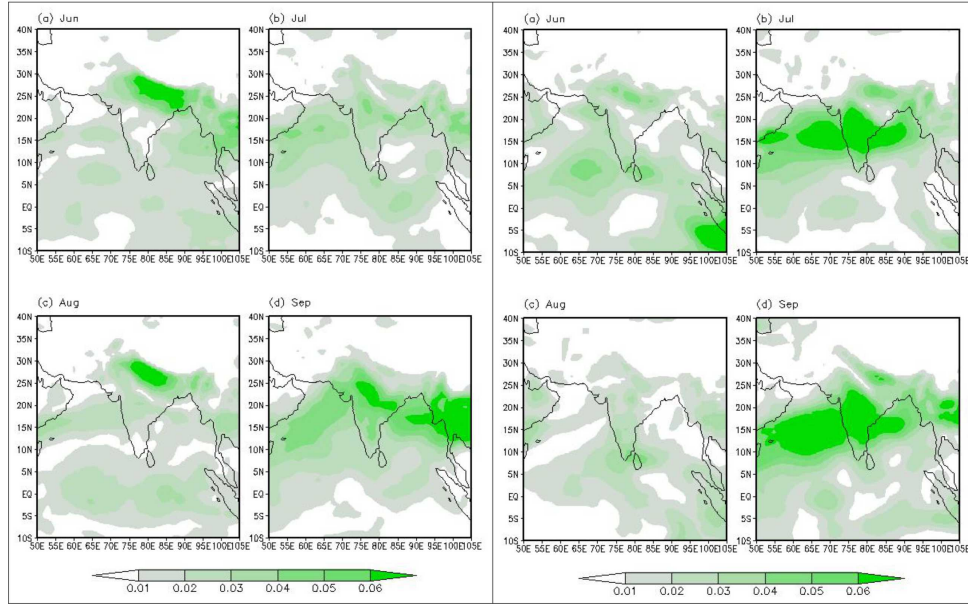


FIGURE 3.6: Moisture convergences calculated using zonal and meridional wind. The figure shows the anomaly relative to the JJAS mean for (i) the year 2012 and (ii) 2013 respectively.

Bengal in general is characterized by $P/E > 1$ during the monsoon season (Shenoi et al., 2002), which is more pronounced in September in the studied years. We have estimated the moisture convergence ($Q = (q_u, q_v)$, where q is the specific humidity (g kg^{-1}) and u, v being the zonal and meridional wind vector (ms^{-1}) for the JJAS season.

Figure 3.6 show the anomaly (relative to the JJAS mean for each year) for the individual months showing the relative difference of moisture convergence during the monsoon season of 2012 and 2013 respectively. As evident from these figures that the northern Bay of Bengal experienced higher moisture convergence during September, asserting the Moore et al. (2013) hypothesis. 98 hours back trajectory calculations also show that moistures were originated mainly in the equatorial Indian Ocean region during September in both the years. However, the Figure 3.6 (right panel) also shows significant amount of moisture convergence during July 2013, implying that this month also experienced similar characteristics as September. The $\delta^{18}\text{O}$ time series (Figure 3.2) for 2013 indeed shows such kind of behavior, which is very similar $\delta^{18}\text{O}$ pattern in these two months albeit with reduced amplitude in July 2013. Like September 2013, positive d-excess anomaly in July 2013 also provides supportive evidence.

Isotopic variability of the low pressure systems

The tropical cyclones (TC) are known to produce most depleted isotopic values. A qualitative isotopic analysis is presented on cyclones that occurred during the later part of the year 2013. In the first week of October 2013, a low pressure system originated east of the Andaman Island. This caused heavy rainfall: 55 mm on 4th Oct at Port Blair. The following three days there was little rain but heavy rain (91 mm) was

recorded on 9th Oct at Port Blair. The $\delta^{18}\text{O}$ ($\delta^2\text{H}$) of precipitation during all these days had a close range of $-4.9 \pm 0.60\text{‰}$ (-25.87 ± 3.8). The same day the depression intensified and eventually turned into a Super Heavy Cyclonic Storm (near 13°N , 93.5°E , "Phailin"). The following day it crossed Andaman Islands and moved northwards (IMD report on cyclone). On 9th and 10th October the recorded rainfall at Port Blair was ca. 73 mm and 10 mm respectively. But the $\delta^{18}\text{O}$ of rain further depleted and achieved a value ca. -5.5‰ on these days. The storm tracks are shown in Figure A.4. The cyclonic effect continued and the Port Blair site recorded moderate rain on 13th Nov (13.8 mm). There was little rain on 23rd Nov but the $\delta^{18}\text{O}$ showed nearly the same values (10.4‰) on both these days. Mean time, another depression formed south east of Andaman island around 19th November 2013. When it reached the island it turned to Cyclonic Storm (the Lehar, Figure A.3.3) and caused heavy rain in the southern parts of the Andaman Island. The recorded rainfall on 24th and 25th November 2013 were 21 mm and 213 mm respectively (Figure 3.2). Interestingly, the isotopic values observed during these two days were nearly the same, $\delta^{18}\text{O} \sim -17\text{‰}$ ($\delta^2\text{H} \sim -118\text{‰}$) despite there was one order of magnitude difference in rainfall amount. This is also to be noted here that isotopic values reflected the intensity of the cyclonic storm as well. The Phailin track was relatively far from the rain sampling location (~ 160 km), compared to that of Lehar (~ 25 km). Hence the most depleted $\delta^{18}\text{O}$ ($\delta^2\text{H}$) values recorded during Phailin was -5.8‰ (-31.84‰), but the same for Lehar was -17.1‰ (-118.5‰). It appears that the isotopic data do not show linear behaviour with the rainfall amount during the cyclonic storms. During the first few days of Phailin the rainfall showed a wide variability; from near zero to 91 mm, but the $\delta^{18}\text{O}$ remained nearly constant at $-4.6 \pm 0.44\text{‰}$. During the Lehar cyclonic activity rainfall again showed a large variability from near zero (on 23rd November) to over 200 mm (on 25th November). But isotopic composition of rainfall remained nearly the same ($\delta^{18}\text{O} \sim -17\text{‰}$ and $\delta^2\text{H} \sim -118\text{‰}$). It also implies that the isotopic values depends more on the available moisture amount rather than the rain, but in this process it carries the 'memory' of the rainfall, as discussed below.

We have investigated the effect of convective activities on rainwater $\delta^{18}\text{O}$, similar to studies undertaken elsewhere (e.g., Risi et al., 2008; Moerman et al., 2013). $\delta^{18}\text{O}$ of rain has been correlated with the rainfall (and OLR) integrated for T_i (say) days preceding the event. Figure 3.7 shows the pattern of correlation coefficient with increasing values of T_i . The analysis shows that on short time scale the correlation is low either with rainfall amount or with OLR, but improves when rainfall amount (also OLR) is integrated for several days. The maximum correlation is obtained for $T_i = 18$ (21) days. The year 2013 also shows similar characteristics, but the time band is 24 - 27 days. Risi et al. (2008) provided an explanation of such kind of behavior in the context of rain isotopic analysis in Niamey, Niger. Each convective event causes depletion a little more to the low-level vapor; the isotopic composition feeding a convective system is thus influenced by the cumulative effect of the previous convective

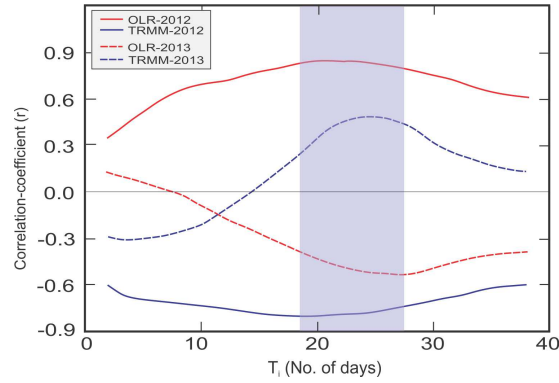


FIGURE 3.7: The progress of correlation between $\delta^{18}\text{O}$ and the convective parameters (rainfall amount and OLR) integrated over a time period T_i . The rainfall and OLR data have been integrated over a grid size of $90^\circ\text{E} - 95^\circ\text{E}$ and $7.5^\circ\text{N} - 12.5^\circ\text{N}$ centered at Port Blair. The blue (red) curves represent the rainfall (OLR). The solid (dashed) lines are for the year 2012 (2013).

systems. This means that a minimum time frame is required for rainwater $\delta^{18}\text{O}$ in order to respond strongly to the convective systems, which in the case of Bay of Bengal is about 20 - 27 days.

This also explains why the amount effect is poor on daily scale, but gets improved on longer time scale (i.e., > 3 weeks). The improved correlation between $\delta^{18}\text{O}$ - rainfall on higher temporal domain, implies that the isotopic properties of rainfall are controlled more by the integrated effect rather than the discrete events of rainfall. In other words, the isotopic tracers carry a 'memory' of the past rain (Risi et al., 2008; Moerman et al., 2013; Vimeux et al., 2005). This kind of memory effect has also been observed in case of rainfall during severe cyclonic events, as mentioned earlier. Also it means that when the individual local convective events become an organized convection the isotopic composition of rain water responds better to this large scale system rather than the isolated events. Such kind of observations have also been reported especially in the tropical region whereby precipitation isotope fractionation processes have been shown to integrate across wider spatial scales and longer time periods (Kurita, 2013; Moerman et al., 2013; Vimeux et al., 2005; Cobb et al., 2007).

Rain Isotopes Lead-lag Analysis

The lead-lag analysis of any two meteorological parameters is a well established method to understand the timescales of the governing processes of the atmosphere. However, such kind of analysis is rarely done in rain isotope studies. The isotope and rainfall lead-lag relationship helps understand the nature of the amount effect in the framework of large-scale convective systems. Since a large scale system slowly evolves with time, the correlation would decay slowly with time as compared to the localized convective activity with short lifespan where correlation falls fast with lead-time.

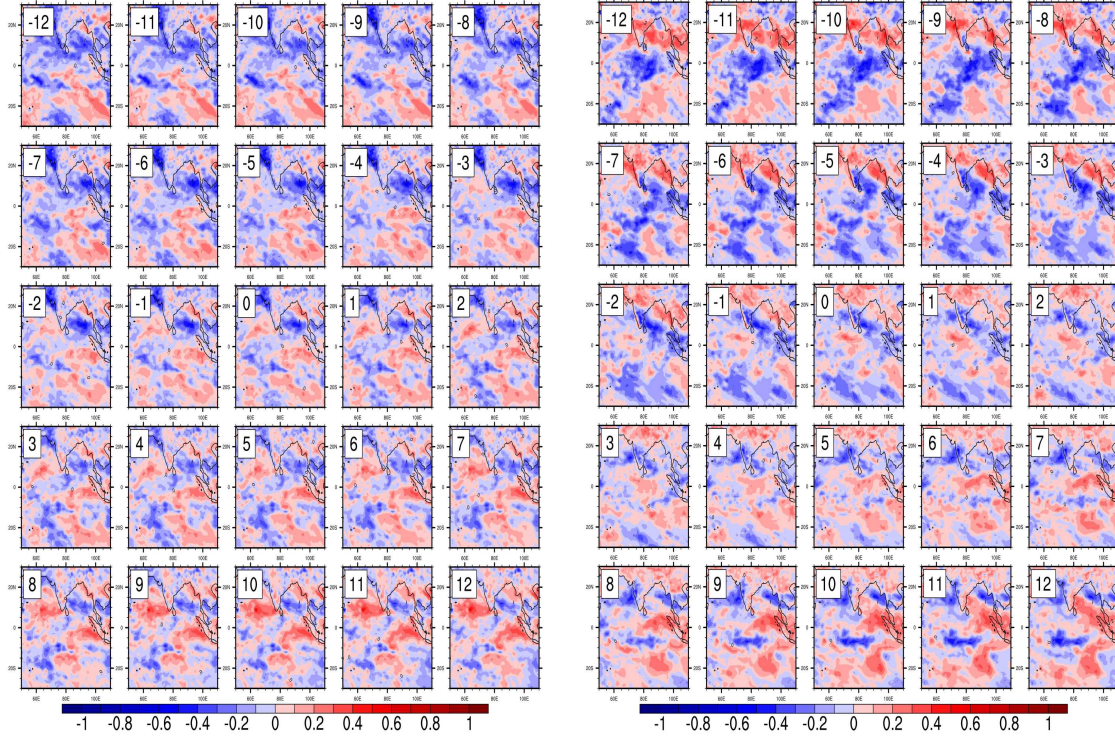


FIGURE 3.8: Spatial (30°S - 30°N , 50°E - 110°E) correlation coefficient between $\delta^{18}\text{O}$ (reference) and TRMM derived daily rainfall (sliding) data in year 2012 (left panel) and 2013 (right panel). Unlike 2012 where the negative correlation is visible mainly in Bay of Bengal in this year the negative correlation manifests in the Indian Ocean.

We have investigated the nature of the $\delta^{18}\text{O}$ -rainfall relationship by analyzing their spatial correlation pattern in order to understand the spatial variability and also the variation of amount effect in these two years. Figure 3.8 shows the lead-lag correlation spatial diagram with $\delta^{18}\text{O}$ data as the reference (fixed) time series and TRMM daily rainfall data at each grid point over the Indian Ocean region for the year 2012 during JJAS as the other (sliding) time series. The lag correlation plot showing sequential development of correlation pattern at each grid from lag 12 to lag +12 is shown here in separate panels. Strong inverse correlation was observed in 2012 at lag 12 days. The correlation progressively weakens and vanishes at lag +12 days. This behavior essentially shows a sinusoidal behavior of relationship between rainfall amount and its $\delta^{18}\text{O}$ values with a periodicity of about 24 - 25 days. The timescales observed by correlation analysis appears to be linked to the monsoon intraseasonal oscillation (ISO) that shows spectral signature on this time frame during monsoon season over the Indian subcontinent implying that rain $\delta^{18}\text{O}$ is a likely recorder of monsoon ISO. Additionally, the correlation band (the region where correlation is negative) is restricted to northern Indian Ocean (Arabian Sea and Bay of Bengal); but negligible or weakly positive in the Indian Ocean.

The year 2013 shows similar cycle but the usual negative $\delta^{18}\text{O}$ -rainfall correlation band shifts from the north Indian Ocean to the equatorial region. Whereas, the

northern Indian Ocean region unlike the year 2012, display positive correlation. This demonstrates that the expected rainfall- $\delta^{18}\text{O}$ negative correlation or the amount effect has a spatial variability; as evident in Figure 3.9, the spatial extent is >1000 km. This kind of variability may arise due to the seasonality (i.e. season to season variation) of the monsoon intraseasonal oscillation. The seasonality of monsoon ISO is linked to monsoon interannual variability (Sharmila et al., 2015). For example, the year 2012 is characterized by relatively low rainfall (Khole et al., 2013) (ISMR: 93% relative to Long Period Average, LPA), positive SST anomaly in distinct areas of the Indian Ocean during the JJAS period representing relatively restricted moisture source regions. On the other hand, the year 2013 experienced higher than normal rainfall (ISMR: 106% relative to LPA), strong intra-seasonal variability, the fastest spread of monsoon in India in the last 41 years, neutral SST anomaly from most parts of the Indian Ocean representing diverse moisture source areas (Devi and Yadav, 2014).

Section Conclusion

The rainwater isotopic compositions over southern Bay of Bengal show systematic depletions seem to vary with the seasonal cycle of monsoon as well as seasonality of the intraseasonal oscillation. Relatively low humid condition but strong circulation in the early phase of monsoon cause moderate level of raindrop re-evaporation, which in turn contributes to amount effect. However, the extent of evaporation diminishes, caused by altered atmospheric condition at the mature phase of monsoon when amount effect seems to be controlled more by the moisture flux convergence than the local evaporation. On seasonal time scale, the d-excess shows lower values during the monsoon but higher values during the non-monsoon time. This appears to be controlled by the moisture source, originated in the equatorial Indian Ocean during monsoon but from continental and non-Indian Ocean region during the non-monsoon time; this has also been confirmed by back trajectory analysis. However, higher values of d-excess could also arise as isolated events during the monsoon which is caused by re-cycling of water vapor being systematically fed into a large scale convective system. As per our results during the large scale convection d-excess becomes high, which means ^2H is favored than ^{18}O . The timescale of the positive d-excess anomalies during the monsoon appears to be modulated by the monsoon intraseasonal oscillation. The oxygen and hydrogen isotopic compositions show significant variations depending on the ocean-atmosphere conditions, maximum depletion was observed during the tropical cyclones. Convective activities integrated over a period of time control rainwater isotopic composition more than the isolated events. Hence, the rain $\delta^{18}\text{O}$ carries the signature of previous rainfall better than the individual rain events.

3.4.2 Isotopic investigation of the moisture transport processes

The daily rainfall sampling in Port Blair between 2012 and 2015, the Andaman Island is considered as representative of the BoB (the source area). The Port Blair- $\delta^{18}\text{O}$ has

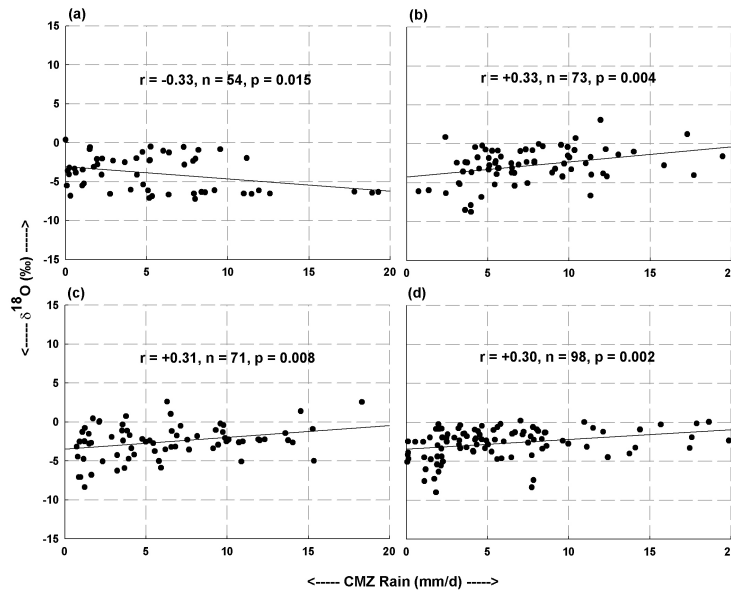


FIGURE 3.9: Scatter diagram between Port Blair- $\delta^{18}\text{O}$ vs. Core Monsoon Zone (CMZ) average rainfall; (a) 2012 (b) 2013 (c) 2014 (d) 2015.

been correlated with the area averaged rainfall over the Port Blair with increasing grid size. The results show that the inverse correlation coefficient (amount effect) increases when the rainfall is averaged over a larger area, reaching a maximum value for an area of $5^\circ\text{lat} \times 5^\circ\text{lon}$ (Section 3.4.4). Analyses of other years' rain-isotope data also yield similar result. The exercise demonstrates that the amount effect remains significant approximately for an area of $550 \text{ km} \times 550 \text{ km}$, however, decreases thereafter. But what would happen when the rain isotopes are correlated with rainfall of a distant region, a region which is physically separated from the rain collection site? To examine this behavior we have analyzed the rainfall over the CMZ; an area about 2.8 million km^2 in central India and is approximately $2,000 \text{ km}$ away from the Andaman Island (Figure 3.2 b). The reason for taking the CMZ is that the rainfall over this region is a proxy for all India summer monsoon rainfall variability (Rajeevan et al., 2010). The Port Blair- $\delta^{18}\text{O}$ shows weak but a significant positive correlation with the CMZ rainfall; Figure 3.9 (a-d) depicts the nature of inter-annual variability of the relationship of these two parameters. The year 2012 shows a negative correlation, while the following three successive years (2013-2015) show positive correlations.

For 2015, the correlation (r) between Port Blair- $\delta^{18}\text{O}$ and CMZ average rainfall amount is $+0.35$ ($n = 96$, $p < 0.01$). However, the rainfall at Port Blair does not show any reasonable correlation with the CMZ average rainfall (r varies from 0.014 to 0.091). Here we discuss the possible implications of the Port Blair- $\delta^{18}\text{O}$ and the CMZ-Rainfall relationship. We propose a hypothesis that the above mentioned isotope-rainfall correlation is arising due to moisture flow from the BoB to India during the monsoon season. We test this hypothesis by carrying out a correlation analysis between rain isotope at Port Blair and a central Indian site (Nagpur) followed by two

more sites; these are Kolkata in east and Tezpur in northeast India, both of which are known to receive BoB moistures during the summer monsoon.

Source Area: - BoB

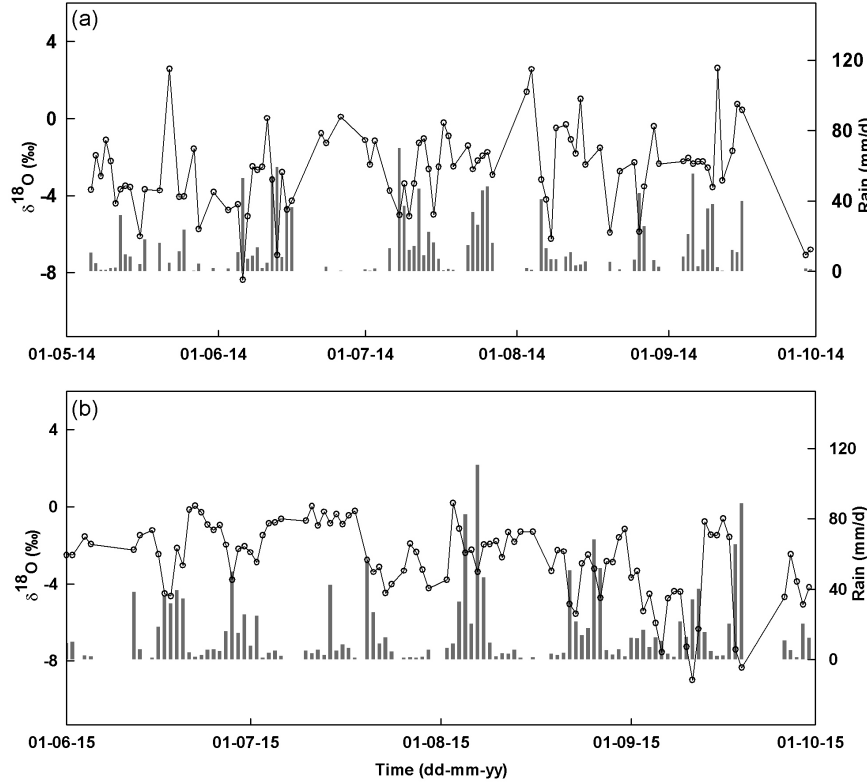


FIGURE 3.10: Oxygen isotope record of Port Blair rainfall (black line) and the rainfall variability (gray bar) for (a) 2014 and (b) 2015.

The time series plots of daily rainfall and its oxygen isotopic composition for the year 2014 and 2015 over the Port Blair site are shown in Figure 3.10. The rainfall- $\delta^{18}\text{O}$ plots for the year 2012-13 have been presented in earlier section Figure 3.2. However, here we summarize Local Meteoric Water Lines (LMWL) for the four years studied in the context of moisture transport. The LMWL of the Port Blair site during JJAS for the years 2012-2015 are given below:

$$\delta^2\text{H} = 7.10 \times \delta^{18}\text{O} + 9.42; R^2 = 0.94 \quad - - > 2012 \quad (3.3)$$

$$\delta^2\text{H} = 6.75 \times \delta^{18}\text{O} + 5.11; R^2 = 0.96 \quad - - > 2013 \quad (3.4)$$

$$\delta^2\text{H} = 6.47 \times \delta^{18}\text{O} + 3.29; R^2 = 0.96 \quad - - > 2014 \quad (3.5)$$

$$\delta^2\text{H} = 7.72 \times \delta^{18}\text{O} + 8.71; R^2 = 0.91 \quad - - > 2015 \quad (3.6)$$

The slope varies from 6.5 to 7.7, a slope lower than that of the global meteoric water line (slope = 8.0, Craig, 1961, indicates a significant amount of moisture production

underwent kinetic fractionation, and/or raindrops were subjected to evaporation below the cloud base.

Propagation of the rain band

Before analyzing the precipitation isotope data of these two regions (BoB vs. Mainland), the propagation of the rain/convection band over the BoB and their possible implications on precipitation isotopes are crucial to understand. Time latitude Hovmöller diagram of the unfiltered OLR anomaly has been shown in Figure 3.11(a) to illustrate the northward propagations for the years 2012 through 2015. It is clear that all the years (except 2012) show strong northward propagation as revealed by the black arrows. It is observed that the northward propagation is largely dominated by

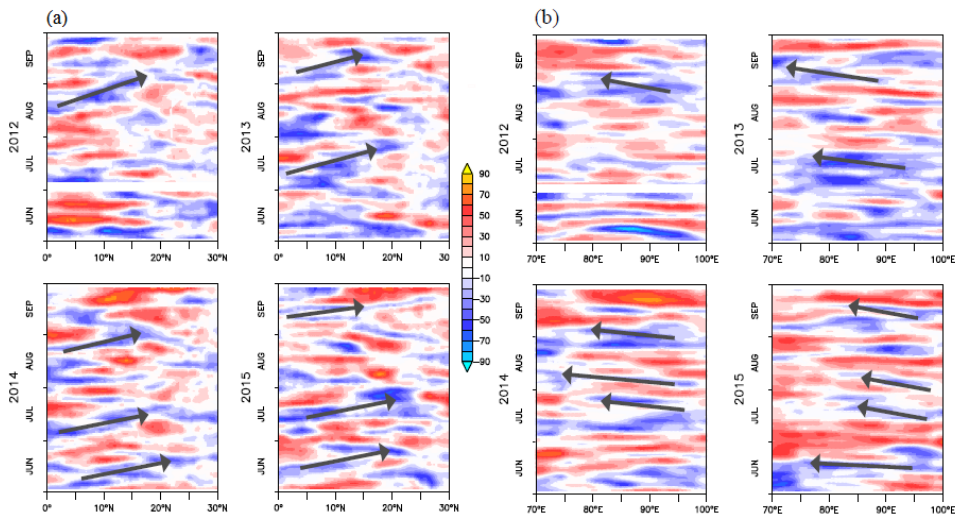


FIGURE 3.11: (a) Time latitude Hovmöller diagrams of daily outgoing longwave radiation anomaly to reveal the northward propagation for the summer monsoon Jun-Sept, 2012-2015. (b) Time longitude Hovmöller diagrams showing the westward propagation of anomalies in daily outgoing longwave radiation (Wm^{-2}) for the summer monsoon Jun-Sept, 2012-2015. Arrows denote dominant eastward/westward propagating bands of anomalous (-ve) convection.

30-60 day mode. To illustrate the westward propagation, time-longitude Hovmöller diagram has been plotted (Figure 3.11(b)). It is noted that while the 30-60 day mode is weak during the drought year of 2012, the 10-20 day mode also seems to be relatively less active during this year. The weak propagation of rain band, and in turn, the moisture flow in the year 2012 are most probably responsible for making this year characteristically different in terms of the isotopic signature compared to other years (2013-2015). One possible implication is that the central Indian region in 2012 may have received the maximum moisture from the Indian Ocean/Arabian Sea and relatively small amount from the BoB.

The spectral analysis revealed that $\delta^{18}\text{O}$ of Port Blair rain is characterized by a periodicity band of 10 to 25 days. Figure 3.12(a)-(d), shows the spectral characteristics of

the rain isotope (upper panel) and rainfall record (lower panel) for the years 2012-15. The periodicity band of 10-25 day is probably associated with the 10-20 day mode of monsoon sub-seasonal variations (Chatterjee and Goswami, 2004) and appears to be distinctly different from the synoptic scale variations which take place in time scales ≤ 10 days. On the other hand, spectral analysis of Port Blair vapor $\delta^{18}\text{O}$ record for 2015 yields significant peak at 12-14 days (Figure 3.12(e), left panel) in accordance with the rainfall record (middle panel). Both the periodicities also show strong coherency as shown in the right panel of the Figure 3.12(e). Hence, we believe that the interpolated values (in rain $\delta^{18}\text{O}$) do not incorporate any significant error in estimating the spectral features and hence the derived periodicities may be considered as representative values. Comparison of interpolated method with Lomb-Scargle periodogram is presented in Appendix A.1 (Figure A.1).

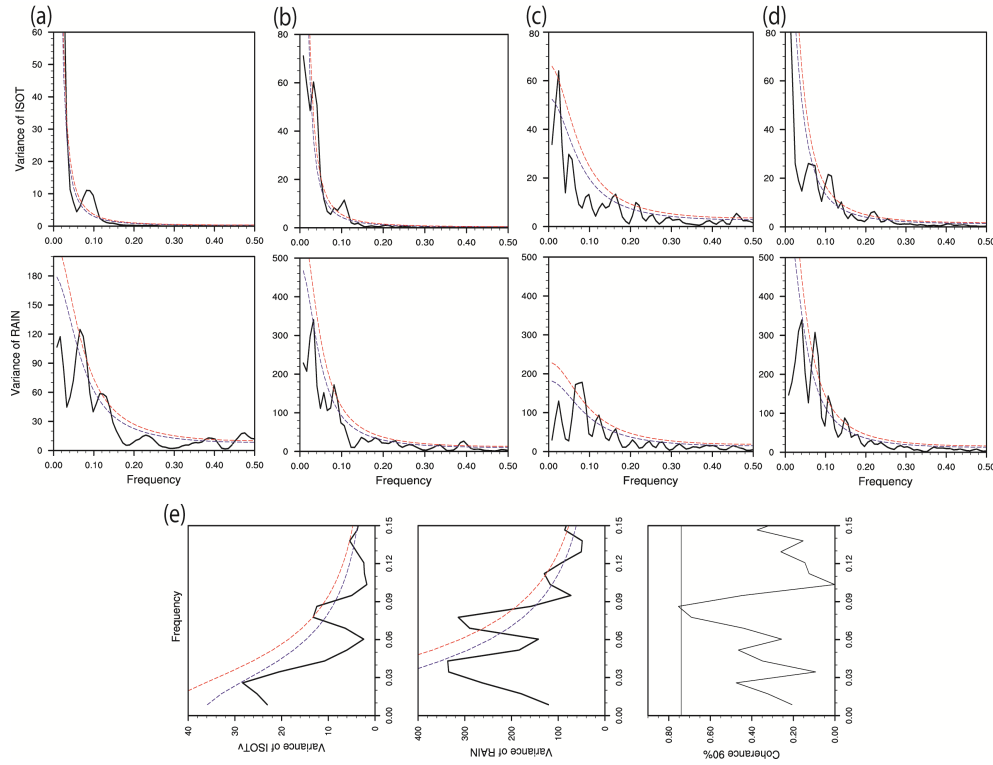


FIGURE 3.12: Spectral peaks calculated for daily interpolated $\delta^{18}\text{O}$ (ISOT) and summer rainfall (RAIN) of Port Blair for (a) 2012, (b) 2013, (c) 2014 (d) 2015 and (e) $\delta^{18}\text{O}$ of ambient vapor (ISOTv) and rainfall (RAIN) for the year 2015, for this case, we calculated the coherency in ISOTv and RAIN. The significant peaks have been marked for each year. The red line and blue line represent 90% and 80% significance levels respectively.

It has been observed that the 2015 monsoon was strongly affected by the El-Niño Southern Oscillation (ENSO), though the effect was subdued (strong) in the early (later) phase of the monsoon (IITM Monsoon Report 2015; <http://www.tropmet.res.in/~lip/Publication/RR-pdf/RR-185.pdf>). The CMZ rainfall anomaly for 2015 is reported in Appendix A (Figure A.5). The calculated anomaly shows that during

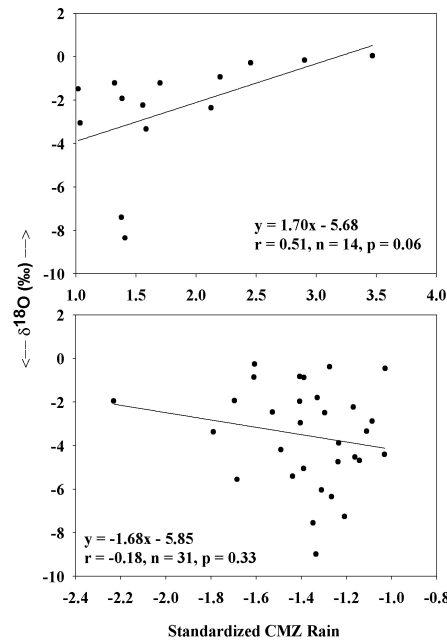


FIGURE 3.13: Response of Port Blair-Rain- $\delta^{18}\text{O}$ to active (upper) and break phase (lower) of rainfall for the year 2015. While, the active phase of rainfall strongly modulates the rain isotopes, the break phase of rainfall seems to have little effect on it.

the month of June and later part of July, the CMZ had positive rainfall anomaly, while August and September were mostly characterized by negative rainfall anomaly. In order to compare the Port Blair- $\delta^{18}\text{O}$ with the 2015 CMZ rainfall anomaly, this anomaly diagram is re-plotted by subtracting the individual days of rainfall from the June-September mean.

It has been found that the pattern of variability in CMZ anomaly (Figure A.5 (a)) is quite similar to that of Port Blair- $\delta^{18}\text{O}$ (Figure A.5 (b)). That is, the characteristic features of monsoon were also manifested in the $\delta^{18}\text{O}$ record of Port Blair rain as revealed in the mean variability, showing positive (negative) anomaly during the initial phase of the monsoon. This may have implications in studying the large scale behaviour of monsoon based on limited isotopic records of rainfall from the Andaman Island e.g. the effect of ENSO or West Pacific on Indian monsoon. But due to the lack of long term rainwater isotopic records, it is not possible to make a comprehensive assessment of this effect at this moment. It has been found that the Port Blair- $\delta^{18}\text{O}$ also responds to the active phase of rainfall. The active (break) phase of the monsoon is characterized by intense (subdued) rain; hence $\delta^{18}\text{O}$ is expected to show strong (week) correlation with the rainfall of the respective phases of active (break), via the amount effect.

Figure 3.13, shows a scatter diagram between CMZ standardized rainfall and the Port Blair- $\delta^{18}\text{O}$ for both the phases. For active case the correlation is quite strong, but for the break period is nearly non-existent. Since the monsoon intraseasonal oscillation is related to the active/break phases of monsoon, the characteristic periodicity of

10-14 days observed for the year 2015 (Figure 3.12(e)) in Port Blair Rain- $\delta^{18}\text{O}$ strongly indicates that rain isotopes in this region responds to the active periods and in turn, to the westward propagation.

This section may be summarized as follows: the moisture flow is a dynamical process; the advected moisture flows from Indian Ocean/Arabian Sea in about 10 to 20 days, considering a mean wind speed of 7ms^{-1} . While reaching the BoB, it also gets a component from the BoB. Secondly, the moisture is continuously recycled, where a significant amount may come from the evaporation of raindrops. The recycled moisture is fed into the cloud system, which slowly builds up over a time period of 10-25 days. It is now being realised that the rain isotopic composition is not completely dependent on the moisture source, but cumulative convective processes from the source region to the deposition site (Galewsky et al., 2016). However, the large scale convective processes occur in a timescales of 10-20 days and 30-60 days. In this context, this is to be noted that the other mode of monsoon variability characterized by 30-60 day periodicity is difficult to identify, mainly due to the lack of long time records.

Spatial variability of the isotope-rainfall relationship

Figure 3.14, shows the spatial correlation between Port Blair- $\delta^{18}\text{O}$ data as reference (fixed) time series and TRMM derived daily rainfall data at each grid point over the Indian sub-continent for the studied years during the JJAS period. Latitudinal averaged (20°N - 25°N) values show the sequential development of correlation pattern at each longitudinal grid (0.25°) from lead 0 to lead 12 (days) in rain, shown top to bottom for the years 2012-15 (Figure 3.14(a-d)). The correlation pattern has been examined for the central Indian part (gray bar). In all the years, but, 2012 Port Blair- $\delta^{18}\text{O}$ shows significant positive correlation with the rain over CMZ at 0 lead. As an exception, a significant negative correlation is noted with the rainfall in the western part of India for the year 2012 at 0 lead. With increased lead time the positive correlation gets improved and reaches maximum at lead time of 9-12 days for 2012. On the other hand, for the cases of 2013-15, the Port Blair- $\delta^{18}\text{O}$ shows better positive correlation with the rain at 0 lead time. Further the correlation decreases and becomes negative as the BoB moistures move westward/eastward with increased lead time of 6 to 12 days as shown in Figure 3.14(b-d). Interestingly, we found that the BoB moisture may contribute directly through westward propagation (year 2013) or sometime takes a reversal from east to west (year 2014 and 2015). The moisture transport timescale and pathways are discussed in Appendix A.6.

The positive correlation is most prominent in the year 2015; the pattern remains strong, even at lead time of 6 days and moved eastward. Afterwards, the positive correlation vanishes and it turns significantly negative at lead time 12. This analysis shows that the correlation pattern between rain isotope of the Andaman Island and the rainfall over central India oscillates with a period of 10-12 days. The coherent nature of correlations appears to arise due to the interplay between the 10-20 day mode and the 30-60 day mode of summer monsoon variability. In some cases the

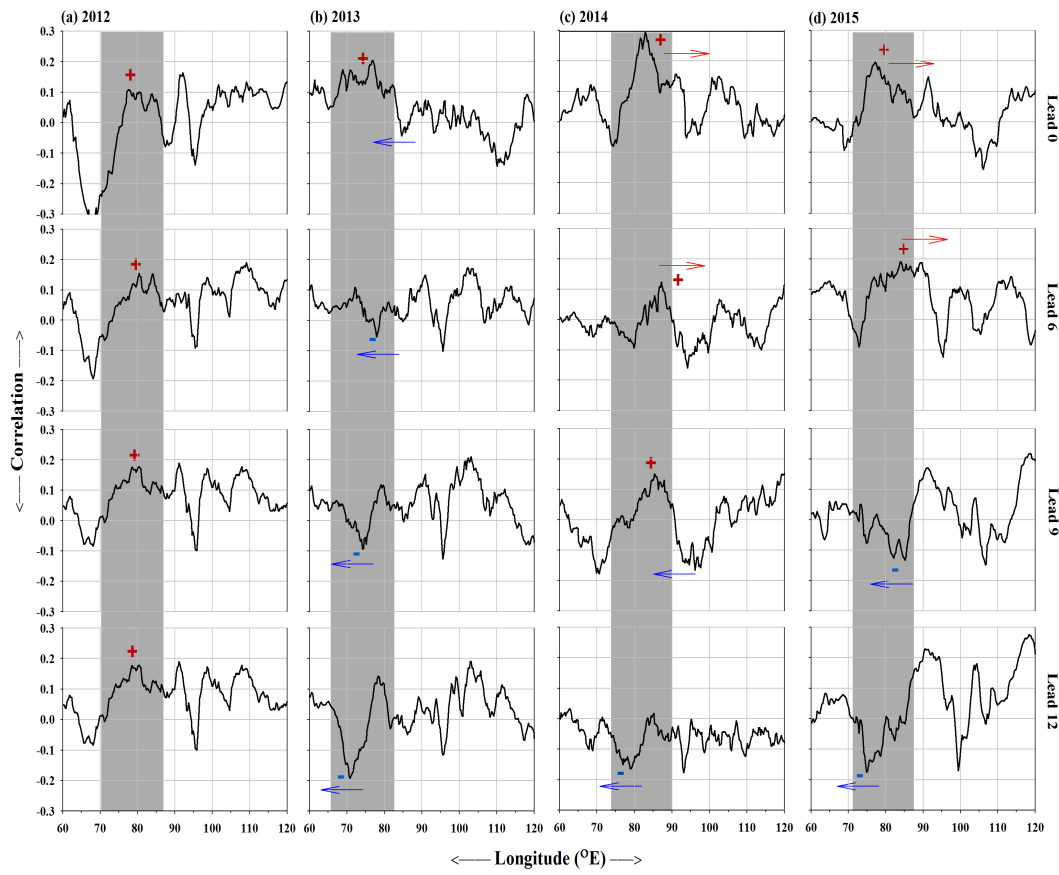


FIGURE 3.14: Correlation between Port Blair rain- $\delta^{18}\text{O}$ time series with the spatial rain has been calculated and latitudinal averaged (20°N - 25°N) values are plotted. The gray bars are showing central India, as mostly the changes in the correlation pattern were found with lead in rain (0 - 12 days). + (red) and - (blue) are showing signs of correlation. Red and blue arrows are showing direction of eastward and westward propagation respectively.

transport of moisture from BoB is negligible over central India (year 2012), though in general, the moisture from the BoB plays a significant role in rainfall over the Indian subcontinent.

Lag relations between the Island and mainland $\delta^{18}\text{O}$ time series

If moisture from the BoB is transported to central India then the Port Blair- $\delta^{18}\text{O}$ should be associated with the CMZ-Rain $\delta^{18}\text{O}$, with proper lag adjustment for moisture travel time (see Figure A.6). A one to one correlation may not be done due to uneven occurrence of rain events and difference in sample numbers between Port Blair and available sampling sites on the Indian mainland.

A comprehensive rain- $\delta^{18}\text{O}$ time series from the central Indian region was not available, but a lower resolution record is available from Nagpur (21°N , 79°E). 18 rain samples were collected in 2015 during the summer monsoon season and analyzed for isotope. A scatter diagram and time-series between Port Blair- $\delta^{18}\text{O}$ and Nagpur- $\delta^{18}\text{O}$

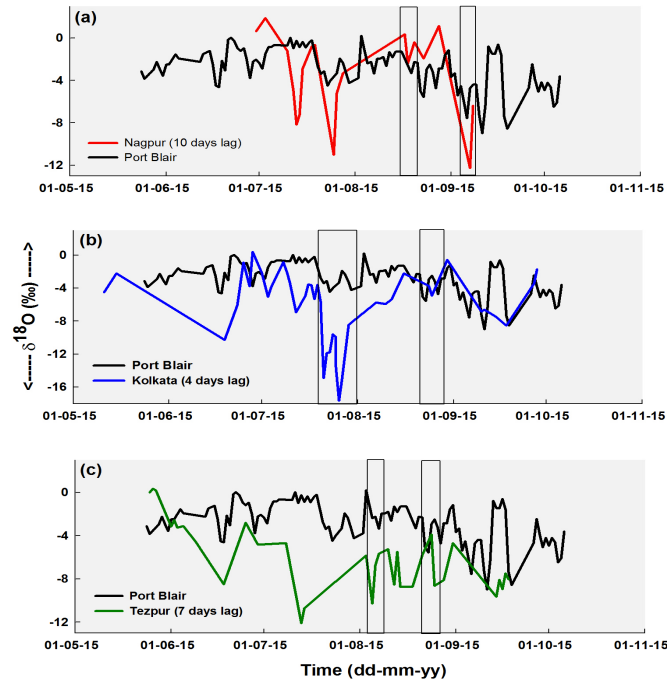


FIGURE 3.15: Correlation between Port Blair rain- $\delta^{18}\text{O}$ time series with the spatial rain has been calculated and latitudinal averaged (20°N - 25°N) values are plotted. The gray bars are showing central India, as mostly the changes in the correlation pattern were found with lead in rain (0 - 12 days). +(red) and -(blue) are showing signs of correlation. Red and blue arrows are showing direction of eastward and westward propagation respectively.

practically shows no correlation or trend ($r = 0.09$, $n = 18$), but when the Nagpur- $\delta^{18}\text{O}$ values are lagged by 10 days (moisture travel time), a similar time varying pattern of $\delta^{18}\text{O}$ was found between these two time series (Figure 3.15(a)). In comparison to Port Blair rain $\delta^{18}\text{O}_{avg}$ (-2.86‰), Nagpur isotopic variation in the year 2015 has an average $\delta^{18}\text{O}$ value of -3.41‰ which is around 0.55‰ depleted and characterized by higher variability (Min = -12.27‰ , Max = $+1.89\text{‰}$) as moisture get depleted in the heavy isotope due to rainout process. Thus, isotopic characteristic of the target region may be depleted in heavy isotope as well as influenced by the signature of other moisture source and local moisture convection. Apart from the above observations, the difference in $\delta^{18}\text{O}$ values and some mismatch particularly the high depletions may be explained as follows. Firstly, the moisture that produces rain over the Andaman Island only a small fraction reaches the Indian region, while the majority of them move off the Indian landmass as stated earlier.

Forward trajectory analysis using the HYSPLIT model on a weekly timescale with Port Blair being the source area clearly shows this kind of behaviour. Out of the 23 cases analyzed (that is 23 weeks from May week-1 to September week-5) only 8-9 of them showed that moistures moved to the Indian region while in the rest of the

cases they moved elsewhere (Figure A.6 (a), dashed curves). Secondly, when the BoB moisture reaches mainland, the transport pathways were not always directly to India, in several cases it first moved to east and northeast and then suffered inversion and moved towards India (Figure A.6 (a), solid curves).

The mechanism of the BoB moisture reversal is discussed later. While traveling to the continental regions of the South-East Asian countries, it may have picked up recycled moisture, which in turn, diluted the initial isotopic signature of the moisture originally derived from the BoB. Nevertheless, the similar variations in $\delta^{18}\text{O}$ provide a strong indication that part of the BoB moisture eventually travelled to the central Indian location (Nagpur), directly or indirectly in about 10 days. An example of heavy depletion in $\delta^{18}\text{O}$ has been discussed later.

We have also tested this hypothesis for another location - Kolkata that lies in the peripheral region of the easternmost boundary of CMZ. A similar trend was also found in this case. Kolkata is known to receive sufficient vapors from the BoB (Sengupta and Sarkar, 2006) that cause intense precipitation over this region. We have collected about 50 samples in 2015 and $\delta^{18}\text{O}$ ($\delta^{18}\text{O}_{avg} = -6.05\text{‰}$) time series has been constructed with 4 days lag and superimposed over Port Blair- $\delta^{18}\text{O}$ (Figure 3.15(b)). Interestingly, back trajectories have shown that on many occasions moisture was sourced from BoB (Figure A.6 (b)). The precipitation isotopes ($\delta^{18}\text{O}$) achieved the lowest values at Kolkata (-14‰) in the last week of July and the first week of August. Further analysis also shows that the major amount of moisture was generated in the northern BoB caused intense rain during this time in the south Bengal region including Kolkata and its surrounding areas. This is the time when a low pressure system (LPS) formed over north of BoB and adjoining areas of Bangladesh and the Gangetic West Bengal, which rapidly concentrated into a depression over north east BoB (at 22°N , 90.8°E on 26/July/2015; IMD daily weather report). For the next couple of days it remained stationary and caused heavy rain and thunderstorm at most places in Gangetic West Bengal on 29th July 2015. On 30th July it moved north-westward and intensified into cyclonic storm KOMEN cantered at about 300 km east-southeast of Kolkata. The isotopic results support the notion that LPS transport moisture from the BoB to the mainland (Sikka, 1977; Goswami, 1987) but contradict the so called 'single source' of BoB moisture to the Kolkata region (Sengupta and Sarkar, 2006).

North East India is also known to receive a significant amount of BoB vapor (Figure A.6 (c)); hence we test our hypothesis at one of the sites Tezpur in Assam. About 52 rain samples were collected from April to September in 2015 and found very similar isotopic variations as over the Port Blair region. A well matched pattern was found when 7 days (moisture travel time) lagged time series of Tezpur- $\delta^{18}\text{O}$ ($\delta^{18}\text{O}_{avg} = -6.01\text{‰}$) was plotted over Port Blair- $\delta^{18}\text{O}$ (Figure 3.15(c)). It is evident from the rain isotope and trajectory analyses that the moisture source for the Tezpur region was mostly from the BoB.

It is known that the moisture travel time depends on circulation pattern and may vary within the season. Thus, all the three sites over mainland show some $\delta^{18}\text{O}$ peaks

that may also match well with isotopic variations of Port Blair rain if the lag time adjusted with speculated error of ± 1 day for the particular period of time (marked by rectangles, Figure 3.15).

Reversal of south BoB moisture

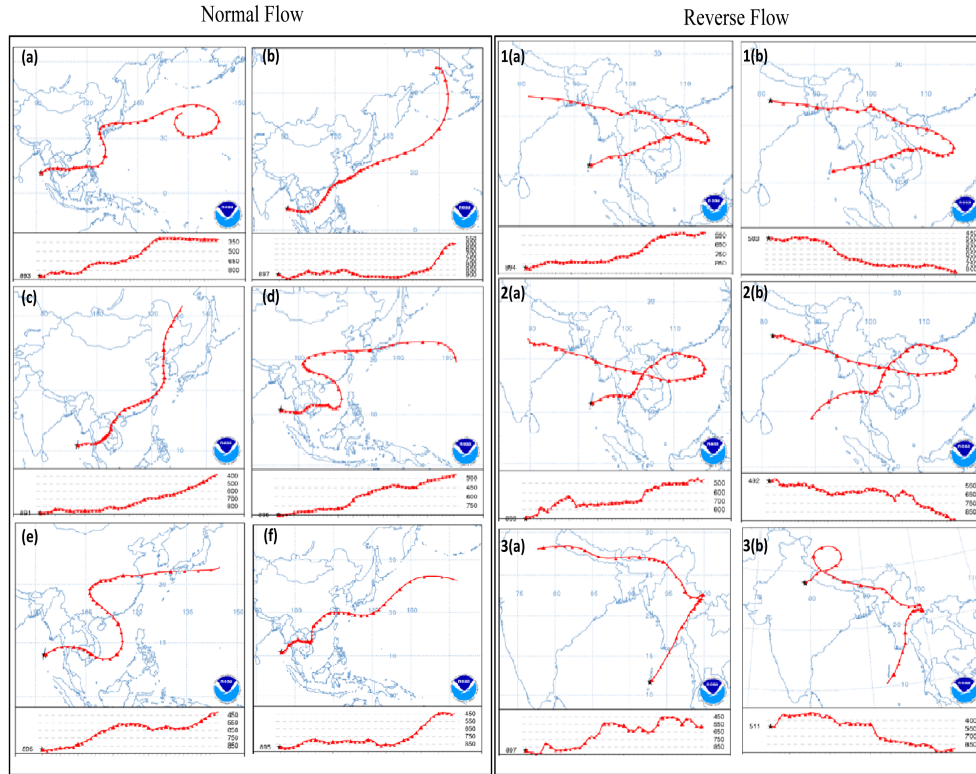


FIGURE 3.16: Left-panel showing forward trajectories ((a) to (f)) as some examples of Normal Flow during the Indian summer monsoon (ISM) and the right-panel showing the forward (1(a), 2(a), 3(a)) and corresponding backward (1(b), 2(b), 3(c)) trajectories during ISM as some examples of Reverse Flow (case-II years). Star (★) is the source (for forward) and end (for backward) point, Port Blair (11.66°N, 92.73°E, 1000 m, 10-12 days) for forward trajectory chosen as the source and in case of backward trajectories the source (5500 m, 10-12 days) was chosen to endpoint ($\pm 0.5^\circ$) of corresponding forward trajectory.

As discussed above, the isotopic variation in the southern BoB region was temporally dependent with the average rainfall over the Core Monsoon Zone of India. The results indicated a retrograde motion of the BoB circulations, occasionally driving the south BoB moisture either directly (Normal Flow) or through a reverse flow around the western Pacific region (Reverse Flow), reaches the Indian landmass. Some examples of observed BoB moisture trajectories are shown in Figure 3.16. The individual

trajectory plot that has two segments; the upper segment depicts the moisture trajectory while the lower segment shows the corresponding pressure levels (in hPa). Some examples of Normal Flow using forward trajectories represent that the moistures originated in the south BoB reach the north-western Pacific via Southeast Asian region (Figure 3.16, left panel: a-f). On the other hand, a few examples of Reverse Flow using the forward trajectories show the moisture flow gets reversed at around the South China Sea (100°E-120°E, 500-600 hPa) toward the Indian landmass (Figure 3.16, 1a, 2a, 3a). For the reversal events, we also calculated the corresponding back trajectory, which is shown on the right side of the forward trajectory panel, i.e., Figure 3.16: 1b, 2b, 3b. It is interesting to note that the back trajectories almost identically retraced the forward moisture movement if the pressure level (500-600 hPa) and the source ($\pm 0.5^\circ$) had been selected appropriately.

It implies that the mid-level moisture over the central Indian region also has one of the sources from the south BoB through the reversed branch. An analogous pathway for forward and backward trajectories for the reversal events support that the moisture originated from south BoB suffers inversion at around the South China Sea and reached the central Indian part in due course of time. This section is about the mechanism and circumstances explaining the reversal of the south BoB moisture flow. In Appendix A.7: the examined years for reversal event the climatological features of reversal of the BoB moisture to the Indian region and its role in modulating the spatial pattern of rainfall are discussed.

Mechanism of moisture path reversal

Calculation of surface temperature and pressure anomalies over the Indian and the western Pacific regions has been carried out to understand the driving mechanism for the observed reversal events. The prerequisite of high surface pressure (and associated low temperature) over the western Pacific has been used as a constraint to examine the Reverse Flow toward the Indian landmass (low pressure). It is known that one of the possible scenarios is the inducing anomalous mass subsidence over the western Pacific region, leads to the positive surface pressure anomaly (i.e., negative temperature anomaly) during the El-Niño years. Hence, the El-Niño year with positive pressure anomalies over the western Pacific and simultaneous coexistence of negative anomaly over the central Indian region may evolve such reverse pathways of the south BoB branch. However, negative pressure anomaly (high temperature) over the central Indian region is significantly noticeable only during the monsoon season (June-September) and has variability on an intraseasonal timescale. As a consequence, the reversal of the south BoB branch cannot be observed for the whole month or season.

All the El-Niño years ($\text{ONI} \geq +0.8$, JJA) and/or the years (e.g., year 2014) showing negative temperature anomalies over the western Pacific and positive over central India are examined. Out of six (1982, 1987, 2002, 1997, 2014, 2015) strong El-Niño

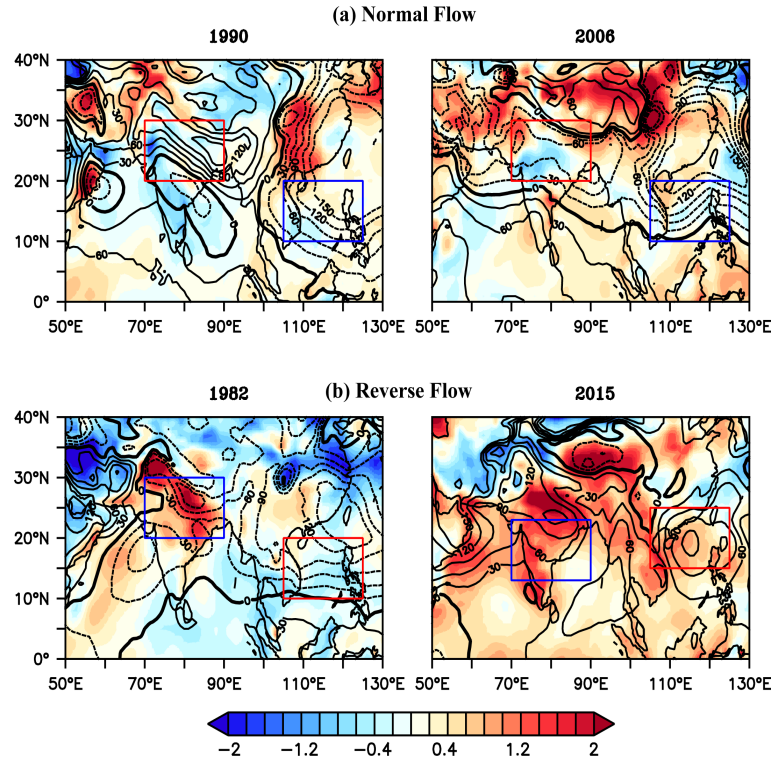


FIGURE 3.17: Surface temperature (shaded, K) and Pressure (contour, Pa) anomaly for a month (e.g. Jul or Aug) of Indian summer monsoon. Two examples of corresponding Normal and Reverse Flow circumstances, i.e. (a) Case I: 1990 & 2016 and (b) Case II: 1982 & 2015 respectively.

years, as per the above mentioned criteria, only four years (1982, 2002, 2014, 2015) have shown the events of reversal during the ISM months. The reversal patterns for those years ISM months are validated through the examination of the monthly wind circulations and trajectories. Further, normal years with Normal Flow ($-0.2 < \text{ONI} < +0.2$, JJA) were chosen (1983, 1990, 1993, 2003, 2006, 2012) to compare against the four years that comprise with Reverse Flow. The methodology and a few examples are discussed below.

Firstly, surface temperature analysis for individual ISM months over the study region. NASA Goddard Institute for Space Studies Surface temperature analysis (GISSTEMP) online portal (<https://data.giss.nasa.gov/gistemp/maps/>) has been used. The spatial temperature anomaly plots reveal two distinct circumstances, i.e. July, 1982 & 1990, base years 1980 - 2015 using data source; Land: GISS and Ocean: ERSST_v5. It has been seen that the relatively negative (positive) temperature anomalies over the Indian region and positive (negative) over the western Pacific may cause the Normal (Reverse) Flow. Secondly, monthly surface temperature and pressure anomalies are plotted; two examples from each case are shown (Figure 3.17). The red box represents an area of positive pressure anomalies (negative temperature anomalies) relative to an area enclosed by the blue box. We found that the changes in relative pressure anomalies over the two regions may modulate the normal wind flow of

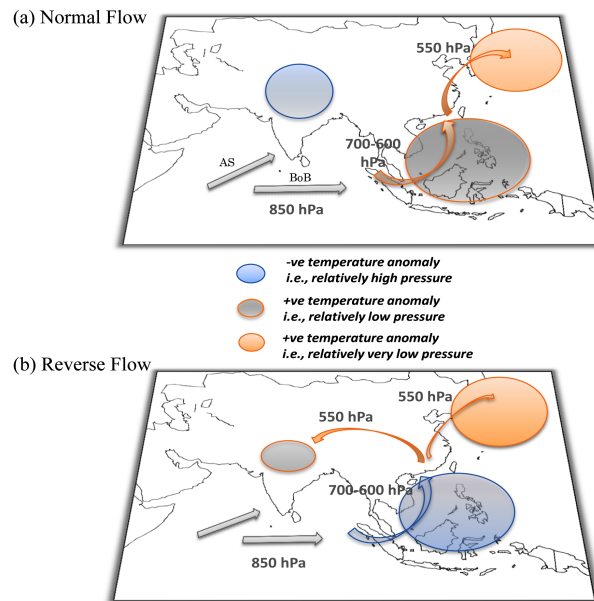


FIGURE 3.18: (a) Normal and (b) Reverse Flow of the south BoB branch during Indian summer monsoon. Temperature and pressure anomalies are based on the years 1980-2015 climatology. Arrows represent wind circulation with pressure levels derived from investigation of monthly wind circulations on different levels and daily trajectory analysis.

the south BoB branch. We examined several cases (not shown) and found that such reversals may evolve with the weakening of low-pressure over the Southeast Asian region and extent of low pressure over central India. For the Normal Flow, temperature (pressure) anomaly over the central Indian region during mid-monsoon months found to be negative (positive) as compared to the western Pacific (Figure 3.17(a)). However, Figure 3.17(b) shows the Reverse Flows are evolved through just opposite circumstances and appeared to have developed during the strong El-Niño years. One more point to be noted here is that due to the low pressure area and strong westerlies over the north-western Pacific, only a fraction of the south BoB or the Pacific moisture may contribute to the Indian region via such kind of reversals. Observed wind patterns at different levels, the role of surface wind drivers, and trajectory analysis help schematically illustrate the two distinct pathways of the south BoB branch shown in Figure 3.18, Normal Flow (upper panel) and Reverse Flow (lower panel).

Timescale of the event: The reversal of the south BoB branch from the western Pacific to central Indian region discussed here as an event. To investigate the matter further towards the timescale of the event. We found that the Reverse Flow occurs through the changes in the anomaly of surface parameters (pressure/temperature) over central India (-ve/+ve) and the western Pacific (+ve/-ve), otherwise Normal Flow. Although, the positive pressure anomaly over the western Pacific may persist during the El-Niño years, but the monsoon intraseasonal oscillations (MISOs) govern the movement of low pressure zone (Inter Tropical Convergence Zone, ITCZ) over

the Indian region (Yasunari, 1979; Sikka and Gadgil, 1980) and result from superposition of 10-20 day and 30-60 day oscillations. Hence, considering high pressure over the western Pacific during the event, the variability of low pressure over the Indian central region will regulate the timescales of the event (Reverse Flow). Thus, the El-Niño may be a necessary condition but not sufficient enough to initiate a reversal of the south BoB branch. That is, the movement of the ITCZ toward the central Indian region on intraseasonal timescale coupled with monthly to seasonally persistent high pressure over the western Pacific may be governing the reversal events. Additionally, the daily trajectory analysis revealed ca. 35% reversal events take place in a month. In brief, the investigations show a reversal of the south BoB branch of monsoon circulation during certain El-Niño year takes place on the sub-monthly scale.

Seasonality in rain isotopes

From 2014 onwards, efforts were made for continuous rainwater sampling in the post monsoon season at the Port Blair site, i.e., between October and December (winter monsoon). The change in wind direction (Figure 3.1), in turn, source moisture over the Andaman region results in seasonality in the isotopic composition of rainwater. Initial investigations (2014 - 15) show an abrupt shift in the average $\delta^{18}\text{O}$ values during the transition from summer to winter monsoon. To investigate the robustness of the observed variations in rain isotopes due to seasonality in rainfall, years 2016 and 2017 rain - isotope data have been analyzed with a focus on winter monsoon rainwater sampling. The details of the sampling between 2014 and 2017 with the calculated average $\delta^{18}\text{O}$ values during summer and winter monsoon at the Port Blair site are given in Table 3.2.

TABLE 3.2: Port Blair $\delta^{18}\text{O}$ average values during summer and winter monsoon.

S.No.	Year	Summer Monsoon Avg $\delta^{18}\text{O}$ (‰)	Winter Monsoon Avg $\delta^{18}\text{O}$ (‰)	Summer - Winter Diff - $\Delta\delta^{18}\text{O}$ (‰)
1.	2014	-2.64	-5.53	2.89
2.	2015	-2.71	-4.20	1.49
3.	2016	-1.83	-5.11	3.28
4.	2017	-2.54	-4.69	2.15

Figure 3.19 shows the time series of $\delta^{18}\text{O}$ between May and December for the years 2014 to 2017. This result suggested an anomalous seasonality (enriched in summer & depleted in winter) in rain isotopes for Port Blair. Climatological (average of 2012 to 2017) variations of monthly mean $\delta^{18}\text{O}$ values of rainwater at Port Blair are shown in Figure 3.20a. Similar pattern of variability has also been reported for the south west coast of India. Warriar et al. (2016) reported the isotopic variations of rainfall at Kozhikode (11.28°N, 75.86°E; Figure 3.20b) having higher values in summer and

lower values in winter. These observations indicate that the isotopic value of rain-water in this latitude range (ca. 11°N - 13°N) show an opposite behavior than that observed in other parts of India, especially in the northern Indian region. One of the reasons for the depleted values in the post monsoon/winter time is the occurrence of tropical cyclone that is known to cause anomalously low rainwater isotopic values in this region (as discussed above).

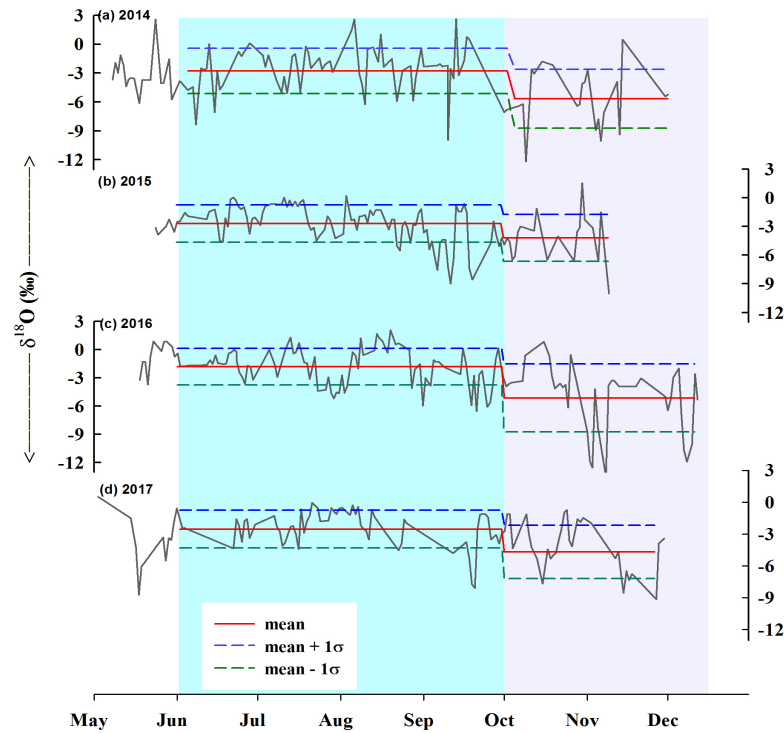


FIGURE 3.19: $\delta^{18}\text{O}$ time series (2014-2017): Y-axis in ‰ suggests seasonal contrast and an abrupt shift from the transition of summer (left) to winter (right) monsoon, shown by two different shades of colors.

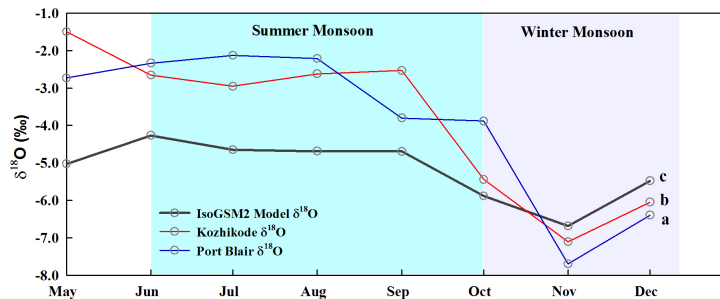


FIGURE 3.20: $\delta^{18}\text{O}$ monthly climatology (a) Port Blair, (b) Kozhikode (c) IsoGSM2 Model data, summer (left) and winter (right) monsoon shown by two different shades of colors.

Furthermore, a similar change was also observed in monthly oxygen isotopes derived from IsoGSM2 model data plotted (climatology, 1979-2013) for two different seasons (Figure 3.20c). The $\delta^{18}\text{O}$ values are calculated over the Port Blair region (10-12°N, 91-93°E), for the summer season $\delta^{18}\text{O}$ values are above -5‰, whereas for the winter season the $\delta^{18}\text{O}$ values are below -6‰. Area averaged rain $\delta^{18}\text{O}$ value show seasonal difference of $\sim 1.3\text{‰}$ over Port Blair region.

As discussed above, the rain isotopic ratios strongly depend on the isotopic values of the source moisture. The rain-isotope depletion in Port Blair region of $\sim 3.0\text{‰}$ (point source) and $\sim 1.3\text{‰}$ (area average) through observation and model data respectively, were found during the transition from summer to winter monsoon. The isotopic composition of rainfall is known to be a function of various ocean-atmospheric parameters. This seasonal contrast appears to be driven by the atmospheric variables that also show strong seasonality. Thus, the abrupt changes in rain-isotopes and its association with the other meteorological parameters (such as, wind, outgoing longwave radiation, moisture parameters, etc) may have the potential to estimate the monsoon withdraw phase in this region.

Section Conclusions

Dual site analysis of daily rainwater isotope, instead of the traditional method of the single (destination) site analysis, seems to offer an alternative method and a better understanding of the moisture dynamical processes. The basic foundation of this assertion is the presence of a significant correlation between the isotopic records on the source area (BoB) and at the target area (CMZ), though the rainfall in these places seems to be independent. The nature of the correlation between the two isotopic records appears to be modulated by the propagation of the rain/cloud band from the BoB to the Indian landmass and the associated moisture transport pathways. That has a seminal role in the monthly mean circulation of ISM, thus, may control the seasonal/monthly spatial moisture and rainfall distribution especially in the central Indian region. The moisture transport time and the time frame to build a large scale convective system (10-20 days) are intricately related. The spectral characteristics of the isotopic time series provide compelling evidence that the isotopic composition of moisture/rainfall respond to this timeframe, and in turn get modulated by these processes.

3.4.3 Rain - Vapor Interaction

Based on a robust oxygen and hydrogen isotopic data sets of ambient vapor and rainwater from Port Blair for 2015, this section discusses (i) the isotopic relationship between water vapor and rain, (ii) the role of source moisture on the isotopic compositions of ambient vapor and rainwater, and (iii) the extent of isotopic fractionation arising primarily due to exchange between the raindrops and the ambient water vapor over the Andaman Islands region.

During the ISM season, strong southwesterly (SW) winds from the south BoB are the dominating moisture source over the Andaman Islands. The origin of air masses is assumed to be approximate to the moisture source direction for the water vapor and rainfall at the study site (Draxler et al., 2010). Though, a large amount of moisture over the site is expected to have come from the south BoB. As the underlying ocean surface water contribution to the convective systems are the major source of moisture, particularly over the BoB region, which maintains a relatively high sea surface temperature during ISM (Shenoi et al., 2002). A few studies also reported that the northeastern BoB contributes significant amount of vapor to the summer monsoon rains (Achyuthan et al., 2013). Ocean surface water oxygen isotopic composition average value over the south BoB was determined for the ISM months and found to be 0.10‰ (Achyuthan et al., 2013). The Craig-Gordon Model (C-G Model) used for the calculation (Equation 1.6) of emanating vapor from the ocean surface water near the site (south-west of Port Blair) over the chosen area ($2^\circ \times 2^\circ$) (Appendix A.8). Sampling strategy, number of the respective samples collected, and notations used are given in Table 3.3.

TABLE 3.3: Characterization of rainwater and ambient vapor samples, corresponding notations used for oxygen isotopic values and number of samples collected with sampling hours are reported.

Sampling Strategy	Vapor (Rain)	Ambient Vapor / Rainwater
		<i>No. of samples collected (duration of sample collection hours)</i>
Sampling on daily basis	$\delta^{18}O_v$ ($\delta^{18}O_r$)	107 (3) / 110 (24)
Rain and vapor for same dates	$\delta^{18}O'_v$ ($\delta^{18}O'_r$)	85 (3) / 85 (24)
Rain during vapor sampling*	$\delta^{18}O_{v-r}$ ($\delta^{18}O_{r-v}$)	27 (3)

*Rain samples were collected in a separate sampler

$\delta^{18}\text{O}$ and $\delta^2\text{H}$ of rain and vapor

Rain $\delta^{18}O_r$ (δ^2H_r) values show a range of +0.20‰(+7.59‰) to -8.99‰(-65.68‰) with an average value of -2.86 ± 1.91 ‰(-13.24 ± 15.45 ‰). The Local Meteoric Water Line (LMWL) is given as $\delta^2H_r = (7.70 \pm 0.23) \times \delta^{18}O_r + (8.82 \pm 4.079)$. The observed slope and intercept of the LMWL for the Port Blair site are not significantly different from the Global Meteoric Water Line (GMWL), i.e. $\delta^2H = 8 \times \delta^{18}O + 10$ (Craig, 1961).

It indicates that the contribution of secondary moisture or evapo-transpired moisture source is negligibly small (Kumar et al., 2010). However, slightly low values of slope and intercept may be a result of post-condensation effects, such as isotopic exchange and/or raindrop re-evaporation (Araguás-Araguás et al., 2000). The process

of raindrop evaporation and isotopic exchange between raindrops and the ambient vapor both make the rainwater enriched in heavier isotopes, but during the high humidity condition the exchange process prevails over the raindrop evaporation (Friedman et al., 1962; Miyake et al., 1968). Further, our result shows that $\delta^{18}\text{O}_r$ and deuterium excess (d-excess) correlation is very weak, $R^2 = 0.015$, implying insignificant raindrop re-evaporation (Gat, 1996). Hence, the observed isotopic variations in this site are likely to be predominantly driven by the isotopic exchange between raindrops and ambient vapor for the ISM season of 2015.

In case of GLV, the range of isotopic values, i.e. $\delta^{18}\text{O}_v$ ($\delta^2\text{H}_v$), varied from -9.78‰ (-64.06‰) to -17.39‰ (-113.98‰) with an average value of $-12.48 \pm 1.59\text{‰}$ ($-79.12 \pm 10.23\text{‰}$). The vapor line in $\delta^{18}\text{O}$ - $\delta^2\text{H}$ space defined by the equation $\delta^2\text{H}_v = (5.69 \pm 0.29) \times \delta^{18}\text{O}_v - (8.43 \pm 3.67)$ shows a strong linear correlation ($r = +0.88$). The difference between the isotopic compositions of rainwater and GLV, i.e. $\Delta(\delta_r - \delta_v)$ is $9.5 \pm 3.5\text{‰}$ for ^{18}O and $65.8 \pm 25.6\text{‰}$ for ^2H . The observed values of $\Delta(\delta_r - \delta_v)$ for ^{18}O and ^2H are close to the calculated equilibrium enrichment factor (ϵ) at average air-temperature (28.4°C); i.e., $^{18}\epsilon = 9.10\text{‰}$ and $^2\epsilon = 75.6\text{‰}$. Thus, our observations suggest that GLV and rainwater maintained a near isotopic equilibrium. However, it is to be noted that the monsoon season also comprises of break phases, which are characterized by low rainfall and decreased humidity. For this condition, the isotopic equilibrium between raindrops and ambient vapor will be weakened resulting some discrepancy in observed and theoretically calculated values (e.g., $^2\epsilon - (\delta^2\text{H}_r - \delta^2\text{H}_v) = 9.8\text{‰}$). This may justify the uncertainty levels, 3.5‰ and 25.6‰ for $\delta^{18}\text{O}$ and $\delta^2\text{H}$ respectively. Therefore, it is important to consider the non-rainy and rainy conditions separately, during the vapor sampling hours to investigate the rain and vapor interactions. Hence, the rain-vapor isotopic interaction has been investigated in the present study by way of rain and vapor samples collected simultaneously, although, the coexistence of rain events during vapor sampling hours were relatively less.

Rain and vapor isotopic characteristics

The rainwater and GLV samples are categorized into two groups. The rainwater samples integrated for 24 hrs, (termed as 'daily scale') and rainwater samples integrated for 3hrs (synchronous with vapor sampling hours) belong to the first group. The second group consists of GLV samples collected during the rainy and non-rainy conditions. A comparative analysis of their isotopic characteristics is presented in this section. Figure 3.21 shows the scatter plots of $\delta^{18}\text{O}$ and $\delta^2\text{H}$ and their corresponding regression lines for various combinations. Isotopic compositions of rainwater during vapor sampling hours show a slope, $s_1 = 6.90$ (green) that is lower than that of the daily scale rainwater slope ($s_2 = 7.67$, red) (Figure 3.21(a)).

The meteoric water line with a lower slope (s_1) implies rainwater during the vapor sampling hours may have been isotopically enriched as a result of the isotopic exchange between raindrops and the ambient vapor. This is to be noted that the

contribution of evapo-transpired moisture over the site was negligible and $\delta^{18}\text{O}$ and d-excess for the rainfall collected during the vapor sampling hours also exhibited a poor correlation ($R^2 = 0.043$, $n = 27$). However, when the $\delta^{18}\text{O}$ - $\delta^2\text{H}$ relationship is examined on daily timescale, the slope ($s_2 = 7.67 \pm 0.27$) does not differ significantly from 8 (i.e., the slope of GMWL). This observation indicates that the isotopic composition of rainfall on the daily timescale did not show the effect of isotopic interaction. The reason for this distinct behavior due to different sampling timescales may be explained as follows. The synchronized rainwater and vapor collection (3hrs) period experienced mostly rainy and high humid condition throughout this time period. Whereas, the 24hrs rain collection period was punctuated by no-rain condition perhaps for several hours. Hence, the isotopic interaction during the 24hrs rain collection period was much less compared to the 3hrs synchronized collection of vapor and rainwater.

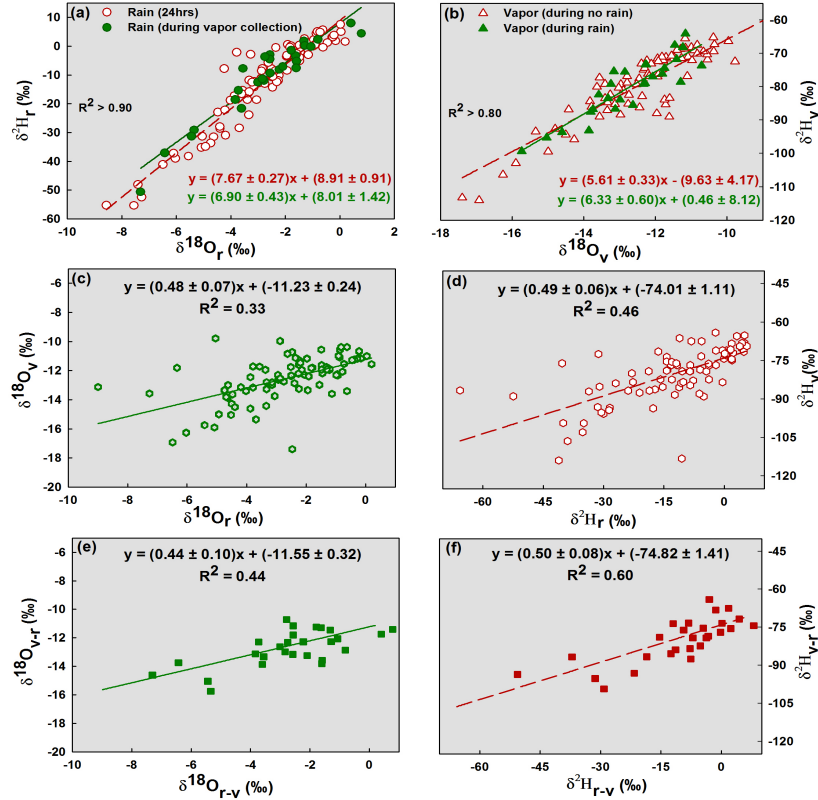


FIGURE 3.21: (a) and (b) show a linear regression between $\delta^{18}\text{O}$ and $\delta^2\text{H}$ of rain and vapor respectively for the two sets. First, the 24 hours rain and 3 hours rain (during vapor-sampling) and second, vapor for the non-rainy and rainy conditions; (c) and (d) show the cross-correlation between $\delta^{18}\text{O}$ of rain (r) and vapor (v) (green open hexagon) as well as same for $\delta^2\text{H}$ (red open hexagon) respectively; (e) and (f) show the cross-correlation between $\delta^{18}\text{O}$ of rain during vapor sampling (r-v) and vapor during rain (v-r) (green filled square) as well as same for $\delta^2\text{H}$ (red filled square) respectively.

On the other hand, slope of the vapor line during the rain event shows a higher value ($s_3 = 6.33$, green) than that of the vapor line of the non-rainy days ($s_4 = 5.61$, red) (Figure 3.21(b)). The difference in slopes can be explained as, during rainfall and humid condition net diffusion from the boundary of raindrops to the atmosphere would dominate than the raindrop re-evaporation. Hence, the more diffusive $^1\text{H}^1\text{H}^{16}\text{O}$ species would escape from the raindrops faster than the heavy isotope species of $^1\text{H}^1\text{H}^{18}\text{O}$ and $^1\text{H}^2\text{H}^{16}\text{O}$. The opposite phenomenon takes place in the vapor phase. We also calculate the changes in slope for the water line as well as for the vapor line as a result of isotopic distribution between ambient vapor and rainwater. The differences ' $s_2 - s_1$ ' and ' $s_4 - s_3$ ' were found to be nearly the same, 0.77 and 0.72 respectively. This clearly implies that the isotopic interaction between rain and vapor plays a dominating role, while other factors exert only nominal effect.

Out of 107 GLV and 110 rainwater samples collected, 85 samples were of common dates, corresponding isotopic values are denoted as $\delta^{18}\text{O}'$ and $\delta^2\text{H}'$ (Table 3.3). Figure 3.21(c) and (d) show linear relationships between $\delta^{18}\text{O}'_r$ and $\delta^{18}\text{O}'_v$ ($r = +0.55$, $n = 85$, $p < 0.01$) and $\delta^2\text{H}'_r$ and $\delta^2\text{H}'_v$ ($r = +0.65$, $n = 85$, $p < 0.01$) respectively. The result implies a significant co-variation in the isotopic composition of vapor and rain phases. The isotopic values of vapor considering isotopic equilibrium ($\delta^{18}\text{O}_{eq}$) using $\delta^{18}\text{O}'_r$ and ambient air-temperature (Majoube, 1971) and its comparison with the observed values $\delta^{18}\text{O}'_v$ ($r = +0.57$, $n = 85$, $p < 0.01$) shows that rainwater and ambient vapor isotopic values are indeed consistence on the seasonal timescale. Such kind of agreement was also observed by Lekshmy et al. (2018) in the coastal region of Kerala, southwest India. Both of these exercises imply that GLV and rainwater were close to isotopic equilibrium.

Further, the vapor-rain interaction has been estimated for the 3hr sampling interval when both GLV and rainwater were collected separately (Figure 3.21(e) and (f)). The isotopic notations used in this exercise are: $\delta^{18}\text{O}'_{r-v}$ represents the oxygen isotopic values of rain collected (3 hrs) during vapor sampling. While $\delta^{18}\text{O}'_{v-r}$ represents the oxygen isotopic values of GLV collected during rainy condition (Table 3.3). Similar notations are used for hydrogen isotopes as well. The correlation between $\delta^{18}\text{O}'_{r-v}$ and $\delta^{18}\text{O}'_{v-r}$ was found to be reasonably strong ($r = 0.66$, $n = 27$, $p = 0.02$). The same for the hydrogen isotopes i.e. $\delta^{18}\text{O}'_{r-v}$ vs. $\delta^{18}\text{O}'_{v-r}$ was $r = 0.77$ ($n = 27$, $p < 0.01$). Interestingly, coefficients of the regression equations for both the cases, that is non-rainy and rainy conditions are almost the same, shown in Figure 3.21(c) and (d) and Figure 3.21(e) and (f) respectively (equations are shown in the respective figures). Though the different number of samples in these cases may give rise to sampling artifact, however, the agreement observed in both the cases (hydrogen and oxygen) almost rules out this possibility. A close correlation value also implies that the isotopic time-series of GLV during the rainy condition could be used to estimate theoretically the isotopic composition of rainwater for the entire monsoon season. However, one

important factor is the isotopic composition of the source moisture, which could be one of the causes for the isotopic variations in ambient vapor and in turn, of the rainfall. Since consideration of the daily variation in the isotopic composition of source moisture is likely to give a better understanding of the rain-vapor isotopic interaction over a specific site (viz. coastal regions), subsequent section is focused on the controls of the source moisture in the isotopic composition of ambient vapor and the regional rainfall.

Role of source moisture

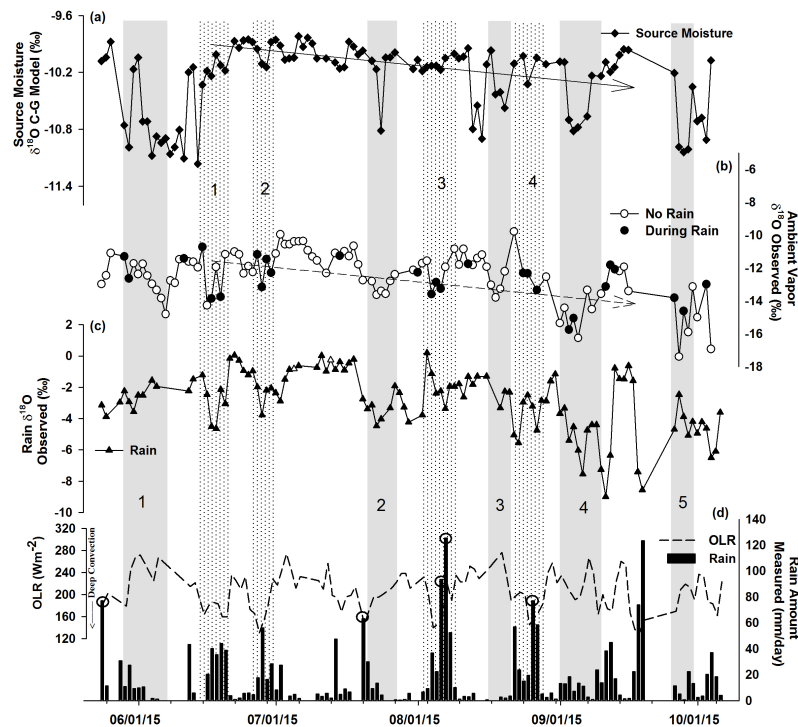


FIGURE 3.22: Time series of isotopic records of rain, vapor and atmospheric variables: (a) source moisture oxygen isotope ratio (C-G Model); (b) isotopic composition of the ambient vapor during the non-rainy (open circle) and rainy (closed circle) hours; the arrows indicate a declining trend in isotopic composition during the monsoon season (c) oxygen isotope record of rainfall (closed triangle); (d) the outgoing longwave radiation (OLR; dashed curve) superimposed on the daily rainfall record (bars; small circle overhead the bars are rainfall recorded during the events of deep convection). Columns (in grey and stippled) highlight the co-variation of isotopic time series of different components (source moisture - vapor - rain) during less/no rain and heavy/continuous rain conditions respectively.

The meteorological parameters (namely, Rain and OLR) and isotopic variations in source moisture, ambient vapor, and rainwater over the site (Figure 3.22) and their comparative evaluation on daily timescale are presented. The source moisture oxygen isotopes (i.e., R_e is considered as source moisture over the site) show variations on daily time scale with a declining trend in isotopic composition between the period

June through September (-9.82‰ to -11.16‰ , Avg. = -10.27‰), besides several deep depletions were observed with standard deviation (σ) of 0.38‰ . The highly depleted $\delta^{18}\text{O}$ values (below $\pm 1\sigma$ of the average) of source moisture correspond to higher SST ($r = -0.61$), this situation is in conformity with less or no rainfall conditions over the site (Black bars, Figure 3.22(d)), also corroborated by high OLR ($> 200\text{Wm}^{-2}$) values (dashed line, Figure 3.22(d)). The general trend (arrows) and the deep depletion in $\delta^{18}\text{O}$ values (filled gray bars) of the source moisture (Figure 3.22(a)) are in concordance with the GLV (Figure 3.22(b)), but rainwater $\delta^{18}\text{O}$ ratios (Figure 3.22(c)) are not always in agreement with the other two variables.

The GLV and the rainwater oxygen isotopes have shown analogous variations during the deep convection (dotted gray bars) and OLR between $\sim 180\text{--}200\text{Wm}^{-2}$. For the periods of daily rain condition (active period of ISM), all ($\delta^{18}\text{O}$ of source moisture - ambient vapor - rainwater) have shown a similar variation, e.g., 1 and 2 dotted bars and 2, 3, and 4 filled bars (Figure 3.22). Some cases of very deep convection (OLR $< 180\text{Wm}^{-2}$) do not show any concurrency between the $\delta^{18}\text{O}$ ratios of source moisture - ambient vapor - rainwater, few of them are marked with a small circle over the rain bars (Figure 3.22, listed in Table 3.4).

So far, the isotopic values of source moisture, ambient vapor and rainwater are discussed only qualitatively, however, a quantitative understanding is warranted under the different atmospheric conditions (e.g. rainy versus non-rainy condition). It will give a better understanding of atmospheric controls on isotopic composition and the role of source moisture on the isotopic composition of rainfall. Henceforth, the calculated as well as measured isotopic compositions (namely, $\delta^{18}\text{O}$) are separated out depending upon heavy rain, moderate rain, light rain, and no rain conditions during the ISM of 2015. To characterize the rainfall, the IMD criteria of heavy to light rain has been followed (<http://imd.gov.in/section/nhac/termglossary.pdf>), and shown in Table 3.4.

TABLE 3.4: Correlation Coefficients between $\delta^{18}\text{O}_e$ (Source moisture), $\delta^{18}\text{O}_v$ (Ambient vapor), and $\delta^{18}\text{O}_r$ (Rain) for different rainfall (mm/d) scenarios of the year 2015.

Rain →	(a)heavy (>35.6) n = 16	(b)moderate ($35.5\text{--}7.6$) n = 28	(c)light ($7.5\text{--}2.6$) n = 19	(d)very light ($2.5\text{--}0.1$) n = 19	(e)no rain n = 19
Correlation (r)					
I. $\delta^{18}\text{O}_v$ & $\delta^{18}\text{O}_r$	0.22	0.64	0.71	0.81	-
II. $\delta^{18}\text{O}_e$ & $\delta^{18}\text{O}_v$	-0.14	0.46	0.66	0.62	0.43
III. $\delta^{18}\text{O}_r$ & $\delta^{18}\text{O}_e$	-0.03	0.33	0.76	0.51	-

Numbers in bold are significant at the 95% confidence level

At Port Blair, the oxygen isotopic ratios of GLV ($\delta^{18}\text{O}_v$) and rainwater ($\delta^{18}\text{O}_r$) are

significantly correlated over a wide range of rainfall amount, i.e. moderate to very-light rain (Table 3.4, row I). The high correlation observed between $\delta^{18}\text{O}_v$ and $\delta^{18}\text{O}_r$ is most likely arising due to isotopic interaction leading to equilibrium condition between vapor and rainwater. $\delta^{18}\text{O}$ variations in source moisture, GLV, and rainwater also show a strong correlation with each other for the light rainfall condition (Table 3.4, column (c)), thus, implies an equilibrium condition between "source moisture - ambient vapor - rainwater" with a minimum contribution of secondary moisture from the other sources. On the other hand, the low correlation between source moisture and GLV oxygen isotope values during no-rain condition (Table 3.4, column (e)) implies the large fraction of secondary moisture generated locally (evapo-transpiration) may be due to low humid conditions. The lack of a relationship between the calculated and measured isotopic ratios during the heavy rainfall day (Table 3.4, column (a)) indicates a failure of C-G Model and known physical mechanisms of isotopic fractionation. So, even considering the local moisture contribution constant, it can be seen that the isotopic variation of ambient vapor, in turn, the isotopic composition of rainwater also depend on the source moisture. Moreover, during the rainfall period of moderate to very-light intensity, the crucial controlling factor for the variation in the isotopic composition is rain-vapor interaction over the site. A high correlation was found between $\delta^{18}\text{O}_v$ and source moisture ($\delta^{18}\text{O}_e$) during light rainfall (discussed above) and also after combining the moderate and very-light rainfall conditions ($r = 0.48$, $n = 66$, $p = 0.052$). Similarly, in case of $\delta^{18}\text{O}_e$ and $\delta^{18}\text{O}_v$, $r = 0.54$, $n = 66$, $p = 0.014$. The significant positive correlation between the evaporated vapor (C-G Model) and rainwater isotopic ratios strongly suggests source moisture controls on the isotopic composition of rainfall over the site.

Considering non-rainy and rainy conditions during vapor sampling hours, measured GLV oxygen isotopic ratios are plotted and shown by open and filled circles respectively in Figure 3.22(b). Theoretically, the rainwater should be enriched while vapors are depleted in heavy isotopes due to isotopic exchange process. Though a quantitative evaluation of the isotopic exchange process may not be possible for the individual event, but one can address only the statistical properties. Towards this, calculation of the isotopic variations through the interaction between rain and ambient vapor is presented in the next section.

Rain and vapor isotopic interaction

The mean seasonal isotopic variations in "source moisture - ambient vapor - rainwater" have been examined and attempted to quantify the isotopic interaction for two cases; GLV samples collected during (i) non-rainy and (ii) rainy conditions. The arithmetic averages of oxygen isotope ratios of evaporated moisture from the ocean surface ($\delta^{18}\text{O}_e$) during non-rainy (no. of sample = 80) and rainy conditions (number of samples = 27) at the site are -10.26‰ and -10.32‰ respectively. The values are the same within the $\pm 1\sigma$ uncertainty limit, implying the source moisture isotopic properties did

not vary significantly on the seasonal timescale for the Andaman region. But, as mentioned earlier, they did show some variation on a daily timescale. Now, assuming that the same moisture was advected to the observation site, the $\delta^{18}\text{O}_v$ was recalculated (GLV) as -12.32‰ and -12.73‰ for non-rainy and rainy conditions respectively. The observed depletion for the GLV is presumably due to the preceding rainout process and moisture mixing from the surface. However, these factor is likely to be operative for both the conditions (non-rainy and rainy) during vapor sampling, thus, a more depleted value (0.41‰ , 1σ analytical uncertainty level is 0.1‰) of average $\delta^{18}\text{O}_v$ during the rainy condition clearly indicates that the ambient vapors indeed suffered from isotopic fractionation due to isotopic interaction. This led to isotopic enrichment in the collected rainwater samples. This was corroborated by our observation, i.e., the rainwater samples during the vapor sampling hours, on an average were isotopically enriched (-2.65‰) than that of the 24hrs cumulative rainfall (-2.77‰) collection. The isotopically depleted vapors are subsequently fed to the cloud system and the rainwater produced from this secondary moisture would also be isotopically depleted. This is one of the reasons of a relatively strong amount effect observed for the year 2015 (Rainfall vs. $\delta^{18}\text{O}$, $r = -0.48$) compared to the years 2012 and 2013, which were characterized by lower amount effect (Section 3.4.4).

According to Rayleigh-type distillation during the rainout process,

$$\delta^{18}\text{O}_v \approx \delta^{18}\text{O}_e + \delta^{18}\text{O}_r \quad (3.7)$$

Where, $\delta^{18}\text{O}_v$, $\delta^{18}\text{O}_e$, and $\delta^{18}\text{O}_r$ are the oxygen isotopic values for the vapor after the first rainout, evaporated moisture from the ocean surface, and rainwater respectively. However, there will also be the other factors, such as re-evaporation of raindrops, isotopic interaction, and evapo-transpiration that may have some additional effect which may have negative or positive feedback (F) on the ambient vapor and rainwater isotopic compositions. Hence the equation (2) needs to be modified by an additive factor, F.

$$\delta^{18}\text{O}_v \approx \delta^{18}\text{O}_e + \delta^{18}\text{O}_r \pm F \quad (3.8)$$

In order to calculate the feedback factor, few assumptions would be considered for the study site. i) The site receives the first rain from the source moisture and ii) During the rainy and humid conditions, the only factor that affects the isotopic compositions is the isotopic exchange due to the interaction between ambient vapor and raindrops.

Using the assumption (i), the feedback factor is estimated for the Port Blair site using the calculated average isotopic values for the non-rainy condition, i.e., $\delta^{18}\text{O}_v = -12.32\text{‰}$, $\delta^{18}\text{O}_e = -10.26\text{‰}$, and $\delta^{18}\text{O}_r = -2.77\text{‰}$. From Equation 3.7, the feedback factor (F) has been found to be 0.71‰ (notably this value is much higher than the experimental uncertainty level of 0.1‰). On the other hand, for the rainy condition during

vapor sampling hours, the average isotopic values are $\delta^{18}\text{O}_{v-r} = -12.73\text{‰}$, $\delta^{18}\text{O}_e = -10.32\text{‰}$, and $\delta^{18}\text{O}_{r-v} = -2.65\text{‰}$. So, the calculated feedback factor (F) for the rainy and humid conditions is 0.24‰ (Equation 3.8). Hence, it can be inferred from these calculations that the contribution of other factors to alter the isotopic composition of rain and vapor is 0.47‰ ($0.71 - 0.24$). This is approximately 70% of the maximum variation of 0.71‰ , and the remaining 30% may be accounted for solely due to the isotopic interaction between vapor and rain.

Section Conclusion

For the summer months (ISM season) of 2015, the study of ground level vapor (GLV) and rainwater isotopic variations provided a means to make a quantitative estimate of their interaction over the BoB region. Using the isotopic values of rainwater and vapor and theoretically calculated (Craig-Gordon Model, 1965) isotopic composition of source moisture, we explored the interaction among the source moisture, ambient vapor, and rainwater in the Bay of Bengal region. The isotope study of vapor and rainwater provided valuable insight in understanding their interaction vis-à-vis source and ambient vapor control on the variations in isotopic composition of regional rainfall. The isotopic relationship between the source moisture, ambient vapor, and rainfall varied on the basis of isotopic variability in the source moisture and the rainfall amount on a daily timescale. Oxygen isotope ratios of ambient vapor and rainwater were significantly correlated over a wide range of rainfall amount, i.e. moderate to very-light rain. But, for heavy rainfall conditions ($>35\text{mm/day}$), a weak correlation was found, indicating limitations of the Rayleigh fractionation and Craig-Gordon model. The result shows that the isotopic exchange between ambient vapor and raindrops could lead to measurable depletion in the isotopic composition of ambient vapor (0.41‰), this, in turn; helps determine the subsequent isotopic enrichment in rainwater. Further, we estimated that the isotopic interaction may account for up to 30% in the observed variability of the isotopic composition of rain and vapor over the site.

3.4.4 Spatial and temporal variability in amount effect

The amount effect results primarily due to the preferential removal of the heavier isotopes during moisture condensation followed by the rainout process. Amount effect induced depletion is typically observed in monsoonal regions during the seasonal intensification of monsoonal frontal and convective systems (Hoffmann and Heimann, 1997) and in tropical depressions (Vuille et al., 2003). An extreme case is tropical cyclone precipitation, where moisture may undergo multiple depletive convection cycles (Lawrence and Gedzelman, 1996). The effect is scale dependent and a better knowledge of its scale dependency may help us improve its application in paleo-monsoon study. The basic premise of the amount effect is that heavy rainfall depletes the isotopic composition of the rainfall, but never been documented using

modern days isotopic vis-à-vis rainfall data over a large spatial and temporal domain. It is, therefore essential to understand the mechanism(s) that control the amount effect over a wide region. On the other hand, quantification of the amount effect is required for specific sites where speleothem/tree-ring based rainfall reconstruction is envisaged.

The reason for not attempting such an exercise is the lack of a robust precipitation isotope dataset on the daily scale over a wide region. The Global Network of Isotopes in Precipitation (GNIP) is a robust data repository that monitors the isotopic composition of precipitation. The data produced from this network over the Indian region are very limited and that too for short periods. Only a few reasonably long-term data available from GNIP on monthly timescale are for New Delhi (1960 - 2012) and Bombay (1960 - 1978), representing two different regions of the Indian Monsoon (Bhattacharya et al., 2003). There are different types of effects which the isotopic composition may vary spatially and at different timescales (such as continental, altitude, seasonal, and amount effect). However, these effects once established for a particular place or region may not change much except amount effect, unless climatic and hydrological regimes change considerably.

Compilation of GNIP database: Indian Region

A total of 36 stations data are available on GNIP for the Indian region, however, few sites have only isotope ratios ($\delta^{18}\text{O}$, $\delta^2\text{H}$) or only precipitation data. A compilation of GNIP data is presented to delineate a broad picture of the amount effect and its variability on spatial and temporal scale (Figure 3.23).

The first column of Figure 3.23 displays the name of the Indian sites and second is corresponding Köppen's climatic zone classification (<http://koeppen-geiger.vu-wien.ac.at/present.htm>). The correlation between the amount of rainfall and $\delta^{18}\text{O}$ are reported on different timescales, such as on monthly and annual scales. In the Figure 3.23, the green texts are showing negative (-ve) correlation, i.e. amount effect is valid, and red labels having positive values reveal absence of amount effect in those sites. It has been found that, few sites validate the amount effect on monthly but not on annual timescale (less number of data points). The sites having less than six data points are discarded and marked as not available (NA). Most of the sites available at GNIP are not showing significant amount effect due to short data periods as well as some sites rainfall is strongly seasonal (winter monsoon is more depleted in ^{18}O than summer). So, a definitive conclusion may be lacking to characterize a region/site based on rainfall and its isotopic composition (except for a few sites, such as New Delhi, Mumbai, Hyderabad) using the GNIP database.

Observation: Rain Isotopes

As discussed above, the amount effect shows a varying characteristic in the Indian subcontinent. While most of the places obey this relation on monthly and longer

Global Network of Isotopes in Precipitation (GNIP)									
Name of site	Climate Zone	Start Year	End Year	Rain Vs d18O Correlation (+ve or -ve)					
				Monthly			Annual		
				r	n	p	r	n	p
MINICOY ISLAND	Am	1965	1968	NA	NA	NA	NA	NA	NA
MUMBAI	Am	1960	1978	0.15	50	0.288	0.52	11	0.050
OOTACAMUND	Cwb	1959	1960	NA	NA	NA	NA	NA	NA
HYDERABAD	Aw	1997	2001	0.41	33	0.008	0.53	4	NA
NA SARAM	Aw	1977	1977	0.93	5	NA	NA	NA	NA
CHINPAK	Aw	1977	1977	0.54	5	NA	NA	NA	NA
BHOPALPALLI	Aw	1977	1977	0.58	5	NA	NA	NA	NA
TUNDLA BUZURG	Aw	1977	1977	0.89	5	NA	NA	NA	NA
SALAGIRI	Aw	1977	1977	0.67	5	NA	NA	NA	NA
KAMALAPUR	Aw	1977	1977	0.76	5	NA	NA	NA	NA
ALLAHABAD	Csa	1980	1980	0.77	5	NA	NA	NA	NA
NEW DELHI	BSh	1960	2012	0.47	341	<0.0001	0.40	45	0.005
SHILLONG	Cwb	1966	1978	0.20	31	0.140	0.38	7	0.200
KOZHICODE(CALICUT)	Am	1997	2007	0.33	87	0.001	0.53	11	0.050
BELGAUM	Aw	2003	2005	0.18	12	0.287	0.61	3	NA
DEVPRAYAG	Cwb	2004	2006	0.63	14	0.007	0.64	3	NA
GANGOTRI	Dwc	2004	2006	0.42	13	0.070	0.72	3	NA
GOMUKH	ET	2004	2006	0.09	12	0.400	0.80	3	NA
GUWAHATI	Cwa	2003	2004	0.19	11	0.278	NA	NA	NA
JAMMU	Cwa	2003	2006	0.45	27	0.009	0.27	4	NA
KAKINADA	Aw	2003	2006	0.41	24	0.023	0.78	4	NA
KOLKATA	Aw	2004	2006	0.18	13	0.278	0.99	3	NA
LUCKNOW	Cfa	2003	2004	0.34	8	0.200	NA	NA	NA
MANERI	Cwb	2005	2006	0.70	11	0.007	NA	NA	NA
PATNA	Cwa	2003	2005	0.72	5	NA	NA	NA	NA
RISHIKESH	Cwb	2005	2006	0.50	8	0.103	NA	NA	NA
ROORKEE	BSh	2003	2006	0.09	12	0.390	0.35	3	NA
SAGAR	Aw	2003	2006	0.35	14	0.109	0.30	3	NA
TEHRI	Cwb	2004	2006	0.71	17	0.001	0.99	3	NA
THARAMANI*	As	2001	2004	NA	NA	NA	NA	NA	NA
TIRUNELVELI	Aw	2003	2005	0.26	12	0.207	NA	NA	NA
UTTARKASHI	Cwb	2004	2006	0.41	26	0.010	0.92	3	NA
NAINITAL	Cwb	1995	1995	0.32	6	0.260	NA	NA	NA
BANGLORE (JUN-NOV)	Aw	2003	2004	0.31	13	0.151	NA	NA	NA
DOBRANI	Dwb	2004	2006	0.68	8	0.030	NA	NA	NA
LAKE SAST HAMKOTTA~	Am	2001	2002	NA	NA	NA	NA	NA	NA

*only precipitation data available NA = Not Available ~only isotopes data available

FIGURE 3.23: GNIP database Compilation for the Indian region.

timescale, some places, such as northeast India, west coast of India and parts of south India show notable exceptions (Bhattacharya et al., 2003; Yadava et al., 2007; Breitenbach et al., 2012). A detailed study on isotopic characteristics of Indian precipitation is reported in Kumar et al. (2010). These authors have considered differences in sites geographic and meteorological conditions and their associated atmospheric processes (i.e., ambient temperature, humidity, and source of vapor masses). The sample collection sites presented in Kumar et al., 2010 are shown in Figure 3.24; they analyzed about 900 precipitation samples during the study period (2003-2006) on monthly timescale. The study has shown the amount effect is valid for all seasons in the northern Indian and western Himalayan stations, whereas the effect was seen only during the summer monsoon period for the rest of the stations.

Since amount effect is related to various atmospheric conditions, such as, rainwater re-evaporation (Dansgaard, 1964; Risi et al., 2008), the degree of organized convection (Lawrence et al., 2004; Kurita et al., 2009), moisture flux convergence (Moore et al., 2013) etc. it is also important to examine which processes are operative in the

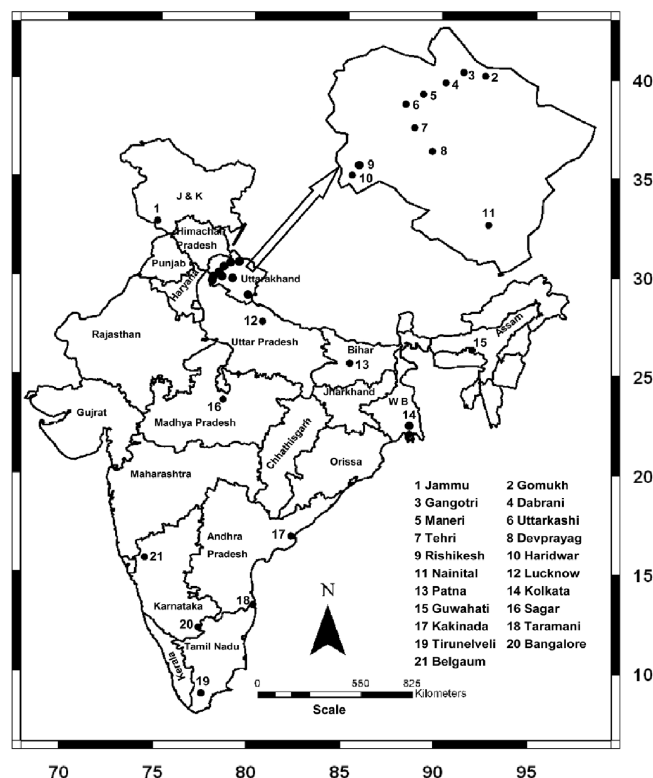


FIGURE 3.24: Location map of sample collection sites (Kumar et al., 2010).

study region. In the present study, the distinct characteristics of amount effect in the Andaman region (namely Port Blair) are investigated.

Port Blair

Amount effect seems to be valid over the Andaman region (Laskar et al., 2013). However, rain isotopes undergo systematic depletions in response to the organized convection occurring over a large area and are modulated by the integrated effect of convective activities. As discussed above, the rain isotopes appear to be linked with the monsoon intraseasonal variability in addition to synoptic scale fluctuations. On the daily timescale, Port Blair rainfall and its isotopic variation is analyzed for the summer monsoon of years 2012-2015.

The year 2012 shows a good negative correlation ($r = -0.30$, $n = 90$, $p = 0.002$) between amount of daily rainfall and their respective $\delta^{18}\text{O}$ values, while 2013 and 2014 show poor ($r = -0.09$, $n = 83$) and relatively good ($r = -0.24$, $n = 89$) correlations respectively. The year 2015 shows the best correlation ($r = -0.40$, $n = 98$, $p < 0.0001$), implying that amount effect undergoes considerable inter-annual variability. The relationship is improved only on longer timescale. On monthly timescale the correlations are -0.73 and -0.59 for 2012 and 2013 respectively. The above observations clearly indicate that amount effect is differently manifested in these years. This kind of variability appears to be arising due to the interannual variability of monsoon. Considering two

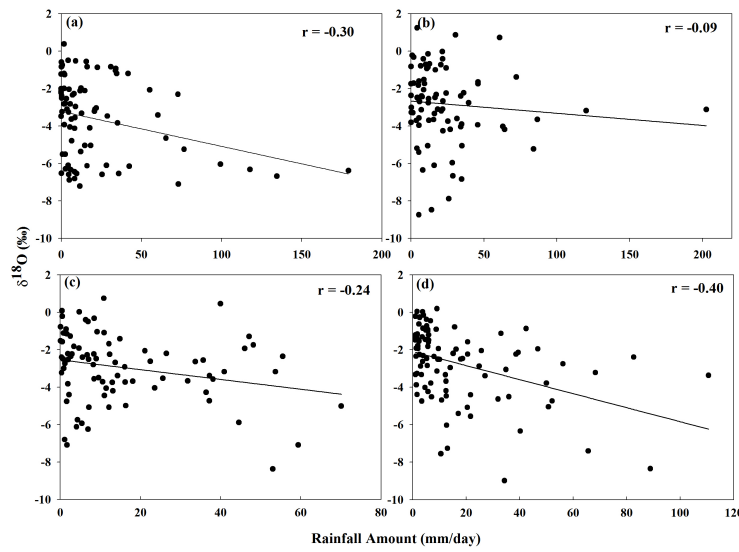


FIGURE 3.25: Scatter diagram between rainfall amount and $\delta^{18}\text{O}$ for the years (a) 2012, (b) 2013, (c) 2014, (d) 2015.

consecutive contrasting years, the year 2012 is characterized by relatively low rainfall (ISMR: 93% relative to long period average, LPA), high intraseasonal variability, positive SST anomaly in distinct areas of the Indian Ocean during the JJAS period representing relatively restricted moisture source regions. On the other hand the year 2013 experienced higher than normal rainfall (ISMR: 106% relative to LPA), the fastest spread of monsoon in Indian landmass in the last 41 years, neutral SST anomaly from most part of the Indian Ocean representing diverse moisture source areas (Monsoon Report, 2012 and 2013, IMD, Pune). The average rain rate (11.4 mm/day; GPCP data) over the Andaman region in 2012 is lower than that for the year 2013 (12.61 mm/day). Since rain re-evaporation is inversely proportional to rain rate (Risi et al., 2008) the average re-evaporation rate of raindrops for year 2012 being higher compared to 2013 resulting relatively stronger amount effect in 2012. When the rainfall is integrated either on temporal or spatial domain the variability is reduced, but the extent of variability in case of time integrated $\delta^{18}\text{O}$ is much less than the rainfall amount. This means that local or the small scale effects induce relatively high degree of noise on rainfall variability but not on its isotopic composition. Similar inference is drawn by Kurita et al. (2009) who noted that rainfall variability at some places in south Asian region gets affected by local conditions, such as topography results no correlation between rainfall and its isotopic ratios on daily time scale. The improved correlation between $\delta^{18}\text{O}$ - rainfall on higher temporal domain as we observe here implies that the isotopic properties of rainfall are controlled more by the integrated effect rather than the discrete events of rainfall. Similar behavior was observed when we examined the relationship between rain $\delta^{18}\text{O}$ and the rainfall variability averaged over T_i days preceding the event (Figure 3.7). This is similar to the analysis done by Moerman et al. (2013) who studied the relationship between daily rainfall - $\delta^{18}\text{O}$ and

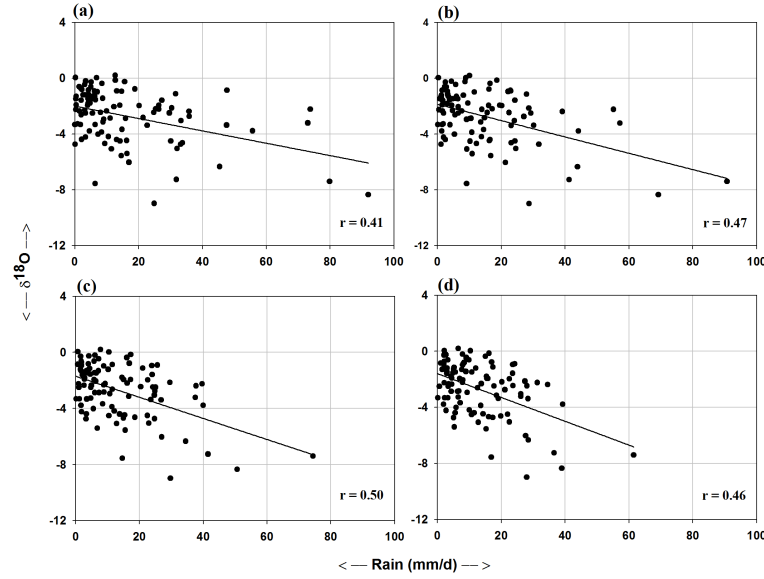


FIGURE 3.26: Scatter diagram showing the relationship between Port Blair- $\delta^{18}\text{O}$ and the area averaged rainfall with increasing area grid size (a) $1^\circ \times 1^\circ$, (b) $3^\circ \times 3^\circ$, (c) $5^\circ \times 5^\circ$, and (d) $7^\circ \times 7^\circ$.

the running means of rainfall variability. Oxygen isotopic composition of daily rain (for September 2012/2013 when it rained almost every day) was correlated with the time integrated rainfall variability for increasing number of days including the day for which $\delta^{18}\text{O}$ is being considered. Figure 3.8 shows the progress of correlation coefficient with the number of days. The correlation is improved with increased number of days and peaks around five days ($r \sim -0.7$). This probably implies that the isotopic composition of the rainwater was controlled more by the moisture dynamics rather than the individual rain events. It also helps estimate the average moisture residence time at BoB ca. 5 days. Secondly the integrative capacity of $\delta^{18}\text{O}$ could be used as a good proxy for the precipitation variability in association with other meteorological parameters. In other words the isotopic tracers carry a 'memory' of past several days of rain. This implies that isotopic composition of rain water in this region is not only controlled by the local processes but also by the large scale processes. Such kind of observations have also been reported especially in the tropical region whereby precipitation isotope fractionation processes have been shown to integrate across wider spatial scales and longer time periods (Cobb et al., 2007; Kurita et al., 2009).

In 2015, we have also investigated the effect of heavy rainfall events on $\delta^{18}\text{O}$ in order to examine whether a few heavy rainfall events could affect the rainfall- $\delta^{18}\text{O}$ correlation significantly. Six events had been identified when rainfall was more than mean $+2\sigma$. The correlation coefficient (r) was recalculated after excluding those events and found to be $r = -0.35$ ($n = 92$, $p < 0.01$). A similar analysis was done with the Port Blair rainfall data (daily updated IMD website data) and r value was found to be -0.37 . This exercise demonstrates that the amount effect dominantly represented by the normal rain events and anomalously high rain events does not affect it significantly. In addition to station data, the Port Blair $\delta^{18}\text{O}$ and the IMD gridded ($1^\circ \times 1^\circ$) rainfall

data has also been plotted (Figure 3.25) to examine the effect of larger scale rainfall variability on rain water isotopic composition. Towards this, the Port Blair- $\delta^{18}\text{O}$ has been correlated with the area averaged rainfall over the Port Blair (IMD gridded data) with increasing grid size. The results show that the correlation coefficient increases when the rainfall is averaged over a larger area, reaching a maximum value ($r = -0.50$, $n = 98$, $p < 0.01$) for an area of $5^\circ \times 5^\circ$. Analysis of other years' rain-isotope data also yield similar result.

With the updated dataset of rain isotopes (2012-2017) from the Port Blair site, the amount effect has been recalculated on monthly timescales, considering May to September of each year (except 2017, rainfall data not available). The monthly record has been generated by the arithmetic mean of daily datasets of $\delta^{18}\text{O}$ and rainfall amount. The scatter diagrams are plotted between monthly rainfall amount and $\delta^{18}\text{O}$, shown in Figure 3.27(a). The regression analysis reveals a significant amount effect on longer time scale ($r = -0.45$), as discussed earlier that the correlation increases for in a few years on monthly timescale (e.g., 2012 & 2013). The correlation is improved if the weighted average values of $\delta^{18}\text{O}$ were considered ($r = -0.72$) (Figure 3.27(b)).

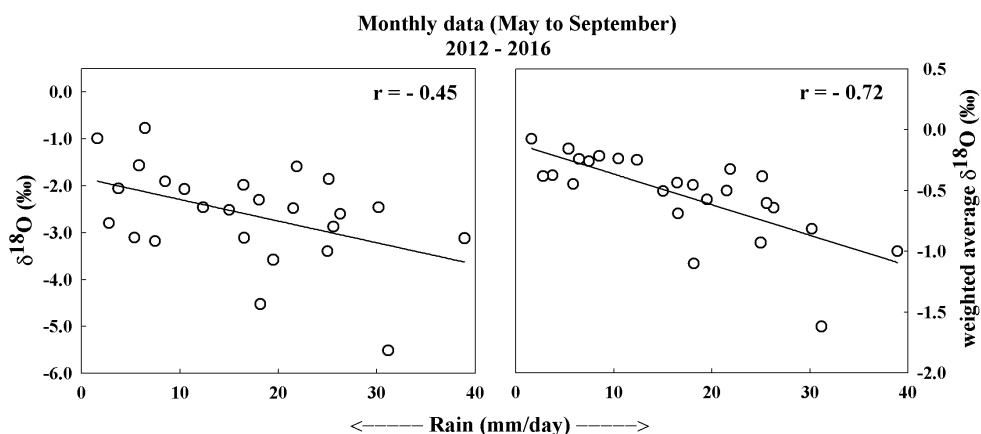


FIGURE 3.27: Scatter diagram between monthly average rainfall amount and (a) $\delta^{18}\text{O}$ and (b) weighted average $\delta^{18}\text{O}$.

The $\delta^{18}\text{O}$ records from speleothems have been widely used to reconstruct the Indian monsoon variability (e.g. Yadava and Ramesh, 2005; Yadava et al., 2004). These studies have documented the impact of amount effect (Dansgaard, 1964) in speleothem's $\delta^{18}\text{O}$ signature from the Indian region. The field survey and collection of the speleothems from the Andaman region as well as Indian peninsular region have been successfully executed to study the past monsoonal variations (Chapter 2). The collected speleothem samples were processed (cutting and drilling); however, only sub-samples of speleothem collected from peninsular region (Kadapa cave, (14.52°N , 77.99°E)) have been isotopic analyzed for $\delta^{13}\text{C}$ and $\delta^{18}\text{O}$ due to time constraint (Chapter 4).

In general, $\delta^{18}\text{O}$ of rainfall in the central and peninsular Indian regions varies with the amount of rainfall. Kumar et al. (2010) collected and analyzed rainwater

isotopes for a few sites near the Kadapa cave region (namely Kakinada and Bangalore). The data of $\delta^{18}\text{O}$ of rainfall and rainfall amount from Kakinada and Bangalore as well as Hyderabad (from GNIP dataset) show a weak but negative correlation. Vuille et al. (2005) used the ECHAM-4 AGCM model fitted with isotope tracers to explore the amount effect across the Asian monsoon. They argue that over most of the monsoon-affected areas (sea to land) circulation generates increased convection, and subsequently an observable amount effect. Furthermore, an isotope incorporated model (discussed in next paragraph) output datasets with the resolution $\sim 200 \times 200$ km have also been used. Model data of precipitation rate and its $\delta^{18}\text{O}$ averaged over the Kadapa region ($14.286\text{--}16.19^\circ\text{N}$, $76.87\text{--}78.75^\circ\text{E}$) show a highly significant negative correlation ($r_{(\text{Jan--Dec})} = -0.31$, $n = 366$, $p < 0.0000001$, $r_{(\text{Jun--Oct})} = -0.43$, $n = 174$, $p < 0.0001$).

Isotope Enabled Model: Rain Isotopes

The Isotope incorporated Global Spectral Model (IsoGSM, Yoshimura et al., 2008) data available from 1979-2013 (IsoGSM2, updated) with the resolution $\sim 200 \times 200$ km have been used to study rain isotopes spatial variability.

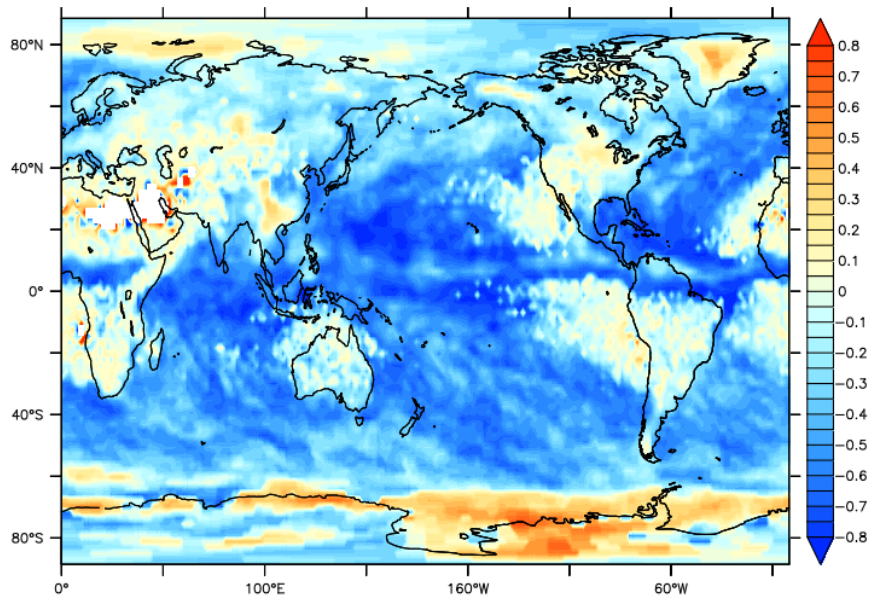


FIGURE 3.28: Spatial correlation between rainfall amount and its oxygen isotope ratios using IsoGSM2.0 dataset for the period 1979-2013.

IsoGSM data is first multi-decadal global 3-D isotope ($^1\text{H}^2\text{HO}$, H_2^{18}O) simulation data, which are consistent to the well-known global "quasi-observational" data. The IsoGSM derived isotopic values of precipitation agree reasonably well with the observed data. It means that it can be used for reference or input values for comparison purposes. The model incorporates various components, such as water vapor, precipitation and evaporation. In the absence of any actual observation based on rainwater sampling on longer timescale, existence of long-term amount effect can be checked

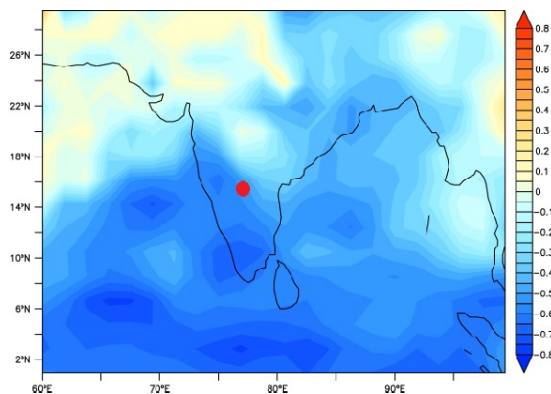


FIGURE 3.29: Spatial correlation between rainfall amount and its oxygen isotope ratios over the Indian subcontinent using IsoGSM2.0 dataset for the period 1979-2013. Red dot indicates the speleothem study site situated in Andhra Pradesh region of India.

using IsoGSM. Figure 3.28 shows the spatial correlation between precipitation and its oxygen isotopic ratios. In the tropics, $\delta^{18}\text{O}$ of rainwater is inversely correlated to amount of rainfall. That support the various observational studies carried out in the tropic, such as Rozanski et al. (2013). This has been explained in terms of very high tropical rainfalls at times of the passage of the Intertropical Convergence Zone (ITCZ), characterised by towering clouds and strong downdrafts, causing extreme depletion in $\delta^{18}\text{O}$ and $\delta^2\text{H}$. Among island stations in the tropics, where temperature variations are small, a dependence of $\delta^{18}\text{O}$ on rain amount is observed to the extent of $-1.5\text{‰}/100\text{mm}$ of monthly rainfall.

However, the amount effect pattern shows spatial variability within the tropical belt. For instance, IsoGSM output shows that the amount effect is valid over peninsular India as well as over the west and central northeast Indian region, but not valid over major parts of the northwest and northeast India (Figure 3.29). Thus, in the present study, the peninsular region has been chosen for the paleo-monsoon investigation using speleothems red dot, Figure 3.29). The collected sample details and output are discussed in chapter 4.

3.5 Chapter Conclusions

Isotopic analysis of rainfall over the Andaman Island, Bay of Bengal was carried out for the years 2012 - 2015 in order to study the atmospheric controls on rainwater isotopic variations and moisture transport processes. The oxygen and hydrogen isotopic compositions are typical of the tropical marine sites but show significant variations depending on seasonal weather conditions; maximum depletion was observed during the tropical cyclones. The results suggest that the isotopic composition of rainwater seems to be controlled by the dynamical nature of the moisture rather than the individual rain events. Precipitation isotopes undergo systematic depletions in response to the organized convection occurring over a large area and are modulated

by the integrated effect of convective activities. Precipitation isotopes appear to be linked with the monsoon intraseasonal variability in addition to synoptic scale fluctuations. The integrative characteristics of rain isotope and in turn the amount effect manifest the best in a time scale of 3 - 4 weeks that appear to be linked to the monsoon intraseasonal variability which is a very specific characteristics of the Bay of Bengal. Since the amount effect responds to integrated effect of convective activities, it depends basically on the mean state of monsoon operating on intraseasonal time scale; that is, spatially over 1000 km and temporarily approximately 12 - 27 days. The monsoon between 2012 and 2015 underwent different intraseasonal variability and hence amount effect also showed very different behavior in these years. During the early to mid monsoon the amount effect arose primarily due to rain re-evaporation but in the later phase it was driven by moisture convergence rather than evaporation.

It was observed that the Port Blair rainwater oxygen isotope ratios ($\delta^{18}\text{O}$) maintain a temporally dependent correlation with the average rain variation over the Core Monsoon Zone (CMZ) of India, though the rainfall over these two regions appears to be mutually independent. The moisture transport processes over the Bay of Bengal have been investigated by means of isotopic analysis of daily rainfall at the moisture source (BoB) as well as on the moisture destination (CMZ) sites. The nature of the correlation between the isotopic records from source and destination sites appears to be modulated by the isotope amount effect, propagation of the rain/cloud band from the BoB to the Indian landmass and the associated moisture transport pathways. The study also establishes the timescale of the moisture transport and the building of the convective systems by means of isotopic characteristics. Building up of the large scale convective system, specifically in the northern Indian Ocean is known to happen in 10-20 days and 30-60 days time scale, which manifest in the form of westward and northward propagation of the rain/cloud band. During this timeframe the moisture is steadily fed into the convective clouds. On the other hand, the transport of moisture from the equatorial Indian Ocean to the Bay of Bengal takes about the same time (10-20 days). The study demonstrates that the moisture transport time and the time frame to build a large scale convective system is intricately related. Further, it was observed that the Port Blair rain isotopic values were strongly modulated by the seasonally reversing monsoon circulations. This kind of contrasting behavior in atmospheric variables as well as in the isotopic composition of rainfall in this region may provide an alternative means to estimate the monsoon withdrawal dates.

It has been observed that the isotopic controls of the source moisture on ambient vapor could be one of the reasons for the observed discrepancy, in turn, on the isotopic variations of the rainfall. Hence, the isotopic interaction between vapor and rain can be a function of variation in the isotopic composition of the source moisture due to variability in meteorological parameters on daily timescale. Thus, isotopic variability in source moisture should also be considered for the comprehensive isotopic studies

over the coastal regions. Study shows that the isotopic exchange between ambient vapor and raindrops could lead to measurable depletion in isotopic composition of vapor, in turn, subsequent enrichment in rainwater. The isotopic interaction may account up to 30% in the observed variability of the isotopic composition of rain and vapor over the BoB region.

Since precipitation isotopes are strongly modulated by the moisture dynamics in the subseasonal scale, including the moisture generated from the sea surface, its systematic study would be helpful to monitor the long term changes in the subseasonal moisture transport and hence the temporal variability pattern of precipitation derived from the BoB moisture over the Indian subcontinent. One of the potential applications of this moisture transport process could be to investigate how the moisture generation and in turn the transport process in the BoB would respond to the global warming in the coming decades.

According to current understanding, amount effect implies more the rain, more is the isotopic depletion. But this study shows that increased amount of rainfall does not necessarily mean a higher depletion in ^{18}O or ^2H . Since amount effect is caused by different atmospheric processes which occur in different scales, their interactions introduce non-linearity in the observed amount effect. This is an intricate attribute of the amount effect which is likely to have important implications in paleo-monsoon reconstruction. Hence, this characteristic behavior of amount effect is a limiting factor for paleo-monsoon reconstruction on annual to sub annual time scale using speleothem or tree ring. Currently the spatial pattern of ISM rainfall and its isotopic variability simulated by global circulation models show good agreement with the observations, but large discrepancies exist in the magnitude of simulated amount effect (Midhun and Ramesh, 2016). Our study is expected to provide a better understanding of the amount effect in the Indian region which in turn is likely to help in reducing the discrepancy between observation and the model simulation.

Chapter 4

Reconstruction of high-resolution monsoonal record using stalagmite

Large parts of this chapter are published in

Nitesh Sinha, Naveen Gandhi, S. Chakraborty, R. Krishnan, M. G. Yadava, R. Ramesh, (2018). Abrupt climate change at ~2800 yr BP evidenced by a stalagmite record from peninsular India. *The Holocene*. <https://doi.org/10.1177/0959683618788647>.

In this chapter, the past monsoonal variability over the Indian region is investigated. Using high-resolution speleothem proxy record from the Indian subcontinent, it focuses on the multi-decadal to centennial scale variability of the ISM. The chapter is divided into two sections, firstly it presents an analysis of the ISM rainfall variations for a 1460-year period (1720-3180 yr BP), based on a long record of a U-Th dated stalagmite record from the Kadapa cave in peninsular India (Section 4.1). The second section synthesizes the available paleoclimate records of speleothems as well as a few other proxy records from the Indian subcontinent (Section 4.2). Thus, after successful reconstruction of past ISM rainfall and compilation of proxy derived rain data, this chapter is dedicated to address objectives 3 and 4.

4.1 ISM rainfall reconstruction using a stalagmite record from peninsular India

4.1.1 Introduction

The oxygen isotope ($\delta^{18}\text{O}$) records of speleothems from Indian subcontinent have been widely used to reconstruct the Indian monsoon variability (e.g., Yadava et al., 2004; Yadava and Ramesh, 2005). These studies have documented the impact of amount effect (Dansgaard, 1964) in speleothems $\delta^{18}\text{O}$ signature from the Indian region. Evidence of climatic change and paleo-hydrological conditions in the past can also be inferred from trace element profiles derived from stalagmites (Fairchild et al., 2001; Fairchild and Treble, 2009). Yadava and Ramesh (2001) suggested that variations of

trace elements in tropical speleothems can be used as potential indicators of past rainfall variability. Most stalagmites currently used for paleo-climate reconstruction are calcitic, while aragonitic stalagmites are less abundant (Holmgren et al., 2003). The processes determining speleothem isotopic and elemental composition, however, are complex (Fairchild et al., 2006; Lachniet, 2009). Thus, it is still not entrenched how changes in crystallographic structure are linked with variations of the Indian monsoon in the past. One of the major constraints in understanding the long-term monsoonal variability (interannual and decadal timescales) is the lack of high-resolution speleothem records from the subcontinent. To the best of our knowledge, only a short term record of 900 years (450 to 1350 yr BP) from Dandak Cave (Sinha et al., 2007) and 50 years (-16 to -72 yr BP) record of the Mawmluh cave (Myers et al., 2015) exist based on annual and sub-annual resolutions respectively.

Natural forcing and ISM

Solar variability is known to have influenced some of the major climatic events on centennial to millennial scales during the late Holocene. Such as Iron Age cold epoch, north Atlantic ice debris events, warm/cold European climate (Bond et al., 2001; Engels, Stefan and van Geel, Bas, 2012). Furthermore, millennial-scale variations of the Indian monsoon are reported to have linkages with ITCZ movements associated with the changes in the solar insolation (Gupta et al., 2003). In particular, the decline of the ISM during the middle to late Holocene is linked to the southward migration of the ITCZ (Fleitmann et al., 2007). While instrumental records during the 19th and 20th century and climate model simulations provide evidence for decadal-scale variations in the Indian monsoon rainfall (e.g., Krishnan and Sugi, 2003; Meehl and Hu, 2006). However, the signatures of decadal-to-centennial variability of monsoon rainfall are not yet adequately investigated for terrestrial proxies from the Indian subcontinent.

The aim of this study is to understand the ISM variability on long timescales (decadal to centennial) and comprehend their underlying mechanisms. Keeping this in view, the chapter presents (i) a 1460 years long $\delta^{18}\text{O}$ stalagmite record (1720-3180 yr BP) with \sim annual resolution collected from a cave situated in peninsular India; (ii) trace elemental ratios and crystallographic structure information on major environmental changes; (iii) a discussion on various climatic events between 1720 and 3180 yr BP and their possible forcing factors.

4.1.2 Cave location and regional climate

Stalagmite NK-1305, \sim 22 cm (8.66") long, was collected from the Nakarallu cave, Kadapa (14.52°N, 77.99°E; also known as Cuddapah); on 03 June 2013. Kadapa is located at the south-central part of Andhra Pradesh, India (blue star, Figure 4.1(a)). The cave has a very narrow entrance followed by a path stretches nearly vertically down to about 7-8 m followed by a 400 m rugged walk (Figure 4.1(b), (c): rough sketch not

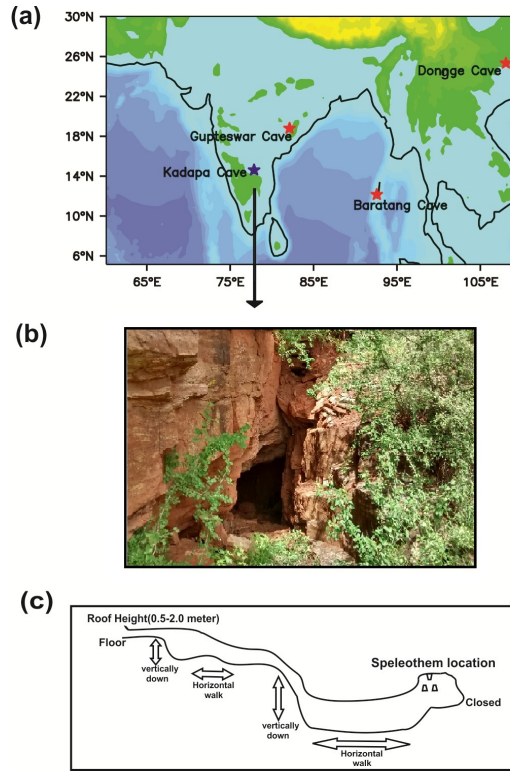


FIGURE 4.1: (a) Location of the Kadapa cave (blue star) and other speleothem caves locations (red star) with records of common periods (Section 4.2.3). (b) Cave entrance, (c) Rough sketch of pathway inside the cave (not to scale).

to scale). Being located far from the nearest village, there are major challenges in entering the cave due to the rugged terrain, the near vertical passage at the entry point and complete darkness along the path after 10-15 m from the cave entrance. Thus, the cave in its current form seems not to have suffered human intervention. The cave site is at an elevation of ~ 280 m above the mean sea level. During sampling, the cave temperature was 28°C and relative humidity $> 96\%$ with hot and dry conditions outside the cave (Air temperature = 38°C and $\text{RH} < 50\%$). Rainwater samples over or near the cave could not be collected due to its isolation from the human-habitation.

The cave is hereafter referred to as the Kadapa cave. Regional climate is semi-arid with mean annual rainfall of ~ 710 mm. The region receives rain mostly during the summer monsoon (Jun-Oct, $\sim 75\%$) and scanty rainfall during the winter monsoon (Nov-Dec, $\sim 18\%$) (www.imdhyderabad.gov.in/ap/site/andhraindex.html). The Arabian Sea is the major moisture source over the study site during the Indian summer monsoon (Figure B.1). The mean annual temperature of Kadapa is 27°C . The monthly climatological (1979 - 2013) variations of rain, temperature, and rain oxygen isotope ratio (IsoGSM2) over the Kadapa region are shown in Figure B.2. The vegetation of the region is dry savannah and poor steppe with shrubs.

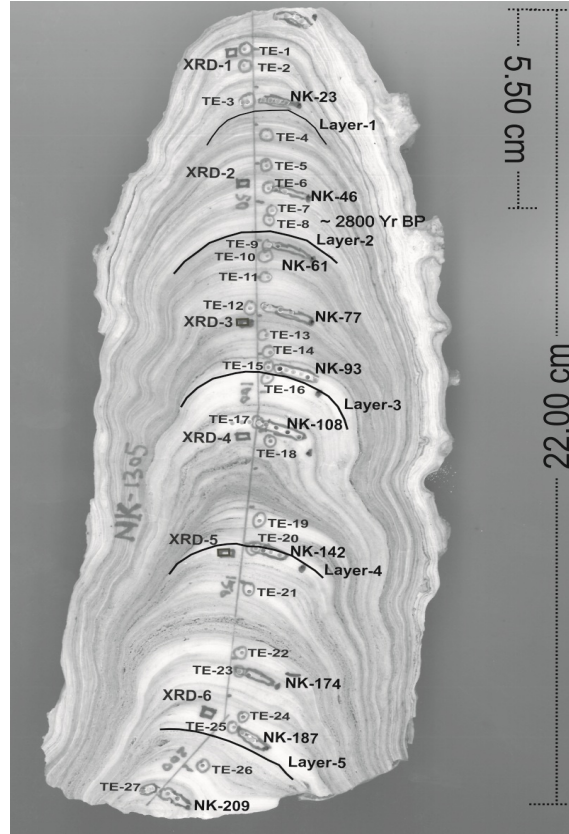


FIGURE 4.2: The Kadapa stalagmite sample drilling positions for: XRD (black rectangles), trace elements (gray circles), U-Th dating (NK-1 to NK-209), Hendy's test (black curved lines) and 1134 sub-samples drilled along the growth direction shown by thick gray line for oxygen isotopic measurements. The vertical line on the right is showing the scaling of 22.00 cm long stalagmite sample and 2800 yr BP event marked at 5.50 cm (approx.) from the top.

4.1.3 Methods

Eleven sub-samples (200 mg) were extracted along the growth axis from different layers of the stalagmite (Figure 4.2, marked NK-1 to NK-209) for dating, depending on the measured concentration of U/Th. A precise chronology of the sample was established in April 2015, using U-Th dating by Multi-Collector Inductively Coupled Plasma Mass Spectrometer (MC-ICPMS) at the University of Queensland, Australia; the dating was carried out using the method described in Hellstrom (2003).

Approximately 1 mg sub-samples were extracted from 6 different layers for X-ray diffraction (XRD) analyses (Figure 4.2, marked as a black box, XRD-1 to XRD-6) to ascertain the calcite and aragonite proportions in the sample. The measurements were carried out on Bruker Powder XRD at the Indian Institute of Science Education and Research, in Pune. The Rietveld method and International Centre for Diffraction Data- Reference Intensity Ratio (ICDD RIR) method was used for crystallographic characterization (Details are given in Mukherjee et al., 2017).

For stable isotope analyses, a total of 1134 carbonate samples were extracted along

the growth axis of stalagmite using a micro-mill sampling system (New Wave Research) (Figure 4.2, marked as a thick gray line connecting the bottom to top) at the Physical Research Laboratory (PRL), Ahmedabad, India. Samples were analyzed on stable Isotope Ratio Mass Spectrometer (Thermo-Fisher Delta V plus IRMS) for $\delta^{18}\text{O}$ and $\delta^{13}\text{C}$ with a precision better than $\pm 0.1\%$ at IITM. NBS-19 and Laboratory standards (PRL, Makrana Marble) were run along with samples to check the reproducibility and accuracy of the measurements (Laskar et al., 2013).

To validate the isotopic equilibrium, a qualitative test, known as "Hendys test" (Hendy, 1971) has been performed. Here the measured $\delta^{18}\text{O}$ values remain constant along a single growth layer and there is no correlation between $\delta^{18}\text{O}$ and $\delta^{13}\text{C}$. To perform the test, 28 samples from 5 different layers (5-6 subsamples from each layer (Layer-1 to Layer-5); Figure 4.2, marked as black curve) were extracted using hand-held dental drill and isotopic analysis has been done. Further to check the kinetic fractionation, the correlation between $\delta^{18}\text{O}$ and $\delta^{13}\text{C}$ along the stalagmite growth axis has been investigated; the result has been presented in Appendix B (Figure B.3).

Sub-samples of 2-3 mg were drilled by a hand-held dental drill from 27 layers (Figure 4.2, marked as small gray circles (TE-1 to TE-27) for trace element analysis. While drilling sub-samples for trace elements measurements, care was taken to avoid brown (dark) layers as these layers might have more detritus materials. Samples for TEs were analyzed using Thermo X-series II ICP-MS at University of Queensland, Australia. The USGS standard W-2 was used as the calibration standard and the measurement was carried out using the protocol of Eggins et al. (1997). Calcium (Ca) being the major element, it could not be measured on the ICP-MS along with other trace elements. Therefore, element/Ca ratios (by weight) were obtained by dividing the values by 382,000,000 (which is the nominal Ca concentration in ppb in CaCO_3).

4.1.4 Results

U-Th based chronology

U-Th dates of eleven samples are given in Table B.6 with associated errors. Errors associated with the age quoted in the text are $\pm 2\sigma$. The dating yields the youngest date of 1740 ± 7 yr BP for the sample depth 1 mm from the top and the oldest date 3164 ± 12 yr BP with depth ~ 6 mm from the base. The U content of 4-72 ppm allowed measurement of ages with uncertainties smaller than 0.03ka (kilo annum). Interpolation between discrete dating points has been done using COPRA1.0 model (Breitenbach et al., 2012). The model uses Monte-Carlo simulation and a translation procedure is used to assign a precise time scale to climate proxies and to translate dating uncertainties to uncertainties in the proxy values. COPRA adds small random numbers drawn from a normal distribution and interpolates the ages to the proxy record. Repeating this many times (Monte Carlo simulation; Gilks and Roberts, 1996) makes it possible to generate several slightly differing age models required for populating the

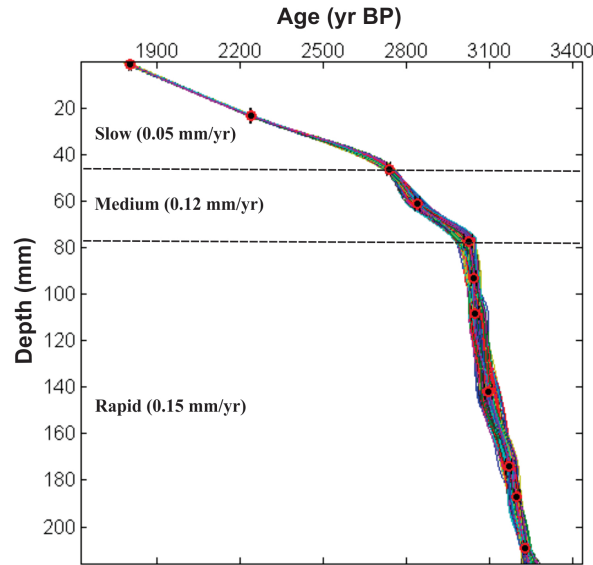


FIGURE 4.3: Variation of U-Th dates with depth in the stalagmite. The uncertainties associated with the ages vary between 6 and 32 years (at 2 sigma level; for details see Figure B.6). COPRA median age model for stalagmite (blue bold line) with 95% confidence bounds are constrained by eleven U-series dates (black dots with error bars). Marked periods 3180-3020 yr BP, 3020-2800 yr BP and 2800-1720 yr BP show rapid, medium and slow growth of carbonate precipitation, respectively.

confidence intervals for the dating points. Thus, the final age model results from a series of different Monte Carlo simulations.

A COPRA median age model for stalagmite with 95% confidence bounds, constrained by eleven U-series dates, is shown in Figure 4.3. The Age-depth relationship of samples reveals that there were no age reversals or hiatuses in the sample. The growth of the sample is from 3180-1720 yr BP, the rate of growth, however, has varied during its course of deposition. The change in growth rates is observed at ~ 50 mm and ~ 75 mm (from the top) corresponding to 2800 ± 20 yr BP and 3020 ± 32 yr BP, respectively. The growth rate of the stalagmite has been calculated using the U-Th ages at respective sampling positions. Thus, the stalagmite growth can be divided into three segments viz. 3180-3020 yr BP (rapid, ± 0.15 mm/yr), 3020-2800 yr BP (medium, ± 0.12 mm/yr) and 2800-1720 yr BP (slow, ± 0.05 mm/yr).

XRD data

XRD peaks, obtained for six layers (Figure B.4, XRD 1-6), show that calcite (aragonite) is approximately 70% (30%) in the layers 3-6, while the layers 1-2 show about 35% (65%) respectively. Chronologically, the layers 1-2 and 3-6 belong to the periods 1720-2665 yr BP and 2935-3180 yr BP, respectively. XRD analyses show that the precipitated carbonate in the stalagmite was a mixture of calcite and aragonite with varying proportions. Inorganic carbonate precipitation under controlled laboratory

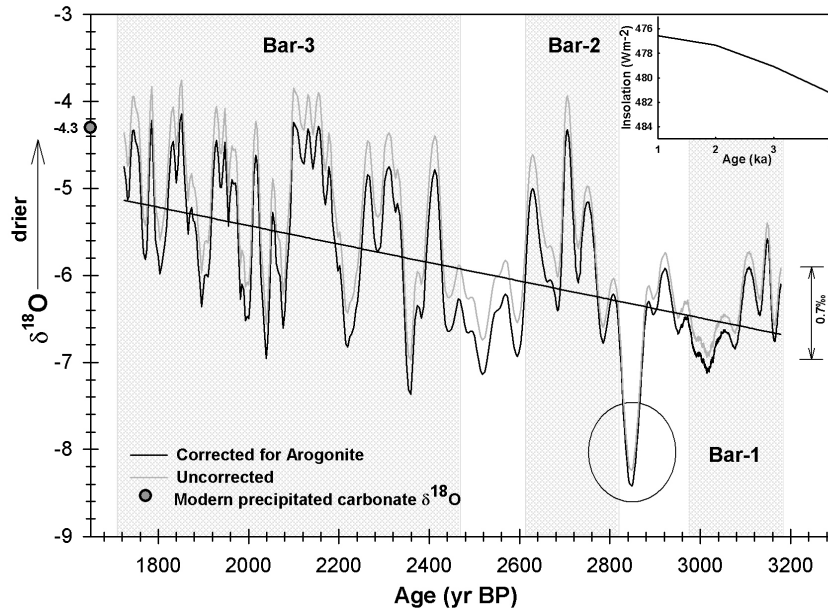


FIGURE 4.4: Variations of $\delta^{18}\text{O}$ with the U-Th ages in yr BP of the Kadapa Cave stalagmite. Circle marked to show highly depleted ^{18}O values at ~ 2850 yr BP. The trend line shows that the ISM gets drier from 3180 to 1720 yr BP following northern hemispheric solar insolation (shown in inset; source: Laskar, J. et al., 2004). Three distinct bars (1, 2, and 3) marked to show observed variability in monsoon associated with different periods.

conditions show that the aragonite is enriched in the heavier isotope compared to calcite by $\sim 0.6\text{‰}$ and 1.8‰ at 25°C for oxygen and carbon, respectively (Tarutani et al., 1969; Robinson and Clayton, 1969). In such cases, the measured speleothem $\delta^{18}\text{O}$ has been corrected based on the aragonite proportion present in the mixture to get an equivalent calcite speleothem ($\delta^{18}\text{O}_{\text{corrected}} = \delta^{18}\text{O}_{\text{measured}} - (\% \text{ of aragonite} \times 0.6)$; Yadava et al. (2014)).

Oxygen Isotope

Measured (uncorrected) values of $\delta^{18}\text{O}$ vary from -3.8‰ to -8.2‰ (with an average of -6.1‰) with respect to Vienna Pee Dee Belemnite (VPDB). Following Yadava et al. (2014), the measured $\delta^{18}\text{O}$ values were thus corrected based on the aragonite proportion present in the mixture. Corrected $\delta^{18}\text{O}$ varies from -4.1‰ to -8.4‰ (with an average value of -6.3‰). The corrected and uncorrected values are plotted together in Figure 4.4. Both corrected and uncorrected values are positively correlated ($R^2 = 0.99$) and the maximum correction in $\delta^{18}\text{O}$ values, due to the varying amounts of aragonite, is 0.3‰ . This small correction (0.3‰) has an insignificant impact on the overall variability over the entire time interval between 3180 and 1720 yr BP. An average increase of 1.8‰ ($r = 0.63$; $n = 1134$; $p < 0.01$) in $\delta^{18}\text{O}$ from 3180 to 1720 yr BP is evident from the

regression analysis of reconstructed data. Measured modern precipitated carbonate $\delta^{18}\text{O}$ is -4.3‰ (shown by filled circle symbol in Figure 4.4).

The stalagmite has potentially captured the various climatic fluctuations of the past on varying time scales. An average depletion in $\delta^{18}\text{O}$ value is -0.7‰ (-6.1‰ to -6.8‰) between 3000 and 3180 yr BP (Figure 4.4 Bar-1). Low isotopic variability during initial speleothem formation coincides with the high carbonate precipitation rate. A sharp depletion in the $\delta^{18}\text{O}$ values can be observed around 2900-2850 yr BP (see the circle in Figure 4.4). During this time period of ~ 50 years, there was a gradual depletion in $\delta^{18}\text{O}$ (24 data points) values from -6.3‰ to -8.4‰ . On the other hand, an abrupt enrichment in average $\delta^{18}\text{O}$ ratios is observed after 2800 ± 20 yr BP (Figure 4.4 Bar-2). The $\delta^{18}\text{O}$ values between 1720-2500 yr BP varied from -7.3‰ to -4.7‰ , for example, the depletion in $\delta^{18}\text{O}$ near 2350 yr BP is about -7.3‰ and similar depletions can be seen subsequently, at intervals of 100 to 200 years, with an average enrichment in $\delta^{18}\text{O}$ values (Figure 4.4 Bar-3).

Hendy's Test

Hendy's test was carried out along the five distinct lateral layers. $\delta^{18}\text{O}$ and $\delta^{13}\text{C}$ with distance (in cm) from the central axis are plotted and shown in Figure 4.5 1(a)-5(a). Correlations between $\delta^{18}\text{O}$ and $\delta^{13}\text{C}$ for each layer have also been calculated (Figure 4.5 1(b)-5(b)). The co-variation or trend either in $\delta^{18}\text{O}$ or $\delta^{13}\text{C}$ along the layers have not been observed, except for the layer 1 (Figure 4.5 1(a)). For layer 1, variation in $\delta^{18}\text{O}$ is $<1\%$ on both sides of the central axis, but is larger in the case of $\delta^{13}\text{C}$. Nonetheless, there is an insignificant correlation between $\delta^{18}\text{O}$ and $\delta^{13}\text{C}$ for the layer 1 as well as for the other layers (except layer 5, which shows a statistically significant correlation between $\delta^{18}\text{O}$ and $\delta^{13}\text{C}$ ($R^2=0.55$; $p < 0.05$; Figure 4.5 5(b)). For Hendy's test samples need to be extracted from a single layer, since even a slight mixing with the adjacent layer may cause a significant variation in $\delta^{18}\text{O}$ and/or $\delta^{13}\text{C}$. Variation in $\delta^{13}\text{C}$ along the layer 1 and significant correlation between $\delta^{18}\text{O}$ and $\delta^{13}\text{C}$ for the layer 5 could be a result of accidental mixing of the adjacent layers during sample drilling. Mickler et al. (2006) assessed the isotopic equilibrium of modern speleothem formation using carbon and oxygen isotope values. They show that a significant relationship between $\delta^{18}\text{O}$ and $\delta^{13}\text{C}$ along stalagmite growth axes could signify kinetic fractionation. However, Kadapa cave sample records (along the growth axis) show an irrational correlation between $\delta^{18}\text{O}$ and $\delta^{13}\text{C}$ (Figure B.3). Therefore, considering the cave environment and above test results, it is appropriate to conclude that mostly carbonate precipitated under isotopic equilibrium.

Trace Elements

Sr/Ca, Ba/Ca and U/Ca show significant variations along the growth axis of stalagmite. An interesting point to note here is the sharp change in elemental concentrations

at 2800 ± 20 yr BP (Figure 4.6 a, b, c). Samples prior to 2800 yr BP have very low concentrations but the later part witnesses an order of magnitude increase. Low trace element concentrations coincided with a higher growth rate of carbonate as well as dominant calcite precipitation. In the Kadapa stalagmite, the average value of the Ba/Sr ratio for the period 1720-2800 yr BP is 8.2 ± 1.5 and it sharply changes to 14.7 ± 1.3 between 2800-3180 yr BP (Figure 4.6 d). These trace element ratio changes are likely related to the mineralogical transition and the different crystallography of aragonite and calcite (Figure 4.6 e).

4.1.5 Discussion

Indian Monsoon Variability

The U-Th dated stalagmite spans 1460 years (1720-3180 yr BP) of paleo-monsoon record with \sim annual resolution. Interpolated ages (COPRA model) reveal the resolution varying from annual (during 3180-3010 yr BP) to four years (during 2600-1720 yr BP), yielding an average resolution of 1.5 years for the entire time series. The $\delta^{18}\text{O}$ of speleothem in most of the tropical caves is primarily governed by the $\delta^{18}\text{O}$ of rain, and rain isotopic compositions are climatically controlled. Lower $\delta^{18}\text{O}$ values, over the tropics, correspond to a high amount of rainfall and vice versa, which is known as the Amount effect (Dansgaard, 1964). The Kadapa region receives >75% of annual rainfall during summer monsoon season with much of the moisture coming from the Arabian Sea. Continental effect is more or less constant for a particular site and is averaged out for the records of long time period. Hence, the overall oxygen isotopic variability over Kadapa is considered to be a reflection of variation of ISM rainfall amount. On the same lines, some recent works based on the Valmiki cave stalagmite (15.15°N ; 77.81°E) located a few kilometres from the Kadapa cave, have discussed the ISM variability (Lone et al., 2014; Raza et al., 2017).

Since the Kadapa cave region receives maximum moisture from the Arabian Sea branch of ISM, an increase in $\delta^{18}\text{O}$ by 1.8‰ of the Kadapa stalagmite between 3180 and 1720 yr BP is indicative of the decline in ISM strength. The overall declining trend in the ISM rainfall seems to be associated with the southward migration of the ITCZ, associated with lower northern hemispheric summer insolation during the study period (Figure 4.4 inset). The decline of ISM as a result of the decrease in solar insolation since the last \sim 8k years has been widely reported from various proxy records, e.g., sediment core studies (e.g., Gupta et al., 2003) and speleothem records (e.g., Dominik et al., 2003; Kathayat et al., 2016). It is known that the decrease in solar insolation lead to migration of ITCZ southwards, which in turn, weakens the ISM (e.g., Fleitmann et al., 2007). Our results corroborate the previous observations of the weakening of ISM rainfall for the study period under the influence of ITCZ southward movement. Figure 4.4 represents the overall oxygen isotopic variation for the study period (shown from right to left). A rapid growth of stalagmite sample for initial 200 years indicates

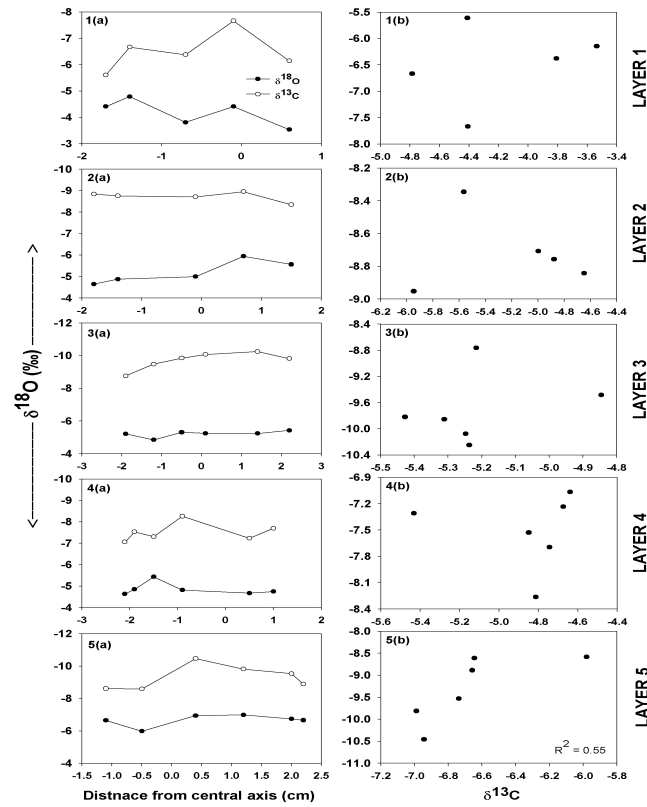


FIGURE 4.5: Left panel 1(a)-5(a): $\delta^{18}\text{O}$ (filled circles) and $\delta^{13}\text{C}$ (open circles) variations with distance from the central growth axis on either side for the five layers (layers shown in Figure 1d) of the stalagmite for Hendy's test. Right panel 1(b)-5(b): correlation between $\delta^{18}\text{O}$ and $\delta^{13}\text{C}$ for the same five layers.

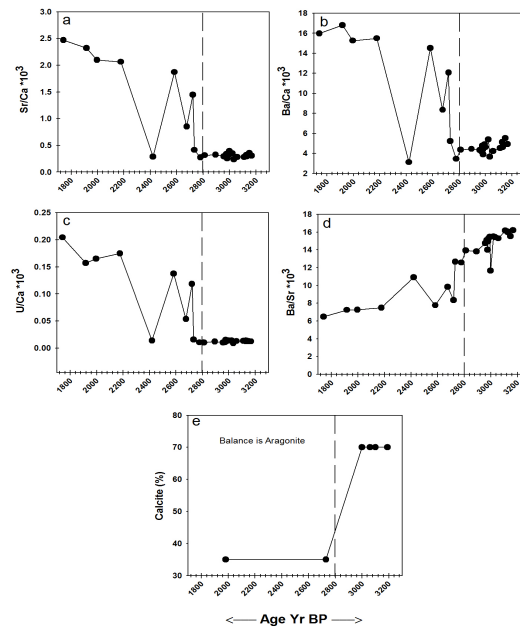


FIGURE 4.6: Variations of trace elemental ratios of (a) Sr/Ca (b) Ba/Ca (c) U/Ca and (d) Ba/Sr with age, dotted line at ~ 2800 yr BP (e) % of calcite with age.

a wetter period as evidenced by the depleted $\delta^{18}\text{O}$ values (Figure 4.4, Bar-1, the average variation in $\delta^{18}\text{O}$ is 0.7‰). An observed anomalous depletion in ^{18}O shown by a circle in Figure 4.4 has been discussed in the subsequent paragraph. An abrupt enrichment in ^{18}O values is observed at 2800 ± 20 yr BP, which corresponds to a major reduction in rainfall amount over the region (Figure 4.4, Bar-2). The variations in $\delta^{18}\text{O}$ between 1720 and 2500 yr BP are from -7.3‰ to -4.2‰, correspond to a reduction in the monsoonal rainfall on decadal to centennial time scales. Furthermore, depletion in $\delta^{18}\text{O}$ values near 2350 ± 6 yr BP of about -7.3‰ and consecutive reductions have been observed after the interval of 100 to 200 years (Figure 4.4, Bar-3). Similar multi-decadal to century scale, prolonged wet/drought periods have been found during the Holocene in several speleothem as well as lake records from central India and coherent with Kadapa record under chronological uncertainty. For example, a high resolution speleothem $\delta^{18}\text{O}$ record of Dandak Cave (Sinha et al., 2011b) and sediment core record from Lonar Lake (Prasad et al., 2014) in the central India document a near millennial long history of monsoon rainfall and drought variability those lasted for several years to decades. Although the trend in Kadapa stalagmite $\delta^{18}\text{O}$ indicated dry weather during (1800-2100 yr BP), there are several short intervals within for which the depletion in ^{18}O values is suggestive of intermittent wet periods.

The high resolution stalagmite records capture fluctuations in the isotopic values that occurred at small time intervals. For example, an anomalous depletion in ^{18}O between 2900 and 2850 yr BP has been observed (Figure 4.4, marked by a circle). The anomalous depletion during the period could be due to: 1) strong ISM (via Amount effect), or 2) weakening of ISM with stronger winter monsoon as rainfall from the latter is depleted in $\delta^{18}\text{O}$ (Figure B.5) as compared to that of the former (GNIP data set, IAEA/WMO, 2006; Warrier et al., 2010; Yadava et al., 2007), or 3) heavy rain events associated with intense cyclonic activity (Lawrence and Gedzelman, 1996; Lawrence et al., 2004), as the Kadapa region occasionally receives moisture from the Bay of Bengal via cyclonic activities (Raghavan and Rajesh, 2003). Similar anomalous depleted $\delta^{18}\text{O}$ signatures, approximately at the same time period (under chronological uncertainty) was observed in carbonate shells from the Banni grasslands (23.31°N to 23.86°N latitude and 68.93°E to 70.53°E) of western India (See Fig. 5A in Pillai et al., 2017) and in the speleothem $\delta^{18}\text{O}$ record from the Andaman Islands (12.08°N , 92.75°E), Bay of Bengal (Laskar et al., 2013). Pillai et al. (2017) interpreted the signal in terms of ISM variability as the west Indian region receives rainfall mostly during ISM (>90%; http://www.cgwb.gov.in/District_Profile/Gujarat/Kachchh.pdf). Therefore, enhancement of ISM seems to be a more probable reason than that of the possibility of stronger winter monsoon with the weakening of ISM. Cyclones originating from the Bay of Bengal or the Arabian Sea can also give rise to the highly depleted ^{18}O rainfall over the east coast, peninsular India and Andaman regions. Cyclone tracks for the period AD 1891 to 2015, available at the India Meteorological Department (<http://www.imd.gov.in>), show that cyclones originating

from the Arabian Sea fail to reach Kadapa region in peninsular India. On the other hand, some of the cyclones originating from the Bay of Bengal have the potential to reach the west coast of India. Thus, it is not unlikely that some of the severe cyclones originating at the Bay of Bengal could have potentially influenced the Kadapa region during the period between 2900 and 2850 yr BP. Such a scenario can explain the similar $\delta^{18}\text{O}$ signals in stalagmites from the Andaman Islands and the Kadapa and Banni grasslands of western India.

Growth rate and Mineralogy

The Kadapa stalagmite witnessed variable growth rates with a sharp change at 2800 ± 20 yr BP. Prior to 2800 yr BP, the growth rate was relatively higher (> 0.10 mm/yr), which later slowed down to about 0.05 mm/yr. Coincidentally, XRD data also suggest a major shift in crystallographic forms of CaCO_3 between the period 2665 and 2935 yr BP. Since the time around 2800 yr BP lies within the time window (2665 and 2935 yr BP), we examined other evidences (next paragraph), which allow us to infer the time of transition of crystallographic structure around 2800 yr BP. Calcite was the dominant mineral in the precipitated carbonate (70%) prior to 2800 yr BP, whereas aragonite was found to be $>70\%$ after ~ 2800 yr BP. Prior calcite precipitation affects the Mg/Ca ratio and the CaCO_3 saturation state of the drip water, and therefore prior calcite precipitation is known to be an essential process for inducing aragonite precipitation (Tooth and Fairchild, 2003). Increasingly arid climate results in reduced drip rates, which can cause prior calcite precipitation (Fairchild et al., 2000). Wassenburg et al. (2012) noted that the weakening of rainfall intensity in the northern Morocco region was featured in the isotopic composition of aragonite (caves in the Middle Atlas). Our results from the Kadapa stalagmite indicate that carbonate precipitation rates varied with rainfall and the abrupt decline in rainfall is suggestive of reduced drip rate or drying up of the existing seepage path in the Kadapa cave. The major changes in trace elemental concentrations also indicate the association of higher aragonite with low rainfall. However, drip water and cave mineralogy data are needed to strengthen the above inferences.

Trace elements as evidence of abrupt climatic change

Trace elemental ratios Sr/Ca, Ba/Ca, and U/Ca also showed a similar abrupt change at (2795 ± 20) yr BP (~ 2800 yr BP) (Figure 4.6, marked as dashed lines). We examine the Ba/Sr ratios in order to investigate the possible mechanisms that can explain the abrupt change in trace elements and crystallographic structures (Figure 4.6d). Ba/Sr remains constant during the growth of the stalagmite if the bedrock constituents and seepage pathways do not change significantly during its formation (Yadava and Ramesh, 2001). Hence, an abrupt change in Ba/Sr at 2800 yr BP (dashed line in Figure 4.6d) suggests a change in the seepage pathway and/or reduction in drip rate. Wassenburg et al. (2012) demonstrated that the aragonite composition has higher

concentration of trace elements compared to calcite (e.g. Ba, Sr, U), however, that too coincides with enriched $\delta^{18}\text{O}$ ratios (see Fig 6 in Wassenburg et al., 2012). Low growth rate and the mineralogy change at this point (~ 2800 yr BP) can be likewise explained by drier conditions, though this is not proven in this study given the lack of bedrock/drip-water samples and lack of high resolution TE data immediately near the transition from calcite to aragonite.

Influence of Solar activity on ISM

Prominent short term climatic changes can be a result of solar variability and its influence on the Earth's climate (Bond et al., 2001; Engels, Stefan and van Geel, Bas, 2012). Cosmogenic radio nuclei Carbon-14 (^{14}C) are formed by the interactions of the galactic cosmic rays with atomic nuclei of nitrogen in the atmosphere (Libby, 1946). There is an inverse relationship between solar activity and the incidence of galactic cosmic rays (Forbush, 1954). Thus, the variation in the production of atmospheric ^{14}C is considered as a proxy for the past solar activity (Engels, Stefan and van Geel, Bas, 2012). To examine the effect of variable solar activity on monsoon rainfall, the Kadapa stalagmite $\delta^{18}\text{O}$ data is plotted along with the $\Delta^{14}\text{C}$ record (representative of atmospheric radiocarbon activity, Reimer et al., 2004) (Figure 4.7 a & b respectively). There is a marked similarity in an abrupt rise in $\Delta^{14}\text{C}$ and the associated decline in monsoon activity, particularly for the period around 2350 and 2800 yr BP (Figure 4.7, gray bars). Similar abrupt climatic change at ~ 2800 yr BP, in the form of an unusual cold environment in the North Atlantic and continental Europe triggered by a decline in solar activity, has been widely reported (Geel et al., 1996; Geel et al., 1997; Raspopov et al., 2001; Bond et al., 2001; Blaauw et al., 2004). Also, the period (1800-2100 yr BP) overlaps with the periods 1600-2250 yr BP (Roman Warm Period; RWP, arrows Figure 4.7) of unusually warm weather in Europe and the North Atlantic. Time overlap of the dry conditions of the ISM and the warm climate of Europe indicate the possibility of both ISM and European climate are linked through teleconnection or driven by similar forcing during RWP.

Synchronous variability in the ISM and the East Asian monsoon (EAM) can be expected, since water vapor over South China is primarily transported from the Indian Ocean (Wang and Chen, 2012). To examine the coherency between the ISM and EAM, the Kadapa stalagmite record is compared with the Dongge cave data (Wang et al., 2005) for the common period (Figure 4.7c). A similar declining trend of monsoonal rainfall in both the records is noted, and both the records show concordant variation in $\delta^{18}\text{O}$ during the RWP (2250-1750 yr BP; shown by arrows in Figure 4.7). However, the scale of variability in both the records ($\delta^{18}\text{O}$ values vary -6.8‰ to -7.9‰ and -4.1‰ to -8.4‰ for the Dongge and the Kadapa caves, respectively) is different due to the distinct seasonal variation and different cave settings. Lone et al. (2014) found a similar synchronous variability between the speleothem records from the Dongge and the Valmiki caves (Kurnool, Andhra Pradesh, India) for the period 15700-14700

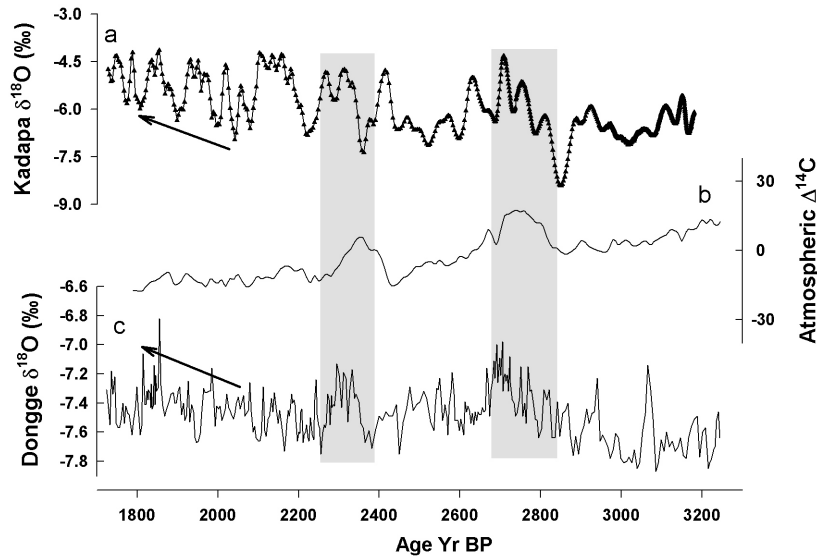


FIGURE 4.7: Comparison of (a) Kadapa cave- $\delta^{18}\text{O}$, and (b) atmospheric $\Delta^{14}\text{C}$ (a surrogate for solar activity) for the common period. Gray bars show the decline in rainfall associated with the two major rises in atmospheric $\Delta^{14}\text{C}$ values at 2350 yr BP and 2800 yr BP. (c) Dongge cave record for the common time period. Arrows show the general declining trend in rainfall coincides with the Roman Warm Period (RWP).

yr BP. Furthermore, the peaks in $\Delta^{14}\text{C}$ variations around 2350 and 2800 yr BP coincide with periods of decreased ISM (Kadapa record) and EAM (Dongge record) indicative of the effects of reduced solar activity (Figure 4.7, gray bars). The synchronous behavior of the ISM and EAM systems is a topic of wide interest (Dykoski et al., 2005; Yang et al., 2010).

4.2 Synthesis of proxies derived past ISM variability

4.2.1 Introduction

Although, many different types of measurements have been made on speleothems, but the changes in $\delta^{18}\text{O}$ are primarily a signal of change in precipitation amount over the tropics and have also been widely used to reconstruct changing atmospheric circulation patterns (e.g. Bar-Matthews et al., 1999; Luetscher et al., 2015). There are some works in the context of providing climate reconstructions or datasets (e.g. Bolliet et al., 2016; Caley et al., 2014; Harrison et al., 2014; Shah et al., 2013). The main open-access multi-proxy databases are available on the NOAA (www.ncdc.noaa.gov/data-access/paleoclimatology-data) and PANGAEA (www.pangaea.de) websites. However, there was no standard practice for specifically archiving the growing number of stable isotope records obtained from speleothems, until some efforts emerged

recently to create a data-bank by SISAL (Speleothem Isotope Synthesis and Analysis) group set up in 2017 (www.dx.doi.org/10.17864/1947.139). However, none of them provide a comprehensive coverage of the speleothem records from the Indian subcontinent.

Uses of speleothem to reconstruct the past monsoon began more than four decades ago (Hendy and Wilson, 1968). However, only a few significant works have been done on speleothems from the Indian subcontinent. To date, they have shown the potential for reconstructing the Indian monsoon for longer durations which goes from millennial to orbital scales and with variable temporal resolutions of annual to 100 years, depending on sampling resolution (e.g. Yadava and Ramesh, 2005; Sinha et al., 2007; Berkelhammer et al., 2010; Sinha et al., 2015; Kathayat et al., 2016). Speleothem caves are widely distributed over the Indian subcontinent, however, less explored and this makes crucial to compile available records to enhance our understanding of regional climate and its impact on global scale. The present work aimed to produce a compilation of existing speleothem oxygen isotope records from the Indian subcontinent. The cave sites explored so far for the past climate studies are shown and associated authors are listed in Figure 4.8. Several factors influence the oxygen isotopic variability in precipitation and subsequently in the speleothem calcite that is formed, specifically a source effect, an elevation effect, and an amount effect over the Indian subcontinent. Thus, the speleothem derived records from various sites show an uneven range of variation in the stable isotope ratios for the same time period, although, variability are similar.

4.2.2 Speleothem records from the Indian subcontinent

The speleothem oxygen isotope records from the Indian peninsular regions significantly reflected the monsoonal rainfall variations (e.g., Yadava et al., 2004; Sinha et al., 2007; Berkelhammer et al., 2010; Sinha et al., 2011b), as at these locations, the influence of changing cave temperature has been considered as negligible. The studies from the northern part of India reveal impacts of westerlies from Mediterranean/Atlantic and suggested monsoonal variations during some major events (e.g., LIA) contrast to peninsular India (e.g., Kotlia et al. (2015) and Kotlia et al. (2016)). Furthermore, the northeast region is the first morphological barrier for northward moving moisture during ISM and moisture majorly sourced from BoB (e.g., Berkelhammer et al., 2010; Lechleitner et al., 2017). Likewise, the cave sites were selected with the goal of minimizing other complicating influences, but uncertainties still exist. In addition, the climate models explicitly simulate water isotopes as a tool for understanding and characterizing the atmospheric hydrological cycle (e.g. Sturm et al., 2010; Werner et al., 2011). However, evaluations against paleo-records such as the $\delta^{18}\text{O}$ records from speleothems necessitate the evaluations of isotope-enabled climate models.

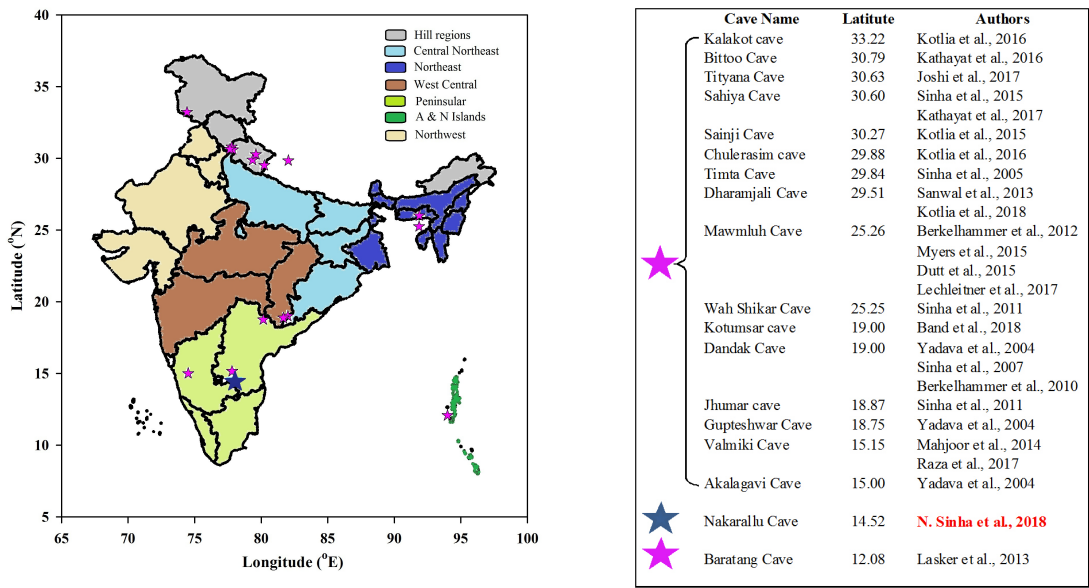


FIGURE 4.8: Speleothem sites over the Indian subcontinent studied so far: the left panel shows the map of India (IMD's Sub Divisions in different colors) marked with the sites location as star (★) and corresponding cave name and authors are listed on the right panel in order of decreasing latitudes (see Table 4.1). The dark blue star represents studied site of the present thesis and the pink stars show sites explored earlier by the other authors.

Towards this, synthesis and evaluation of available speleothem records are presented here. The compilation of 26 studies from 18 caves around the Indian subcontinent provides oxygen isotope measurements from speleothems. These datasets mostly (n=17) cover last 4000 years, records from the Himalayan region and caves from northeast India enveloped period up to 20000 years (n=7), and a very few sites (n=2) from the Indian subcontinent have data records on longer periods (> 20000 years). Most of these dataset are not in public domain, although published, a few were previously archived by the original principal investigators at the NOAA web-site and some have been provided by the authors on personal request (the original references are cited). The detail of the speleothem studies from the Indian caves with their location and periods covered are listed in Table 4.1.

Compilation of rainfall record for the last 4000 years

In order to understand the present and future of the Indian monsoon variability, we must synthesis the past record over a range of timescales, and it becomes imperative to study the unpredictability of trend in ISM on a longer timescales (e.g., millennium), that will help understand the robustness of the multi-decadal periodicity reported by the climate researcher (e.g., Goswami et al., 2014). This section summarizes what is known about past monsoonal change prior to the instrumental record, reconstructed

TABLE 4.1: Speleothem studies from the Indian subcontinent, and periods are mentioned in year Before Present (yr BP) with respect to 1950.
 \times = not available and \checkmark = available.

S.No.		Cave	Area	lat($^{\circ}$ N), lon($^{\circ}$ E)	Age (yr BP)	Authors	Data
1	1	Akalagavi	Karnataka	15.00, 74.51	(-16) – 285	Yadava et al., 2004	\times
2	2	Baratang	North Andaman	12.08, 92.75	0 – 3911	Laskar et al., 2013	\checkmark
3	3	Bittoo	Uttarakhand	30.79, 77.78	0 – 280000	Kathayat et al., 2016	\checkmark
4	4	Chulerasim	Central Himalaya	29.88, 79.35	0 – 328	Kotlia et al., 2016	\times
5	5	Dandak	Chhattisgarh	19.00, 82.00	12 – 1234, 3205 – 3693	Yadava et al., 2004	\checkmark
6					450 – 1350	Sinha et al., 2007	\checkmark
7					400 – 1350	Berkelhammer et al., 2010	\checkmark
8	6	Dharamjali	Central Himalaya	29.51, 80.23	0 – 1800	Sanwal et al., 2013	\times
9					1900 – 4000	Kotlia et al., 2018	\times
10	7	Gupteshwar	Odisha	18.75, 80.16	17 – 3400	Yadava et al., 2004	\checkmark
11	8	Jhumar	Chhattisgarh	18.87, 81.67	(-58) – 875	Sinha et al., 2011	\checkmark
12	9	Wah Shikar	Meghalaya	25.25, 91.86	(-57) – 551	Sinha et al., 2011	\checkmark
13	10	Kalakot	Northwest Himalaya	33.22, 74.42	9500 – 16300	Kotlia et al., 2016	\times
14	11	Kotumsar	Chhattisgarh	19.00, 82.00	5600 – 8500	Band et al., 2018	\times
15	12	Mawmluh	Meghalaya	25.26, 91.88	3653 – 12395	Berkelhammer et al., 2012	\times
16					(-16) – (-66)	Myers et al., 2015	\times
17					5500 – 33800	Dutt et al., 2015	\times
18					6500 – 16000	Lechleitner et al., 2017	\checkmark
19	13	Nakarallu	Andhra Pradesh	14.52, 77.99	1720 – 3180	N. Sinha et al., 2018	\checkmark
20	14	Sahiya	Uttarakhand	30.60, 77.87	(-56) – 2090	Sinha et al., 2015	\times
21					0 – 2000	Kathayat et al., 2017	\times
22	15	Sainji	Central Himalaya	30.27, 79.60	0 – 4000	Kotlia et al., 2015	\times
23	16	Timta	Western Himalaya	29.84, 82.03	11700 – 15200	Sinha et al., 2005	\checkmark
24	17	Tityana	Central-Lesser Himalaya	30.63, 77.65	1600 – 4000	Joshi et al., 2017	\times
25	18	Valmiki	Andhra Pradesh	15.15, 77.81	14700 – 15700	Mahjoor et al., 2014	\times
26					13160 – 15610	Raza et al., 2017	\times

using oxygen isotope records of speleothems. These changes are driven by global factors, including climate change and major climatic events (such as LIA, MWP), or regional responses as ISM manifests variability on intra-seasonal, inter-annual to inter-decadal timescales.

As discussed earlier, $\delta^{18}\text{O}$ of speleothem in most of the central and peninsular caves are primarily governed by the $\delta^{18}\text{O}$ of rainfall. Therefore, the time series of speleothem-derived rainfall from these regions are plotted in Figure 4.9, viz., Baratang cave, Andaman Island (Laskar et al., 2013); Kadapa cave, Andhra Pradesh (present study); Gupteshwar Cave, Orissa (Yadava et al., 2004); Jhumar Cave (Sinha et al.,

[2011b] and Dandak cave (Yadava et al., [2004]; Sinha et al., [2007]; Berkelhammer et al., [2010]). These caves are situated in the Indian subcontinent and encounter the same monsoon system, thus expected to show similar variability. However, because of different locations and altitude effect, the speleothem $\delta^{18}\text{O}$ ratios show an uneven range of variations. This is perhaps because of different cave settings (soil productivity or vegetation type), regional responses, temperature etc. Besides, air-mass pathways can also play an important role in isotopic variations in rainwater, in turn, imprinted in cave deposits.

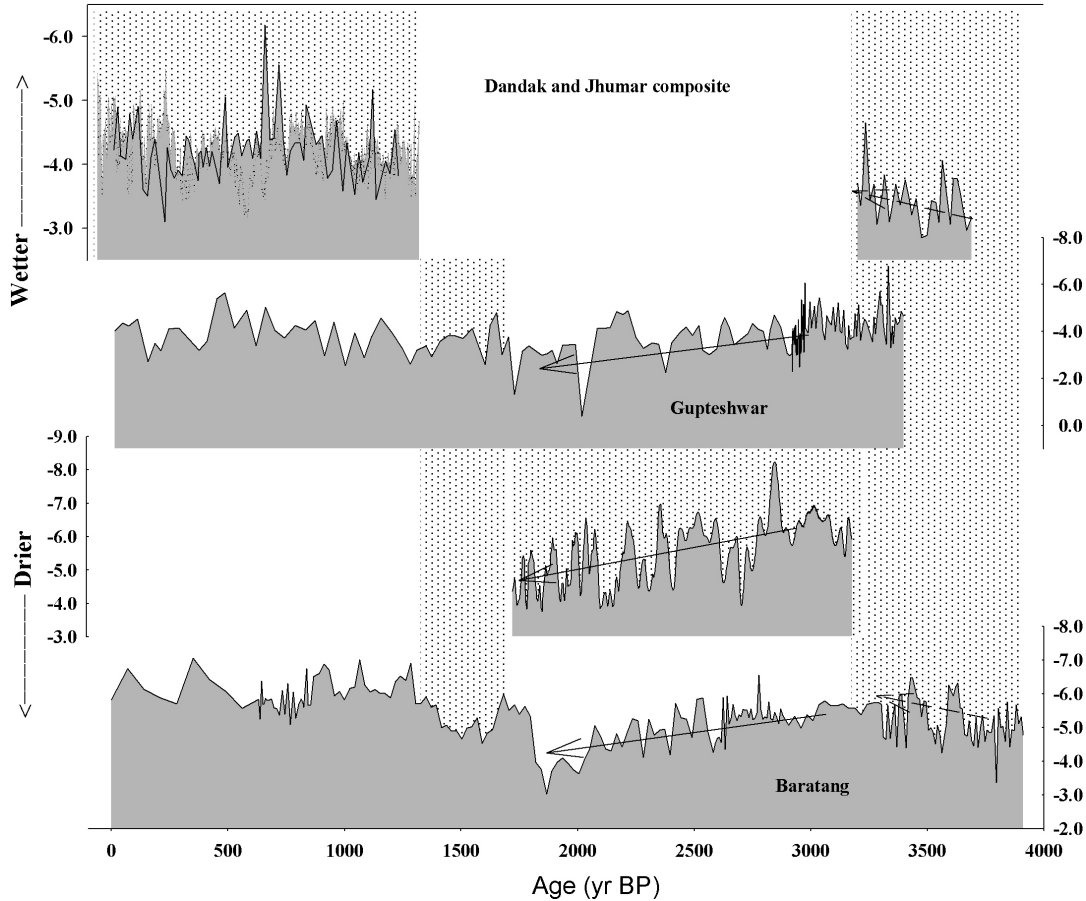


FIGURE 4.9: Compilation of $\delta^{18}\text{O}$ (y-axis, ‰) variations in the speleothems from central and peninsular Indian regions for the last 4000 years. Higher to lower values of $\delta^{18}\text{O}$ show drier to wetter conditions, i.e. in the positive y-axis direction, arrows are showing trend in rainfall for those particular periods (see text for detail). The stippled bars are showing the datasets considered for that particular period to compile and generate a high-resolution record of last 4000 years (Figure [4.10]).

Figure [4.9] is plotted in an order of low to high latitudes (bottom to up) and a standardized chronology across different speleothems are adopted, i.e., ages are reported in yr BP with respect to 1950. The dry/wet conditions can be interpreted by increasing/decreasing $\delta^{18}\text{O}$ ratios, and the area below the curve also represents the rainfall variation for the respective time series (i.e., low area corresponds to weak monsoon; not to scale). The resemblance in the $\delta^{18}\text{O}$ variations and long-term trends for the

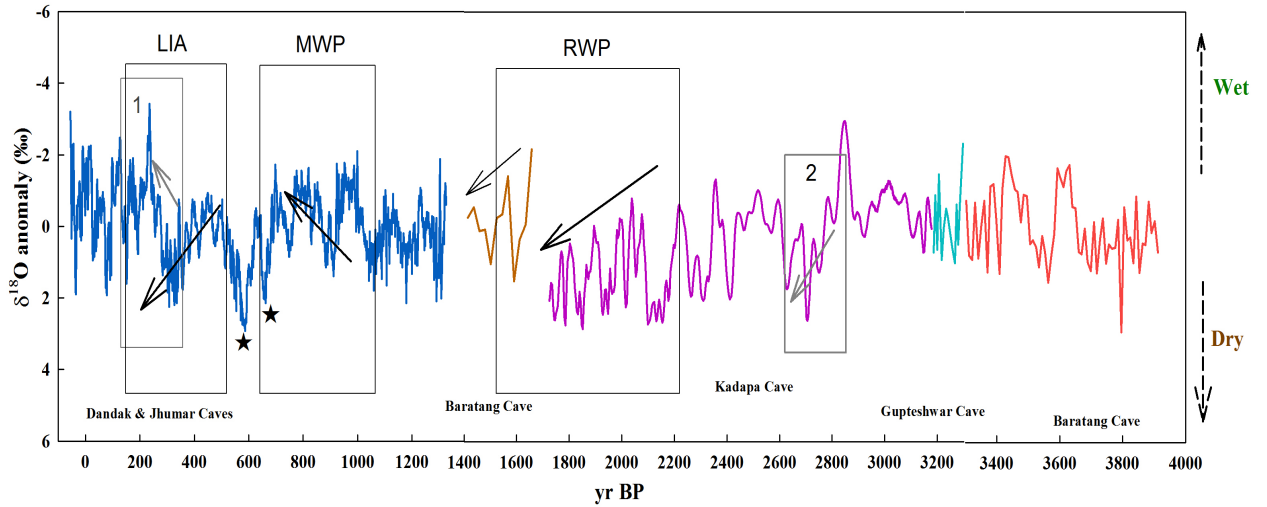


FIGURE 4.10: Synthesis of speleothem $\delta^{18}\text{O}$ variations to generate a high-resolution monsoonal record for the last 4000 years. Most of the records are from monsoon zone of India, region representative of the ISM. Major climatic events of the past, such as, LIA, MWP, RWP (black boxes) are captured in the Indian speleothems records, trends are shown by the arrows. Abrupt changes in monsoonal strength (gray box 1 & 2) as well as major drought periods (Sinha et al., 2011a; few marked as stars) over the Indian region are potentially reflected in the speleothem records.

common periods (e.g., Kadapa cave with Baratang and Gupteshwar caves) across the locations signifies that the major climatic variations are well captured in all the caves within the limits of chronological uncertainty (arrows, Figure 4.9).

Using these datasets, an attempt to compile and generate a continuous high resolution monsoon record has been made. Towards this, available high-resolution records are mostly preferred, such as composite of Dandak and Jhumar caves for the period 0 - 1350 yr BP and Kadapa cave record for the period 1720 - 3180 yr BP. For the intermittent periods, dataset with better resolution (more number of data points) as well as the only those periods are considered which shows similar variations with the other available record(s). For instance, between the periods 1350 - 1720 yr BP, 3180 - 3400 yr BP, and 3400 - 4000 yr BP, datasets of Baratang cave, Gupteshwar cave, and again Baratang cave are used, respectively. The oxygen isotope anomaly has been calculated because of their uneven variations for different caves and compiled record (stippled gray bars, Figure 4.9) is plotted (Figure 4.10). A few gaps in the time series are due to the poor resolution of available records for those particular periods, thus, discounted.

The record of 4000 years of rainfall influenced by some major climatic events, such as LIA, MWP, and RWP illustrated here by combining the Kadapa, Jhumar and Dandak caves records (Figure 4.10, black boxes); arrows represent the declining trends in the Indian monsoon rainfall during RWP (1550 - 2200 yr BP) and LIA (100 - 550 yr

BP) and enhanced during MWP (650 - 1050 yr BP). However, these events are not elegantly manifested in the Baratang cave or Gupteswar cave records perhaps because of their coarser temporal resolution. A few abrupt climatic changes were observed as enhanced (~ 300 yr BP, Sinha et al., 2011b) and suppressed monsoon (~ 2800 yr BP, present work) in Jhumar cave and Kadapa cave speleothem records respectively (Figure 4.10; gray box 1 & 2 respectively). Apart from these, the record suggests the presence of the significant low frequency (multi-decadal to centennial) variability in the climate system, leads to large discrepancies between models and paleoclimate data at low frequencies. Many hypotheses were put forth, such as, the Indian monsoon and ENSO are thought to be a manifestation of a global-scale oscillation on a multi-decadal (60 yr) timescale (Goswami, 2006); frequency distribution of active break periods driver the ISM variability on centennial timescales (Sinha et al., 2011b); ISM linkage with Pacific sea surface temperatures (Krishnan and Sugi, 2003; Goswami, 2006) and also with the Atlantic Multi-decadal Oscillation (AMO - Goswami, 2006; Lu et al., 2006). So, it is still a matter of debate that the multi-decadal mode of Indian monsoon is an intrinsic mode of the Asian monsoon or an integral part of a global multi-decadal mode of variability (Goswami et al., 2014).

4.2.3 ISM Multi-decadal Variability

The spectral characteristics of hydroclimate observations from speleothems spanning the last few millennia show significant periods in the range of 20 - 80 years (e.g., Lone et al., 2014; Sinha et al., 2015). Spectral analysis of Kadapa stalagmite $\delta^{18}\text{O}$ record also reveals multi-decadal variability which strongly demonstrates a ~ 50 year periodicity in the monsoon rainfall between 1420 - 3180 yr BP (Figure 4.11 a). The high-resolution Kadapa record potentially captured the typical 4-5 years oscillations related to ENSO as well as quasi-biannual oscillation¹ (e.g., Baldwin et al., 2001) signals, however, out of the limit of age error uncertainty ($2\sigma = \pm 6$ years). The Kadapa region receives maximum rainfall during the southwest monsoon (ISM, discussed above), thus, the observed periodicity is perhaps representing a multi-decadal mode of variability in the Asian monsoon.

From the Indian subcontinent, only a few studies have reported speleothem $\delta^{18}\text{O}$ records for common time periods (i.e., 1700 - 3300 yr BP) and made available, namely, the Baratang Cave, Gupteshwar cave, and the Sahiya cave. The present thesis also considers a speleothem record from the Southeast Asian region (Dongge cave) for re-examining the climatological teleconnection between ISM and EAM on multi-decadal timescales. The records from India as well as from South China corroborate the existence of multi-decadal oscillations of the periodicity ranging from 40-50 years (Figure 4.11 b-e).

¹The quasi-biennial oscillation (QBO) is a near-periodic, large-amplitude, downward propagating oscillation in zonal (westerly) winds in the equatorial stratosphere.

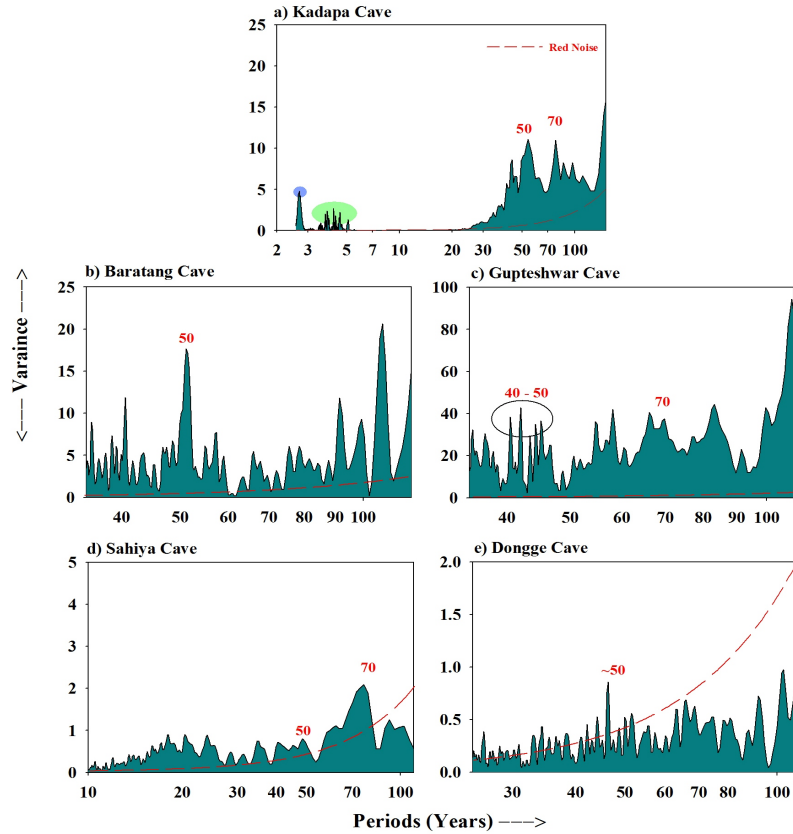


FIGURE 4.11: Power spectrum of the speleothem oxygen isotope records from the Indian subcontinent caves (a - d) and from the South China cave (e). The spectral analysis of the unevenly spaced paleoclimatic records are obtained using SPECTRUM program (Schulz and Statteger, 1997). Red dashed lines represents the Red Noise.

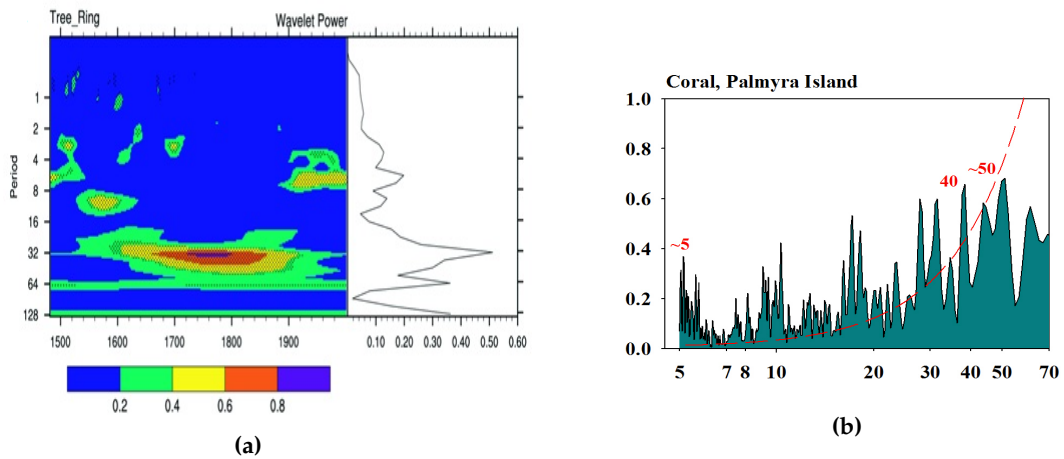


FIGURE 4.12: (a) Wavelet power spectrum of the Teak tree width index, dots represents significance at 95% confidence level. (b) Power spectrum of the Palmyra Island coral $\delta^{18}\text{O}$, dashed line shows red noise.

Similarly, multi-decadal variability was also reported in East African region (Tierney et al., 2013), which has connections with monsoon rainfall variability (e.g. Vizy and Cook, 2003) over India. It is also known that the Indian monsoon variability has

been mostly explained through the indirect effect of El-Niño event on large scale circulation (Kumar et al., 2006). A study of Southern India shows association of deficient ISM and El-Niño events using tree-Ring Width Index (RWI) of Teak as a proxy (Borgaonkar et al., 2010). Northeast Indian stalagmite records Pacific decadal climate change and its high correlation with weakening of the central Indian rainfall. Recent study on drought reconstructions based on tree-ring records by Li et al. (2011) reveals a quasi-regular cycle of 50 - 90 years modulation of ENSO amplitude.

The amplitude modulation of ENSO is closely coupled with changes in the tropical Pacific mean state, implies that the variability of central tropical Pacific climate on multi-decadal timescale may lead to diverse response on ocean-atmospheric large scale circulation. In view of these, power spectrum analysis on the RWI (Borgaonkar et al., 2010) and fossil-coral oxygen isotopic records ($\delta^{18}\text{O}_c$) from the Palmyra Island (6°N, 162°W; Cobb et al., 2003) has been performed, as both the studies implicate either indirectly or directly the ENSO variability. Figure 4.12 shows wavelet power spectrum for RWI (continuous record) and spectral peaks for $\delta^{18}\text{O}_c$, it should be noted that the $\delta^{18}\text{O}_c$ derived mean SST for the months of Nov-Jan (peak of ENSO) have been used. Both the records also show a presence of multi-decadal variability of periodicity 40-50 years, maybe arising due to amplitude modulation of ENSO. It is known that the El-Niño and weakening of Indian monsoon are strongly associated but their negative correlation fails during the recent decades. Therefore, we hypothesize that amplitude modulation in the ENSO might be associated with the observed multi-decadal variability in the Asian monsoon and play a vital role in the El-Niño and Indian monsoon varying relationship. However, modern high-resolution proxy records from the Indian as well as from the Pacific region are needed to strengthen this conjecture.

4.3 Chapter Conclusions

A U-Th dated stalagmite from the Kadapa cave provides a 1460 year (1720-3180 yr BP) record of stable isotopic variations ($\delta^{18}\text{O}$) with annual resolution. The achieved time-resolution for such a long time period is one of the best so far from the Indian region. This stalagmite record shows an overall increase of 1.8‰ in $\delta^{18}\text{O}$ during the 1460-yr period, which corresponds to progressively drier conditions over the peninsular Indian region, indicative of a southward migration of the ITCZ due to a reduction in the northern hemispheric summer insolation. The Kadapa stalagmite record also displays several notable wet and dry periods on multi-decadal to centennial scales. A major depletion of ^{18}O is noted between 2900 and 2850 yr BP (50 years) which may correspond to either an intensification of the ISM and/or enhancement of heavy rain events due to intense cyclonic activities. The abrupt change seen from the Kadapa stalagmite $\delta^{18}\text{O}$ record at ~2800 yr BP is reflected in changes in the trace elemental ratios and crystallographic structure. Furthermore, the abrupt change at 2800 yr BP coincides with the unusual cold event in the North Atlantic (Iron Age cold epoch) having linkages with low solar activity. The Kadapa stalagmite also shows drier conditions

intercepted with the short wet spells during the RWP, which lasted for several centuries. Importantly, drier periods at 2800 (± 20) and 2350 (± 6) yr BP are found to be related to reduced solar activity as evidenced from the co-variation of the speleothem $\delta^{18}\text{O}$ and the atmospheric $\Delta^{14}\text{C}$ records. The coherency between the Kadapa and Dongge cave records point to a synchronous variability between the ISM and EAM systems. Active stalagmite from the same cave will be needed for bridging the gap from the present to 1720 yr BP in the high resolution record, in order to cover the late Holocene climate variability.

A detailed investigation and comparison with the other speleothem records for the common timeframe from the Indian subcontinent have been performed. The long-term (1460 year) trend and major multi-decadal and centennial changes of the Kadapa stalagmite $\delta^{18}\text{O}$ data match well with other stalagmite records from the Indian region. Synthesis of available high-resolution speleothem records help generate last 4000 years of ISM variation, which reflects past major climatic events as well as abrupt changes. Using spectrum analysis, study finds that the oxygen isotope derived ISM has variability on multi-decadal scale of approximately 50 years periodicity. The observed periodicity is also corroborated by the other proxy records (including speleothems) from the Indian subcontinent and South China region. Furthermore, ~ 50 Yr of periodicity is also found in other paleo-climatic proxies such as tree ring (southern India) and fossil-coral (central Pacific). We hypothesized that this kind of variability arise due to amplitude modulation of ENSO, lending support to observed Indian monsoon and ENSO negative correlation failure during recent decades. However, modern high-resolution speleothem record reconstruction from Indian monsoon zone and its potential to capture Pacific climate variability needs to be established. In addition, the past proxy records from the ENSO centric Pacific region are needed to strengthen our conjecture of ISM and ENSO linkage on multi-decadal timescales. Further study on the mechanisms that are responsible for producing such ISM multi-decadal periodicity and ENSO amplitude modulation will help shed light on ISM - ENSO dynamics.

Chapter 5

Summary, Discussion & Outlook

5.1 Summary

In this thesis, the spatial and temporal variability of the amount effect under recent condition is analyzed using modern rainwater isotopes from the Indian subcontinent, namely, Andaman Islands, Bay of Bengal (BoB) and a few sites from the Indian mainland (Nagpur, Tezpur, and Kolkata). Daily rain and vapor sampling were done during the Indian summer monsoon of 2015, to understand the rain and vapor isotopic interaction. In the next phase of this thesis, the analyses of the speleothem sample from the Indian peninsular region are discussed and reconstructed time series of monsoon variability and synthesis of speleothem derived rainfall records are presented.

The above mentioned tasks have been organized into four objectives:

- **Objective 1:** Investigation of precipitation isotopes and their relationship with the meteorological parameters.
- **Objective 2:** Systematic study of the amount effect from different areas including the speleothem sampling sites.
- **Objective 3:** Reconstruction of monsoon rainfall using the isotopic analysis of speleothem from the Indian subcontinent.
- **Objective 4:** Synthesis of speleothems and other proxy derived rain data in and around the Indian subcontinent.

This thesis explores the possible connection between the isotopic composition of rainfall over the Andaman Island and the rainfall over the Indian mainland. Isotopic analysis of rainfall over the Port Blair sites, Andaman Islands was carried out for the year 2012 and 2013 in order to study the atmospheric controls on rainwater isotopic variations. In continuation of that, isotopic analysis of daily rain samples (2012-2017) from Port Blair as well as from some sites on the Indian mainland (2015) namely Nagpur, Kolkata, and Tezpur have been carried out. The dual site (source-receiver) isotopic analysis has been performed with the aim to understand moisture

transport processes and rain-isotope linkage with the monsoon intra-seasonal oscillations (MISOs). Furthermore, a quantitative approach to estimate the isotopic interaction between ambient vapor and raindrops over the BoB is presented. The rain-amount and oxygen isotope ratio database is available from literature, GNIP, as well as the Model output, are evaluated for the Indian region. Additions to that, the study drew a special focus on observed variability in the amount effect by analyzing the daily to monthly rainwater isotopes.

The second part of this thesis work investigates Indian Summer Monsoon (ISM) for the period between 1700 and 3200 yr BP deduced from stable oxygen isotope ($\delta^{18}\text{O}$) and trace element (e.g. Sr, Ba, U) analyses of a stalagmite (Kadapa cave, 14.52°N, 77.99°E) sample collected from peninsular India. A detailed investigation and comparison with the other speleothem records from the Indian subcontinent have been performed (i.e., synthesis). The analysis focuses on the presence of multi-decadal variability in ISM using robust statistical methods, to estimate the periodicity and, explain their coherent behavior.

5.2 Discussion

Discussion on main results

5.2.1 Modern Rain Isotope Study

Results obtained in this study support the recent understanding of the rain and isotope linkage and relationship with meteorological processes, but give new insights into amount effect variability, which should be taken into account for future paleoclimate studies from a proxy as well as model-based perspective.

This part explores the possible connection between the isotopic composition of rainfall over the Andaman Island and the rainfall over the Indian mainland. The oxygen and hydrogen isotopic compositions are typical of the tropical marine sites but show significant variations depending on the ocean-atmosphere conditions; maximum depletion was observed during the tropical cyclones. The isotopic composition of rainwater seems to be controlled by the dynamical nature of the moisture rather than the individual rain events. Precipitation isotopes undergo systematic depletions in response to the organized convection occurring over a large area and are modulated by the integrated effect of convective activities. During the early to mid monsoon, the amount effect arose primarily due to rain re-evaporation but in the later phase, it was driven by moisture convergence rather than evaporation. According to current understanding, amount effect implies - more the rain, more is the isotopic depletion. But this study shows that increased amount of rainfall does not necessarily mean a higher depletion in ^{18}O or ^2H . Since amount effect is caused by different atmospheric processes which occur in different scales, their interactions introduce non-linearity resulting in a variable amount effect.

The isotopic analysis of daily rain samples (2012-2015) from Port Blair, the Andaman Islands, as well as from some sites on the Indian mainland (2015) reveals interesting observations, that is the Port Blair rainwater oxygen isotope ratios ($\delta^{18}\text{O}$) maintained a temporally dependent correlation with the average rain variation over the Core Monsoon Zone (CMZ) of India. The correlation between the isotopic records from the two regions (BoB and CMZ) appears to arise from the propagation of the rain/cloud band from the Bay to the Indian landmass and its association with MISOs. Consequently, the correlation between rainfall over the CMZ and $\delta^{18}\text{O}$ of Port Blair rain provides conclusive evidence of the transport of the Bay of Bengal moisture to some parts of the Indian mainland during the summer monsoon season. The spatial dependency of Port Blair rain-isotopes with the CMZ rain shows interannual variability and also indicates different pathways of the BoB moisture to the Indian mainland within a season. The pathways are identified by the trajectory analysis with Port Blair being the source area. The spectral analysis revealed that $\delta^{18}\text{O}$ of Port Blair rain (vapor) is characterized by a periodicity band of 10 to 25 days for the years 2012-2015 (Figure 3.12). The periodicity band of 10-25 day is probably associated with the 10-20 day mode of monsoon sub-seasonal rainfall variations over the CMZ. Like rainfall, the $\delta^{18}\text{O}$ at these two regions may be modulated by MISOs. We observed analogous variation in $\delta^{18}\text{O}$ of island precipitation and $\delta^{18}\text{O}$ of mainland precipitation at the studied sites (Figure 3.15). The study establishes the time scale of the moisture transport and the building of the convective systems by means of isotopic characteristics. Further, it has been demonstrated that the moisture transport time and the time frame to build a large-scale convective system is intricately related. One of the potential applications of this moisture transport process could be to investigate how the moisture generation and in turn the transport process in the BoB would respond to the global warming in the coming decades.

Further, the analysis focusing on a process by which the spatial distribution pattern of rainfall variability to be arising. In general, southwest wind flows en-route the Southeast Asian region from the south BoB to the western Pacific during the ISM (Normal Flow), however, under certain circumstances, part of the south BoB branch of circulation reverses back to the Indian landmass (Reverse Flow) (Figure 3.18). It has been observed that the south BoB branch of monsoon could extend up to the western Pacific for several years. The study presented that the changes in surface parameters play an important role in the redistribution of Indian monsoon rainfall. Thus, we proposed a mechanism by which the south BoB monsoon flow interacts with the western Pacific atmospheric system, thereby facilitating a pathway of the west Pacific moisture intrusion into the Indian subcontinent. The south BoB branch of ISM appears to be governed by the warm western Pacific climate (mainly near the SCS). However, negative temperature anomalies for some years (e.g., El-Niño) may cause Reverse Flow of the south BoB branch under the well developed low-pressure condition over the central Indian region. A low-pressure zone (i.e., ITCZ) during the ISM exhibits

variability on the intraseasonal timescale. So in this respect, the event (i.e., reversal) takes place on an interannual timescale (during El-Niño). However, the occurrence of this event in a given year may affect the moisture distribution and rainfall pattern on the sub-monthly time scale. The present study brings out one of the causes of significant changes in the rainfall pattern over the Indian region. Most of the studies on rainfall distribution were only limited to seasonal monsoon rainfall only through SW monsoonal flow. For the first time, the present study discussed the contribution from reversal of south BoB branch of SW flow for the major rain-producing month's (i.e. June, July, August, and September) in annual rainfall.

With an aim to improve the understanding of the isotopic composition of rain and vapor as tracers of water-movement in the atmosphere, an effort was made to investigate the important factors of fractionation in rain and vapor phase. Towards this, the isotopic interaction between ambient vapor and raindrops over the Port Blair, Andaman Islands was investigated. Daily rainwater and vapor sample were analyzed for the Indian summer monsoon months of 2015. Isotopologues of rainwater and ambient vapor were found to be positively correlated ($r = 0.55-0.65$) with an average difference of 9.5‰ (65.8‰) in $\delta^{18}\text{O}$ ($\delta^2\text{H}$) on a seasonal timescale. Isotopic controls of the source moisture on ambient vapor and fractionation due to the isotopic exchange can define the isotopic variability of the region rainfall. The study estimated that the interaction between vapor and raindrops can account for approximately 30% variations in the isotopic composition of rainwater. Thus, it is worth mentioning that the isotopic variability in source moisture should also be considered for the comprehensive isotopic studies over the coastal regions.

Earlier studies showed that the amount effect shows a varying characteristic in the Indian subcontinent (e.g., Kumar et al., 2010). While most of the places obey this relation on monthly and longer timescale, some places, such as northeast India, west coast of India and parts of south India show notable exceptions (Bhattacharya et al., 2003; Yadava et al., 2007; Breitenbach et al., 2012). The results of the present study show that the rain isotopes appear to be linked with the monsoon intraseasonal variability in addition to synoptic scale fluctuations. However, rain isotopes undergo systematic depletions in response to the organized convection occurring over a large area and are modulated by the integrated effect of convective activities. Further, the study examines the effect of larger scale rainfall variability on rainwater isotopic composition. The exercise demonstrates that the amount effect remains significant approximately for an area of $5^\circ\text{lat} \times 5^\circ\text{lon}$, but, decreases thereafter. However, a significant correlation between the CMZ rainfall (area 2,000 km away from the Andaman Island) and rainwater isotopic variation of the Port Blair site exists. The spatial dependency of Port Blair rain-isotopes with the CMZ rain shows interannual variability and also indicates different pathways of the BoB moisture to the Indian mainland within a season. Currently, the spatial pattern of ISM rainfall and its isotopic variability simulated by global circulation models show good agreement with the observations, but large

discrepancies exist in the magnitude of simulated amount effect. The characteristic behavior of amount effect is a limiting factor for paleo-monsoon reconstruction on annual to sub-annual time scale using speleothem or tree ring. Our study is expected to provide a better understanding of the amount effect in the Indian region which in turn is likely to help in reducing the discrepancy between observation and the model simulation.

Compilation of earlier studies reveals that $\delta^{18}\text{O}$ of rainfall in the central and peninsular Indian regions varies with the amount of rainfall (Yadava and Ramesh, 2005; Yadava et al., 2004; Kumar et al., 2010). The data of $\delta^{18}\text{O}$ of rainfall and rainfall amount from Kakinada and Bangalore as well as Hyderabad (from GNIP dataset) show a weak but negative correlation. Vuille et al. (2005) show that over most of the monsoon-affected areas (sea to land) circulation generates increased convection, and subsequently an observable amount effect. Furthermore, an isotope incorporated model (IsoGSM2) output datasets (precipitation rate and its $\delta^{18}\text{O}$) with the resolution $\sim 200 \times 200$ km averaged over the Kadapa region show a significant negative correlation (Figure 3.29). Thus, in the present study, the peninsular region (namely Andhra Pradesh) has been chosen for the paleo-monsoon investigation using speleothems.

5.2.2 Past Monsoon Study

This part presents an analysis of the ISM rainfall variations for a 1460-year period (1720-3180 yr BP), based on a long record of a U-Th dated stalagmite record from the Kadapa cave in peninsular India. Overall, results are valuable as the achieved time resolution (~ 1 yr) for this time period is one of the highest so far from the Indian region (up to the authors knowledge). Thus, this record might build the basis for a more in-depth analysis of the impact of annual time-scales on multi-decadal to centennial variability of the Indian monsoon.

The collected speleothem (stalagmite) sample from Kadapa, Andhra Pradesh was analyzed for $\delta^{13}\text{C}$ and $\delta^{18}\text{O}$ and U-Th dating was undertaken on (11 sub-samples) samples to produce a robust time series. The stalagmite proxy record captures variations associated with wet and dry monsoons on decadal to centennial time-scales, together with a general declining trend in the ISM during the 1460 year period (Figure 4.4). It is noted that the declining trend of the ISM follows the northern hemispheric summer insolation, which is known to influence the location and strength of the Inter Tropical Convergence Zone (ITCZ). Furthermore, the Kadapa stalagmite also shows drier conditions intercepted with the short wet spells during the Roman Warm Period (RWP), which lasted for several centuries. The Kadapa stalagmite record indicates an abrupt climate change, characterized by the decline of ISM around 2800 yr BP, as manifested in the enrichment of ^{18}O values. Furthermore, the enriched ^{18}O values around 2800 yr BP are interrelated by changes in the stalagmite growth rate, its trace elemental ratios (Sr/Ca, Ba/Ca, Th/Ca and U/Ca) and crystallographic structure. In addition, the decline of ISM around 2800 yr BP coincides with a sudden rise in the

atmospheric $\Delta^{14}\text{C}$, indicative of reduced solar activity. This period around 2800 yr BP is widely reported as the cold European climate associated with ice debris events in the North Atlantic (also known as the Iron Age Cold Epoch), which were reportedly forced by low solar activity. Synthesis of the published stalagmite records from the Indian region, during the overlapping time-frame, show coherent variations with the Kadapa stalagmite and also the Dongge cave stalagmite (Southern China), pointing to synchronous variations of the Indian and the East Asian monsoon systems (Figure 4.7). Active stalagmite from the same cave could bridge the gap from the present to 1720 yr BP in the high-resolution record, in order to cover the late-Holocene climate variability. Fortunately, in the second expedition to the Kadapa cave, a sample was collected and the U-Th dates confirmed that the sample covered periods between the present and ~ 1700 yr BP, the discussion of the results, however, is beyond the scope of this thesis.

The second section of this part presents the synthesis of the available speleothem derived rainfall records. Speleothem caves are widely distributed over the Indian subcontinent, however, less explored and this makes it a crucial point to compile the available records to enhance our understanding of regional climate and its impact on a global scale. The speleothem oxygen isotope records from the Indian peninsular regions significantly reflected the monsoonal rainfall variations, as at these locations, the influence of changing cave temperature has been considered as negligible. The synthesis of 26 studies from 18 caves around the Indian subcontinent provides oxygen isotope measurements from speleothems (Table 4.1). Compilation of high-resolution records for the last 4000 years reveals that the Indian monsoon influenced by various major climatic events, such as LIA, MWP, and RWP (Figure 4.10).

A detailed investigation and comparison with the other speleothem records for the common time frame (1700-3300 yr BP) from the Indian subcontinent have been performed to understand the mechanism of multi-decadal variability in ISM. Spectral analysis of oxygen isotopic time series from the Indo-China region indicates the presence of a strong periodicity of ~ 50 yrs in almost all the records (Figure 4.11). Furthermore, ~ 50 Yrs of periodicity is also found in other paleo-climatic proxies such as tree ring (southern India) and coral (central Pacific). It is known that the Indian monsoon variability has been mostly explained through the indirect effect of El-Niño event on large scale circulation (Kumar et al., 2006). A study of Southern India shows an association of deficient ISM and El-Niño events using tree-Ring Width Index (RWI) of Teak as a proxy (Borgaonkar et al., 2010). Northeast Indian stalagmite records Pacific decadal climate change and its high correlation with weakening of the central Indian rainfall. A recent study by Li et al. (2011) reveals a quasi-regular cycle of 50 - 90 years modulation of El-Niño & Southern Oscillation (ENSO) amplitude. The ISM variability could be related to amplitude modulation of ENSO. Although El-Niño and weakening of the Indian monsoon are strongly associated but their negative correlation fails during recent decades. We hypothesize that amplitude modulation in the

El-Niño might play a vital role in the observed El-Niño and Indian monsoon varying correlations. Furthermore, similar multi-decadal variability was also reported in the East African region (Tierney et al., 2013, which has connections with monsoon rainfall variability over India. Thus, recent (2-4 ka) high-resolution records from Indian as well as proxy records from the India and the Pacific Ocean are needed to strengthen our present understanding of multi-decadal variability of ISM. This study raises a possibility of regional ocean dynamics role in monsoon variability due to varying surface land-sea thermal response to monsoonal flow that may help understand sporadic lack of teleconnection with tropic and extra-tropic climate.

5.3 Outlook

The work presented in this thesis represents the first detailed study of rain-isotope variability and its relationship with the meteorological parameters from the Indian subcontinent. Most of the earlier studies and the hypothesis are based on global/regional rain-isotope data on monthly to annual timescales. This thesis takes the initiative of analyzing the isotopic characteristics of daily rain samples to understand the atmospheric controls on the rain isotopes over the Indian region on intraseasonal timescale, specifically over the Bay of Bengal and the surrounding landmasses. The advantage of this approach is the applicability to a range of variability and seasonality in rain-isotope, in turn, to understand spatial and temporal variability in rainfall. The reason for not using such method was due to high-resolution data availability on both spatial extent and temporal scales. However, a method based on daily timescale including other variables may describe, inconsistent patterns of amount effect, atmospheric circulation on intraseasonal timescale (e.g. active and break spells), moisture transport processes, seasonality in rain-isotope and its linkage with monsoon intraseasonal variability.

For a better understanding of the rain and isotope relationship over a specific region, further work is warranted. First of all, it is necessary to increase the network of sampling sites to have an extensive dataset on various timescales (possibly sub-daily to daily). The present study is basically based on rain-isotope observation from the Andaman region (Port Blair) and it would be interesting to investigate the observed rain-isotope variability responses for the other part of the Indian subcontinent (e.g., the Arabian Sea, central India). The rain and isotope relationship seem to be governed by the intensity of active and break spells, however, number of such cases (active and break) need to be investigated for better characterization based on rain-isotopes. Further, the study proposed a dual site (moisture source and destination) analysis of daily rainwater isotope, instead of the traditional method of the single (destination) site analysis. That is an alternative method and perhaps offers a better understanding of the moisture dynamical processes. Since rain isotopes are strongly modulated by the moisture dynamics in the subseasonal scale, including the moisture

generated from the source (Ocean), its systematic study would be helpful to monitor the long-term changes in the subseasonal moisture transport and hence the temporal variability pattern of rain, for instance, rainfall derived from the BoB moisture over the Indian subcontinent. One of the potential applications of this moisture transport process could be to investigate how the moisture generation and in turn the transport process in the BoB would respond to the global warming in the coming decades. Increased use of river water for the societal needs may reduce the continental runoff in the foreseeable future. Additionally, the melting of mountain glaciers may worsen this problem. This, in turn, is likely to have an adverse effect on the BoB stratification process and hence the monsoon rainfall. The situation may get further aggravated due to the decreasing trend of moisture transport from the Indian Ocean as a result of weakening trends of low-level wind speed and moisture content (Konwar et al., 2012).

The above analysis on moisture transport processes reveals that the BoB branch of ISM has two distinct types of moisture pathways on intraseasonal timescale under certain circumstances. That is in some of the years during the summer monsoon, BoB branch suffered a retrograde path and reversed back (at around the South China Sea) to Indian landmass. Further analysis consisting of several years of observation is required to quantify the reverse flow moisture contribution and to determine its timescale and to fully characterize the drivers of the reversal events. Once the south BoB branch of circulation is well understood its interpretation in terms of Pacific teleconnection in General Circulation Models may improve the prediction/simulation of summer monsoon rainfall pattern over the Indian continent.

An attempt to understand the rain-vapor interaction based on rain and vapor time series on daily timescale over BoB could be valuable to estimate the isotopic fraction due to isotopic exchange. The study investigated the isotopic relationship between the major components, i.e., "source moisture - ambient vapor - rainwater" on the basis of rainfall amount, which reveals complexity in estimation during the heavy rainfall events. However, current experimental setup is not adequate enough to overcome this limitation, but high frequency (such as on hourly timescale using an isotope analyzer) analysis of rain and vapor samples is likely to offer a better understanding of the physical mechanisms controlling the variations of the isotopic composition during heavy rainfall conditions.

A major focus of the present work was to augment the high-resolution records of past monsoon to understand the ISM variability on various timescales. In this context, peninsular India speleothems are promoted to be very good archives for paleomonsoon studies. However, temperature reconstruction is feasible using oxygen isotopes, especially in tropical speleothems. Fluid inclusions in speleothems could be very useful for paleo-temperature reconstruction using the concentration of dissolved noble gases and $\delta^2\text{H}$ ($\delta^{18}\text{O}$ of fluids may not be very useful due to isotopic exchange with carbonates) (Kluge et al., 2008), this may hold immense potential in the Indian

context. A better understanding of paleoclimate (e.g. rainfall and temperature) is important for modelling future climate and the response of the changing climate on monsoon variability. One more aspect that needs to be improved is better instrumental facilities, such as, organic geochemistry laboratory to measure organic biomarkers, Multi-collector Inductively Coupled Plasma Mass Spectrometer (MC-ICPMS) dating techniques (for U-Th dating), which are either not available or not efficiently practiced at present in India. It would be interesting to estimate the error occurred in radiocarbon dating in comparison to U-Th dates of the same sample, in turn, estimation of dead carbon in cave deposits and to improve understanding of complex nature of the geochemical processes associated with recharge and carbonate precipitation.

Speleothem derived stable isotopic variations from the Indian subcontinent as well as few sites (e.g. South China) those come under the broader domain of the same Asian monsoon system show an uneven range of variation in isotopic composition for the same time period, although, variability are similar. This may be because of different cave settings (soil productivity or vegetation type), location (latitude, longitude), temperature etc. In this context, it is important to focus on the organic geochemical aspect of variations in speleothem proxies. Besides, source moisture of the cave region and air-mass pathways can also play an important role in isotopic variations in rainwater, in turn, imprinted in cave deposits. It will involve detailed study of available speleothem records from different regions. On the other hand, it needs to derive a model that comprises an estimation of the isotopic composition of source moisture (Harmon and Gordon, 1965) and fractionation at all stages of the pathway from source region through to condensation (rainwater isotope data for at least 10 years) over the site.

Synthesis of past records of monsoon rainfall from Indian subcontinent reveal various wet and dry periods on decadal to centennial timescales. Notably, the mid 14th - 15th centuries witnessed a series of dry monsoon phases (droughts) that each lasted for several years to decades (Sinha et al., 2011a; Borgaonkar et al., 2010). Studies have shown the linkage between tropical Pacific variability and weakening of south Asia monsoon (e.g., Rasmusson and Carpenter, 1982); however, the relation failed more than half of the times during instrumental data records (Kumar et al., 2002). Moreover, a few records suggest La-Niña like conditions persisted at times of mega-drought over Asia (Moy et al., 2002; Conroy et al., 2008). Another theory is Inter-Tropical convergence zone (ITCZ) movement and its association with global monsoon on centennial to millennial scale (e.g., Wang et al., 2001; Dykoski et al., 2005; Overpeck et al., 1996, etc); however, under this view explaining discrete multi-decadal weakening of monsoon is still a matter of debate. In addition to these, the monsoon variability is fundamentally connected with the seasonal dynamics of convection, moisture pathways, troposphere wind and temperature (e.g., Krishnan et al., 2006; Gadgil et al., 2007; Sun et al., 2010). In a recent study, the multi-decadal monsoonal variability in the East African region found to be driven by Indian Ocean, which has connections

with monsoon rainfall variability over India. These studies raise a possibility of regional ocean dynamics role in monsoon variability due to varying surface land-sea thermal response to monsoonal flow and sporadic lack of teleconnection with tropic and extra-tropic climate. The proxy-based studies reveal multi-decadal variability in ISM rainfall at a timescale of 50-80 years in periodicity. This could be considered as a 'mode' of variability of the Asian monsoon (Goswami et al., 2014). However, neither the periodicity, nor the stationarity of the variability, or its mechanism are established and remain an active area of research. The past changes may help understand changes in the ISM that may occur in future, which has large societal impacts for associated regions starting from East Africa to the Indian subcontinent and extended up to East Asian countries.

This thesis contributes to a growing body of literature suggesting that rainfall and speleothem $\delta^{18}\text{O}$ reflect not just rainfall amount, but various hydro-climatic processes. Despite this source of uncertainty, well-dated speleothem records remain important archives of paleo-climatic information, which are increasingly being supported by instrumental monitoring and numerical modelling studies. In particular, this thesis highlights the importance of rain-isotope variation in the modern time period and terrestrial moisture transport in understanding the causes of $\delta^{18}\text{O}$ systematic across the Indian region. The existing network of rainwater sampling and cave sites across the Indian subcontinent needs to be improved to obtain a robust database. Future multi-proxy approach will exploit ongoing improvements to isotope-enabled GCMs at regional scales, constraints on hydrological processes, and karst hydrology modelling to provide quantitative tests of the fidelity of $\delta^{18}\text{O}$ -based paleo-monsoon reconstructions. Not least because this highly populous region depends greatly upon seasonal rainfall, establishing an accurate understanding of past ISM variability is an important scientific goal.

Appendix A

Chapter I

Supplementary Materials for Chapter 3

A.1 Spectral Analysis

The periodicities in the $\delta^{18}\text{O}$ of rain samples (2012 - 2015) using the Lomb-Scargle periodogram method and compared with the interpolated method (Figure 3.12), the results are found to be similar (Figure A.1). The significant peaks from both the spectral analyses methods are marked and common peaks are circled with the same color.

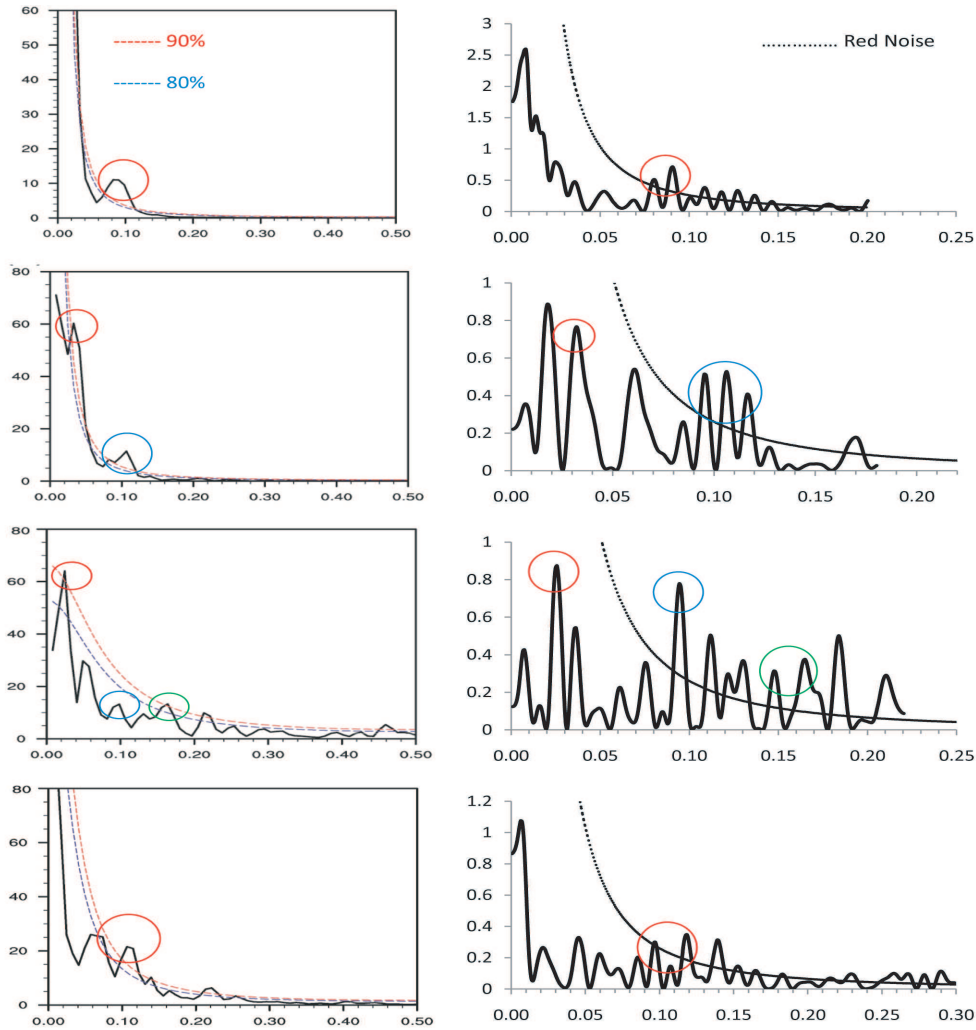


FIGURE A.1: Left column shows the spectral analysis performed on interpolated $\delta^{18}\text{O}$ for the years 2012-2015 (top to bottom). In the right column, the Lomb-Scargle periodogram outputs are shown for the corresponding years, uneven $\delta^{18}\text{O}$ values are used as input. Comparisons between both the results reveal similar significant peaks, marked with same color circles in both the column on the peaks.

A.2 Source Moisture over Port Blair

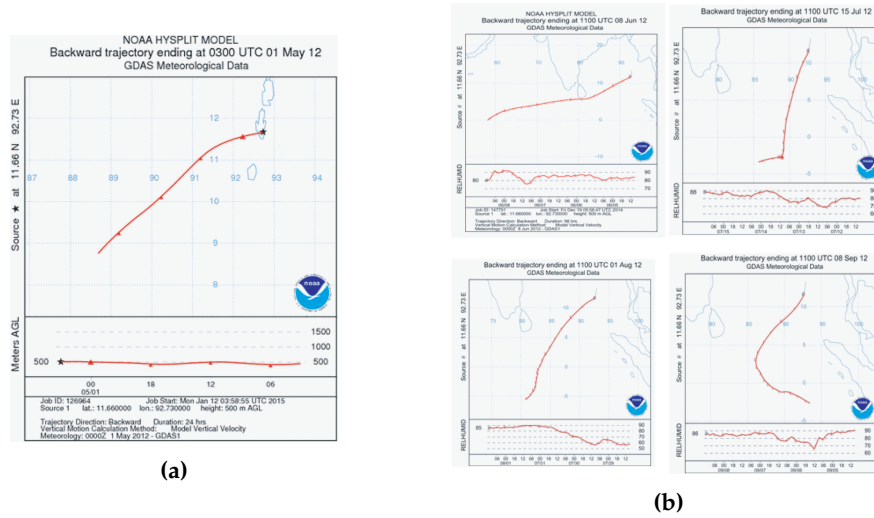


FIGURE A.2: (a) 24hr wind back trajectory plot for May 1-7, 2012, produced by Hysplit model showing the air movement from the southern portion of the Bay of Bengal to the sample site (Port Blair, indicated as star). (b) 98hr wind back trajectory plot for monsoon season (JJAS) showing the major moisture source at the sampling site is from the remote Indian Ocean. Latitudes and longitudes are marked on the grids. The bottom panel shows the temporal variation of the heights of the air masses in meters.

A.3 Relative humidity and Wind

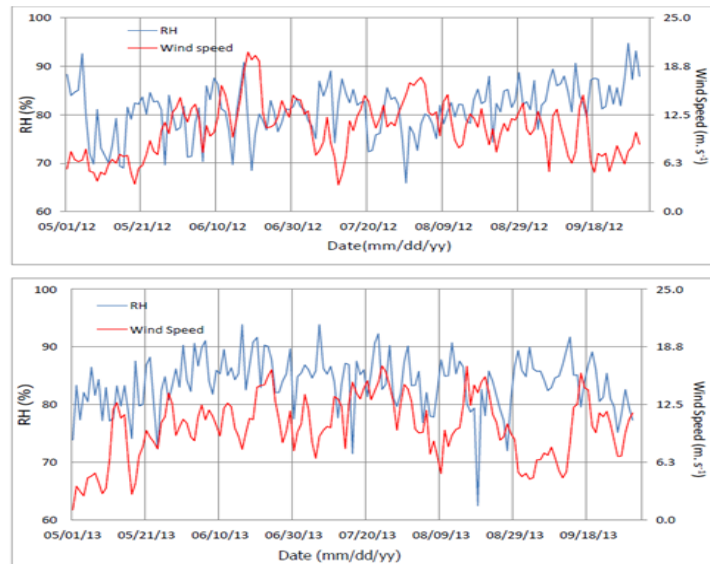


FIGURE A.3: Relative humidity, RH (in blue, left Y-axis) and Wind Speed (in red, right Y-axis) at 850 hPa on a 5×5 grid box over Port Blair. Upper panel is for the year 2012 and the lower panel is for the year 2013.

A.4 Cyclone Tracks

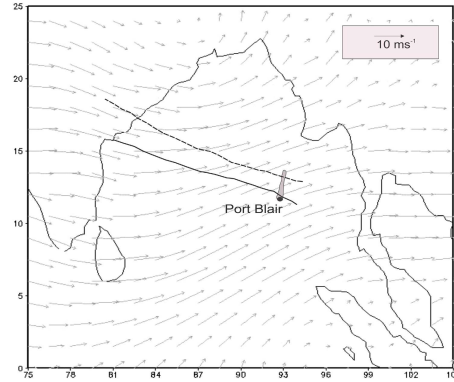


FIGURE A.4: The Andaman and Nicobar Island (in grey, not to scale); Port Blair (solid circle) is the rain sampling location. The two curve lines show the cyclonic tracks: Phailin (dotted) and Lehar (solid) that caused heavy rain in and around the Islands in November-2013. The mean wind pattern during the monsoon season (JJAS) of 2012 has also been shown (grey arrows).

A.5 CMZ Rain and Port Blair- $\delta^{18}\text{O}$ anomaly

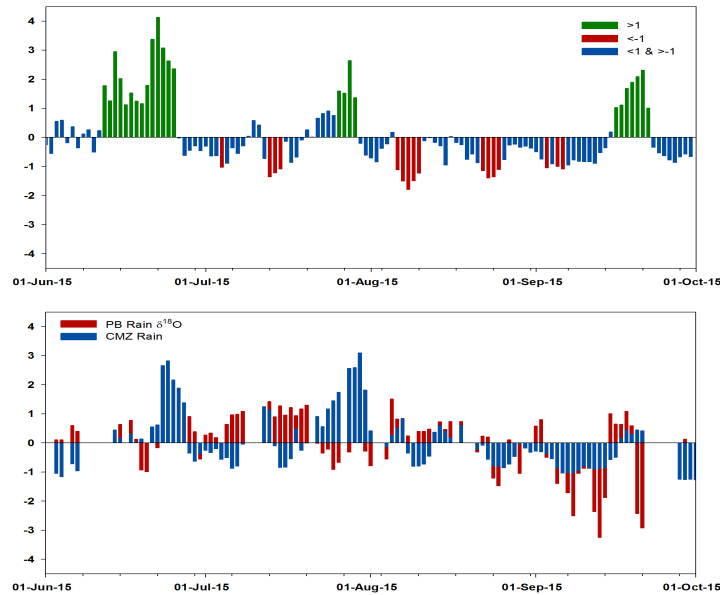


FIGURE A.5: (a) Anomalies constructed by subtracting the climatological mean (reference years 1950-2000) from the 2015 CMZ rainfall data. (b) 2015 anomalies in CMZ rain amount and Port Blair $\delta^{18}\text{O}$ with respect to year 2015. The active periods (defined as rainfall $> +1\sigma$ for three successive days) are shown by green bars, and the break periods (defined as rainfall $< -1\sigma$ for three successive days) are noted by red bars. The intervening periods are denoted by blue bars.

A.6 Timescale of moisture transport

Forward/backward trajectories have been calculated to estimate the moisture transport time from BoB to the three mainland sites, namely Nagpur, Kolkata, and Tezpur (Figure A.6 (a), (b), and (c) respectively). The respective average travel time for the central Indian, east and north-eastern Indian region was found to be 10, 4 and 7 days respectively. It was also observed that the BoB moisture near the Andaman Island usually travelled to the western Pacific through the Southeast Asian region. However, few trajectories have shown direct moisture pathways from the island (Port Blair) to the mainland (Figure A.6 (a), dashed curves) and in some anomalous cases, moisture paths suffered an inversion at around the Southeast Asian region and reached the Indian mainland (Figure A.6, solid curves).

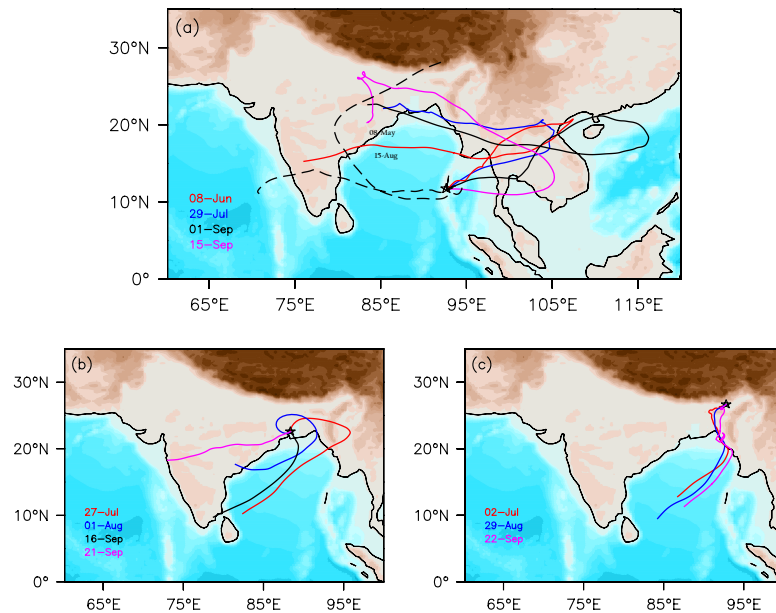


FIGURE A.6: HYSPLIT model trajectory (a) Examples of a few forward trajectories (run time = 190 - 240 hrs) showing the direct and reversed pathway of BoB (Port Blair) moisture to the Indian mainland during JJAS, 2015. (b) Backward trajectories showing a few examples of the moisture contribution from BoB to Kolkata (run time = 48 hrs) during JJAS, 2015. (c) Same as (b) but for Tezpur (run time = 168 hrs). Sites are marked with stars and the background depicts the general topography.

A.7 Circulation pattern of the south BoB branch during ISM

The study of mean-monthly winds reveals two types of circulation pattern of the south BoB branch during ISM, which needs to be investigated in detail. Firstly, wind flows from the south BoB to the western Pacific via the Southeast Asian region (e.g., Figure 3.16 (a)). This is a general circulation flow of the south BoB branch during the

ISM season (Normal Flow). On the other hand, one part of the south BoB branch gets reversed at around the South China Sea toward the Indian landmass (e.g., Figure 3.16 (b)); this anomalous reversal pattern has been observed only for a few years during the ISM months (Reverse Flow). Detailed analyses of monthly wind and surface meteorological parameters help characterize the years, which occasionally experience the reverse circulation patterns during the ISM months. The reverse wind patterns are observed only for a few specific years under certain circumstances during ISM. A possible mechanism of the reversal and year characterization criteria are described in subsequent sections. We divide these characteristics into two cases (Table A.1); Case-I: the years with Normal Flow of the south BoB branch during ISM months and, Case-II: the years that occasionally show the monthly Reverse Flow patterns of the south BoB branch during the ISM months.

TABLE A.1: Case-I: Years with Normal Flow of the south BoB branch and Case-II: years those comprise Reverse Flow of the south BoB branch, during Indian summer monsoon (June-September).

	Year
Case - I	1983, 1990, 1993, 2003, 2006, 2012
Case - II	1982, 2002, 2014, 2015

A.7.1 Spatial rainfall distribution during the summer monsoon

To gain insight on the changes in moisture or rainfall spatial patterns, if any, due to the distinct flow of the south BoB branch. Firstly, we examined the vertical moisture variations in the two Cases. Calculated longitudinally averaged ($75^{\circ}\text{E} - 85^{\circ}\text{E}$) specific humidity has been plotted with latitudes (Figure A.7). The Plot shows the vertically integrated latitudinal variations of seasonal (Jun-Sep) mean moisture content over the Indian region for the years belonging to the two Cases (Table-A.1), as well as two exceptions (1987 and 1997). The vertical moisture contents (Figure A.7, red curves) for the years that comprise Reverse Flow are found comparably equivalent to years with Normal Flow of the south BoB branch during ISM (Figure A.7, black curves). Although, corresponding years of Case-I and Case-II (Table A.1) have had normal and poor summer monsoonal rainfall respectively. All the four years that have shown the events of reversal of the south BoB branch are El-Niño years, and also rainfall was below normal considering India as a whole. However, the convergence of the red curves between the latitudes $20^{\circ}\text{N} - 30^{\circ}\text{N}$ shows that there is an additional moisture source over central India. It can be interpreted that the reversal of the south BoB branch during these years could be the source of moisture, thereby weakening the effect of El-Niño which is known to suppress the seasonal rainfall over the Indian landmass. As we mentioned, there are two years with no Reverse Flow of the south

BoB branch, although they are strong El-Niño years.

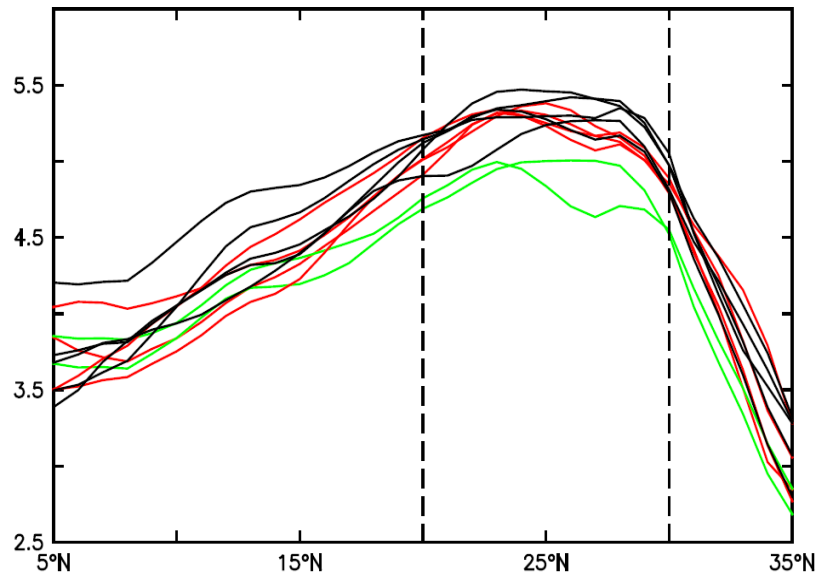


FIGURE A.7: Vertically Integrated specific humidity (Kg/Kg) averaged over longitudes 75°E - 85°E and plotted along the latitude between 5°N and 35°N. Dashed straight lines are representing central India (20°E & 30°E). Black and red curves showing the variation in moisture content for the years (Table A.1) with Normal Flow and Reverse Flow during ISM respectively, the green curves are for the two El-Niño years without Reverse Flow (1987 and 1997).

These are 1987 and 1997 coinciding with conditions of drought and below normal rainfall over the central Indian region respectively (www.tropmet.res.in/pub/data/rain/iitm-regionrf.txt). The low seasonal moisture content over central India (A.7 green curve) and observed wind patterns for those years also indicate a weak summer monsoon. Investigations reveal that the positive temperature anomaly and low pressure zone is shifted towards the west of India and dominant dry winds are ascendant from the northwest direction. Hence, we speculated that this could be one of the reasons for deficit monsoon conditions.

The spatial distribution of rainfall during ISM over the Indian subcontinent has been shown for the respective Case I and Case II year's monthly composite plots in Figure A.8. Rainfall patterns in latitudinal belt 15°N-30°N over central India in both the cases are found to be similar particularly during the mid months (Jul and Aug) of the ISM. However, deviation in rainfall patterns and shifting in rain bands toward central and northeast Indian region manifested for the composite of the Case II years. A report of the National Climate Centre (Guhathakurta and Rajeevan, 2007) documented the trends in rainfall pattern over India for the period 1901-2003. They have reported that the mean rainfall in July and August contributes up-to 45.4% of annual rainfall out of mean southwest monsoon (74.2%, 877.2 mm).

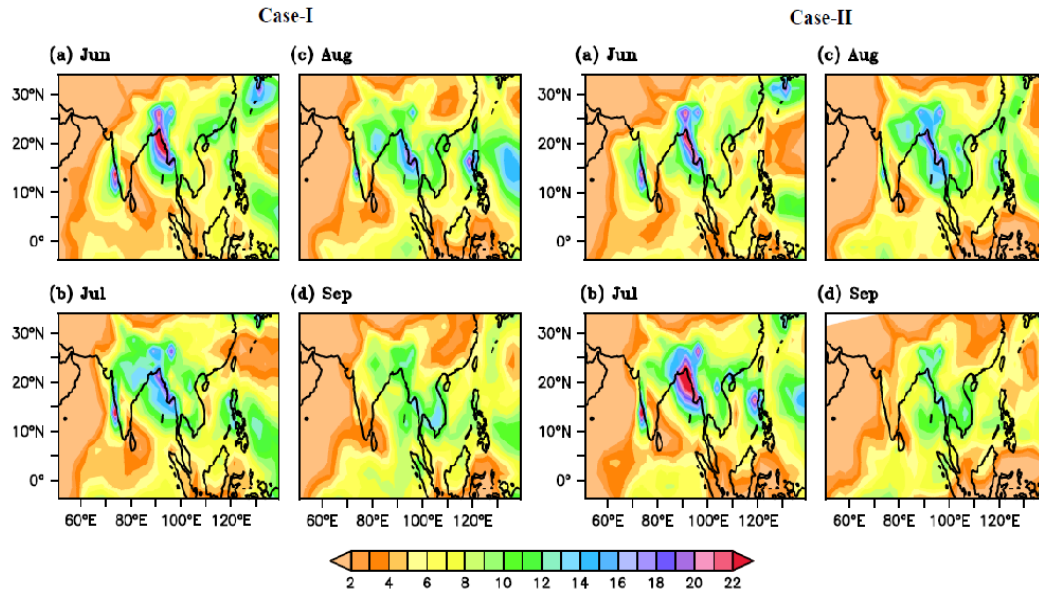


FIGURE A.8: Composite of rainfall (mm) amount during ISM months to compare the change in rainfall patterns for the years (Case-I) with Normal Flow and the years (Case-II) comprises Reverse Flow of the south BoB branch.

Furthermore, the standard deviation and coefficient of variability for 1901-2003 rainfall time series are reported 71.0 mm, 8.1% respectively. Consistent with the reported variability, calculated coefficient of variability for composites of ISM mid months of Case I and Case II years show low variance (< 0.3) particularly over central/northeast India as compared to the other regions. The main result regarding the change in rainfall pattern during ISM mid-months can be summarized as similar rainfall distribution over central and north-east India for both the cases, change in rainfall pattern and slight shifting of rainfall centre toward east of India for case II. We have examined the changes in the ISM circulation patterns for the case II years over the region, which may be useful to explain the corresponding changes in the rainfall pattern. The synoptic systems like low-pressure areas extension through the reversed branch of BoB and centred depression over the BoB is responsible for the rainfall distribution over central north and northeast India and adjacent areas of North Bay of Bengal.

A.8 Vapor Sampling Site

The Port Blair site is situated in the southern part of the Andaman Islands in the BoB and characterized by tropical wet climate. The site location is indicated as a red dot in Figure A.8, the vectors represent the mean wind pattern between June-September (ISM season) 2015. During the ISM season, strong southwesterly winds from the south BoB are the dominating moisture source over the Andaman Islands. It is also corroborated by the back trajectory analysis, as the origin of air-masses is

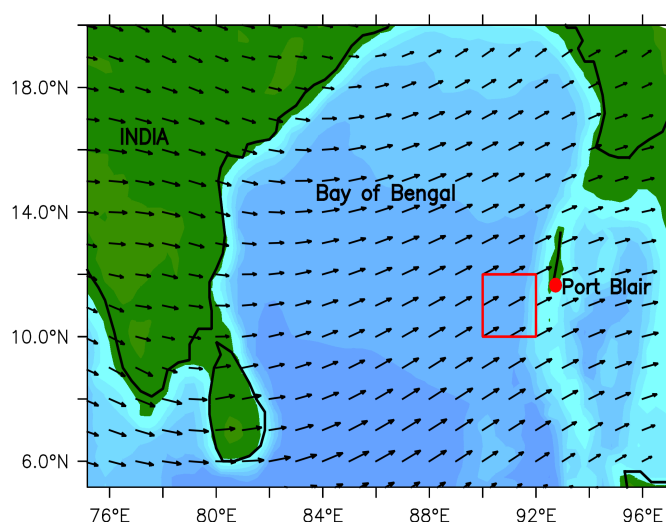


FIGURE A.9: Shows a horizontal view of the site location (red filled circle) and mean wind pattern (vector) for the Indian summer monsoon, 2015.

assumed to be approximate to the moisture source direction for the water vapor and rainfall at the study site (Draxler et al., 2010). However, a large amount of moisture over the site is expected to have come from the south BoB. As the underlying ocean surface water contribution to the convective systems are the major source of moisture, particularly over the BoB region (Shenoi et al., 2002). A few studies also reported that the northeastern BoB contributes a significant amount of vapor to the summer monsoon rains (e.g. Achyuthan et al., 2013). Therefore, an area of $2^\circ \times 2^\circ$ ($10^\circ\text{N} - 12^\circ\text{N}$, $90^\circ\text{E} - 92^\circ\text{E}$) in the southwest of the Port Blair site has been considered to calculate R_e using the C-G Model (red box, Figure A.9).

Appendix B

Chapter II

Supplementary Materials for Chapter 4

B.1 Moisture Source Region: Kadapa Cave

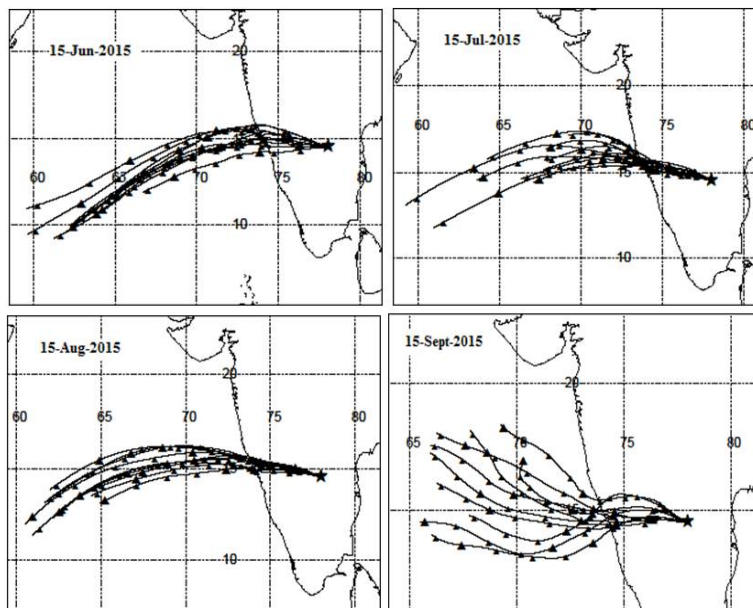


FIGURE B.1: Forty-eight-hour backward wind trajectories for the qualitative identification of moisture sources at the Kadapa Cave during the monsoon (June to Sep). The trajectories are obtained at a height of 1000 m from the ground level using the NOAA Hybrid Single Particle Lagrangian Integrated Trajectory (HYSPLOT) Model for some selected dates of monsoon months of 2015: 15th June, 15th July, 15th August, and 15th September.

B.2 Monthly Climatology: Andhra Pradesh Region

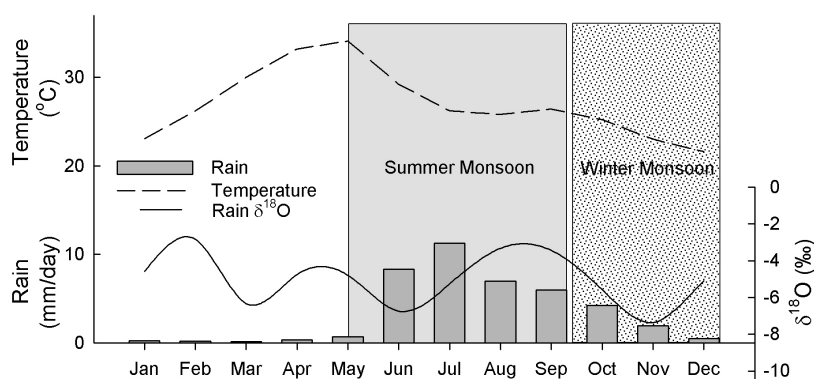


FIGURE B.2: Monthly climatological variation of rain, temperature, and rain oxygen isotope ratio ($\delta^{18}\text{O}$) over the Kadapa region using IsoGSM2 data (Yoshimura et al., 2008). Climatology has been calculated for the period of 1979-2013 at box area of $\sim 2^\circ \times 2^\circ$ over the study site. During the Indian summer monsoon, depleted values of $\delta^{18}\text{O}$ correspond to high rainfall amount. On the other hand, rainfall during the winter monsoon is more depleted for even low rainfall amount.

B.3 $\delta^{18}\text{O}$ and $\delta^{13}\text{C}$ Correlation

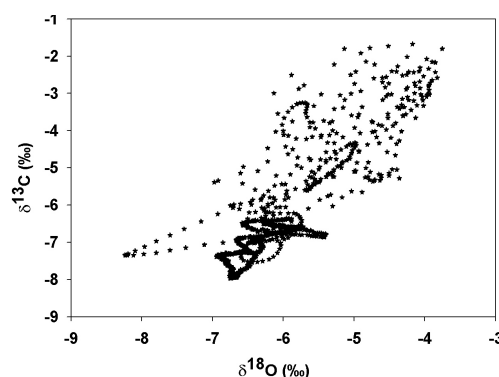


FIGURE B.3: Scatter plot of $\delta^{18}\text{O}$ versus $\delta^{13}\text{C}$ values along the growth axis.

B.4 Crystallography Results: Kadapa Stalagmite Sample

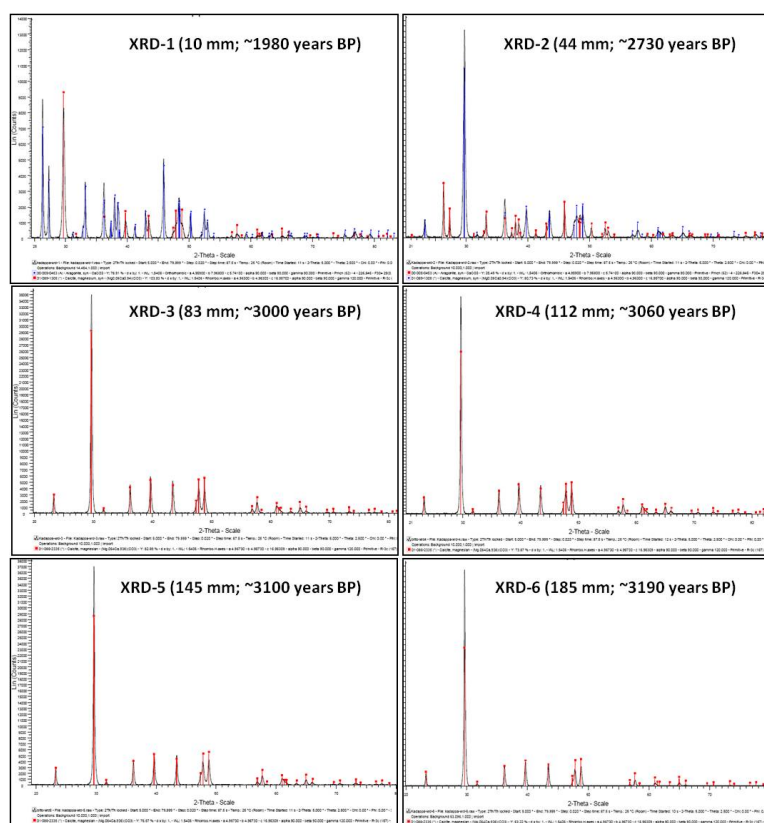


FIGURE B.4: XRD peaks of six sub-samples from Kadapa Cave stalagmite (see Figure 4.2 for sample drilled positions). In (a) and (b), red and blue peaks are of Aragonite; syn CaCO_3 and Calcite-magnesium; syn $(\text{Mg}_{0.06}\text{Ca}_{0.94}) (\text{CO}_3)$, respectively. In (c) to (f) red peaks are of Calcite -magnesium; syn $(\text{Mg}_{0.06}\text{Ca}_{0.94}) (\text{CO}_3)$.

B.5 Amount Effect: Kadapa Region

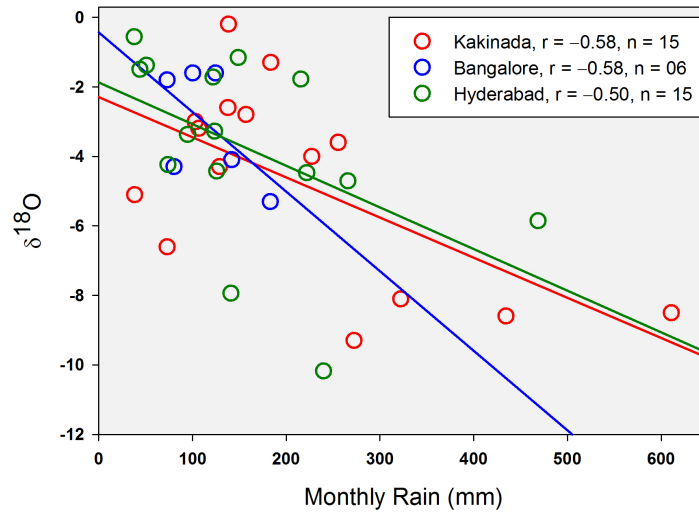


FIGURE B.5: The inverse correlation between $\delta^{18}\text{O}$ and monthly rainfall amount for the few sites from Kumar et al. (2010), namely, Kakinada, and Bangalore as well as Hyderabad (from GNIP data set). The $\delta^{18}\text{O}$ and rainfall amount of these sites show a weak negative correlation.

B.6 U-Th Dating: Kadapa Stalagmite Samples

Depth (mm)	Sample code	Weight (mg)	^{238}U (ppm)	^{232}Th (ppb)	$\delta^{234}\text{U}$ (a)	$\pm 2\sigma$	$(^{230}\text{Th}/^{238}\text{U})$ $\pm 2\sigma$	$(^{230}\text{Th}/^{232}\text{Th})$ $\pm 2\sigma$	Age uncorrected (Yr before 2015)	$\pm 2\sigma$	Age corrected (Yr before 2015)	$\pm 2\sigma$	Age corrected (Yr BP)	$\delta^{234}\text{U}_{\text{initial}}$ (b)	$\pm 2\sigma$	
1	NK-1	11.61	63.0271	0.0384	2.854	0.008	559.45	1.29	1.5595	0.0013	1717.97	7.79	1806	7	562.32	1.30
23	NK-23	11.68	72.1467	0.0356	4.125	0.006	545.92	1.05	1.5459	0.0011	1670.69	4.64	2241	6	549.40	1.06
46	NK-46	10.97	16.0168	0.0050	0.477	0.006	437.90	1.30	1.4379	0.0013	3639.05	46.72	2738	14	441.31	1.31
61	NK-61	11.98	4.1650	0.0019	1.458	0.005	444.71	1.23	1.4447	0.0012	323.18	2.40	2841	20	448.34	1.24
77	NK-77	12.83	4.5624	0.0059	6.830	0.019	498.08	1.68	1.4981	0.0017	84.00	0.81	3055	29	502.57	1.70
93	NK-93	15.24	4.7906	0.0044	0.762	0.003	506.40	1.87	1.5064	0.0019	792.66	5.80	3047	20	510.80	1.88
108	NK-108	09.78	4.9632	0.0084	1.250	0.004	480.07	1.65	1.4801	0.0017	493.30	4.36	3054	26	484.26	1.66
142	NK-142	13.18	4.1818	0.0049	0.627	0.004	529.55	1.71	1.5296	0.0017	868.53	9.01	3099	25	534.23	1.73
174	NK-174	10.25	5.0937	0.0018	1.934	0.006	507.88	0.85	1.5079	0.0009	346.74	2.51	3178	21	512.51	0.86
187	NK-187	11.87	5.6947	0.0051	0.228	0.003	529.05	0.96	1.5291	0.0010	3352.80	51.11	3200	26	533.86	0.98
209	NK-209	10.15	5.2379	0.0020	1.440	0.004	514.46	1.22	1.5145	0.0012	489.41	2.29	3234	12	519.22	1.24

Formula used:

$$(a) \delta^{234}\text{U} = ([^{234}\text{U}/^{238}\text{U}] - 1) \times 1000$$

$$(b) \delta^{234}\text{U}_{\text{initial}} = \{([^{234}\text{U}/^{238}\text{U}]_{\text{corrected initial}} - 1) \times 1000\} \times e^{\lambda_{234} \cdot T}, T \text{ is corrected age and } \lambda_{234} = 2.8263 \times 10^{-6} \text{ yr}^{-1}$$

FIGURE B.6: Uranium and Thorium isotopic compositions and U-Th ages measured by MC-ICPMS for 11 subsamples of stalagmite NK-1305 from Kadapa cave. Here, yr BP refers to before present 1950 AD.

Bibliography

- Achyuthan, H. et al. (2013). "Stable isotopes and salinity in the surface waters of the Bay of Bengal: Implications for water dynamics and palaeoclimate." In: *Marine Chemistry* 149, pp. 51 –62. URL: <https://dx.doi.org/10.1016/j.marchem.2012.12.006>.
- Adler, Robert F. et al. (2003). "The Version-2 Global Precipitation Climatology Project (GPCP) Monthly Precipitation Analysis (1979 - Present)". In: *Journal of Hydrometeorology* 4.6, pp. 1147 –1167. DOI: [10.1175/1525-7541\(2003\)004<1147:TVGPCP>2.0.CO;2](https://doi.org/10.1175/1525-7541(2003)004<1147:TVGPCP>2.0.CO;2).
- Araguás-Araguás, L., K. Froehlich, and K. Rozanski (2000). "Deuterium and oxygen-18 isotope composition of precipitation and atmospheric moisture". In: *Hydrological Processes* 14.8, pp. 1341 –1355. DOI: [10.1002/1099-1085\(20000615\)14:8<1341::AID-HYP983>3.0.CO;2-Z](https://doi.org/10.1002/1099-1085(20000615)14:8<1341::AID-HYP983>3.0.CO;2-Z).
- Araguás-Araguás, Luis, Klaus Froehlich, and Kazimierz Rozanski (1998). "Stable isotope composition of precipitation over southeast Asia". In: *Journal of Geophysical Research: Atmospheres* 103.D22, pp. 28721 –28742. DOI: [10.1029/98JD02582](https://doi.org/10.1029/98JD02582).
- Baker, Andy et al. (1998). "Testing Theoretically Predicted Stalagmite Growth Rate with Recent Annually Laminated Samples: Implications for Past Stalagmite Deposition". In: *Geochimica et Cosmochimica Acta* 62.3, pp. 393 –404. DOI: [10.1016/S0016-7037\(97\)00343-8](https://doi.org/10.1016/S0016-7037(97)00343-8).
- Baldini, James U.L. et al. (2008). "Very high-frequency and seasonal cave atmosphere PCO₂ variability: Implications for stalagmite growth and oxygen isotope-based paleoclimate records". In: *Earth and Planetary Science Letters* 272.1, pp. 118 –129. DOI: <https://doi.org/10.1016/j.epsl.2008.04.031>.
- Baldwin, M. P. et al. (2001). "The quasi-biennial oscillation". In: *Reviews of Geophysics* 39.2, pp. 179–229. DOI: [10.1029/1999RG000073](https://doi.org/10.1029/1999RG000073).
- Bar-Matthews, Miryam et al. (1999). "The Eastern Mediterranean paleoclimate as a reflection of regional events: Soreq cave, Israel". In: *Earth and Planetary Science Letters* 166.1, pp. 85 –95. ISSN: 0012-821X. DOI: [https://doi.org/10.1016/S0012-821X\(98\)00275-1](https://doi.org/10.1016/S0012-821X(98)00275-1).
- Bavadekar, S. N. and D. A. Mooley (1981). "Use of the equation of continuity of water vapor for computation of average precipitation over peninsular India during summer monsoon". In: *Cambridge University Press*, pp. 261 –268.
- Berkelhammer, Max et al. (2010). "Persistent multidecadal power of the Indian Summer Monsoon". In: *Earth and Planetary Science Letters* 290.1, pp. 166 –172. ISSN: 0012-821X. DOI: <https://doi.org/10.1016/j.epsl.2009.12.017>.

- Bhattacharya, S. K., S. K. Gupta, and R. V. Krishnamurthy (1985). "Oxygen and hydrogen isotopic ratios in groundwaters and river waters from India". In: *Proceedings of the Indian Academy of Sciences - Earth and Planetary Sciences* 94.3, pp. 283–295. DOI: [10.1007/BF02839206](https://doi.org/10.1007/BF02839206).
- Bhattacharya, S. K. et al. (2003). "Isotopic variation in Indian Monsoon precipitation: Records from Bombay and New Delhi". In: *Geophysical Research Letters* 30.24. DOI: [10.1029/2003GL018453](https://doi.org/10.1029/2003GL018453).
- Blaauw, Maarten, Bas van Geel, and Johannes van der Plicht (2004). "Solar forcing of climatic change during the mid-Holocene: indications from raised bogs in The Netherlands". In: *The Holocene* 14.1, pp. 35–44. DOI: [10.1191/0959683604hl687rp](https://doi.org/10.1191/0959683604hl687rp).
- Bolliet, T. et al. (2016). "Water and carbon stable isotope records from natural archives: a new database and interactive online platform for data browsing, visualizing and downloading". In: *Climate of the Past* 12.8, pp. 1693–1719. DOI: [10.5194/cp-12-1693-2016](https://doi.org/10.5194/cp-12-1693-2016).
- Bond, Gerard et al. (2001). "Persistent Solar Influence on North Atlantic Climate During the Holocene". In: *Science* 294.5549, pp. 2130–2136. DOI: [10.1126/science.1065680](https://doi.org/10.1126/science.1065680).
- Borgaonkar, H. P. et al. (2010). "El Niño and related monsoon Droughts signals in 523-year-long ring width records of teak (*Tectonagrandis* L.F.) trees from South India". In: *Palaeogeogr. Palaeocli.* 285, pp. 74–84.
- Breitenbach, S. F. M. et al. (2012). "COnstructing Proxy Records from Age models (COPRA)". In: *Climate of the Past* 8.5, pp. 1765–1779. DOI: [10.5194/cp-8-1765-2012](https://doi.org/10.5194/cp-8-1765-2012).
- Breitenbach, Sebastian F.M. et al. (2010). "Strong influence of water vapor source dynamics on stable isotopes in precipitation observed in Southern Meghalaya, NE India". In: *Earth and Planetary Science Letters* 292.1, pp. 212–220. DOI: <https://doi.org/10.1016/j.epsl.2010.01.038>.
- Cadet, Daniel L. and Steve Greco (1987). "Water Vapor Transport over the Indian Ocean during the 1979 Summer Monsoon. Part I: Water Vapor Fluxes". In: *Monthly Weather Review* 115.3, pp. 653–663. DOI: [10.1175/1520-0493\(1987\)115<0653:WVTOTI>2.0.CO;2](https://doi.org/10.1175/1520-0493(1987)115<0653:WVTOTI>2.0.CO;2).
- Caley, T. et al. (2014). "Oxygen stable isotopes during the Last Glacial Maximum climate: perspectives from data-model (iLOVECLIM) comparison". In: *Climate of the Past* 10.6, pp. 1939–1955. DOI: [10.5194/cp-10-1939-2014](https://doi.org/10.5194/cp-10-1939-2014).
- Chatterjee, Piyali and B. N. Goswami (2004). "Structure, genesis and scale selection of the tropical quasi-biweekly mode". In: *Quarterly Journal of the Royal Meteorological Society* 130.599, pp. 1171–1194. DOI: [10.1256/qj.03.133](https://doi.org/10.1256/qj.03.133).
- Cheng, Hai et al. (2012). "The Global Paleomonsoon as seen through speleothem records from Asia and the Americas". In: *Climate Dynamics* 39.5, pp. 1045–1062. DOI: [10.1007/s00382-012-1363-7](https://doi.org/10.1007/s00382-012-1363-7).
- Cheng, Hai et al. (2016). "The Asian monsoon over the past 640,000 years and ice age terminations". In: *Nature* 534, pp. 640–646. URL: [10.1038/nature18591](https://doi.org/10.1038/nature18591).

- Clark, I. D. and P. Fritz (1997). "Environmental Isotopes in Hydrogeology. Boca Raton Fla". In:
- Cobb, Kim M. et al. (2003). "El Niño/Southern Oscillation and tropical Pacific climate during the last millennium". In: *Nature* 424, pp. 271–276. DOI: [10.1038/nature01779](https://doi.org/10.1038/nature01779).
- Cobb, Kim M. et al. (2007). "Regional-scale climate influences on temporal variations of rainwater and cave dripwater oxygen isotopes in northern Borneo". In: *Earth and Planetary Science Letters* 263.3, pp. 207–220. DOI: <https://doi.org/10.1016/j.epsl.2007.08.024>.
- Conroy, Jessica L. et al. (2008). "Holocene changes in eastern tropical Pacific climate inferred from a Galápagos lake sediment record". In: *Quaternary Science Reviews* 27.11, pp. 1166–1180. DOI: <https://doi.org/10.1016/j.quascirev.2008.02.015>.
- Craig, Harmon (1961). "Isotopic Variations in Meteoric Waters". In: *Science* 133.3465, pp. 1702–1703. DOI: [10.1126/science.133.3465.1702](https://doi.org/10.1126/science.133.3465.1702).
- Dansgaard, W (1964). "Stable isotopes in precipitation". In: *Tellus* 16.4, pp. 436–468. DOI: [10.1111/j.2153-3490.1964.tb00181.x](https://doi.org/10.1111/j.2153-3490.1964.tb00181.x).
- Dar, S. S. and P. Ghosh (2017). In: *Earth Syst. Dynam.* 8, pp. 313–321. DOI: <https://doi.org/10.5194/esd-8-313-2017>.
- Datta, P.S., S.K. Tyagi, and H. Chandrasekharan (1991). "Factors controlling stable isotope composition of rainfall in New Delhi, India". In: *Journal of Hydrology* 128.1, pp. 223–236. DOI: [https://doi.org/10.1016/0022-1694\(91\)90139-9](https://doi.org/10.1016/0022-1694(91)90139-9).
- Dee, D. P. et al. (2011). "The ERA-Interim reanalysis: configuration and performance of the data assimilation system". In: *Quarterly Journal of the Royal Meteorological Society* 137.656, pp. 553–597. DOI: [10.1002/qj.828](https://doi.org/10.1002/qj.828).
- Deshpande, R. D. et al. (2010). "Rain-vapor interaction and vapor source identification using stable isotopes from semiarid western India". In: *Journal of Geophysical Research: Atmospheres* 115.D23. DOI: [10.1029/2010JD014458](https://doi.org/10.1029/2010JD014458).
- Deshpande, R.D. et al. (2011). "TWIN National Programme: New Hydrological Insights. Aggarwal S.K. P.G. Jaison A. Sarkar (Eds) Proceedings 15th ISMAS Symposium cum Workshop on Mass Spectrometry". In: vol. 28, pp. 7–11.
- Devi, Sunitha S. and B. P. Yadav (2014). "Characteristics features of southwest monsoon 2013: accessed on 12-12-2014. eds Pai D. S. and Bhan S. C." In: India Meteorological Department. Chap. 1, pp. 1–17. URL: <http://imdpune.gov.in>.
- Dewan and co authors (1984). "Flux of air and moisture in BoB in summer monsoon". In: *Mausam* 35, pp. 493–498.
- Dominik, Fleitmann et al. (2003). "Holocene Forcing of the Indian Monsoon Recorded in a Stalagmite from Southern Oman". In: *Science* 300.5626, pp. 1737–1739. DOI: [10.1126/science.1083130](https://doi.org/10.1126/science.1083130).
- Dorale, Jeffrey A. et al. (1998). "Climate and Vegetation History of the Midcontinent from 75 to 25 ka: A Speleothem Record from Crevice Cave, Missouri, USA". In: *Science* 282.5395, pp. 1871–1874. DOI: [10.1126/science.282.5395.1871](https://doi.org/10.1126/science.282.5395.1871).

- Draxler, Roland R., Paul Ginoux, and Ariel F. Stein (2010). "An empirically derived emission algorithm for wind-blown dust". In: *Journal of Geophysical Research: Atmospheres* 115.D16. DOI: [10.1029/2009JD013167](https://doi.org/10.1029/2009JD013167).
- Dreybrodt, Wolfgang and Denis Scholz (2011). "Climatic dependence of stable carbon and oxygen isotope signals recorded in speleothems: From soil water to speleothem calcite". In: *Geochimica et Cosmochimica Acta* 75.3, pp. 734–752. DOI: <https://doi.org/10.1016/j.gca.2010.11.002>.
- Dykoski, Carolyn A. et al. (2005). "A high-resolution, absolute-dated Holocene and deglacial Asian monsoon record from Dongge Cave, China". In: *Earth and Planetary Science Letters* 233.1, pp. 71–86. ISSN: 0012-821X. DOI: <https://doi.org/10.1016/j.epsl.2005.01.036>. URL: <http://www.sciencedirect.com/science/article/pii/S0012821X05000865>.
- Edwards, R. Lawrence, J.H. Chen, and G.J. Wasserburg (1987). "²³⁸U/²³⁴U/²³⁰Th/²³²Th systematics and the precise measurement of time over the past 500,000 years". In: *Earth and Planetary Science Letters* 81.2, pp. 175–192. DOI: [https://doi.org/10.1016/0012-821X\(87\)90154-3](https://doi.org/10.1016/0012-821X(87)90154-3).
- Eggins, S.M. et al. (1997). "A simple method for the precise determination of 40 trace elements in geological samples by ICPMS using enriched isotope internal standardisation". In: *Chemical Geology* 134.4, pp. 311–326. DOI: [https://doi.org/10.1016/S0009-2541\(96\)00100-3](https://doi.org/10.1016/S0009-2541(96)00100-3).
- Engels, Stefan and van Geel, Bas (2012). "The effects of changing solar activity on climate: contributions from palaeoclimatological studies". In: *J. Space Weather Space Clim.* 2, A09. DOI: [10.1051/swsc/2012009](https://doi.org/10.1051/swsc/2012009).
- Epstein, S and T Mayeda (1953). "Variation of O18 content of waters from natural sources". In: *Geochimica et Cosmochimica Acta* 4.5, pp. 213–224. ISSN: 0016-7037. DOI: [https://doi.org/10.1016/0016-7037\(53\)90051-9](https://doi.org/10.1016/0016-7037(53)90051-9). URL: <http://www.sciencedirect.com/science/article/pii/0016703753900519>.
- Fairchild, Ian J and A Baker (2012). "Speleothem science: from process to past environments". In: *Wiley-Blackwell*, p. 450.
- Fairchild, Ian J. and Pauline C. Treble (2009). "Trace elements in speleothems as recorders of environmental change". In: *Quaternary Science Reviews* 28.5, pp. 449–468. DOI: <https://doi.org/10.1016/j.quascirev.2008.11.007>.
- Fairchild, Ian J et al. (2000). "Controls on trace element (Sr/Mg) compositions of carbonate cave waters: implications for speleothem climatic records". In: *Chemical Geology* 166.3, pp. 255–269. DOI: [https://doi.org/10.1016/S0009-2541\(99\)00216-8](https://doi.org/10.1016/S0009-2541(99)00216-8).
- Fairchild, Ian J. et al. (2001). "Annual to sub-annual resolution of multiple trace-element trends in speleothems". In: *Journal of the Geological Society* 158.5, pp. 831–841. DOI: [10.1144/jgs.158.5.831](https://doi.org/10.1144/jgs.158.5.831).
- Fairchild, Ian J. et al. (2006). "Modification and preservation of environmental signals in speleothems". In: *Earth-Science Reviews* 75.1. Isotopes in PALaeoenvironmental

- reconstruction (ISOPAL), pp. 105–153. DOI: <https://doi.org/10.1016/j.earscirev.2005.08.003>.
- Feng, Xiahong, Anthony M. Faiia, and Eric S. Posmentier (2009). “Seasonality of isotopes in precipitation: A global perspective”. In: *Journal of Geophysical Research: Atmospheres* 114.D8. DOI: [10.1029/2008JD011279](https://doi.org/10.1029/2008JD011279).
- Findlater, J. (1969a). “A major low-level air current near the Indian Ocean during the northern summer”. In: *Quarterly Journal of the Royal Meteorological Society* 95.404, pp. 362–380. DOI: [10.1002/qj.49709540409](https://doi.org/10.1002/qj.49709540409).
- (1969b). “Interhemispheric transport of air in the lower troposphere over the western Indian Ocean”. In: *Quarterly Journal of the Royal Meteorological Society* 95.404, pp. 400–403. DOI: [10.1002/qj.49709540412](https://doi.org/10.1002/qj.49709540412).
- Fleitmann, Dominik et al. (2007). “Holocene ITCZ and Indian monsoon dynamics recorded in stalagmites from Oman and Yemen (Socotra)”. In: *Quaternary Science Reviews* 26.1, pp. 170–188. DOI: <https://doi.org/10.1016/j.quascirev.2006.04.012>.
- Forbush, Scott E. (1954). “World-wide cosmic ray variations, 1937–1952”. In: *Journal of Geophysical Research* 59.4, pp. 525–542. DOI: [10.1029/JZ059i004p00525](https://doi.org/10.1029/JZ059i004p00525).
- Friedman, Irving, Lester Machta, and Ralph Soller (1962). “Water-vapor exchange between a water droplet and its environment”. In: *Journal of Geophysical Research* 67.7, pp. 2761–2766. DOI: [10.1029/JZ067i007p02761](https://doi.org/10.1029/JZ067i007p02761).
- Froehlich, K., J. J. Gibson, and P. Aggarwal (2002). “Deuterium excess in precipitation and its climatological significance. Proc. Int. Conf. on Study of Environmental Change Using Isotope Techniques”. In: Vienna, Austria, International Atomic Energy Agency: C & S Papers Series 13-P, pp. 54–66.
- Fuller, L. et al. (2008). “Isotope hydrology of dripwaters in a Scottish cave and implications for stalagmite palaeoclimate research”. In: *Hydrology and Earth System Sciences* 12.4, pp. 1065–1074. DOI: [10.5194/hess-12-1065-2008](https://doi.org/10.5194/hess-12-1065-2008).
- Gadgil, S., M. Rajeevan, and P.A. Francis (2007). “Monsoon variability: links to major oscillations over the equatorial Pacific and Indian oceans”. In: *Current Science* 93, pp. 182–194.
- Gadgil, Sulochana (2003). “The Indian monsoon and its variability”. In: *Annual Review of Earth and Planetary Sciences* 31.1, pp. 429–467. DOI: [10.1146/annurev.earth.31.100901.141251](https://doi.org/10.1146/annurev.earth.31.100901.141251).
- Galewsky, Joseph et al. (2016). “Stable isotopes in atmospheric water vapor and applications to the hydrologic cycle”. In: *Reviews of Geophysics* 54.4, pp. 809–865. DOI: [10.1002/2015RG000512](https://doi.org/10.1002/2015RG000512).
- Gascoyne, Melvyn (1983). “Trace-element partition coefficients in the calcite-water system and their paleoclimatic significance in cave studies”. In: *Journal of Hydrology* 61.1. V.T. Stringfield Symposium - Processes in Karst Hydrology, pp. 213–222. DOI: [https://doi.org/10.1016/0022-1694\(83\)90249-4](https://doi.org/10.1016/0022-1694(83)90249-4).

- Gascoyne, Melvyn, Henry P Schwarcz, and Derek C Ford (1980). "A palaeotemperature record for the mid-Wisconsin in Vancouver Island". In: *Nature* 285, pp. 474–746. URL: <http://dx.doi.org/10.1038/285474a0><http://10.0.4.14/285474a0>.
- Gat, J. R. (1981). "The isotopes of hydrogen and oxygen in precipitation". In: Elsevier, pp. 1–21.
- Gat, J. R. (1996). "Oxygen and hydrogen isotopes in the hydrologic cycle". In: *Annual Review of Earth and Planetary Sciences* 24, pp. 225–262. URL: <https://doi.org/10.1146/annurev.earth.24.1.225>.
- Gat, J. R. (2000). "Atmospheric water balance - the isotopic perspective". In: *Hydrological Processes* 14.8, pp. 1357–1369. DOI: [10.1002/1099-1085\(20000615\)14:8<1357::AID-HYP986>3.0.CO;2-7](https://doi.org/10.1002/1099-1085(20000615)14:8<1357::AID-HYP986>3.0.CO;2-7).
- Gat, J. R. (2005). "Some classical concepts of isotope hydrology - Isotope in the Water Cycle: Past, Present and Future of a Developing Science, edited by P. K. Aggarwal, J. R. Gat, and K. F. O. Froehlich". In: *Int. At. Energy Agency*, pp. 127–137.
- Gedzelman, Stanley David and James R. Lawrence (1990). "The Isotopic Composition of Precipitation from Two Extratropical Cyclones". In: *Monthly Weather Review* 118.2, pp. 495–509. DOI: [10.1175/1520-0493\(1990\)118<0495:TIC0PF>2.0.CO;2](https://doi.org/10.1175/1520-0493(1990)118<0495:TIC0PF>2.0.CO;2).
- Geel, Van B. et al. (1996). "Archaeological and palaeoecological indications of an abrupt climate change in The Netherlands, and evidence for climatological teleconnections around 2650 BP". In: *Journal of Quaternary Science* 11.6, pp. 451–460. DOI: [10.1002/\(SICI\)1099-1417\(199611/12\)11:6<451::AID-JQS275>3.0.CO;2-9](https://doi.org/10.1002/(SICI)1099-1417(199611/12)11:6<451::AID-JQS275>3.0.CO;2-9).
- Geel, Van B. et al. (1997). "The Sharp Rise of ^{14}C ca. 800 cal BC: Possible Causes, Related Climatic Teleconnections and the Impact on Human Environments". In: *Radiocarbon* 40.1, pp. 535–550. DOI: [10.1017/S0033822200018403](https://doi.org/10.1017/S0033822200018403).
- Genty, Dominique et al. (2001a). "Dead carbon in stalagmites: carbonate bedrock paleodissolution vs. ageing of soil organic matter. Implications for ^{13}C variations in speleothems". In: *Geochimica et Cosmochimica Acta* 65.20, pp. 3443–3457. DOI: [https://doi.org/10.1016/S0016-7037\(01\)00697-4](https://doi.org/10.1016/S0016-7037(01)00697-4).
- Genty, Dominique, Andy Baker, and Barbara Vokal (2001b). "Intra- and inter-annual growth rate of modern stalagmites". In: *Chemical Geology* 176.1, pp. 191–212. ISSN: 0009-2541. DOI: [https://doi.org/10.1016/S0009-2541\(00\)00399-5](https://doi.org/10.1016/S0009-2541(00)00399-5). URL: <http://www.sciencedirect.com/science/article/pii/S0009254100003995>.
- Gilks, W R. and G. O. Roberts (1996). "Improving MCMC mixing. eds W R. Gilks, S. Richardson and D. J. Spiegelhalter". In: *Markov Chain Monte Carlo in Practice*.
- Gimeno, Luis et al. (2012). "Oceanic and terrestrial sources of continental precipitation". In: *Reviews of Geophysics* 50.4. DOI: [10.1029/2012RG000389](https://doi.org/10.1029/2012RG000389).
- Gonfiantini, R. (1981). *The δ -notation and the mass spectrometric measurement techniques*. In: J. R. Gat and R. Gonfiantini (Eds.) *Stable Isotope Hydrology: Deuterium and Oxygen-18 in the Water Cycle*, pp. 35–84.
- Goswami, B. N. (1987). "A mechanism for the West Northwest movement of the monsoon depressions". In: *Nature* 326, pp. 376–370.

- (2006). "The Asian monsoon: Inter-decadal variability. The Asian Monsoon, B. Wang, Ed." In: Praxis Springer Berlin Heidelberg, pp. 295–328.
- Goswami, B. N. and Mohan R. S. Ajaya (2001). "Intraseasonal Oscillations and Interannual Variability of the Indian Summer Monsoon". In: *Journal of Climate* 14.6, pp. 1180–1198. DOI: [10.1175/1520-0442\(2001\)014<1180:IOAIV0>2.0.CO;2](https://doi.org/10.1175/1520-0442(2001)014<1180:IOAIV0>2.0.CO;2)
- Goswami, B. N. and Prince K. Xavier (2005). "Dynamics of internal interannual variability of the Indian summer monsoon in a GCM". In: *Journal of Geophysical Research: Atmospheres* 110.D24. DOI: [10.1029/2005JD006042](https://doi.org/10.1029/2005JD006042)
- Goswami, B. N. et al. (2014). "Multi-Decadal Variability in Indian Summer Monsoon Rainfall Using Proxy Data". In: *Climate Change: Multidecadal and Beyond*. Chap. Chapter 21, pp. 327–345. DOI: [10.1142/9789814579933_0021](https://doi.org/10.1142/9789814579933_0021)
- Griffiths, Michael L. et al. (2010). "Younger Dryas-Holocene temperature and rainfall history of southern Indonesia from 18O in speleothem calcite and fluid inclusions". In: *Earth and Planetary Science Letters* 295.1, pp. 30–36. DOI: <https://doi.org/10.1016/j.epsl.2010.03.018>
- Guhathakurta, P. and M. Rajeevan (2007). "Trends in the rainfall pattern over India". In: *International Journal of Climatology* 28.11, pp. 1453–1469. DOI: [10.1002/joc.1640](https://doi.org/10.1002/joc.1640)
- Gupta, AK, Anderson DM, and Overpeck JT (2003). "Abrupt changes in the Asian southwest monsoon during the Holocene and their links to the North Atlantic Ocean". In: *Nature* 421, pp. 354–357.
- Gupta, S. K. and co authors (2005). "Ground water d18O and dD from central Indian Peninsula: influence of the Arabian Sea and the Bay of Bengal branches". In: *Journal of Hydrology* 303, pp. 38–55.
- Gupta, S. K. and Deshpande R. D. (2005). "The need and potential applications of a network for monitoring of isotopes in waters of India". In: *Current science* 88, pp. 117–118.
- Harmon, Craig and Louis Irwin Gordon (1965). *Deuterium and Oxygen 18 Variations in the Ocean and the Marine Atmosphere*. Pisa: Consiglio nazionale delle ricerche.
- Harmon, Russell S. et al. (2004). "Paleoclimate Information from Speleothems: The Present as a Guide to the Past". In: *Studies of Cave Sediments*. Ed. by Ira D. Sasowsky and John Mylroie. Boston, MA: Springer US, pp. 199–226.
- Harrison, S. P. et al. (2014). "Climate model benchmarking with glacial and mid-Holocene climates". In: *Climate Dynamics* 43.3, pp. 671–688. DOI: [10.1007/s00382-013-1922-6](https://doi.org/10.1007/s00382-013-1922-6)
- Hellstrom, John (2003). "Rapid and accurate U/Th dating using parallel ion-counting multi-collector ICP-MS". In: *J. Anal. At. Spectrom.* 18 (11), pp. 1346–1351. DOI: [10.1039/B308781F](https://doi.org/10.1039/B308781F)
- Hendy, C. H. (1971). "The isotopic geochemistry of speleothems - I: The calculation of the effects of different modes of formation on the isotopic composition of speleothems and their applicability as paleoclimatic indicators". In: *Geochimica et Cosmochimica Acta* 35, pp. 801–824.

- Hoffmann, Georg and Martin Heimann (1997). "Water isotope modeling in the Asian monsoon region". In: *Quaternary International* 37, pp. 115–128. DOI: [https://doi.org/10.1016/1040-6182\(96\)00004-3](https://doi.org/10.1016/1040-6182(96)00004-3).
- Holmgren, Karin et al. (2003). "Persistent millennial-scale climatic variability over the past 25,000 years in Southern Africa". In: *Quaternary Science Reviews* 22.21, pp. 2311–2326. DOI: [https://doi.org/10.1016/S0277-3791\(03\)00204-X](https://doi.org/10.1016/S0277-3791(03)00204-X).
- Hughes, Malcolm K. and Henry F. Diaz (1994). "Was there a 'medieval warm period', and if so, where and when?" In: *Climatic Change* 26.2, pp. 109–142. DOI: [10.1007/BF01092410](https://doi.org/10.1007/BF01092410).
- Johnson, Kathleen R. et al. (2006). "Seasonal trace-element and stable-isotope variations in a Chinese speleothem: The potential for high-resolution paleomonsoon reconstruction". In: *Earth and Planetary Science Letters* 244.1, pp. 394–407. DOI: <https://doi.org/10.1016/j.epsl.2006.01.064>.
- Joseph, Porathur V., Jon K. Eischeid, and Robert J. Pyle (1994). "Interannual Variability of the Onset of the Indian Summer Monsoon and Its Association with Atmospheric Features, El Niño, and Sea Surface Temperature Anomalies". In: *Journal of Climate* 7.1, pp. 81–105. DOI: [10.1175/1520-0442\(1994\)007<0081:IVOT00>2.0.CO;2](https://doi.org/10.1175/1520-0442(1994)007<0081:IVOT00>2.0.CO;2).
- Kalnay, E. et al. (1996). "The NCEP/NCAR 40-Year Reanalysis Project". In: *Bulletin of the American Meteorological Society* 77.3, pp. 437–472. DOI: [10.1175/1520-0477\(1996\)077<0437:TNYRP>2.0.CO;2](https://doi.org/10.1175/1520-0477(1996)077<0437:TNYRP>2.0.CO;2).
- Kathayat, Gayatri et al. (2016). "Indian monsoon variability on millennial-orbital timescales". In: *Scientific Reports* 6, p. 24374. URL: <http://dx.doi.org/10.1038/srep24374>.
- Kendall, C. and J.J. McDonnell (1998). *Isotope Tracers in Catchment Hydrology*. Isotope Tracers in Catchment Hydrology. Elsevier Science. ISBN: 9780444501554. URL: <https://books.google.co.in/books?id=kiLo1U0cm1IC>.
- Kluge, T. et al. (2008). "A new tool for palaeoclimate reconstruction: Noble gas temperatures from fluid inclusions in speleothems". In: *Earth and Planetary Science Letters* 269.3, pp. 408–415. DOI: <https://doi.org/10.1016/j.epsl.2008.02.030>.
- Konwar, Mahen, Anant Parekh, and B. N. Goswami (2012). "Dynamics of east-west asymmetry of Indian summer monsoon rainfall trends in recent decades". In: *Geophysical Research Letters* 39.10. DOI: [10.1029/2012GL052018](https://doi.org/10.1029/2012GL052018).
- Kotlia, Bahadur Singh et al. (2012). "Climatic fluctuations during the LIA and post-LIA in the Kumaun Lesser Himalaya, India: Evidence from a 400 y old stalagmite record". In: *Quaternary International* 263. Late Quaternary morphodynamics in East Asia, pp. 129–138. DOI: <https://doi.org/10.1016/j.quaint.2012.01.025>.
- Kotlia, Bahadur Singh et al. (2015). "Precipitation variability in the Indian Central Himalaya during last ca. 4,000 years inferred from a speleothem record: Impact of Indian Summer Monsoon (ISM) and Westerlies". In: *Quaternary International* 371. Updated Quaternary Climatic Research in parts of the Third Pole Selected

- papers from the HOPE-2013 conference, Nainital, India, pp. 244–253. DOI: <https://doi.org/10.1016/j.quaint.2014.10.066>.
- Kotlia, Bahadur Singh et al. (2016). “Stalagmite Inferred High Resolution Climatic Changes through Pleistocene-Holocene Transition in Northwest Indian Himalaya”. In: *Journal of Earth Science & Climatic Change* 7.3, pp. –. DOI: [10.4172/2157-7617.1000338](https://doi.org/10.4172/2157-7617.1000338).
- Krishnamurthy, R.V. and S.K. Bhattacharya (1991). “In: Taylor, H.P.J., O’Neil, J.R., Kaplan, I.R. (Eds.), Stable Isotope Geochemistry: A Tribute to Samuel Epstein”. In: vol. 3, pp. 187–193.
- Krishnamurti, T. N. and H. N. Bhalme (1976). “Oscillations of a Monsoon System. Part I. Observational Aspects”. In: *Journal of the Atmospheric Sciences* 33.10, pp. 1937–1954. DOI: [10.1175/1520-0469\(1976\)033<1937:00AMSP>2.0.CO;2](https://doi.org/10.1175/1520-0469(1976)033<1937:00AMSP>2.0.CO;2).
- Krishnan, R. and M. Sugi (2003). “Pacific decadal oscillation and variability of the Indian summer monsoon rainfall”. In: *Climate Dynamics* 21.3, pp. 233–242. DOI: [10.1007/s00382-003-0330-8](https://doi.org/10.1007/s00382-003-0330-8).
- Krishnan, R. et al. (2006). “Indian Ocean-monsoon coupled interactions and impending monsoon droughts”. In: *Geophysical Research Letters* 33.8. DOI: [10.1029/2006GL025811](https://doi.org/10.1029/2006GL025811).
- Kumar, Bhishm et al. (2010). “Isotopic characteristics of Indian precipitation”. In: *Water Resources Research* 46.12. DOI: [10.1029/2009WR008532](https://doi.org/10.1029/2009WR008532).
- Kumar, K. K. et al. (2006). “Unraveling the Mystery of Indian Monsoon Failure During El Niño”. In: *Science* 314.5796, pp. 115–119. DOI: [10.1126/science.1131152](https://doi.org/10.1126/science.1131152).
- Kumar, R.R. et al. (2002). “Climate Change in India”. In: New Delhi, India: Tata McGraw Hill, pp. 24–75.
- Kurita, N et al. (2009). “The relationship between the isotopic component of precipitation and precipitation amount in tropical region”. In: *J. Geochem. Explor.* 102, pp. 113–122.
- Kurita, Naoyuki (2013). “Water isotopic variability in response to mesoscale convective system over the tropical ocean”. In: *Journal of Geophysical Research: Atmospheres* 118.18, pp. 10,376–10,390. DOI: [10.1002/jgrd.50754](https://doi.org/10.1002/jgrd.50754).
- Kurita, Naoyuki et al. (2011). “Intraseasonal isotopic variation associated with the Madden-Julian Oscillation”. In: *Journal of Geophysical Research: Atmospheres* 116.D24. DOI: [10.1029/2010JD015209](https://doi.org/10.1029/2010JD015209).
- Lachniet, Matthew S. (2009). “Climatic and environmental controls on speleothem oxygen-isotope values”. In: *Quaternary Science Reviews* 28.5, pp. 412–432. DOI: <https://doi.org/10.1016/j.quascirev.2008.10.021>.
- Landais, A. et al. (2010). “Combined measurements of ^{17}O excess and δ -excess in African monsoon precipitation: Implications for evaluating convective parameterization”. In: *Earth Planet. Sci. Lett.* 298, pp. 104–112.
- Laskar, Amzad H. et al. (2011). “Potential of Stable Carbon and Oxygen Isotope Variations of Speleothems from Andaman Islands, India, for Paleomonsoon Reconstruction”. In: *Journal of Geological Research*, p. 7. DOI: [10.1155/2011/272971](https://doi.org/10.1155/2011/272971).

- Laskar, Amzad H. et al. (2013). "A 4 kyr stalagmite oxygen isotopic record of the past Indian Summer Monsoon in the Andaman Islands". In: *Geochemistry, Geophysics, Geosystems* 14.9, pp. 3555–3566. DOI: [10.1002/ggge.20203](https://doi.org/10.1002/ggge.20203).
- Laskar, J. et al. (2004). "A long-term numerical solution for the insolation quantities of the Earth". In: *A&A* 428.1, pp. 261–285. DOI: [10.1051/0004-6361:20041335](https://doi.org/10.1051/0004-6361:20041335).
- Lawrence, James Robert et al. (2004). "Stable isotopic composition of water vapor in the tropics". In: *Journal of Geophysical Research: Atmospheres* 109.D6. DOI: [10.1029/2003JD004046](https://doi.org/10.1029/2003JD004046).
- Lawrence, Robert James and David Stanley Gedzelman (1996). "Low stable isotope ratios of tropical cyclone rains". In: *Geophysical Research Letters* 23.5, pp. 527–530. DOI: [10.1029/96GL00425](https://doi.org/10.1029/96GL00425).
- Lechleitner, Franziska A. et al. (2017). "Climatic and in-cave influences on ^{18}O and ^{13}C in a stalagmite from northeastern India through the last deglaciation". In: *Quaternary Research* 88.3, pp. 458–471. DOI: [10.1017/qua.2017.72](https://doi.org/10.1017/qua.2017.72).
- Lee, Jung-Eun et al. (2007). "Analysis of the global distribution of water isotopes using the NCAR atmospheric general circulation model". In: *Journal of Geophysical Research: Atmospheres* 112.D16. DOI: [10.1029/2006JD007657](https://doi.org/10.1029/2006JD007657).
- Lekshmy, P. R. et al. (2014). " ^{18}O depletion in monsoon rain relates to large scale organized convection rather than the amount of rainfall". In: *Scientific Reports* 4.5661. DOI: [10.1038/srep05661](https://doi.org/10.1038/srep05661).
- Lekshmy, P.R., M. Midhun, and R. Ramesh (2018). "Influence of stratiform clouds on D and ^{18}O of monsoon water vapour and rain at two tropical coastal stations". In: *Journal of Hydrology* 563, pp. 354–362. ISSN: 0022-1694. DOI: <https://doi.org/10.1016/j.jhydrol.2018.06.001>.
- Lewis, Sophie C. et al. (2011). "High-resolution stalagmite reconstructions of Australian/Indonesian monsoon rainfall variability during Heinrich stadial 3 and Greenland interstadial 4". In: *Earth and Planetary Science Letters* 303.1, pp. 133–142. DOI: <https://doi.org/10.1016/j.epsl.2010.12.048>.
- Li, Hong-Chun et al. (2011). "The ^{18}O and ^{13}C records in an aragonite stalagmite from Furong Cave, Chongqing, China: A-2000-year record of monsoonal climate". In: *Journal of Asian Earth Sciences* 40.6. Quaternary Paleoclimate of the Western Pacific and East Asia: State of the Art and New Discovery, pp. 1121–1130. DOI: <https://doi.org/10.1016/j.jseaes.2010.06.011>.
- Li, W.-X. et al. (1989). "High-precision mass-spectrometric uranium-series dating of cave deposits and implications for palaeoclimate studies". In: *Nature* 339, pp. 534–536. URL: <http://dx.doi.org/10.1038/339534a0><http://10.0.4.14/339534a0>.
- Libby, W. F. (1946). "Atmospheric Helium Three and Radiocarbon from Cosmic Radiation". In: *Phys. Rev.* 69 (11-12), pp. 671–672. DOI: [10.1103/PhysRev.69.671.2](https://doi.org/10.1103/PhysRev.69.671.2).
- Lomb, N. R. (1976). "Least-squares frequency analysis of unequally spaced data". In: *Astrophysics and Space Science* 39.2, pp. 447–462. DOI: [10.1007/BF00648343](https://doi.org/10.1007/BF00648343).

- Lone, Mahjoor Ahmad et al. (2014). "Speleothem based 1000-year high resolution record of Indian monsoon variability during the last deglaciation". In: *Palaeogeography, Palaeoclimatology, Palaeoecology* 395, pp. 1 –8. DOI: <https://doi.org/10.1016/j.palaeo.2013.12.010>.
- Lu, Riyu, Buwen Dong, and Hui Ding (2006). "Impact of the Atlantic Multidecadal Oscillation on the Asian summer monsoon". In: *Geophysical Research Letters* 33.24. DOI: [10.1029/2006GL027655](https://doi.org/10.1029/2006GL027655).
- Luetscher, Marc et al. (2015). "North Atlantic storm track changes during the Last Glacial Maximum recorded by Alpine speleothems". In: *Nature Communications* 6, p. 6344. DOI: [10.1038/ncomms7344](https://doi.org/10.1038/ncomms7344).
- Mahakur, M. et al. (2013). "A high resolution outgoing longwave radiation dataset from Kalpana-1 satellite during 2004-2012". In: *Current Science* 105.8, pp. 1124 – 1133.
- Majoube, M. (1971). "Fractionation of oxygen 18 and of deuterium between water and its vapor". In: *J. Chem. Phys.* 68, pp. 1423 –1436.
- Managave, S.R. et al. (2011). "Response of cellulose oxygen isotope values of teak trees in differing monsoon environments to monsoon rainfall". In: *Dendrochronologia* 29.2, pp. 89 –97. DOI: <https://doi.org/10.1016/j.dendro.2010.05.002>.
- Mann, Michael E. (2002). "Little Ice Age. Encyclopedia of Global Environmental Change". In: vol. 1. Chichester: John Wiley & Sons, Ltd.
- McDermott, Frank (2004). "Palaeo-climate reconstruction from stable isotope variations in speleothems: a review". In: *Quaternary Science Reviews* 23.7. Isotopes in Quaternary Paleoenvironmental reconstruction, pp. 901 –918. DOI: <https://doi.org/10.1016/j.quascirev.2003.06.021>.
- McMillan, Emily A. et al. (2005). "Annual trace element cycles in calcite aragonite speleothems: evidence of drought in the western Mediterranean 12001100yrBP". In: *Journal of Quaternary Science* 20.5, pp. 423–433. DOI: [10.1002/jqs.943](https://doi.org/10.1002/jqs.943).
- Meehl, Gerald A. and Aixue Hu (2006). "Megadroughts in the Indian Monsoon Region and Southwest North America and a Mechanism for Associated Multidecadal Pacific Sea Surface Temperature Anomalies". In: *Journal of Climate* 19.9, pp. 1605–1623. DOI: [10.1175/JCLI3675.1](https://doi.org/10.1175/JCLI3675.1).
- Merlivat, Liliane and Jouzel Jean (1979). "Global climatic interpretation of the deuterium-oxygen 18 relationship for precipitation". In: *Journal of Geophysical Research: Oceans* 84.C8, pp. 5029–5033. DOI: [10.1029/JC084iC08p05029](https://doi.org/10.1029/JC084iC08p05029).
- Mickler, Patrick J., Libby A. Stern, and Jay L. Banner (2006). "Large kinetic isotope effects in modern speleothems". In: *GSA Bulletin* 118.1-2, p. 65. DOI: [10.1130/B25698.1](https://doi.org/10.1130/B25698.1).
- Midhun, M. and R. Ramesh (2016). "Validation of $\delta^{18}\text{O}$ as a proxy for past monsoon rain by multi-GCM simulations". In: *Climate Dynamics* 46.5, pp. 1371–1385. DOI: [10.1007/s00382-015-2652-8](https://doi.org/10.1007/s00382-015-2652-8).

- Miyake, Yasuo, Osamu Matsubaya, and Chizuko Nishihara (1968). "An Isotopic Study on Meteoric Precipitation". In: *Papers in Meteorology and Geophysics* 19.2, pp. 243–266. DOI: [10.2467/mripapers1950.19.2_243](https://doi.org/10.2467/mripapers1950.19.2_243).
- Moerman, Jessica W. et al. (2013). "Diurnal to interannual rainfall $\delta^{18}\text{O}$ variations in northern Borneo driven by regional hydrology". In: *Earth and Planetary Science Letters* 369–370, pp. 108–119. ISSN: 0012-821X. DOI: <https://doi.org/10.1016/j.epsl.2013.03.014>.
- Mook, W G (2001). "Part of the global seawater delta oxygen-18 database from reference Mook 1982". In: PANGAEA. URL: <https://doi.org/10.1594/PANGAEA.58089>.
- Mooley, D. A. and J. Shukla (1989). "Main features of the westward-moving low pressure systems which form over the Indian region during the summer monsoon season and their relation to the monsoon rainfall". In: *Mausam* 40.2, pp. 137–152.
- Moore, M., Z. Kuang, and P. N. Blossey (2013). "A moisture budget perspective of the amount effect". In: *Geophysical Research Letters* 41.4, pp. 1329–1335. DOI: [10.1002/2013GL058302](https://doi.org/10.1002/2013GL058302).
- Moy, C.M. et al. (2002). "Variability of El Niño southern oscillation activity at millennial timescales during the Holocene epoch". In: *Nature* 420, pp. 162–165.
- Mukherjee, Soumya et al. (2017). "Polar Pore Surface Guided Selective CO₂ Adsorption in a Prefunctionalized MetalOrganic Framework". In: *Crystal Growth & Design* 17.7, pp. 3581–3587. DOI: [10.1021/acs.cgd.7b00141](https://doi.org/10.1021/acs.cgd.7b00141).
- Myers, Christopher G. et al. (2015). "Northeast Indian stalagmite records Pacific decadal climate change: Implications for moisture transport and drought in India". In: *Geophysical Research Letters* 42.10, pp. 4124–4132. DOI: [10.1002/2015GL063826](https://doi.org/10.1002/2015GL063826).
- Ordóñez, Paulina et al. (2012). "Major moisture sources for Western and Southern India and their role on synoptic-scale rainfall events". In: *Hydrological Processes* 26.25, pp. 3886–3895. DOI: [10.1002/hyp.8455](https://doi.org/10.1002/hyp.8455).
- Overpeck, Jonathan et al. (1996). "The southwest Indian Monsoon over the last 18 000 years". In: *Climate Dynamics* 12.3, pp. 213–225. DOI: [10.1007/BF00211619](https://doi.org/10.1007/BF00211619).
- Pfahl, Stephan and Heini Wernli (2009). "Lagrangian simulations of stable isotopes in water vapor: An evaluation of nonequilibrium fractionation in the Craig-Gordon model". In: *Journal of Geophysical Research: Atmospheres* 114.D20. DOI: [10.1029/2009JD012054](https://doi.org/10.1029/2009JD012054).
- Pillai, Anusree A.S. et al. (2017). "Mid-late Holocene vegetation response to climatic drivers and biotic disturbances in the Banni grasslands of western India". In: *Palaeogeography, Palaeoclimatology, Palaeoecology* 485, pp. 869–878. DOI: <https://doi.org/10.1016/j.palaeo.2017.07.036>.
- Pisharoty, P. R. (1965). "Evaporation from the Arabian Sea and Indian Southwest Monsoon". In: *Proceedings of International Indian Ocean Expedition, Bombay*, pp. 43–54.

- Prasad, Sushma et al. (2014). "Prolonged monsoon droughts and links to Indo-Pacific warm pool: A Holocene record from Lonar Lake, central India". In: *Earth and Planetary Science Letters* 391, pp. 171–182. DOI: <https://doi.org/10.1016/j.epsl.2014.01.043>.
- Raghavan, S. and S. Rajesh (2003). "Trends in Tropical Cyclone Impact: A Study in Andhra Pradesh, India". In: *Bulletin of the American Meteorological Society* 84.5, pp. 635–644. DOI: [10.1175/BAMS-84-5-635](https://doi.org/10.1175/BAMS-84-5-635).
- Rajeevan, M., Jyoti Bhate, and A. K. Jaswal (2008). "Analysis of variability and trends of extreme rainfall events over India using 104 years of gridded daily rainfall data". In: *Geophysical Research Letters* 35.18. DOI: [10.1029/2008GL035143](https://doi.org/10.1029/2008GL035143).
- Rajeevan, M., Sulochana Gadgil, and Jyoti Bhate (2010). "Active and break spells of the Indian summer monsoon". In: *Journal of Earth System Science* 119.3, pp. 229–247. DOI: [10.1007/s12040-010-0019-4](https://doi.org/10.1007/s12040-010-0019-4).
- Ramesh, R. and M.M. Sarin (1992). "Stable isotope study of the Ganga (Ganges) river system". In: *Journal of Hydrology* 139.1, pp. 49–62. DOI: [https://doi.org/10.1016/0022-1694\(92\)90194-Z](https://doi.org/10.1016/0022-1694(92)90194-Z).
- Rasmusson, Eugene M. and Thomas H. Carpenter (1982). "Variations in Tropical Sea Surface Temperature and Surface Wind Fields Associated with the Southern Oscillation/El Niño". In: *Monthly Weather Review* 110.5, pp. 354–384. DOI: [10.1175/1520-0493\(1982\)110<0354:VITSST>2.0.CO;2](https://doi.org/10.1175/1520-0493(1982)110<0354:VITSST>2.0.CO;2).
- Raspopov, O. M. et al. (2001). "Nonlinear character of solar forcing of climatic processes. Geomagnetism and Aeronomy". In: 41.4, pp. 407–412.
- Raza, Waseem et al. (2017). "Indian summer monsoon variability in southern India during the last deglaciation: Evidence from a high resolution stalagmite 18O record". In: *Palaeogeography, Palaeoclimatology, Palaeoecology* 485, pp. 476–485. DOI: <https://doi.org/10.1016/j.palaeo.2017.07.003>.
- Reimer, Paula J et al. (2004). "Intcal04 Terrestrial Radiocarbon Age Calibration, 026 Cal Kyr BP". In: *Radiocarbon* 46.3, pp. 1029–1058. DOI: [10.1017/S0033822200032999](https://doi.org/10.1017/S0033822200032999).
- Ridley, D. A. et al. (2014). "Total volcanic stratospheric aerosol optical depths and implications for global climate change". In: *Geophysical Research Letters* 41.22, pp. 7763–7769. DOI: [10.1002/2014GL061541](https://doi.org/10.1002/2014GL061541).
- Risi, Camille, Bony Sandrine, and Vimeux Françoise (2008). "Influence of convective processes on the isotopic composition (^{18}O and D) of precipitation and water vapor in the tropics: 2. Physical interpretation of the amount effect". In: *Journal of Geophysical Research: Atmospheres* 113.D19. DOI: [10.1029/2008JD009943](https://doi.org/10.1029/2008JD009943).
- Risi, Camille et al. (2008). "What controls the isotopic composition of the African monsoon precipitation? Insights from event-based precipitation collected during the 2006 AMMA field campaign". In: *Geophysical Research Letters* 35.24. DOI: [10.1029/2008GL035920](https://doi.org/10.1029/2008GL035920).

- Rozanski, Kazimierz, Luis Araguás-Araguás, and Roberto Gonfiantini (1992). "Relation Between Long-Term Trends of Oxygen-18 Isotope Composition of Precipitation and Climate". In: *Science* 258.5084, pp. 981–985. DOI: [10.1126/science.258.5084.981](https://doi.org/10.1126/science.258.5084.981).
- Rozanski, Kazimierz, Luis Araguás-Araguás, and Roberto Gonfiantini (2013). "Isotopic Patterns in Modern Global Precipitation". In: *Climate Change in Continental Isotopic Records*. American Geophysical Union (AGU), pp. 1–36. ISBN: 9781118664025. DOI: [10.1029/GM078p0001](https://doi.org/10.1029/GM078p0001).
- Saha, K. R. (1970). "Air and water vapor transport across the equator in the western Indian Ocean during northern summer 1972". In: *Mon. Wea. Rev.* 103, pp. 197–216.
- Sanwal, Jaishri et al. (2013). "Climatic variability in Central Indian Himalaya during the last 1800 years: Evidence from a high resolution speleothem record". In: *Quaternary International* 304. Larger Asian Rivers: Changes in hydro-climate and water environments, pp. 183–192. DOI: <https://doi.org/10.1016/j.quaint.2013.03.029>.
- Scargle, J. D. (1982). "Studies in Astronomical Time Series Analysis II. Statistical Aspects of Spectral Analysis of Unevenly Sampled Data". In: *Astrophysical Journal* 263, pp. 835–853.
- Schmidt, Gavin A. et al. (2005). "Modeling atmospheric stable water isotopes and the potential for constraining cloud processes and stratosphere-troposphere water exchange". In: *Journal of Geophysical Research: Atmospheres* 110.D21. DOI: [10.1029/2005JD005790](https://doi.org/10.1029/2005JD005790).
- Schulz, Michael and Karl Stattegger (1997). "Spectrum: spectral analysis of unevenly spaced paleoclimatic time series". In: *Computers & Geosciences* 23.9, pp. 929–945. DOI: [https://doi.org/10.1016/S0098-3004\(97\)00087-3](https://doi.org/10.1016/S0098-3004(97)00087-3).
- Schwarcz, H. P. (1986). "Geochronology and isotopic geochemistry of speleothems: Fritz P. and Fontes Ch. Eds." In: Amsterdam: Elsevier, pp. 271–303.
- Sengupta, Debasis and M. Ravichandran (2001). "Oscillations of Bay of Bengal sea surface temperature during the 1998 Summer Monsoon". In: *Geophysical Research Letters* 28.10, pp. 2033–2036. DOI: [10.1029/2000GL012548](https://doi.org/10.1029/2000GL012548).
- Sengupta, Saikat and A. Sarkar (2006). "Stable isotope evidence of dual (Arabian Sea and Bay of Bengal) vapour sources in monsoonal precipitation over north India". In: *Earth and Planetary Science Letters* 250.3, pp. 511–521. DOI: <https://doi.org/10.1016/j.epsl.2006.08.011>.
- Shah, Santosh K., Amalava Bhattacharyya, and Mayank Shekhar (2013). "Reconstructing discharge of Beas river basin, Kullu valley, western Himalaya, based on tree-ring data". In: *Quaternary International* 286. Climate and Vegetation Dynamics, eastern Asia, pp. 138–147. DOI: <https://doi.org/10.1016/j.quaint.2012.09.029>.

- Shakun, Jeremy D. et al. (2007). "A high-resolution, absolute-dated deglacial speleothem record of Indian Ocean climate from Socotra Island, Yemen". In: *Earth and Planetary Science Letters* 259.3, pp. 442–456. DOI: <https://doi.org/10.1016/j.epsl.2007.05.004>.
- Sharmila, S. et al. (2015). "Asymmetry in spacetime characteristics of Indian summer monsoon intraseasonal oscillations during extreme years: Role of seasonal mean state". In: *International Journal of Climatology* 35.8, pp. 1948–1963. DOI: [10.1002/joc.4100](https://doi.org/10.1002/joc.4100).
- Shenoi, S. S. C., D. Shankar, and S. R. Shetye (2002). "Differences in heat budgets of the near-surface Arabian Sea and Bay of Bengal: Implications for the summer monsoon". In: *Journal of Geophysical Research: Oceans* 107.C6, pp. 5–1–5–14. DOI: [10.1029/2000JC000679](https://doi.org/10.1029/2000JC000679).
- Sikka, D. R. (1977). "Some aspects of the life history, structure and movement of monsoon depressions". In: *pure and applied geophysics* 115.5, pp. 1501–1529. DOI: [10.1007/BF00874421](https://doi.org/10.1007/BF00874421).
- Sikka, D. R. and Sulochana Gadgil (1980). "On the Maximum Cloud Zone and the ITCZ over Indian, Longitudes during the Southwest Monsoon". In: *Monthly Weather Review* 108.11, pp. 1840–1853. DOI: [10.1175/1520-0493\(1980\)108<1840:OTMCZA>2.0.CO;2](https://doi.org/10.1175/1520-0493(1980)108<1840:OTMCZA>2.0.CO;2).
- Sime, L. C. et al. (2009). "Evidence for warmer interglacials in East Antarctic ice cores". In: *Nature* 462, pp. 342–345. DOI: [10.1038/nature08564](https://doi.org/10.1038/nature08564).
- Sinha, A. et al. (2015). "Trends and oscillations in the Indian summer monsoon rainfall over the last two millennia". In: *Nature Communication* 6.6309. DOI: <https://doi.org/10.1038/ncomms7309>.
- Sinha, Ashish et al. (2007). "A 900-year (600 to 1500 A.D.) record of the Indian summer monsoon precipitation from the core monsoon zone of India". In: *Geophysical Research Letters* 34.16. DOI: [10.1029/2007GL030431](https://doi.org/10.1029/2007GL030431).
- Sinha, Ashish et al. (2011a). "A global context for megadroughts in monsoon Asia during the past millennium". In: *Quaternary Science Reviews* 30.1, pp. 47–62. DOI: <https://doi.org/10.1016/j.quascirev.2010.10.005>.
- Sinha, Ashish et al. (2011b). "The leading mode of Indian Summer Monsoon precipitation variability during the last millennium". In: *Geophysical Research Letters* 38.15. DOI: [10.1029/2011GL047713](https://doi.org/10.1029/2011GL047713).
- Sodemann, H. et al. (2008). "Interannual variability of Greenland winter precipitation sources: 2. Effects of North Atlantic Oscillation variability on stable isotopes in precipitation". In: *Journal of Geophysical Research: Atmospheres* 113.D12. DOI: [10.1029/2007JD009416](https://doi.org/10.1029/2007JD009416).
- Stein, A. F. et al. (2015). "NOAAs HYSPLIT Atmospheric Transport and Dispersion Modeling System". In: *Bulletin of the American Meteorological Society* 96.12, pp. 2059–2077. DOI: [10.1175/BAMS-D-14-00110.1](https://doi.org/10.1175/BAMS-D-14-00110.1).

- Stohl, A. and P.I James (2004). "A Lagrangian Analysis of the Atmospheric Branch of the Global Water Cycle. Part I: Method Description, Validation, and Demonstration for the August 2002 Flooding in Central Europe". In: *Journal of Hydrometeorology* 5.4, pp. 656–678. DOI: [10.1175/1525-7541\(2004\)005<0656:ALAOTA>2.0.CO;2](https://doi.org/10.1175/1525-7541(2004)005<0656:ALAOTA>2.0.CO;2).
- Stohl, A., M. Hittenberger, and G. Wotawa (1998). "Validation of the lagrangian particle dispersion model FLEXPART against large-scale tracer experiment data". In: *Atmospheric Environment* 32.24, pp. 4245–4264. DOI: [https://doi.org/10.1016/S1352-2310\(98\)00184-8](https://doi.org/10.1016/S1352-2310(98)00184-8).
- Stohl, Andreas and Paul James (2005). "A Lagrangian Analysis of the Atmospheric Branch of the Global Water Cycle. Part II: Moisture Transports between Earths Ocean Basins and River Catchments". In: *Journal of Hydrometeorology* 6.6, pp. 961–984. DOI: [10.1175/JHM470.1](https://doi.org/10.1175/JHM470.1).
- Sturm, C., Q. Zhang, and D. Noone (2010). "An introduction to stable water isotopes in climate models: benefits of forward proxy modelling for paleoclimatology". In: *Climate of the Past* 6.1, pp. 115–129. DOI: [10.5194/cp-6-115-2010](https://doi.org/10.5194/cp-6-115-2010). URL: <https://www.clim-past.net/6/115/2010/>.
- Sun, Ying, Yihui Ding, and Aiguo Dai (2010). "Changing links between South Asian summer monsoon circulation and tropospheric land-sea thermal contrasts under a warming scenario". In: *Geophysical Research Letters* 37.2. DOI: [10.1029/2009GL041662](https://doi.org/10.1029/2009GL041662).
- Tierney, J. E. et al. (2013). "Multidecadal variability in East African hydroclimate controlled by the Indian Ocean". In: *Nature* 493, pp. 389–392. DOI: [10.1038/nature11785](https://doi.org/10.1038/nature11785).
- Tooth, Anna F. and Ian J. Fairchild (2003). "Soil and karst aquifer hydrological controls on the geochemical evolution of speleothem-forming drip waters, Crag Cave, southwest Ireland". In: *Journal of Hydrology* 273.1, pp. 51–68. ISSN: 0022-1694. DOI: [https://doi.org/10.1016/S0022-1694\(02\)00349-9](https://doi.org/10.1016/S0022-1694(02)00349-9).
- Treble, Pauline, J.M.G. Shelley, and John Chappell (2003). "Comparison of high resolution sub-annual records of trace elements in a modern (1911–1992) speleothem with instrumental climate data from southwest Australia". In: *Earth and Planetary Science Letters* 216.1, pp. 141–153. DOI: [https://doi.org/10.1016/S0012-821X\(03\)00504-1](https://doi.org/10.1016/S0012-821X(03)00504-1).
- Treble, P.C. et al. (2005). "Synoptic-scale climate patterns associated with rainfall 18O in southern Australia". In: *Journal of Hydrology* 302.1, pp. 270–282. DOI: <https://doi.org/10.1016/j.jhydrol.2004.07.003>.
- Velde, Y. van der et al. (2010). "Nitrate response of a lowland catchment: On the relation between stream concentration and travel time distribution dynamics". In: *Water Resources Research* 46.11. DOI: [10.1029/2010WR009105](https://doi.org/10.1029/2010WR009105).
- Vimeux, Françoise et al. (2005). "What are the climate controls on D in precipitation in the Zongo Valley (Bolivia)? Implications for the Illimani ice core interpretation". In: *Earth and Planetary Science Letters* 240.2, pp. 205–220. DOI: <https://doi.org/10.1016/j.epsl.2005.09.031>.

- Vizy, K. Edward and Kerry H. Cook (2003). "Connections between the summer east African and Indian rainfall regimes". In: *Journal of Geophysical Research: Atmospheres* 108.D16. DOI: [10.1029/2003JD003452](https://doi.org/10.1029/2003JD003452).
- Vollweiler, Nicole et al. (2006). "A precisely dated climate record for the last 9 kyr from three high alpine stalagmites, Spannagel Cave, Austria". In: *Geophysical Research Letters* 33.20. DOI: [10.1029/2006GL027662](https://doi.org/10.1029/2006GL027662).
- Vuille, M. et al. (2005). "Stable isotopes in precipitation in the Asian monsoon region". In: *Journal of Geophysical Research: Atmospheres* 110.D23. DOI: [10.1029/2005JD006022](https://doi.org/10.1029/2005JD006022).
- Vuille, Mathias et al. (2003). "20th Century Climate Change in the Tropical Andes: Observations and Model Results". In: *Climatic Change* 59.1, pp. 75–99. DOI: [10.1023/A:1024406427519](https://doi.org/10.1023/A:1024406427519).
- Wang, Huijun and Huopo Chen (2012). "Climate control for southeastern China moisture and precipitation: Indian or East Asian monsoon?" In: *Journal of Geophysical Research: Atmospheres* 117.D12. DOI: [10.1029/2012JD017734](https://doi.org/10.1029/2012JD017734).
- Wang, Y. J. et al. (2001). "A High-Resolution Absolute-Dated Late Pleistocene Monsoon Record from Hulu Cave, China". In: *Science* 294.5550, pp. 2345–2348. DOI: [10.1126/science.1064618](https://doi.org/10.1126/science.1064618).
- Wang, Yongjin et al. (2005). "The Holocene Asian Monsoon: Links to Solar Changes and North Atlantic Climate". In: *Science* 308.5723, pp. 854–857. DOI: [10.1126/science.1106296](https://doi.org/10.1126/science.1106296).
- Wang, Yongjin et al. (2008). "Millennial- and orbital-scale changes in the East Asian monsoon over the past 224,000 years". In: *Nature* 451, pp. 1090–1093.
- Warrier, C. U. et al. (2010). "Isotopic characterization of dual monsoon precipitation evidence from Kerala, India". In: *Current Science* 98.11, pp. 1487–1495.
- Warrier, C. Unnikrishnan et al. (2016). "Studies on stable isotopic composition of daily rainfall from Kozhikode, Kerala, India". In: *Isotopes in Environmental and Health Studies* 52.3, pp. 219–230. DOI: [10.1080/10256016.2016.1103238](https://doi.org/10.1080/10256016.2016.1103238).
- Wassenburg, Jasper A. et al. (2012). "Climate and cave control on Pleistocene/Holocene calcite-to-aragonite transitions in speleothems from Morocco: Elemental and isotopic evidence". In: *Geochimica et Cosmochimica Acta* 92, pp. 23–47. DOI: <https://doi.org/10.1016/j.gca.2012.06.002>.
- Werner, Martin et al. (2011). "Stable water isotopes in the ECHAM5 general circulation model: Toward high-resolution isotope modeling on a global scale". In: *Journal of Geophysical Research: Atmospheres* 116.D15. DOI: [10.1029/2011JD015681](https://doi.org/10.1029/2011JD015681).
- White, P.W. (2002). In: *ECMWF Reading- United Kingdom*. URL: www.ecmwf.int.
- Xie, Luhua et al. (2011). "Daily ^{18}O and D of precipitations from 2007 to 2009 in Guangzhou, South China: Implications for changes of moisture sources". In: *Journal of Hydrology* 400.3, pp. 477–489. ISSN: 0022-1694. DOI: <https://doi.org/10.1016/j.jhydrol.2011.02.002>.
- Yadava, M. G. and R. Ramesh (1999). "Speleothems - Useful Proxies for Past Monsoon Rainfall". In: *Journal of Scientific & Industrial Research* 58, pp. 339–348.

- Yadava, M. G. and R Ramesh (2001). "Past rainfall and trace element variations in a tropical speleothem from India". In: *Mausam* 52.1, pp. 307–316.
- Yadava, M. G. and R. Ramesh (2005). "Monsoon reconstruction from radiocarbon dated tropical Indian speleothems". In: *The Holocene* 15.1, pp. 48–59. DOI: [10.1191/0959683605h1783rp](https://doi.org/10.1191/0959683605h1783rp).
- Yadava, M. G., R. Ramesh, and G. B. Pant (2004). "Past monsoon rainfall variations in peninsular India recorded in a 331-year-old speleothem". In: *The Holocene* 14.4, pp. 517–524. DOI: [10.1191/0959683604h1728rp](https://doi.org/10.1191/0959683604h1728rp).
- Yadava, M. G., R Ramesh, and K Pandarinath (2007). "A positive amount effect in the Sahayadri (Western Ghats) rainfall". In: *Current Science* 93.2, pp. 560–564.
- Yadava, M. G., A. M. Dayal, and R. Ramesh (2014). "Effects of dead carbon fraction and the mineralogy of speleothem on their stable carbon and oxygen isotopic variations". In: *Gondwana Geological Magazine* 29.1, pp. 53–59.
- Yang, Yan et al. (2010). "Precise dating of abrupt shifts in the Asian Monsoon during the last deglaciation based on stalagmite data from Yamen Cave, Guizhou Province, China". In: *Science China Earth Sciences* 53.5, pp. 633–641. DOI: [10.1007/s11430-010-0025-z](https://doi.org/10.1007/s11430-010-0025-z).
- Yasunari, Tetsuzo (1979). "Cloudiness Fluctuations Associated with the Northern Hemisphere Summer Monsoon". In: *Journal of the Meteorological Society of Japan. Ser. II* 57.3, pp. 227–242. DOI: [10.2151/jmsj1965.57.3_227](https://doi.org/10.2151/jmsj1965.57.3_227).
- (1980). "A Quasi-Stationary Appearance of 30 to 40 Day Period in the Cloudiness Fluctuations during the Summer Monsoon over India". In: *Journal of the Meteorological Society of Japan. Ser. II* 58.3, pp. 225–229. DOI: [10.2151/jmsj1965.58.3_225](https://doi.org/10.2151/jmsj1965.58.3_225).
- Yoshimura, K. (2015). "Stable Water Isotopes in Climatology, Meteorology, and Hydrology: A Review". In: *Journal of the Meteorological Society of Japan. Ser. II* 93.5, pp. 513–533. DOI: [10.2151/jmsj.2015-036](https://doi.org/10.2151/jmsj.2015-036).
- Yoshimura, K. et al. (2008). "Historical isotope simulation using Reanalysis atmospheric data". In: *Journal of Geophysical Research: Atmospheres* 113.D19. DOI: [10.1029/2008JD010074](https://doi.org/10.1029/2008JD010074).
- Yu, W. et al. (2015). "Simultaneous monitoring of stable oxygen isotope composition in water vapour and precipitation over the central Tibetan Plateau". In: *Atmospheric Chemistry and Physics* 15.18, pp. 10251–10262. DOI: [10.5194/acp-15-10251-2015](https://doi.org/10.5194/acp-15-10251-2015). URL: <https://www.atmos-chem-phys.net/15/10251/2015/>.
- Yuan, Daoxian et al. (2004). "Timing, Duration, and Transitions of the Last Interglacial Asian Monsoon". In: *Science* 304.5670, pp. 575–578. DOI: [10.1126/science.1091220](https://doi.org/10.1126/science.1091220).

Establishing a
research team is
equivalent to starting
a new family. The
main priority is
creating organic and
transparent
relationships among
its members.

-By Canan Dagdeviren

Dendroclimatology Lab
IITM, Pune



The Paleo - Pal